



THE UNIVERSITY OF
WAIKATO
Te Whare Wānanga o Waikato

Research Commons

<http://researchcommons.waikato.ac.nz/>

Research Commons at the University of Waikato

Copyright Statement:

The digital copy of this thesis is protected by the Copyright Act 1994 (New Zealand).

The thesis may be consulted by you, provided you comply with the provisions of the Act and the following conditions of use:

- Any use you make of these documents or images must be for research or private study purposes only, and you may not make them available to any other person.
- Authors control the copyright of their thesis. You will recognise the author's right to be identified as the author of the thesis, and due acknowledgement will be made to the author where appropriate.
- You will obtain the author's permission before publishing any material from the thesis.

**Variation in mandible shape and body size of house mice *Mus musculus* across the New Zealand archipelago:
A Trans-Tasman comparison using geometric morphometrics**

A thesis
submitted in partial fulfilment
of the requirements for the degree
of
Master of Science (Research) in Biological Sciences
at
The University of Waikato
by
ANNIE GRACE WEST



THE UNIVERSITY OF
WAIKATO
Te Whare Wānanga o Waikato

2017

ABSTRACT

Islands create unique environments that provide niche expansion opportunities for invading species not previously available on continental areas. This thesis investigates variation in house mouse mandible shape and body size across the New Zealand archipelago, and aims to identify environmental variables that might influence change between island populations using geometric morphometric techniques.

Mice were introduced to New Zealand in the early 19th century with European explorers and settlers. The *Mus* phylogroups currently known in New Zealand include *Mus musculus domesticus*, *M. m. musculus*, and *M. m. castaneus*. Each of these subspecies has a distinct distribution throughout the archipelago, with *M. m. domesticus* dominating the northern New Zealand ‘mainland’.

Past studies have shown habitat composition and co-existence with rats can significantly influence the activity and behaviour of house mice. Additionally, environmental events such as seed masting are known to provide abundant food resources that inflate house mouse density. Consequently, different habitats may promote variation in dietary components. Here I examined variation between house mice inhabiting five different forest environments across the North and South Islands. Significant variation in mandible shape and body size was found between all five forest populations. Annual rainfall was the most significant covariate with mandible shape. General variation in body size somewhat followed rising latitude, supporting the general ecological trend known as Bergmann’s rule. Habitat type, ambient

temperature, and presence of rats were also significant predictors of body size under regression.

Ecological complexity and biodiversity are known to vary with island size. Islands with greater landmass are associated with increased habitat and species diversity which support heightened competition and predation. Small mammals colonising diminutive, remote islands often experience ecological release from these interactions, leading to the largest cases of gigantism currently known. This study investigated variation between six populations of house mice on small, often very remote islands in the New Zealand archipelago. Significant variation in body size and mandible shape was found between all six populations, but again, rainfall was the most significant covariate with mandible shape. The general pattern in body size between island populations followed Bergmann's rule, and is also consistent with previous studies that observe an inverse relationship between island size and body size, peaking at 50° latitudes. Ambient temperature, rainfall, and genetics were also significant predictors of body size.

Significant variation was also found between all New Zealand mouse populations compared with samples from Sydney, Australia. Sydney was an important shipping port during the settlement of New Zealand. Modern Sydney house mice are probably descendants of the original population from which northern New Zealand *domesticus* mice are derived. Sydney mandibles clustered with extreme examples of variation in New Zealand mouse mandible shapes on separate axes. Collectively, these studies describe significant variation between distinct house mouse populations of the New Zealand archipelago, and lay the foundations for further research in this area.

ACKNOWLEDGEMENTS

I would firstly like to thank the University of Waikato for the numerous scholarships awarded during this Master's degree, and the demonstrating opportunities that funded much of my living and course costs. I also thank the New Zealand Freemasons for awarding me a Freemasons University Scholarship that enabled me to attend the Seventh European Congress of Mammalogy in Sweden, a most fantastic conference that I was very humbled to take part in.

Huge thanks must go to my amazing supervisor, Kim King, who provided endless wisdom and support, and ignited my passion for evolutionary biology. Thank you for all the opportunities and guidance you have bestowed on me from my early days as an eager undergraduate student. You will always be remembered and revered.

Of course, I couldn't have completed this project without the help of Bruce Patty, Olivia Patty, Sari Karppinen, Ray Cursons, Lee Laboyrie, and Grant Tempero. Your eternal patience and guidance were greatly appreciated, especially in the face of what became inevitable failure in the cursed rooms of C.2.03. Lee and Grant, sorry for stinking out R-block with poached mouse heads, and thank you for putting up with my endless queries and requests.

Thank you to Max Oulton for providing the detailed maps of New Zealand.

Thank you to Barry O'Brien for his technical help with the photography equipment, and to Lyn Hunt for her help in helping me understand the complicated statistics of geometric morphometrics.

Thank you to all the people and organisations that provided samples and data for my project: Ellie Bradley, Pete McClelland and Russell Trow, James Russell, Kim King, Zealandia Wildlife Park, Andrew Veale, Elaine Murphy, PJ Moors, and Paul Jamieson.

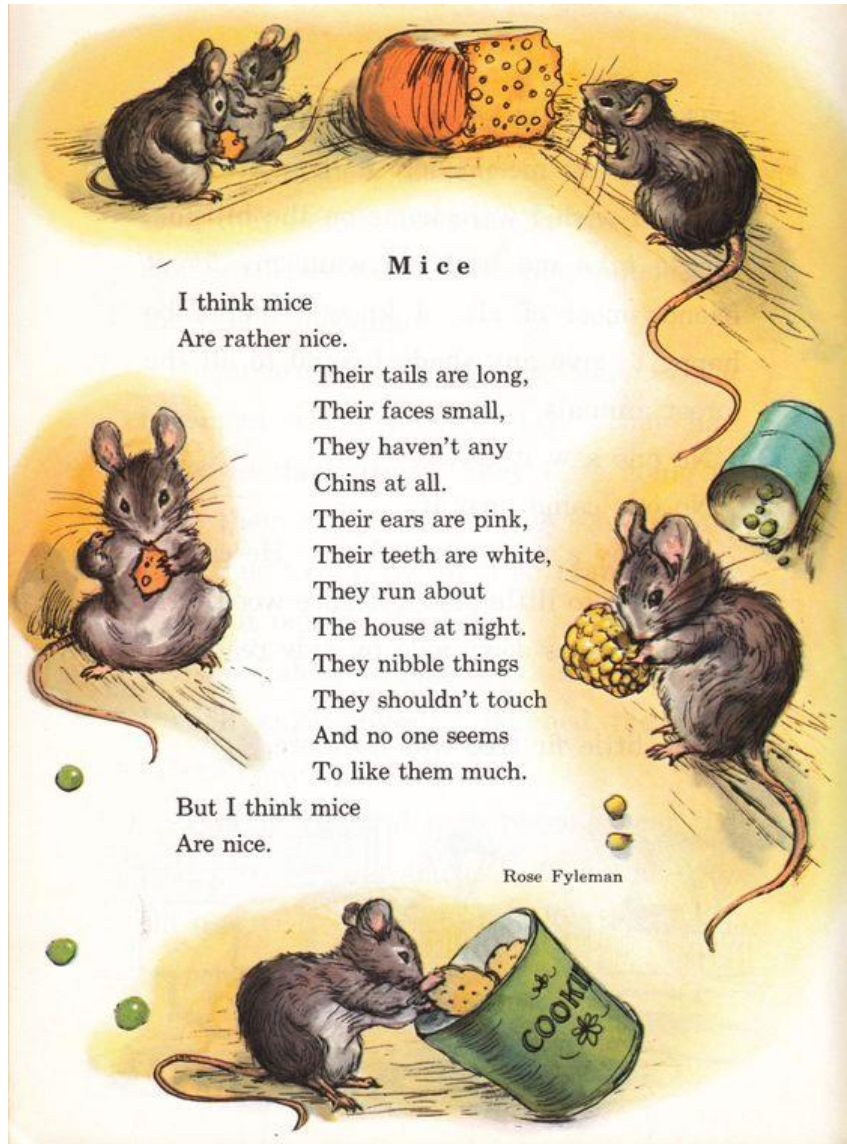
I also need to thank Carly Hill for being a very helpful and understanding twin GM student – sorry again for all the late night messages!

Thank you to all my fellow Masters students for constant reassurance that no-one has finished their writing yet!

Thank you to all my friends and family who supported and entertained me throughout this degree. To my awesome flatmates, thanks for all the Disney movies, wine nights, and late food missions. I could not have completed this thesis without all your tempting distractions.

To my steadfast Jacob, who stayed with me through thick and thin, and was my rock in a sea of despair. Your persistent belief in the strong, intelligent person I aspire to be has undoubtedly laid the foundations for my current and future success, and I am eternally grateful for the person you bring out in me.

And finally, to my wonderful parents – I could not have achieved so much without your constant guidance and support. Your enthusiasm for science, education, and essentially the world has shaped me into the scientist I am today and strive to be. This thesis is as much my accomplishment as it is yours, and I am forever grateful for all the doors you opened, and the opportunities that are to come.



Mice

I think mice
Are rather nice.

Their tails are long,
Their faces small,
They haven't any
Chins at all.
Their ears are pink,
Their teeth are white,
They run about
The house at night.
They nibble things
They shouldn't touch
And no one seems
To like them much.

But I think mice
Are nice.

Rose Fyleman

TABLE OF CONTENTS

ABSTRACT.....	iii
ACKNOWLEDGEMENTS	v
TABLE OF CONTENTS.....	viii
LIST OF TABLES.....	xiii
LIST OF FIGURES	xix
LIST OF APPENDICES.....	xxvi
I. Introduction.....	1
1.1 The house mouse.....	2
1.2 The mandible	8
1.3 Morphometrics.....	12
1.4 Body size.....	16
1.5 Objectives	19
1.6 References.....	23
II. Methodology	39
2.1 Sample collection.....	39
2.2 DNA extraction.....	40
2.3 Purification.....	40
2.4 PCR.....	41
2.6 Mandible cleaning.....	42
2.7 Photography and landmark placement.....	43

2.8 Biomechanical analysis	43
2.9 Statistical analysis	44
2.10 Notes	45
2.11 References	46
III. Comparing house mouse populations in New Zealand Forests.....	51
3.1 Introduction.....	51
3.2 Material	54
Pureora Forest Park	54
Zealandia Wildlife Sanctuary.....	54
Craigieburn Forest Park	55
Eglinton and Hollyford Valleys	55
3.3 Traditional measurements	59
3.2.1 Body Weight	59
3.2.2 Head-Body Length	60
3.2.3 Tail Length.....	60
3.2.4 Regression	62
3.3 Biomechanical analysis	63
3.4 Centroid size.....	66
3.5 Shape analysis	68
3.5.1 Regression and Principal Component Analysis	68
3.5.2 Discriminant Function Analysis.....	76
3.5.3 Canonical Variate Analysis.....	78

3.5.4 Partial Least Squares Analysis	82
3.6 Discussion	85
3.7 References.....	92
IV. Comparison of house mice inhabiting New Zealand offshore islands.....	99
4.1 Introduction.....	99
4.2 Material	102
Ruapuke Island.....	102
Antipodes Island	102
Auckland and Enderby Islands	104
Chatham Island	105
Waikawa Island.....	105
4.3 Traditional measurements	110
4.3.1 Body Weight	110
4.3.2 Head-Body Length.....	111
4.3.3 Tail Length.....	112
4.3.4 Regression.....	114
4.5 Biomechanical analysis.....	115
4.6 Centroid size	118
4.7 Shape analysis.....	120
4.7.1 Regression and Principal Component Analysis (PCA).....	120
4.7.2 Discriminant Function Analysis.....	128
4.7.3 Canonical Variate Analysis.....	131

4.7.4 Partial Least Squares Analysis	137
4.8 Discussion	138
4.9 References	143
V. Variation across the Tasman.....	151
5.1 Introduction.....	151
5.2 Material	152
Sydney.....	152
5.3 Comparison of offshore island and forest mice within the New Zealand archipelago.....	153
5.3.1 Physical measurements and centroid size	153
5.3.2 Shape analysis	153
5.3.2.1 Regression and Principal Component Analysis (PCA).....	153
5.3.2.2 Discriminant Function Analysis.....	155
5.3.3 Discussion	157
5.4 Trans-Tasman forest and Sydney comparison.....	159
5.4.1 Centroid size.....	159
5.4.2 Biomechanical analysis.....	160
5.4.3 Shape analysis	160
5.4.3.1 Regression and Principal Component Analysis	160
5.4.3.2 Discriminant Function Analysis.....	166
5.4.3.3 Canonical Variate Analysis.....	168
5.4.4 Discussion	172

5.5 Offshore island and Sydney comparison	174
5.5.1 Centroid size	174
5.5.2 Biomechanical analysis.....	175
5.5.3 Shape analysis.....	176
5.5.3.1 Regression and Principal Component Analysis	176
5.5.3.2 Discriminant Function Analysis.....	180
5.5.3.3 Canonical Variate Analysis.....	182
5.5.4 Discussion.....	187
5.6 New Zealand mice compared to Sydney mice	190
5.6.1 Shape analysis.....	190
5.6.1.1 Regression and Principal Component Analysis	190
5.6.1.2 Canonical Variate Analysis.....	192
5.6.2 Discussion.....	197
5.7 References.....	199
VI. General discussion and conclusions.....	203
VII. Appendices.....	209
APPENDIX 1.....	209
APPENDIX 2.....	216
ERRATUMS.....	217

LIST OF TABLES

Table III-1 Published and raw body measurements of adult mice on New Zealand offshore islands (mean \pm SD).	57
Table III-2 Environmental variables associated with each forest habitat.	58
Table III-3 P-values from Kruskal-Wallis ANOVA pairwise comparison of forest mouse body weight. Bold, red text indicates significant p-values ≤ 0.05	59
Table III-4 P-values from Kruskal-Wallis ANOVA pairwise comparison of forest mouse head-body length. Bold, red text indicates significant p-values ≤ 0.05	60
Table III-5 P-values from Kruskal-Wallis ANOVA pairwise comparison of forest mouse tail lengths. Bold, red text indicates significant p-values ≤ 0.05	60
Table III-6 Regression percentages of total variation in body weight and length explained by each environmental and genetic covariate. Bold, red text indicates significant percentages with p-values ≤ 0.05	62
Table III-7 P-values from Kruskal-Wallis ANOVA pairwise comparison of the masseter/incisor biomechanical advantage ratio for forest mandibles. Bold, red text indicates significant p-values ≤ 0.05	63
Table III-8 P-values from Kruskal-Wallis ANOVA pairwise comparison of the masseter/molar biomechanical advantage ratio for forest mandibles. Bold, red text indicates significant p-values ≤ 0.05 . Bold italicised text indicates p-values close to 0.05.	64
Table III-9 P-values from Kruskal-Wallis ANOVA pairwise comparison of the temporalis/incisor biomechanical advantage ratio for forest mandibles. Bold, red text indicates significant p-values ≤ 0.05	64
Table III-10 P-values from Kruskal-Wallis ANOVA pairwise comparison of the temporalis/molar biomechanical advantage ratio for forest mandibles. Bold, red text indicates significant p-values ≤ 0.05 . Bold italicised text indicates p-values close to 0.05.	65
Table III-11 P-values from Kruskal-Wallis ANOVA pairwise comparison of forest mandible centroid size. Bold, red text indicates significant p-values ≤ 0.05	66
Table III-12 Eigenvalues for the forest PCA plot that represent more than 5% variance.....	69

Table III-13 P-values from Kruskal-Wallis ANOVA pairwise comparison of PC1 between forest populations. Bold, red text indicates significant p-values ≤ 0.05 .	72
Table III-14 P-values from Kruskal-Wallis ANOVA pairwise comparison of PC2 between forest populations. Bold, red text indicates significant p-values ≤ 0.05 . Bold, italicised text indicates p-values close to 0.05.	73
Table III-15 P-values from Kruskal-Wallis ANOVA pairwise comparison of PC3 between forest populations. Bold, red text indicates significant p-values ≤ 0.05 .	73
Table III-16 P-values from Kruskal-Wallis ANOVA pairwise comparison of PC4 between forest populations. Bold, red text indicates significant p-values ≤ 0.05 . Bold, italicised text indicates p-values close to 0.05.	74
Table III-17 P-values from Kruskal-Wallis ANOVA pairwise comparison of PC5 between forest populations. Bold, red text indicates significant p-values ≤ 0.05 . Bold, italicised text indicates p-values close to 0.05.	74
Table III-18 Misclassification percentages of cross-validation discriminant function analysis for forest mandibles. Bold, red text indicates misclassification levels of $\leq 5\%$. Bold italicised text indicates $\leq 11\%$.	76
Table III-19 Canonical Variate Analysis results for forest mandibles. A) Canonical variates and their associated variance percentages. B) Mahalanobis distances between groups along the first CV axis and their associated p-values. C) Procrustes distances between groups along the first CV axis and their associated p-values. Bold, red text indicates significant p-values ≤ 0.05 . Bold text indicates highest and lowest distance values between pairs.	81
Table III-20 PLS forest loading scores for each covariate, correlation percentage of each PLS, and significance test results after 1000 permutations. Bold, red text indicates significant loading scores, covariation percentages, and p-values ≤ 0.05 .	84
Table IV-1 Published and raw body measurements of adult mice on New Zealand offshore islands (mean \pm SD).	108
Table IV-2 Environmental variables associated with each island habitat.	109

Table IV-3 P-values from Kruskal-Wallis ANOVA pairwise comparison of offshore island mouse body weight. Bold, red text indicates significant p-values ≤ 0.05 . No raw weight data for the Auckland and Chatham Island mice were available. 110

Table IV-4 P-values from ANOVA pairwise comparison of offshore island mouse head-body length. Bold, red text indicates significant p-values ≤ 0.05 . Bold italicised text indicates p-values close to 0.05. 112

Table IV-5 P-values from ANOVA pairwise comparison of offshore island mouse tail length. Bold, red text indicates significant p-values ≤ 0.05 112

Table IV-6 Predicted percentage scores for each island variable. Bold, red text indicates significant regression p-values ≤ 0.05 114

Table IV-7 P-values from Kruskal-Wallis ANOVA pairwise comparison of the masseter/incisor biomechanical advantage ratio for offshore island mandibles. Bold, red text indicates significant p-values ≤ 0.05 . Bold italicised text indicates p-values close to 0.05. 115

Table IV-8 P-values from Kruskal-Wallis ANOVA pairwise comparison of the masseter/molar biomechanical advantage ratio for offshore island mandibles. Bold, red text indicates significant p-values ≤ 0.05 116

Table IV-9 P-values from Kruskal-Wallis ANOVA pairwise comparison of the temporalis/incisor biomechanical advantage ratio for offshore island mandibles. Bold, red text indicates significant p-values ≤ 0.05 116

Table IV-10 P-values from Kruskal-Wallis ANOVA pairwise comparison of the temporalis/molar biomechanical advantage ratio for offshore island mandibles. Bold, red text indicates significant p-values ≤ 0.05 . Bold italicised text indicates p-values close to 0.05. 117

Table IV-11 P-values from Kruskal-Wallis ANOVA pairwise comparison of offshore island mandible centroid size. Bold, red text indicates significant p-values ≤ 0.05 118

Table IV-12 Eigenvalues for the offshore island PCA plot that represent more than 5% variance. Eigenvalues above the ‘lee’ point on the scree plot are italicised. 121

Table IV-13 P-values from Kruskal-Wallis ANOVA pairwise comparison of PC1 between offshore islands. Bold, red text indicates significant p-values ≤ 0.05 123

Table IV-14 P-values from Kruskal-Wallis ANOVA pairwise comparison of PC2 between offshore islands. Bold, red text indicates significant p-values ≤ 0.05	124
Table IV-15 P-values from Kruskal-Wallis ANOVA pairwise comparison of PC3 between offshore islands. Bold, red text indicates significant p-values ≤ 0.05	124
Table IV-16 P-values from Kruskal-Wallis ANOVA pairwise comparison of PC4 between offshore islands. Bold, red text indicates significant p-values ≤ 0.05	125
Table IV-17 P-values from Kruskal-Wallis ANOVA pairwise comparison of PC5 between offshore islands. Bold, red text indicates significant p-values ≤ 0.05	125
Table IV-18 P-values from Kruskal-Wallis ANOVA pairwise comparison of PC6 between offshore islands. Bold, red text indicates significant p-values ≤ 0.05	126
Table IV-19 P-values from Kruskal-Wallis ANOVA pairwise comparison of PC7 between offshore islands. Bold, red text indicates significant p-values ≤ 0.05	126
Table IV-20 Misclassification percentages of cross-validation discriminant function analysis for offshore island mandibles. Bold, red text indicates misclassification levels of $\leq 5\%$. Bold italicised text indicates $\leq 10\%$	129
Table IV-21 Misclassification percentages of cross-validation discriminant function analysis for offshore island haplotypes. Bold, red text indicates misclassification levels of $\leq 5\%$. Bold italicised text indicates $\leq 10\%$	130
Table IV-22 Canonical Variate Analysis results for offshore island mandibles. A) Canonical variates and their associated variance percentages. B) Mahalanobis distances between groups along the first CV axis and their associated p-values. C) Procrustes distances between groups along the first CV axis and their associated p-values. Bold, red text indicates significant p-values ≤ 0.05 . Bold text indicates highest and lowest distances between pairs.....	134
Table IV-23 Canonical Variate results for offshore island mandibles. A) Canonical variates and their associated variance percentages. B) Mahalanobis distances between groups along the first CV axis and their associated p-values. C) Procrustes distances between groups along the first CV axis and their associated p-values. Bold, red text indicates significant p-values ≤ 0.05 . Bold text indicates highest and lowest distance values between pairs.	136

Table V-1 P-values from Kruskal-Wallis ANOVA pairwise comparison between offshore island and forest body measurements and mandible centroid size. Bold, red text indicates significant p-values ≤ 0.05	153
Table V-2 Eigenvalues for the offshore island and forest PCA plot that represent more than 5% variance. Eigenvalues above the 'lee' point on the scree plot are italicised.	154
Table V-3 P-values from Kruskal-Wallis ANOVA pairwise comparison of mandible centroid size between forest and Sydney mice. Bold, red text indicates significant p-values ≤ 0.05	159
Table V-4 P-values from Kruskal-Wallis ANOVA pairwise comparison of the biomechanical advantage ratios between forest and Sydney mandibles. Bold, red text indicates significant p-values ≤ 0.05 . Bold italicised text indicates p-values close to 0.05.	160
Table V-5 Eigenvalues for the forest and Sydney PCA plot that represent more than 5% variance. Eigenvalues above the 'lee' point on the scree plot are italicised.	161
Table V-6 P-values from Kruskal-Wallis ANOVA pairwise comparison of the first five PCs between forest and Sydney mandible shapes. Bold, red text indicates significant p-values ≤ 0.05	165
Table V-7 Misclassification percentage of cross-validation discriminant function analysis for forest and Sydney mandibles. Bold, red text indicates misclassification levels of $\leq 5\%$. Bold italicised text indicates $\leq 10\%$	166
Table V-8 Canonical Variate Analysis results for forest and Sydney mandibles. A) Canonical variates and their associated variance percentages. B) Mahalanobis distances between groups along the first CV axis and their associated p-values. C) Procrustes distances between groups along the first CV axis and their associated p-values. Bold, red text indicates significant p-values ≤ 0.05 . Bold text indicates highest and lowest distance values between pairs.	170
Table V-9 P-values from Kruskal-Wallis ANOVA pairwise comparison of mandible centroid size between offshore island and Sydney mice. Bold, red text indicates significant p-values ≤ 0.05 . Bold, italicised text indicates p-values close to 0.05.....	174
Table V-10 P-values from Kruskal-Wallis ANOVA pairwise comparison of the biomechanical advantage ratios between offshore island and Sydney mandibles. Bold, red text indicates significant p-values ≤ 0.05 . Bold italicised text indicates p-values close to 0.05.....	175

Table V-11 Eigenvalues for the offshore island and Sydney PCA plot that represent more than 5% variance. Eigenvalues above the ‘lee’ point on the scree plot are italicised. 176

Table V-12 P-values from Kruskal-Wallis ANOVA pairwise comparison of the first five PCs between offshore island and Sydney mandible shapes. Bold, red text indicates significant p-values ≤ 0.05 . Bold, italicised text indicates p-values close to 0.05. 179

Table V-13 Misclassification percentages of cross-validation discriminant function analysis for offshore island and Sydney mandibles. Bold, red text indicates misclassification levels of $\leq 5\%$ 180

Table V-14 Misclassification percentages of cross-validation discriminant function analysis for offshore island and Sydney haplotypes. Bold, red text indicates misclassification levels of $\leq 5\%$ 181

Table V-15 Canonical Variate Analysis results for offshore island and Sydney mandibles. A) Canonical variates and their associated variance percentages. B) Mahalanobis distances between groups along the first CV axis and their associated p-values. C) Procrustes distances between groups along the first CV axis and their associated p-values. Bold, red text indicates significant p-values ≤ 0.05 . Bold text indicates highest and lowest distance values between pairs. 184

Table V-16 Canonical Variate Analysis results for offshore island and Sydney haplotypes. A) Eigenvalues and their associated variance percentages. B) Mahalanobis distances between groups along the first CV axis and their associated p-values. C) Procrustes distances between groups along the first CV axis and their associated p-values. Bold, red text indicates significant p-values ≤ 0.05 . Bold text indicates highest and lowest distance values between pairs. 186

Table V-17 Eigenvalues for the New Zealand - Sydney PCA plot that represent more than 5% variance. Eigenvalues above the ‘lee’ point on the scree plot are italicised. 191

Table V-18 Canonical variates and their associated variance percentages for New Zealand and Sydney mandibles. 195

Table V-19 Mahalanobis distances between groups along the first CV axis and their associated p-values for New Zealand and Sydney mandibles. Bold, red text indicates significant p-values ≤ 0.05 . Bold text indicates highest and lowest distance values between pairs. 195

Table V-20 Procrustes distances between groups along the first CV axis and their associated p-values for New Zealand and Sydney mandibles. Bold, red text indicates significant p-values ≤ 0.05 . Bold text indicates highest and lowest distance values between pairs. 196

LIST OF FIGURES

Figure I-A Distinct components of the house mouse mandible. Image retrieved from Michaux et al. (2007).	9
Figure II-A LEFT, placement of 16 landmarks to sample mandible shape. RIGHT, Inlever length (dotted lines) based on muscle attachment zones and Outlever length (solid lines) based on bite zones.	43
Figure III-A Locations of New Zealand forests included in this study. Drawn up by Max Oulton, University of Waikato.	56
Figure III-B Histogram showing mean body weight, head-body length, and tail length values between forest mouse populations.	59
Figure III-C Dot density plots showing the distribution of raw physical measurements within each forest population. Each icon corresponds to an individual mouse.	61
Figure III-D Histogram showing average mandible centroid size values between forest populations. .	67
Figure III-E Group-centred regression of forest mandible shape on log centroid size.	68
Figure III-F Scree plot of the variance explained by each eigenvalue for forest mandibles.	69
Figure III-G LEFT PCA plot of mandible shape differences between forest populations with PC1 and PC2. Each dot represents a specimen, surrounded by equal frequency ellipses. RIGHT Procrustes deformation warped outlines depicting the change in mandible shape along each axis; blue represents mandible shape at far left of the axis, pink represents the mandible shape at far right of the axis.	70
Figure III-H LEFT PCA plot of mandible shape differences between forest populations with PC1 and PC2. Each dot represents a specimen, with 90% confidence ellipses around the mean. RIGHT Procrustes deformation warped outlines depicting the change in mandible shape along each axis; blue represents mandible shape at far left of the axis, pink represents the mandible shape at far right of the axis.	71
Figure III-I LEFT PCA plot of mandible shape differences between forest populations with PC1 and PC3. Each dot represents a specimen, with 90% confidence ellipses around the mean. RIGHT Procrustes deformation warped outlines depicting the change in mandible shape along each axis; blue represents mandible shape at far left of the axis, pink represents the mandible shape at far right of the axis.	72

Figure III-J PCA plot of mandible shape differences between forest genetic haplotypes. Each dot represents a specimen, surrounded by equal frequency ellipses.....	75
Figure III-K PCA plot of mandible shape differences between forest genetic haplotypes. Each dot represents a specimen, with 90% confidence ellipses around the mean.....	75
Figure III-L Procrustes-based superimposition of forest mean mandible shapes obtained from discriminant function analysis. A: Craigieburn (pink) and Eglinton (green), B: Craigieburn (pink) and Pureora (purple), C: Eglinton (green) and Pureora (purple), D: Pureora (purple) and Zealandia (blue).	77
Figure III-M Procrustes-based superimposition of forest haplotype mean mandible shapes obtained from discriminant function analysis. Domesticus (pink) and hybrid (blue).	78
Figure III-N LEFT CVA plot displaying maximum differentiation of pre-defined forest groups with CV1 and CV2. RIGHT Procrustes deformation warped outlines depicting the change in mandible shape along each axis; blue represents mandible shape at far left of the axis, pink represents the mandible shape at far right of the axis.	79
Figure III-O LEFT CVA plot displaying maximum differentiation of pre-defined forest groups with CV1 and CV3. RIGHT Procrustes deformation warped outlines depicting the change in mandible shape along each axis; blue represents mandible shape at far left of the axis, pink represents the mandible shape at far right of the axis.	80
Figure III-P TOP PLS covariation of forest mouse mandible shape with rainfall. Each dot represents an individual specimen. BELOW Warped outline shape change with increasing rainfall.	83
Figure III-Q TOP PLS covariation of forest mouse mandible shape with highest altitude. Each dot represents an individual specimen. BELOW Warped outline shape change with increasing altitude. .	83
Figure IV-A Map of the New Zealand offshore islands included in this study. Drawn up by Max Oulton, University of Waikato.	107
Figure IV-B Histogram showing mean body weight, tail length, and head-body length values between offshore island mouse populations.	111
Figure IV-C Dot density plots representing the distribution of body weight, tail length, and head-body length values within offshore populations. Each icon corresponds to an individual mouse.	113
Figure IV-D Histogram showing average centroid size values between offshore island populations.	119

Figure IV-E Group-centred regression of offshore island mandible shape on log centroid size. 120

Figure IV-F Scree plot of the variance explained by each eigenvalue for offshore island mandibles. 121

Figure IV-G LEFT PCA plot of mandible shape differences between offshore island populations. Each dot represents a specimen, surrounded by equal frequency ellipses. RIGHT Procrustes deformation warped outlines depicting the change in mandible shape along each axis; blue represents mandible shape at far left of the axis, pink represents the mandible shape at far right of the axis. 122

Figure IV-H LEFT PCA plot of mandible shape differences between offshore island populations. Each dot represents a specimen, with 90% confidence ellipses around the mean. RIGHT Procrustes deformation warped outlines depicting the change in mandible shape along each axis; blue represents mandible shape at far left of the axis, pink represents the mandible shape at far right of the axis. 123

Figure IV-I PCA plot of mandible shape differences between offshore island genetic haplotypes. Each dot represents a specimen, with 90% confidence ellipses around the mean. 127

Figure IV-J Procrustes-based superimposition of offshore island mean mandible shapes obtained from discriminant function analysis. A: Antipodes Island (pink) and Chatham Island (light blue), B: Antipodes Island (pink) and Waikawa Island (green), C: Auckland Island (light green) and Enderby Island (blue), D: Enderby Island (blue) and Waikawa Island (green). 129

Figure IV-K Procrustes-based superimposition of mean mandible shapes for offshore island haplotypes obtained from discriminant function analysis. A: Castaneus (pink) and domesticus Clade C (light blue), B: domesticus Clade C (light blue) and domesticus Clade B (green), C: domesticus Clade B (green) and domesticus Clade E (purple). 131

Figure IV-L LEFT CVA plot displaying maximum differentiation of pre-defined offshore island groups. RIGHT Procrustes deformation warped outlines depicting the change in mandible shape along each axis; blue represents mandible shape at far left of the axis, pink represents the mandible shape at far right of the axis. 132

Figure IV-M LEFT CVA plot displaying maximum differentiation of pre-defined offshore island haplotype groups. RIGHT Procrustes deformation warped outlines depicting the change in mandible shape along each axis; blue represents mandible shape at far left of the axis, pink represents the mandible shape at far right of the axis. 135

Figure IV-N TOP PLS covariation of offshore island mandible shape with rainfall. Each dot represents an individual specimen. BELOW Warped outline shape change with increasing rainfall. 137

Figure V-A Group-centred regression of mandible shape on log centroid size for forest and offshore island mandibles. 153

Figure V-B Scree plot of the variance explained by each eigenvalue for forest and offshore island mandibles. 154

Figure V-C LEFT PCA plot of mandible shape differences between offshore island and forest populations. Each dot represents a specimen, with 90% confidence ellipses around the mean. RIGHT Procrustes deformation warped outlines depicting the change in mandible shape along each axis; blue represents mandible shape at far left of the axis, pink represents the mandible shape at far right of the axis. 155

Figure V-D Procrustes-based superimposition of mean mandible shapes for forest and offshore island mandibles obtained from discriminant function analysis. Forest: pink, offshore islands: blue. 156

Figure V-E Dot density plot showing the distribution of centroid size within forest and Sydney populations. Each icon represents an individual mouse. 159

Figure V-F Group-centred regression of mandible shape on log centroid size for forest and Sydney mandibles. 161

Figure V-G Scree plot of the variance explained by each eigenvalue for forest and Sydney mandibles. 162

Figure V-H LEFT PCA plot of mandible shape differences between forest and Sydney populations. Each dot represents a specimen, surrounded by equal frequency ellipses. RIGHT Procrustes deformation warped outlines depicting the change in mandible shape along each axis; blue represents mandible shape at far left of the axis, pink represents the mandible shape at far right of the axis. 163

Figure V-I LEFT PCA plot of mandible shape differences between forest and Sydney populations with PC1 and PC3. Each dot represents a specimen, with 90% confidence ellipses around the mean. RIGHT Procrustes deformation warped outlines depicting the change in mandible shape along each axis; blue represents mandible shape at far left of the axis, pink represents the mandible shape at far right of the axis. 164

Figure V-J PCA plot of mandible shape differences between forest and Sydney genetic haplotypes. Each dot represents a specimen, with 90% confidence ellipses around the mean. 166

Figure V-K Procrustes-based superimposition of forest and Sydney mean mandible shapes obtained from discriminant function analysis. A: Sydney (orange) and Craigieburn (light green), B: Sydney (orange) and Hollyford (blue), C: Sydney (orange) and Pureora (purple)..... 167

Figure V-L Procrustes-based superimposition of mean mandible shapes from forest and Sydney haplotypes obtained from discriminant function analysis. A: Sydney domesticus (pink) and domesticus-castaneusNZ.1 hybrids (blue), B: Sydney domesticus (pink) and forest domesticus Clade E (green). 168

Figure V-M LEFT CVA plot displaying maximum differentiation of pre-defined forest and Sydney groups. RIGHT Procrustes deformation warped outlines depicting the change in mandible shape along each axis; blue represents mandible shape at far left of the axis, pink represents the mandible shape at far right of the axis. 169

Figure V-N LEFT CVA plot displaying maximum differentiation of pre-defined forest and Sydney haplotype groups. RIGHT Procrustes deformation warped outlines depicting the change in mandible shape along each axis; blue represents mandible shape at far left of the axis, pink represents the mandible shape at far right of the axis..... 171

Figure V-O Dot density plot showing the distribution of centroid size within offshore island and Sydney populations. Each icon represents an individual mouse. 174

Figure V-P Group-centred regression of mandible shape on log centroid size for offshore island and Sydney mandibles..... 176

Figure V-Q Scree plot of the variance explained by each eigenvalue for offshore island and Sydney mandibles. 177

Figure V-R LEFT PCA plot of mandible shape differences between offshore island and Sydney populations. Each dot represents a specimen, surrounded by equal frequency ellipses. RIGHT Procrustes deformation warped outlines depicting the change in mandible shape along each axis; blue represents mandible shape at far left of the axis, pink represents the mandible shape at far right of the axis. 178

Figure V-S PCA plot of mandible shape differences between offshore island and Sydney genetic haplotypes. Each dot represents a specimen, with 90% confidence ellipses around the mean. 180

Figure V-T Procrustes-based superimposition of offshore island and Sydney mean mandible shapes obtained from discriminant function analysis. A: Sydney (orange) and Antipodes I. (pink), B: Sydney (orange) and Chatham I. (blue), C: Sydney (orange) and Ruapuke I. (purple). 181

Figure V-U Procrustes-based superimposition of mean mandible shapes for offshore island and Sydney haplotypes obtained from discriminant function analysis. A: Sydney domesticus (orange) and castaneus (pink), B: Sydney domesticus (orange) and dom Clade C (blue), C: Sydney domesticus (orange) and dom Clade E (purple). 182

Figure V-V LEFT CVA plot displaying maximum differentiation of pre-defined offshore island and Sydney groups. RIGHT Procrustes deformation warped outlines depicting the change in mandible shape along each axis; blue represents mandible shape at far left of the axis, pink represents the mandible shape at far right of the axis. 183

Figure V-W LEFT CVA plot displaying maximum differentiation of pre-defined offshore island and Sydney haplotype groups. RIGHT Procrustes deformation warped outlines depicting the change in mandible shape along each axis; blue represents mandible shape at far left of the axis, pink represents the mandible shape at far right of the axis. 185

Figure V-X Group-centred regression of mandible shape on log centroid size for New Zealand and Sydney mandibles. 190

Figure V-Y Scree plot of the variance explained by each eigenvalue for New Zealand and Sydney. 191

Figure V-Z LEFT PCA plot of mandible shape differences between New Zealand and Sydney populations. Each dot represents a specimen, surrounded by equal frequency ellipses. RIGHT Procrustes deformation warped outlines depicting the change in mandible shape along each axis; blue represents mandible shape at far left of the axis, pink represents the mandible shape at far right of the axis. 192

Figure V-AA LEFT CVA plot displaying maximum differentiation of pre-defined New Zealand and Sydney groups. RIGHT Procrustes deformation warped outlines depicting the change in mandible shape along each axis; blue represents mandible shape at far left of the axis, pink represents the mandible shape at far right of the axis. 193

Figure V-BB LEFT CVA plot displaying maximum differentiation of pre-defined New Zealand and Sydney groups with CV1 and CV3. RIGHT Procrustes deformation warped outlines depicting the change in mandible shape along each axis; blue represents mandible shape at far left of the axis, pink represents the mandible shape at far right of the axis. 194

Figure VII-A Corrected PCA plot of mandible shape variation between forest populations with PC1 and PC2. Warped outline plots depict shape change along each axis; blue represents mandible shape at far left of the axis, pink represents mandible shape at far right of the axis. 218

Figure VII-B Corrected PCA plot of mandible shape variation between forest genetic haplotypes with PC1 and PC2. Warped outline plots depict shape change along each axis; blue represents mandible shape at far left of the axis, pink represents mandible shape at far right of the axis. 219

Figure VII-C Corrected PCA plot of mandible shape variation between offshore island populations with PC1 and PC2. Warped outline plots depict shape change along each axis; blue represents mandible shape at far left of the axis, pink represents mandible shape at far right of the axis. 220

Figure VII-D Corrected PCA plot of mandible shape variation between offshore island genetic haplotypes with PC1 and PC2. Warped outline plots depict shape change along each axis; blue represents mandible shape at far left of the axis, pink represents mandible shape at far right of the axis. 221

Figure VII-E Corrected PCA plot of mandible shape variation between offshore island and forest populations with PC1 and PC2. Warped outline plots depict shape change along each axis; blue represents mandible shape at far left of the axis, pink represents mandible shape at far right of the axis. 222

Figure VII-F Corrected PCA plot of mandible shape variation between New Zealand forest and Sydney populations with PC1 and PC2. Warped outline plots depict shape change along each axis; blue represents mandible shape at far left of the axis, pink represents mandible shape at far right of the axis. 223

Figure VII-G Corrected PCA plot of mandible shape variation between New Zealand forest and Sydney genetic haplotypes with PC1 and PC2. Warped outline plots depict shape change along each axis; blue represents mandible shape at far left of the axis, pink represents mandible shape at far right of the axis. 224

Figure VII-H Corrected PCA plot of mandible shape variation between New Zealand offshore island and Sydney populations with PC1 and PC2. Warped outline plots depict shape change along each axis; blue represents mandible shape at far left of the axis, pink represents mandible shape at far right of the axis. 225

Figure VII-I Corrected PCA plot of mandible shape variation between New Zealand offshore island and Sydney genetic haplotypes with PC1 and PC2. Warped outline plots depict shape change along each axis; blue represents mandible shape at far left of the axis, pink represents mandible shape at far right of the axis..... 226

LIST OF APPENDICES

APPENDIX 1.

Raw physical body measurements for forest and offshore island mice.....209

APPENDIX 2.

Environmental and genetic variables used for PLS in Chapters III and IV.....216

ERRATUMS

Corrected PCA plots.....217

I. Introduction

Understanding how morphological traits evolve and change over time has captured the attention of scientists for centuries (Adams et al. 2004; Klingenberg 2010). The progressive ability to accurately describe changes in biological shape has led to the advent of a widespread technique called geometric morphometrics (Bookstein 1986; Rohlf 1990; Bookstein 1991; Rohlf & Marcus 1993; Adams et al. 2004; Rohlf 2005; Slice 2007; Klingenberg 2010; Zelditch et al. 2012). Geometric morphometrics is the mathematical description of shape variables that enable exclusion of influencing variables such as size, rotation, and position, as well as controlling for allometry (Bookstein 1991; Dryden & Mardia 1998; Slice 2007; Klingenberg 2010; Zelditch et al. 2012; Klingenberg 2016). The mathematic basis of this technique offers precise shape description in the form of landmark coordinates, that can be rigorously tested with common-place multivariate statistical analyses (Slice 2007; Cooke & Terhune 2015).

Geometric morphometric methods are now widespread across a number of disciplines that look to quantify morphological variation, from palaeontology to engineering (Cooke & Terhune 2015). Of particular interest to this study is the ability to investigate how shape varies with environmental variables. Improving our capability to accurately describe and monitor shape change and integration is crucial to our understanding of how past morphology may influence future lines of adaptation.

Three subspecies of house mouse currently reside in the New Zealand archipelago: *Musculus musculus domesticus*, *M. m. castaneus*, and *M. m. musculus* (Searle et al. 2009a). The house mouse is a successful generalist, opportunist rodent that has sailed

with humans around the world for centuries, resulting in a global distribution (Searle et al. 2009b; King 2016; Ledevin et al. 2016). House mice were introduced to New Zealand quite recently with European settlement (King 2016).

This thesis aims to investigate how biotic and abiotic factors effect phenotypical variation in house mice across the New Zealand archipelago. Geometric morphometrics will enable the detection of subtle variation between mandibles of distinct mouse populations. Evolutionary responses to island ecology are often reflected in craniodental anatomy, usually associated with changes in diet following ecological release from competition and predation (Van der Greer et al. 2010). The body size of small mammals is also known to vary considerably on islands (Foster 1964; Adler & Levins 1994; Pergams & Ashley 2001; Millien & Damuth 2004; Lomolino 2005; McNab 2010; Lomolino et al. 2012; Martínková et al. 2013), and will be examined in this study. The following literature review introduces previous research on mandible shape and body size of small mammals, mice in particular, and will form the basis for the objectives and hypotheses to be explored by this thesis study.

1.1 The house mouse

The house mouse *Mus musculus* (L. 1758) is a prevalent pest species in New Zealand introduced by European seafarers in the early 19th century. The first published account of mice observed in New Zealand was recorded on Ruapuke Island, Foveaux Strait in 1824 (MacKay et al. 2013; King 2016). Prior to European activity, the

Pacific Rat, *Rattus exulans* (as known as Kiore), was the only introduced mammal in New Zealand, arriving with Polynesian colonists around 1280 AD (Wilmshurst et al. 2008).

1.1.1 *Origins and Genetics*

Evolution of the *Mus* species complex is thought to have originated during the mid-Miocene in a region covering Iran, Afghanistan, Pakistan, and northern India (Suzuki et al. 2015). Past studies indicate two ancient northern and southern *Mus* lineages are thought to have diverged from the ancestral species (Boursot et al. 1993; Suzuki et al. 2015). Dispersal of these phylogroups into Eurasia fostered the three main lineages now observed in New Zealand today. *M. m. domesticus* colonized western Europe and the Mediterranean basin (MacKay et al. 2013; McCormick et al. 2014), and has a long commensal relationship with humans since at least 8000BC (Searle et al. 2009b). In close proximity, *M. m. musculus* expanded into central and eastern Europe, and northern Asia (Searle et al. 2009a; MacKay et al. 2013; McCormick et al. 2014). By contrast, *M. m. castaneus* spread directly east into Southern Asia. All species have since formed multiple haplotypes (Searle et al. 2009a; Suzuki et al. 2015).

The most common mitochondrial D-loop haplotype sequenced in New Zealand is *M. m. domesticus*NZ.4, identical to that of mice originating from Western Europe (Searle et al. 2009a; McCormick et al. 2014; King et al. 2016). *M. m. domesticus* dominates the North Island and upper South Island. The majority of individuals collected in previous New Zealand studies represent this *domesticus*NZ.4 haplotype (Searle et al. 2009a; MacKay et al. 2013; McCormick et al. 2014; King et al. 2016).

When Searle et al. (2009a) sequenced for nuclear DNA markers they found no evidence of *M. m. castaneus* paternal input, yet the maternal mitochondrial *castaneus*NZ.1 haplotype was prevalent throughout the southern South Island. *Castaneus*NZ.1 was also sampled by King et al. (2016) in the Wellington region in conjunction with the only known *M. m. musculus* elements currently known in New Zealand, found inside the Zealandia (Karori) sanctuary. Again, *M. m. musculus* showed no evidence of paternal nDNA input, only maternal mitochondrial elements. *M. m. domesticus* genomic elements were present in all mouse samples, indicating that where *musculus* and *castaneus* DNA are found the respective individuals are hybrids. As there is no evidence of *castaneus* or *musculus* nDNA, King et al. (2016) suggest a selection bias against *castaneus* and *musculus* males, whereby only the female mitochondrial genes are inherited.

In contrast to the North and South Islands, New Zealand's smaller outlying islands support less common haplotypes, and likely represent separate colonisation events (Searle et al. 2009a; King 2016; Bradley et al. 2017). Ledevin et al. (2016) note that founder and genetic effects are important influences in the evolution of island and invasive species, both of which apply to house mice in New Zealand.

1.1.2 *Diet and Habitat*

The invasion of house mice in the New Zealand archipelago has resulted in significant damage to endemic flora and fauna, and continues to threaten endangered wildlife. The global colonisation success of house mice is fuelled primarily by a flexible, omnivorous diet, and a highly commensal relationship with humans (Ruscoe & Murphy 2005; King 2016). House mice in New Zealand feed predominantly on

small invertebrates such as caterpillars, spiders, and weta, but also seeds, lizards, and small avian chicks and eggs (Ruscoe & Murphy 2005; Angel et al. 2009; Wilson & Lee 2010; Goldwater et al. 2012; Russell 2012; Bridgman et al. 2013; Cuthbert et al. 2013; O'Donnell et al. 2017; Samaniego-Herrera et al. 2017). Several studies suggest larvae and spiders are the preferred food items in a New Zealand house mouse diet, but that seeds are also an important portion of diet, especially during summer months (Copson 1986; Marris 2000; Miller & Webb 2001; Le Roux et al. 2002; Smith et al. 2002; Fitzgerald et al. 2004; Angel et al. 2009; Wilson & Lee 2010; Shiels et al. 2013). Yet on Antipodes I. and L'île aux Cochons, mice were suggested to feed more on plant material than invertebrates (Derenne & Mougin 1976; Berry et al. 1978).

Mice are widespread across the North and South Islands, occupying a variety of habitats from tussock sand dunes to alpine forests (Ruscoe et al. 2004; O'Donnell et al. 2017). Dense ground cover tends to be the preferred habitat choice, offering access to both food and safety (King et al. 1996; Ruscoe & Murphy 2005; O'Donnell et al. 2017). Additionally, several studies have shown house mouse populations to irrupt in beech and podocarp forests following a particularly heavy seed year that usually recurs every 3-5 years, commonly termed masting (Norton & Kelly 1988; Murphy 1992; Fitzgerald et al. 1996; Choquenot & Ruscoe 2000; Fitzgerald et al. 2004; Ruscoe et al. 2004; Ruscoe & Murphy 2005; O'Donnell et al. 2017). Beech seed mast events follow a particularly hot summer weather that encourages heavy flowering and seeding (Fitzgerald et al. 1996; Ruscoe et al. 2004). Conversely, Rimu (*Podocarpus*) requires a cooler summer to enable a seed mast event (Ruscoe et al. 2004). The seeds and flowers ultimately drop from the trees and enrich the forest litter. This enrichment enables greater recruitment of invertebrates, especially caterpillars,

resulting in a chain of resource pulses (King 1983; Fitzgerald et al. 1996; Wilson & Lee 2010; O'Donnell et al. 2017). Increased house mouse numbers coincide with greater invertebrate density that follows heavy seedfall (King 1983; Fitzgerald et al. 1996; Wilson & Lee 2010; O'Donnell et al. 2017). House mice in beech forests have been shown to feed predominantly on caterpillars, while also supplementing their diet with nutritious seeds (Murphy 1992; Fitzgerald et al. 1996). Abundant food resources enable extended winter breeding for mice, with populations rapidly increasing in the autumn and winter months after a summer beech mast (King 1983; Fitzgerald et al. 1996; Choquenot & Ruscoe 2000; Ruscoe et al. 2004; O'Donnell et al. 2017). Ruscoe et al. (2004) also found house mice to feed on nitrogenous Rimu seeds during a heavy Rimu mast event.

1.1.3 Competition and Predation

M. musculus has a long history of competition and co-existence with *R. rattus* (Yom-Tov et al. 1999; Caut et al. 2007; Hancock 2008; Bridgman et al. 2013), a related commensal rodent also carried around the world by seafaring voyagers. Both species are generalists with significant dietary and niche overlap, leading to substantial interspecific competition (Innes et al. 1995; Yom-Tov et al. 1999; Ruscoe 2001; Ruscoe & Murphy 2005; Hancock 2008; Bridgman et al. 2013). A previous study by Goldwater et al. (2012) suggested competition from ship rats was the primary factor controlling house mouse populations, in contrast to predation from stoats which had little effect.

Copson (1986) investigated the diets of *M. musculus* and *R. rattus* on sub-Antarctic Macquarie Island. He found mostly diurnal invertebrates in mouse stomachs, and a

greater percentage of plant material in the rats', indicating segregation of food niches and foraging times. In the experimental absence of rats, Hancock (2008) observed that mice foraged more at night when, previously, rat activity levels were highest. The scent of rats also modified *M. musculus* activity and habitat use. The implication is that the removal of rats would benefit mice by increasing the range of habitats available to them for foraging, increasing the time available for activity outside their refuges, and reducing the energy spent on antipredator behaviour (Case 1978; Hancock 2008).

Many previous studies (King et al. 1996; Yom-Tov et al. 1999; Caut et al. 2007; Speedy et al. 2007; Ruscoe et al. 2011; Goldwater et al. 2012) have also observed higher detection rates for mice in the absence of ship rats, so Bridgman et al. (2013) inferred that interactions with rats must limit the activity of mice when rats are present, constricting the realised niche of mice sympatric with rats. On several isolated islands in the New Zealand archipelago house mice were the only invasive rodent, and thus may have experienced ecological release and subsequent niche expansion in the absence of rats.

1.1.4 Arriving in New Zealand

Mice arriving in 19th century New Zealand would have encountered novel environmental conditions that were associated with strong selective pressures, likely prompting adaptive radiation (Michaux et al. 2007; Ledevin et al. 2016). Colonists needed to consume novel food items in order to survive that may have prompted changes in the jaw to facilitate altered mandible function (Michaux et al. 2007; Renaud et al. 2015; Ledevin et al. 2016). The mandible is a very malleable bone that

is responsive to changes in the strength and activity of the muscles pulling on the jaw (Satoh 1997; Michaux et al. 2007; Renaud & Auffray 2010; Baverstock et al. 2013; Anderson et al. 2014). This flexibility can quickly compensate for changes in diet that require altered bite force, making the mandible one of the most utilised materials for detecting adaptive changes, especially in the field of geometric morphometrics (Badyaev & Foresman 2000; Klingenberg & Leamy 2001; Klingenberg et al. 2003; Renaud 2005; Michaux et al. 2007; Renaud & Michaux 2007; Zelditch et al. 2008; Mikula et al. 2010; Renaud & Auffray 2010; Renaud et al. 2010; Boell & Tautz 2011; Klingenberg & Navarro 2012; Renaud et al. 2012; Siah sarvie et al. 2012; Boell 2013; Renaud et al. 2013; Swiderski & Zelditch 2013; Anderson et al. 2014; Pallares et al. 2014; Álvarez et al. 2015; Anthwal et al. 2015; Doudna & Danielson 2015; Renaud et al. 2015).

1.2 The mandible

Distinct components of the mandible include: the ramus, comprised of the coronoid process, angular process, and condyle process, and the alveolar region (Hiemae 1971a; Satoh 1997; Michaux et al. 2007; Renaud & Auffray 2010; Klingenberg & Navarro 2012; Baverstock et al. 2013; Renaud et al. 2015) (Figure I-A).

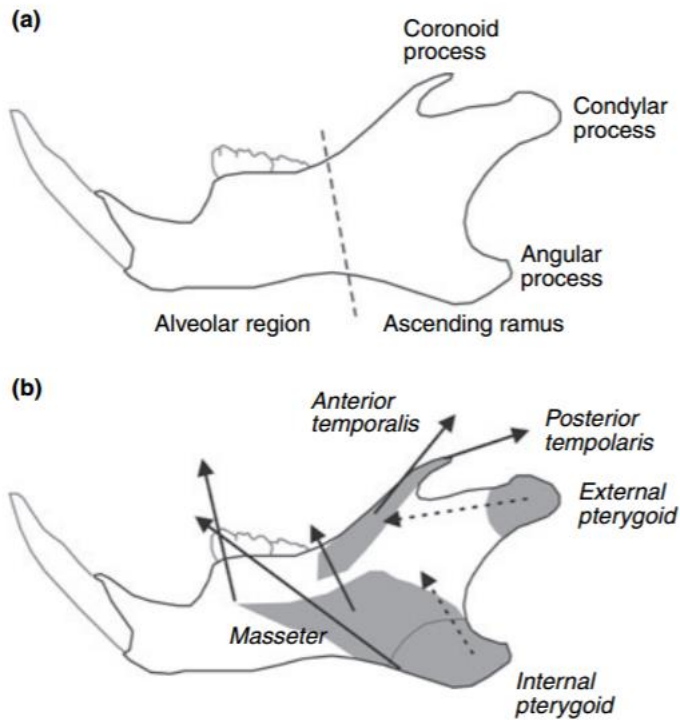


Fig. 1. Mandible of a murine rodent (*Apodemus*) in lateral view. (a) Main anatomical parts. (b) Attachment area and approximate line of action of the main masticatory muscles (after Satoh 1997)

Figure I-A Distinct components of the house mouse mandible. Image retrieved from Michaux et al. (2007).

The ability of the mandible to produce gnawing and chewing actions rely on the muscles that facilitate these movements, and the associated bone regions to which they attach (Hiimae 1971a; Klingenberg & Navarro 2012; Baverstock et al. 2013). The condyle process facilitates interaction of the mandible bone joint with the cranium, whereas the coronoid and angular processes are the respective attachment sites for temporalis and masseter muscles (Hiimae 1971a; Klingenberg & Navarro 2012; Baverstock et al. 2013). Food is broken down in the mouth through grinding and shearing motions i.e. mastication (Hiimae 1971a; Crompton & Parker 1978). The masseter muscle facilitates molar mastication activity, enabling the mouse to grind up tough plant material, whereas the temporalis muscle enables occlusion of the

incisor teeth for gnawing and prey catching activities (Hiimae 1971a, b; Crompton & Parker 1978; Satoh 1997; Michaux et al. 2007; Baverstock et al. 2013; Anderson et al. 2014; Renaud et al. 2015). The mandible effectively acts as a lever (Crompton & Parker 1978; Thomason 1991); force applied to the ramus region enables the teeth to apply pressure to food in order to break it down for digestion. Michaux et al. (2007) note that mandible shape is strongly related to the insertion and activity of the masticatory muscles (Satoh 1997).

1.2.1 The Influence of Hard and Soft foods

Mandible shape is also very sensitive to changes in the relative 'hardness' of food items included in the diet (Renaud & Auffray 2010; Anderson et al. 2014; Renaud et al. 2015). A diet characterised by greater proportions of resistant foods will require a larger mechanical force to process and breakdown compared with softer food items (Michaux et al. 2007; Anderson et al. 2014; Renaud et al. 2015). Michaux et al. (2007) found granivorous rodents displayed mandibles with smaller coronoid processes and extended angular processes. On the other hand, insectivorous rodents showed more developed coronoid processes that facilitate insertion of strong temporalis muscles, providing backwards movement of the mandible to create a grasping action.

Anderson et al. (2014) observed shape changes in the alveolar and ramus regions of mouse mandibles fed either soft or hard food diets over a period of six months that support previous suggestions by Michaux et al. (2007). Mice fed hard foods developed larger coronoid and angular processes, accompanied by a ventral expansion of the incisor and molar regions. Hard food was also associated with

greater integration of the molar region and angular process, whilst those fed soft food only showed weak integration of incisor and condyle areas. Increased integration of the molar and angular modules allows greater bite force to be applied to mechanically resistant foods. Essentially, a shorter, broader mandible was able to apply greater mechanical force than a slimmer, elongated one by increasing the strength of force exerted by the masseter muscle (Sato 1997; Michaux et al. 2007).

1.2.2 Biomechanical Advantage

Biomechanical advantage is the ability and efficiency of the mandible to create bite force (Hiimae 1971b; Anderson et al. 2014; Renaud et al. 2015), and can be quantified by measuring the ratio of the inlever, where mechanical force is created, to the outlever where the force is actioned (Hiimae 1971b; Renaud et al. 2015) (see Figure 1a). Renaud et al. (2015) describe the inlever in house mice as the distance between the edge of the condyle process to the muscle attachment points on the coronoid and angular processes, and the outlever as the distance from the condyle process to the incisor and second molar teeth. The ratio of these measurements gives an estimate for biomechanical advantage i.e. the effectiveness of the mandible to produce bite force.

Renaud et al. (2015) found house mice inhabiting sub-Antarctic Guillou Island, Kerguelen Archipelago, had higher mechanical advantage associated with temporalis function compared to continental mice, but lower masseter function advantage, using geometric morphometric methods. The authors suggested this functional difference was a result of dietary niche shift towards more invertebrate prey, supporting

functional changes observed in mouse mandibles fed soft food items by Anderson et al. (2014).

1.3 Morphometrics

Morphometrics is the study of anatomical shape variation, defined as “all the geometric features of an object excluding size, position and orientation” (Klingenberg 2016), and how this change relates to other variables (Bookstein 1991; Dryden & Mardia 1998; Adams et al. 2004; Slice 2007). Shape is often measured as the outline, length of an object, or an arrangement of morphological landmarks (Klingenberg 2010, 2016). Traditional morphometrics were originally restricted to testing a collection of angles and distances with multivariate statistical techniques, but with the evolution of technology shape can now be quantified mathematically using computer software programs (Bookstein 1991; Rohlf & Marcus 1993; Dryden & Mardia 1998; Adams et al. 2004; Slice 2007).

1.3.1 A Summary of Modern Techniques

Modern geometric morphometric techniques use Cartesian coordinate based landmark software to capture shape information from 2D and 3D images (Rohlf & Slice 1990; Klingenberg 2016). Size, position, and orientation variables are removed from the landmark arrangements to obtain exclusive shape information using a technique called Procrustes superimposition (Rohlf & Slice 1990; Dryden & Mardia 1998; Slice 2007).

Klingenberg (2016) offers the following comprehensible explanation for how Procrustes superimposition measures shape difference:

Centroid size is the measure of size used almost universally in geometric morphometrics: it is the square root of the sum of squared distances of all the landmarks of an object from their centroid (center of gravity, whose location is obtained by averaging the x and y coordinates of all landmarks).

To quantify the shape difference between two landmark configurations, Procrustes superimposition can be used: configurations are scaled to have centroid size 1.0 and are translated and rotated so that the sum of squared distances between corresponding landmarks is minimal (this involves a translation so that both configurations share the same centroid). The square root of the sum of squared distances between corresponding landmarks is called Procrustes distance: it is the discrepancy between the landmark configurations that cannot be removed by scaling, translation, or rotation and is therefore useful as a measure of shape difference. Kendall's shape space is a representation of all possible shapes with a given number of landmarks and a given dimensionality (i.e., coordinates measured in two or three dimensions), so that the distance between the points representing any two shapes corresponds to the Procrustes distance between the respective shapes (Kendall 1984; Small 1996; Dryden & Mardia 1998; Kendall et al. 1999).

A range of multivariate analyses are used to visualise this shape change. Principal components analysis (PCA) is useful for visualising main variation patterns between individual samples. PCA reduces the dimensionality of the data set by "performing a

singular value decomposition of the variance-covariance matrix and extracting the resulting eigenvectors, which then form the principal components” (Slice 2007). Each principal component represents an axis that describes a successional percentage of total variance in shape.

On the other hand, canonical variate analysis (CVA) can be used to investigate the most effective separation of shapes with three or more predefined groups. When comparing only two groups, discriminant function analysis (DFA) can be used in place of CVA. Similar to PCA, CVA builds a new coordinate system whereby specific axes are found that describe the greatest discrimination between group means (Slice 2007). Distances in the canonical variate space are not analogous to those produced in the original Procrustes coordinate space because CVA rescales its axes using within-group variation patterns (Zelditch et al. 2012). For this reason, results must be interpreted carefully.

Partial least squares analysis (PLS) has often been used to investigate covariation of shape variables with biotic and abiotic variables (Monteiro 1999; Zelditch et al. 2012). PLS also reduces the original shape coordinates onto a set of new axes that explain covariation between sets of variables in successional order (Zelditch et al. 2012).

1.3.2 The Influence of Allometry

However, none of these analyses account for allometric variation. Allometry refers to the variation of morphological traits with change in body size (Gould 1966; Mitteroecker and Gunz 2009; Zelditch et al. 2012; Klingenberg 2016). The integration of size and shape can impose considerable constraints on the direction of

shape evolution (Klingenberg 2016). Although size and shape are both important traits used to describe phenotypic variation, it is often useful to study each separately. The study of allometry in morphometric fields is widely debated, but can be pooled under two core schools of thought.

The Huxley-Jolicoeur school does not distinguish size from shape, and rather emphasizes the covariation among different traits that arise from variation in size. In other words, size is assumed to be the greatest contributor to shape variation (Huxley 1924; Klingenberg 2016). By contrast, the Gould-Mosimann school views allometry as the covariation of size and shape, which are considered to be distinct variables, and can therefore be tested for statistical association (Mosimann 1970; Klingenberg 2016). The Gould-Mosimann school of thought forms the basis of the geometric morphometric software used throughout this thesis investigation (Klingenberg 2011).

Multivariate regression can be used to investigate the covariance of shape and size by regressing Procrustes coordinates onto the logarithm of centroid size (Monteiro 1999; Mitteroecker & Gunz 2009). Multivariate regression separates the shape variation into predicted and residual components. A line of best fit is fitted to the predicted data points that represent the covariation of shape with size. Residual components are deviations from this line of prediction that represent non-allometric shape variation. To investigate non-allometric shape variation, the residual components can be used in place of Procrustes coordinates for further statistical analyses (Klingenberg 2010).

All these analyses produce warped outline diagrams that depict the directional shape change along each axis. A warped outline diagram is a collection of interconnecting

lines between selected landmarks that can be warped to visualise shape variation (Slice 2007).

Zelditch et al. (2012) provide a more detailed explanation of these methods in their book *Geometric morphometrics for biologists: a primer*. For useful definitions of the morphometric terms touched on in this literature review see Slice (2007).

1.4 Body size

The body size of small mammals is known to vary significantly with geography and associated environmental variables. Many studies have attempted to describe this global pattern in body size variation by developing ecological ‘rules’.

1.4.1 Bergmann’s Rule

Bergmann’s rule infers that mammals attain larger body size with increasing latitude associated with cooler climates (Mayr 1956; McNab 2010). Larger animals would have an advantage over smaller animals in cooler climates through greater heat retention (higher volume to surface area ratio), greater energy stores, and an increased capability to exploit a wider range of food resources (Meiri & Dayan 2003; Watt et al. 2010; Lomolino et al. 2012; Alhajeri & Steppan 2016). Many researchers argue that latitude is a proxy for temperature, rainfall, and primary production (Boyce 1978; Burnett 1983; Rodríguez et al. 2006; Yom-Tov & Geffen 2006; Meiri et al. 2007; McNab 2010; Huston & Wolverton 2011; Alhajeri & Steppan 2016). These variables inevitably impact the availability of resources, thereby influencing the body size

attainable by small mammals at any given latitude (McNab 2010; Huston & Wolverson 2011).

Primary productivity is the creation of organic plant material through photosynthesis. Sunlight, temperature, and precipitation are the main abiotic variables that influence localised productivity (Huston & Wolverson 2011). McNab (2010) and Huston & Wolverson (2011) suggest geographical variation in net primary productivity (NPP) influences the development of body size through the availability of food. Huston & Wolverson (2011) argue that body size increases in regions where net primary production (NPP) is highest during essential growing and reproductive periods, termed ecologically and evolutionarily relevant NPP (eNPP) i.e. food availability. They propose that “the significance of the eNPP concept is that it specifically addresses the NPP that is available to meet the energetic and nutritional demands of animals (and plants) during that time when they are reproducing and growing”.

1.4.2 The Island Rule

Bergmann’s rule is often associated with another ecological trend in body size called the island rule or syndrome (Foster 1964; Adler & Levins 1994; Pergams & Ashley 2001; Millien & Damuth 2004; Lomolino 2005; McNab 2010; Lomolino et al. 2012; Martínková et al. 2013). Body size has been observed to vary dramatically on islands, as unique insular environments foster rapid and substantial evolutionary change (Berry 1964; Lomolino 1985; Adler & Levins 1994; Yom-Tov et al. 1999; Millien & Damuth 2004; Lomolino 2005; White & Searle 2007; Lomolino et al. 2012; Samaniego-Herrera et al. 2017). Founder and genetic drift events often reduce the genetic diversity of colonising populations, significantly altering allelic frequencies

(Barton & Mallet 1996; Millien 2006; Renaud & Auffray 2010; Millien 2011; Martínková et al. 2013; Cucchi et al. 2014; Gray et al. 2015). Gene flow is also likely to be reduced on isolated islands, if present at all, enabling rapid, directional selection (Pergams & Ashley 2001; Martínková et al. 2013).

The strength of this effect is often attributed to an inverse relationship with island area, and a positive relationship with isolation (Pergams & Ashley 2001; Lomolino 2005; Millien 2011; Lomolino et al. 2012). Lomolino et al (2012) found that the greatest gigantism observed in small mammalian invaders was significantly correlated with smaller, more remote islands lacking other mammalian competitors.

Biodiversity and ecological complexity differ between islands of varying size. Food scarcity is the primary selection pressure on smaller islands, while larger islands can support more species and habitat diversity, and consequently more competition and predation (Adler & Levins 1994; Pergams & Ashley 2001; Lomolino 2005; Millien 2006; Lomolino et al. 2012). On smaller islands, the absence of usual competition and predation pressures often allows small rodent populations to expand their previous realised niche, exploiting the sudden increase in available resources.

Lomolino et al. (2012) summarise by stating “the body size evolution of mammals of isolated islands should be influenced both by ecological character displacement (from conspecifics and from other resident vertebrates, namely birds and reptiles, which tend to be small) and by character release (from mammalian competitors and predators)” (Simberloff et al. 2000; Grant & Grant 2006; Meiri 2011).

Millien (2011) observed a significant negative relationship between island size and the rate of evolutionary change. Smaller islands were observed to foster both faster

and greater change, suggesting species colonising the smallest islands will experience faster and more substantial evolution than those on larger islands.

Past studies on mouse populations show that 100 years is enough time for phenotypic changes to develop, especially in the face of substantial habitat differences and genetic drift often encountered on islands (Berry 1964; Millien 2006; Michaux et al. 2007; Renaud & Auffray 2010; Millien 2011; Renaud et al. 2013; Doudna & Danielson 2015; Renaud et al. 2015).

1.5 Objectives

Previous studies on house mice in New Zealand have focussed on their ecology and, to some extent, dietary habits, especially in relation to beech mast cycles. Despite being prevalent throughout the New Zealand archipelago, there have been no intraspecific comparisons of variation in the house mouse mandible, and how potential shape variation relates to environmental variables. Variation in mouse body size between New Zealand populations has also never been analysed in the context of the island rule. Consequently, the material collected for this thesis investigation invited answers to the following questions.

1. Does mandible shape and body size vary significantly between house mouse populations inhabiting different forest habitats of the New Zealand North and South Islands? If so, what are the covariates available that explain a significant proportion of this observed variation?

2. Does mandible shape and body size of house mice vary significantly between smaller, offshore New Zealand islands that differ significantly in ecology and habitat to the North and South Islands? If so, what are the covariates available that explain a significant proportion of this observed variation?
3. Does mouse mandible shape and body size vary significantly between the larger and smaller islands of New Zealand i.e. comparing forest and offshore island populations?

This thesis investigates the variation in house mouse mandible shape between different types of habitat in New Zealand to understand how shape variation correlates with specific environmental variables.

My first research chapter (Chapter III) explores the mandible shapes and body size of house mice in various forest habitats around New Zealand which differ in the types of food resources and competition or predation experienced by mouse inhabitants. The forests in this particular study include: Eglinton Valley, Hollyford Valley, Craigieburn Forest Park, Zealandia Wildlife Sanctuary, and Pureora Forest.

Chapter IV focuses on mandible and body size variation between mouse populations on offshore islands. Major phenotypic changes are regularly documented on islands, and often proceed at an accelerated rate compared to mainland populations. New Zealand's offshore islands represent important habitat for endemic flora and fauna that are threatened by local mice inhabitants. The variation in island habitats and their degree of isolation creates a unique opportunity to study the adaptation of invasive mice to local conditions. The islands included in this study are: Enderby I., Auckland I., Antipodes I., Ruapuke I., Waikawa I., and Chatham I. House mice have been

inhabiting each of these islands for at least 100 years, and on at least Antipodes and Ruapuke Islands represent single colonization events. The isolation of the Subantarctic (Antipodes I., Auckland I., and Enderby I.) and Chatham Islands renders multiple invasion events unlikely, and has also reduced the possibility of sustained gene flow between insular mouse populations.

Furthermore, the inclusion of house mouse mandibles from Sydney, Australia, enable the comparison of island and continental populations. Insular animals have been shown to diverge rapidly and substantially from their continental counterparts, especially with dietary niche change. Sydney was an important shipping port during the colonization of mice in New Zealand, and may represent an ancestral population for northern New Zealand *domesticus* mice. This statement invites the following question:

1. Does mandible shape of house mice vary significantly between islands (New Zealand) and continents?

This query is addressed in Chapter V, along with a comparison combining the forest and island material from Chapters III and IV.

Traditional morphometric techniques often lack the ability to detect subtle variation in mandible shape among populations. As such, geometric morphometrics is used to quantify small but significant variations in mandible function. Physical body measurements were also available for the mouse samples included in this study.

These data were compared between sites in addition to exploring variation in mandible shape in order to assess any significant differences in body weight or length between study sites.

In the absence of ship rats, several New Zealand-based studies have shown the mean body weight and density of wild mice to increase significantly post-eradication, inferring a widening of food niche breadth to include resources that had previously been controlled by rats. Mice inhabiting Zealandia Wildlife Sanctuary, Antipodes I., Auckland I., Enderby I., Ruapuke I., and Waikawa I. are free from the constraints of predation and competition imposed by other invasive species such as stoats and rats. This ecological release is likely to introduce variation in both mandible and body morphology that reflect a broadening of dietary niche with increased foraging hours.

1.6 References

- Adams DC, Rohlf JF, Slice DE 2004. Geometric morphometrics: ten years of progress following the "revolution". *Italian Journal of Zoology* 71(1): 5-16.
- Adler GH, Levins R 1994. The island syndrome in rodent populations. *The Quarterly Review of Biology* 69(4): 473-90.
- Alhajeri BH, Steppan SJ 2016. Association between climate and body size in rodents: A phylogenetic test of Bergmann's rule. *Mammalian Biology - Zeitschrift für Säugetierkunde* 81(2): 219-225.
- Álvarez A, Perez SI, Verzi DH 2015. The role of evolutionary integration in the morphological evolution of the skull of caviomorph rodents (Rodentia: Hystricomorpha). *Evolutionary Biology* 42(3): 312-327.
- Anderson P, Renaud S, Rayfield E 2014. Adaptive plasticity in the mouse mandible. *BioMed Central Evolutionary Biology* 14(85).
- Angel A, Wanless R, Cooper J 2009. Review of impacts of the introduced house mouse on islands in the Southern Ocean: are mice equivalent to rats? *Biological Invasions* 11(7): 1743-1754.
- Anthwal N, Peters H, Tucker AS 2015. Species-specific modifications of mandible shape reveal independent mechanisms for growth and initiation of the coronoid. *Evodevo* 6(1): 35.
- Badyaev AV, Foresman KR 2000. Extreme environmental change and evolution: Stress-induced morphological variation is strongly concordant with patterns of evolutionary divergence in shrew mandibles. *Proceedings: Biological Sciences* 267(1441): 371-377.

- Barton NH, Mallet J 1996. Natural selection and random genetic drift as causes of evolution on islands [and discussion]. *Philosophical Transactions: Biological Sciences* 351(1341): 785-795.
- Baverstock H, Jeffery NS, Cobb SN 2013. The morphology of the mouse masticatory musculature. *Journal of Anatomy* 223(1): 46-60.
- Berry RJ 1964. The evolution of an island population of the house mouse. *Evolution* 18(3): 468-483.
- Berry RJ, Peters J, van Aarde RJ 1978. Sub-antarctic house mice : colonization, survival and selection *Journal of Zoology* 184: 127-141.
- Boell L 2013. Lines of least resistance and genetic architecture of house mouse (*Mus musculus*) mandible shape. *Evolution & Development* 15(3): 197-204.
- Boell L, Tautz D 2011. Micro-evolutionary divergence patterns of mandible shapes in wild house mouse (*Mus musculus*) populations. *BioMed Central Evolutionary Biology* 11: 306.
- Bookstein FL 1986. Size and shape spaces for landmark data in two dimensions. *Statistical Science* 1(2): 181-222.
- Bookstein FL 1991. *Morphometric tools for landmark data: Geometry and Biology*. Cambridge, UK, Cambridge University Press.
- Boursot P, Auffray JC, Brittondavidian J, Bonhomme F 1993. The evolution of house mice. *Annual Review of Ecology and Systematics* 24: 119-152.
- Boyce MS 1978. Climatic variability and body size variation in the muskrats (*Ondatra zibethicus*) of North America. *Oecologia* 36(1): 1-19.

- Bradley E, Trewick SA, Morgan-Richards M 2017. Genetic distinctiveness of the Waikawa Island mouse population indicates low rate of dispersal from mainland New Zealand. *New Zealand Journal of Ecology* 41(2).
- Bridgman LJ, Innes J, Gillies C, Fitzgerald NB, Miller S, King CM 2013. Do ship rats display predatory behaviour towards house mice? *Animal Behaviour* 86(2): 257-268.
- Burnett CD 1983. Geographic and climatic correlates of morphological variation in *Eptesicus fuscus*. *Journal of Mammalogy* 64(3): 437-444.
- Caut S, Casanovas JG, Virgos E, Lozano J, Witmer GW, Courchamp F 2007. Rats dying for mice: Modelling the competitor release effect. *Austral Ecology* 32(8): 858-868.
- Choquenot D, Ruscoe WA 2000. Mouse population eruptions in New Zealand forests: the role of population density and seedfall. *Journal of Animal Ecology* 69(6): 1058-1070.
- Cooke SB, Terhune CE 2015. Form, function, and geometric morphometrics. *The Anatomical Record* 298(1): 5-28.
- Copson GR 1986. The diet of the introduced rodents *Mus musculus* and *Rattus rattus* on sub-Antarctic Macquarie Island. *Wildlife Research* 13(3): 441-445.
- Crompton A, Parker P 1978. Evolution of the mammalian masticatory apparatus: the fossil record shows how mammals evolved both complex chewing mechanisms and an effective middle ear, two structures that distinguish them from reptiles. *American Scientist* 66(2): 192-201.
- Cucchi T, Barnett R, Martínková N, Renaud S, Renvoisé E, Evin A, Sheridan A, Mainland I, Wickham-Jones C, Tougaard C 2014. The changing pace of insular

- life: 5000 years of microevolution in the Orkney vole (*Microtus arvalis orcadensis*). *Evolution* 68(10): 2804-2820.
- Cuthbert RJ, Louw H, Lurling J, Parker G, Rexer-Huber K, Sommer E, Visser P, Ryan PG 2013. Low burrow occupancy and breeding success of burrowing petrels at Gough Island: a consequence of mouse predation. *Bird Conservation International* 23(2): 113-124.
- Derenne P, Mougin JL 1976. Données écologiques sur les mammifères introduits de l'île aux Cochons, Archipel Crozet (46°06'S, 50°14'E). *Mammalia* 40: 21-53.
- Doudna JW, Danielson BJ 2015. Rapid morphological change in the masticatory structures of an important ecosystem service provider. *Public Library of Science (PLoS) ONE* 10(6): e0127218.
- Dryden IL, Mardia KV 1998. *Statistical shape analysis*. Chichester; New York, John Wiley & Sons.
- Fitzgerald BM, Efford MG, Karl BJ 2004. Breeding of house mice and the mast seeding of southern beeches in the Orongorongo Valley, New Zealand. *New Zealand Journal of Zoology* 31(2): 167-184.
- Fitzgerald BM, Daniel MJ, Fitzgerald AE, Karl BJ, Meads MJ, Notman PR 1996. Factors affecting the numbers of house mice (*Mus musculus*) in hard beech (*Nothofagus truncata*) forest. *Journal of the Royal Society of New Zealand* 26(2): 237-249.
- Foster JB 1964. Evolution of mammals on islands. *Nature* 202(4929): 234-235.
- Goldwater N, Perry GLW, Clout MN 2012. Responses of house mice to the removal of mammalian predators and competitors. *Austral Ecology* 37(8): 971-979.

- Gould SJ 1966. Allometry and size in ontogeny and phylogeny. *Biological Reviews* 41(4): 587-638.
- Grant PR, Grant BR 2006. Evolution of character displacement in Darwin's finches. *Science* 313(5784): 224-226.
- Gray MM, Parmenter MD, Hogan CA, Ford I, Cuthbert RJ, Ryan PG, Broman KW, Payseur BA 2015. Genetics of rapid and extreme size evolution in island mice. *Genetics* 201(1): 213-228.
- Hancock B 2008. The influence of ship rats (*Rattus rattus*) on the habitat preferences of the house mouse (*Mus musculus*). Unpublished Masters thesis, Victoria University of Wellington.
- Hiiemae K 1971a. The structure and function of the jaw muscles in the rat (*Rattus norvegicus* L.) I. Their anatomy and internal architecture. *Zoological Journal of the Linnean Society* 50: 75-99.
- Hiiemae K 1971b. The structure and function of the jaw muscles in the rat (*Rattus norvegicus* L.): III. The mechanics of the muscles. *Zoological Journal of the Linnean Society* 50(1): 111-132.
- Huston MA, Wolverton S 2011. Regulation of animal size by eNPP, Bergmann's rule, and related phenomena. *Ecological Monographs* 81(3): 349-405.
- Huxley JS 1924. Constant differential growth-ratios and their significance. *Nature* 114(2877): 895-896.
- Innes J, Warburton B, Williams D, Speed H, Bradfield P 1995. Large-scale poisoning of ship rats (*Rattus-rattus*) in indigenous forests of the North-Island, New-Zealand. *New Zealand Journal of Ecology* 19(1): 5-17.

- Kendall DG 1984. Shape manifolds, procrustean metrics, and complex projective spaces. *Bulletin of the London Mathematical Society* 16(2): 81-121.
- Kendall DG 1989. A survey of the statistical theory of shape. *Statistical Science* 4(2): 87-99.
- King CM 1983. The relationships between beech (*Nothofagus* sp.) seedfall and populations of mice (*Mus musculus*), and the demographic and dietary responses of stoats (*Mustela erminea*), in three New Zealand forests. *Journal of Animal Ecology* 52(1): 141-166.
- King CM 2016. How genetics, history and geography limit potential explanations of invasions by house mice *Mus musculus* in New Zealand. *Biological Invasions* 18(6): 1533-1550.
- King CM, Innes JG, Flux M, Kimberley MO, Leathwick JR, Williams DS 1996. Distribution and abundance of small mammals in relation to habitat in Pureora Forest park. *New Zealand Journal of Ecology* 20(2): 214-240.
- King CM, Alexander A, Chubb T, Cursons R, MacKay J, McCormick H, Murphy E, Veale A, Zhang H 2016. What can the geographic distribution of mtDNA haplotypes tell us about the invasion of New Zealand by house mice *Mus musculus*? *Biological Invasions* 18(6): 1551-1565.
- Klingenberg CP 2010. Evolution and development of shape: integrating quantitative approaches. *Nature Reviews Genetics* 11(9): 623-635.
- Klingenberg CP 2011. MorphoJ: an integrated software package for geometric morphometrics. *Molecular Ecology Resources* 11: 353-357.
- Klingenberg CP 2016. Size, shape, and form: concepts of allometry in geometric morphometrics. *Development Genes and Evolution* 226(3): 113-137.

- Klingenberg CP, Leamy LJ 2001. Quantitative genetics of geometric shape in the mouse mandible. *Evolution* 55(11): 2342-2352.
- Klingenberg CP, Navarro N 2012. Development of the mouse mandible: a model system for complex morphological structures. In: Macholan M, Baird SJE, Munclinger P, Pialek J ed. *Evolution of the House Mouse*. Cambridge, England, Cambridge University Press.
- Klingenberg CP, Mebus K, Auffray JC 2003. Developmental integration in a complex morphological structure: how distinct are the modules in the mouse mandible? *Evolution & Development* 5(5): 522-531.
- Le Roux V, Chapuis JL, Frenot Y, Vernon P 2002. Diet of the house mouse (*Mus musculus*) on Guillou Island, Kerguelen archipelago, Subantarctic. *Polar Biology* 25: 49-57.
- Ledevin R, Chevret P, Ganem G, Britton-Davidian J, Hardouin EA, Chapuis J-L, Pisanu B, da Luz Mathias M, Schlager S, Auffray J-C and others 2016. Phylogeny and adaptation shape the teeth of insular mice. *Proceedings of the Royal Society B: Biological Sciences* 283(1824).
- Lomolino MV 1985. Body size of mammals on islands: The island rule reexamined. *The American Naturalist* 125: 310-316.
- Lomolino MV 2005. Body size evolution in insular vertebrates: generality of the island rule. *Journal of Biogeography* 32: 1683-1699.
- Lomolino MV, Sax DF, Palombo MR, van der Geer AA 2012. Of mice and mammoths: evaluations of causal explanations for body size evolution in insular mammals. *Journal of Biogeography* 39(5): 842-854.

- MacKay JWB, Alexander A, Hauber ME, Murphy EC, Clout MN 2013. Does genetic variation among invasive house mice in New Zealand affect eradication success? *New Zealand Journal of Ecology* 37(1): 18-25.
- Marris JWM 2000. The beetle (Coleoptera) fauna of the Antipodes Islands, with comments on the impact of mice; and an annotated checklist of the insect and arachnid fauna. *Journal of the Royal Society of New Zealand* 30(2): 169-195.
- Martínková N, Barnett R, Cucchi T, Struchen R, Pascal M, Fischer MC, Higham T, Brace S, Ho SY 2013. Divergent evolutionary processes associated with colonization of offshore islands. *Molecular ecology* 22(20): 5205-5220.
- Mayr E 1956. Geographical character gradients and climatic adaptation. *Evolution* 10(1): 105-108.
- McCormick H, Cursons R, Wilkins RJ, King CM 2014. Location of a contact zone between *Mus musculus domesticus* and *M. m. domesticus* with *M. m. castaneus* mtDNA in southern New Zealand. *Mammalian Biology* 79(5): 297-305.
- McNab BK 2010. Geographic and temporal correlations of mammalian size reconsidered: a resource rule. *Oecologia* 164: 13-23.
- Meiri S 2011. Bergmann's Rule - what's in a name? *Global Ecology & Biogeography* 20(1): 203-207.
- Meiri S, Dayan T 2003. On the validity of Bergmann's rule. *Journal of Biogeography* 30(3): 331-351.
- Meiri S, Yom-Tov Y, Geffen E 2007. What determines conformity to Bergmann's rule? *Global Ecology & Biogeography* 16: 788-794.

- Michaux J, Chevret P, Renaud S 2007. Morphological diversity of Old World rats and mice (Rodentia, Muridae) mandible in relation with phylogeny and adaptation. *Journal of Zoological Systematics and Evolutionary Research* 45(3): 263-279.
- Mikula O, Auffray JC, Macholan M 2010. Asymmetric size and shape variation in the Central European transect across the house mouse hybrid zone. *Biological Journal of the Linnean Society* 101(1): 13-27.
- Miller AP, Webb PI 2001. Diet of house mice (*Mus musculus* L.) on coastal sand dunes, Otago, New Zealand. *New Zealand Journal of Zoology* 28(1): 49-55.
- Millien V 2006. Morphological evolution is accelerated among island mammals. *Public Library of Science (PLOS) Biology* 4(11): 2165-2165.
- Millien V 2011. Mammals evolve faster on smaller islands. *Evolution* 65(7): 1935-1944.
- Millien V, Damuth J 2004. Climate change and size evolution in an island rodent species: New perspectives on the island rule. *Evolution* 58(6): 1353-1360.
- Mitteroecker P, Gunz P 2009. Advances in geometric morphometrics. *Evolutionary Biology* 36(2): 235-247.
- Monteiro LR 1999. Multivariate regression models and geometric morphometrics: The search for causal factors in the analysis of shape. *Systematic Biology* 48(1): 192-199.
- Mosimann JE 1970. Size allometry: size and shape variables with characterizations of the lognormal and generalized gamma distributions. *Journal of the American Statistical Association* 65(330): 930-945.

- Murphy EC 1992. The effects of a natural increase in food-supply on a wild population of house mice. *New Zealand Journal of Ecology* 16(1): 33-40.
- Norton D, Kelly D 1988. Mast seeding over 33 years by *Dacrydium cupressinum* Lamb.(rimu)(Podocarpaceae) in New Zealand: the importance of economies of scale. *Functional ecology*: 399-408.
- O'Donnell CF, Weston KA, Monks JM 2017. Impacts of introduced mammalian predators on New Zealand's alpine fauna. *New Zealand Journal of Ecology* 41(1): 01-22.
- Pallares LF, Harr B, Turner LM, Tautz D 2014. Use of a natural hybrid zone for genomewide association mapping of craniofacial traits in the house mouse. *Molecular Ecology* 23(23): 5756-5770.
- Pergams ORW, Ashley MV 2001. Microevolution in island rodents. *Genetica* 112(1): 245-256.
- Renaud S 2005. First upper molar and mandible shape of wood mice (*Apodemus sylvaticus*) from northern Germany: ageing, habitat and insularity. *Mammalian Biology - Zeitschrift für Säugetierkunde* 70(3): 157-170.
- Renaud S, Michaux JR 2007. Mandibles and molars of the wood mouse, *Apodemus sylvaticus*: Integrated latitudinal pattern and mosaic insular evolution. *Journal of Biogeography* 34(2): 339-355.
- Renaud S, Auffray JC 2010. Adaptation and plasticity in insular evolution of the house mouse mandible. *Journal of Zoological Systematics and Evolutionary Research* 48(2): 138-150.

- Renaud S, Auffray JC, de la Porte S 2010. Epigenetic effects on the mouse mandible: common features and discrepancies in remodeling due to muscular dystrophy and response to food consistency. *BMC Evolutionary Biology* 10(1): 28.
- Renaud S, Alibert P, Auffray JC 2012. Modularity as a source of new morphological variation in the mandible of hybrid mice. *BioMed Central Evolutionary Biology* 12: 16.
- Renaud S, Hardouin EA, Pisanu B, Chapuis JL 2013. Invasive house mice facing a changing environment on the Sub-Antarctic Guillou Island (Kerguelen Archipelago). *Journal of Evolutionary Biology* 26(3): 612-624.
- Renaud S, Gomes Rodrigues H, Ledevin R, Pisanu B, Chapuis J-L, Hardouin EA 2015. Fast evolutionary response of house mice to anthropogenic disturbance on a Sub-Antarctic island. *Biological Journal of the Linnean Society* 114(3): 513-526.
- Rodríguez MÁ, López-Sañudo IL, Hawkins BA 2006. The geographic distribution of mammal body size in Europe. *Global Ecology & Biogeography* 15: 173-181.
- Rohlf FJ 1990. Morphometrics. *Annual Review of Ecology and Systematics* 21(1): 299-316.
- Rohlf FJ 2005. Geometric morphometrics simplified. *Trends in Ecology & Evolution* 20(1): 13-14.
- Rohlf FJ, Slice DE 1990. Extensions of the procrustes method for the optimal superimposition of landmarks. *Systematic Biology* 39(1): 40-59.
- Rohlf FJ, Marcus LF 1993. A revolution morphometrics. *Trends in Ecology & Evolution* 8(4): 129-132.

- Ruscoe WA 2001. Advances in New Zealand mammalogy 1990–2000: House mouse. *Journal of the Royal Society of New Zealand* 31(1): 127-134.
- Ruscoe WA, Murphy EC 2005. House Mouse. In: King CM ed. *The Handbook of New Zealand Mammals*. 2nd ed. Melbourne, AUS, Oxford University Press.
- Ruscoe WA, Wilson D, McElrea L, McElrea G, Richardson SJ 2004. A house mouse (*Mus musculus*) population eruption in response to rimu (*Dacrydium cupressinum*) seedfall in southern New Zealand. *New Zealand Journal of Ecology* 28(2): 259-265.
- Ruscoe WA, Ramsey DSL, Pech RP, Sweetapple PJ, Yockney I, Barron MC, Perry M, Nugent G, Carran R, Warne R and others 2011. Unexpected consequences of control: competitive vs. predator release in a four-species assemblage of invasive mammals. *Ecology Letters* 14(10): 1035-1042.
- Russell JC 2012. Spatio-temporal patterns of introduced mice and invertebrates on Antipodes Island. *Polar Biology* 35(8): 1187-1195.
- Samaniego-Herrera A, Clout MN, Aguirre-Muñoz A, Russell JC 2017. Rodent eradications as ecosystem experiments: a case study from the Mexican tropics. *Biological Invasions*: 1-19.
- Satoh K 1997. Comparative functional morphology of mandibular forward movement during mastication of two murid rodents, *Apodemus speciosus* (Murinae) and *Clethrionomys rufocanus* (Arvicolinae). *Journal of Morphology* 231: 131-142.
- Searle JB, Jamieson PM, Gündüz I, Stevens MI, Jones EP, Gemmill CEC, King CM 2009a. The diverse origins of New Zealand house mice. *Proceedings of the Royal Society B: Biological Sciences* 276(1655): 209-217.

- Searle JB, Jones CS, Gündüz İ, Scascitelli M, Jones EP, Herman JS, Rambau RV, Noble LR, Berry RJ, Giménez MD and others 2009b. Of mice and (Viking?) men: phylogeography of British and Irish house mice. *Proceedings of the Royal Society B: Biological Sciences* 276(1655): 201-207.
- Shiels AB, Flores CA, Khamsing A, Krushelnycky PD, Mosher SM, Drake DR 2013. Dietary niche differentiation among three species of invasive rodents (*Rattus rattus*, *R. exulans*, *Mus musculus*). *Biological Invasions* 15(5): 1037-1048.
- Siahsarvie R, Auffray JC, Darvish J, Rajabi-Maham H, Yu HT, Agret S, Bonhomme F, Claude J 2012. Patterns of morphological evolution in the mandible of the house mouse *Mus musculus* (Rodentia: Muridae). *Biological Journal of the Linnean Society* 105(3): 635-647.
- Simberloff D, Dayan T, Jones C, Ogura G 2000. Character displacement and release in the small Indian mongoose, *Herpestes javanicus*. *Ecology* 81(8): 2086-2099.
- Slice DE 2007. Geometric morphometrics. *Annual Review of Anthropology* 36: 261-268.
- Small CG 1996. *The statistical theory of shape*. Springer, New York.
- Smith VV, Avenant NN, Chown SS 2002. The diet and impact of house mice on a sub-Antarctic island. *Polar Biology* 25(9): 703-715.
- Speedy C, Day T, Innes J 2007. Pest eradication technology-the critical partner to pest exclusion technology: the Maungatautari experience. *Managing vertebrate invasive species*: 49.
- Suzuki H, Yakimenko L, Usuda D, Frisman L 2015. Tracing the eastward dispersal of the house mouse, *Mus musculus*. *Genes and Environment* 37(1): 1-9.

- Swiderski DL, Zelditch ML 2013. The complex ontogenetic trajectory of mandibular shape in a laboratory mouse. *Journal of Anatomy* 223(6): 568-580.
- Thomason JJ 1991. Cranial strength in relation to estimated biting forces in some mammals. *Canadian Journal of Zoology* 69: 2326-2333.
- Van der Greer AA, Lyras G, de Vos J, Dermitzakis M 2010. Evolution of island mammals: adaptation and extinction of placental mammals on islands. Hoboken, New Jersey, Wiley-Blackwell.
- Watt C, Mitchell S, Salewski V 2010. Bergmann's rule; a concept cluster? *Oikos* 119(1): 89-100.
- White TA, Searle JB 2007. Factors explaining increased body size in common shrews (*Sorex araneus*) on Scottish Islands. *Journal of Biogeography* 34: 356-363.
- Wilmshurst JM, Anderson AJ, Higham TFG, Worthy TH 2008. Dating the late prehistoric dispersal of Polynesians to New Zealand using the commensal Pacific rat. *Proceedings of the National Academy of Sciences* 105(22): 7676-7680.
- Wilson DJ, Lee WG 2010. Primary and secondary resource pulses in an alpine ecosystem: snow tussock grass (*Chionochloa* spp.) flowering and house mouse (*Mus musculus*) populations in New Zealand. *Wildlife Research* 37(2): 89-103.
- Yom-Tov Y, Geffen E 2006. Geographic variation in body size: the effects of ambient temperature and precipitation. *Oecologia* 148: 213-218.
- Yom-Tov Y, Yom-Tov S, Moller H 1999. Competition, coexistence, and adaptation amongst rodent invaders to Pacific and New Zealand Islands. *Journal of Biogeography* 26(5): 947-958.

Zelditch M, Swiderski DL, Sheets HD 2012. Geometric morphometrics for
biologists: a primer. Elsevier/Academic Press, Amsterdam.

Zelditch ML, Wood AR, Bonett RM, Swiderski DL 2008. Modularity of the rodent
mandible: Integrating bones, muscles, and teeth. *Evolution & Development*
10(6): 756-768.

II. Methodology

2.1 Sample collection

Pre-cleaned skulls collected from Antipodes Island in 1978 by PJ Moors (unpublished); Auckland and Enderby Islands in 1980 by Kath Walker (see Searle et al. 2009); Hollyford Valley, Eglinton Valley, and Craigieburn Forest Park during 1974-76, 1973-80, and 1975-80 respectively by King (1983); Chatham Island in 2000 and 2007 by PM Jamieson (Searle et al. 2009) and Chubb (2008) respectively; and from Pureora Forest during 1982-87 by King et al. (1996), were provided by the University of Waikato for this study. Approximately 100 whole body samples were donated by Zealandia Wildlife Park in Wellington that were frozen after trapping or baiting over the last two years. Fourteen frozen whole body samples from Waikawa Island were donated by Ellie Bradley from Massey University (Bradley et al. 2017). Seven whole body mice were collected from Ruapuke Island and donated by Russel Trow in November 2016 (unpublished), through Pete McClelland. Fourteen Sydney mice were donated as whole bodies in ethanol by a third party through Andrew Veale. Capture data including gender and physical measurements accompanied the original dissections of the Antipodes I., Waikawa I., Chatham I., Enderby I., Pureora Forest, Eglinton Valley, Hollyford Valley, and Craigieburn Forest mouse samples. Physical measurements were taken for Ruapuke I. and Zealandia Forest mice. This background information was used to compare the body weights, tail lengths, and head-body lengths under univariate analysis of variance (ANOVA) using MYSTAT version 12 from Systat Software, Inc., San Jose California USA, www.sigmaplot.com. Head-body length and weight were also regressed against several environmental variables

using MorphoJ (Klingenberg 2011). The mice collected from Zealandia, Wellington, were haplotyped using a restriction digest in order to identify *M. m. musculus* hybrid individuals.

2.2 DNA extraction

DNA was extracted from mouse ear samples using a Biotool Mouse Direct PCR Kit as per the manufacturer's instructions. Manufacturer's protocol: Place the ear in a 1.5mL centrifuge tube. Thoroughly mix 100µl of fresh Buffer L with 2µl of Protease Plus for a single sample in a separate tube. Add the protease mixture to the mouse tissue tubes with the tissue cut end submerged in it, then incubate at 55°C for 30 minutes (incubation times may vary, depending on sample's digestion rates). After the digestion process, incubate at 95°C for 5 minutes to inactivate protease. The tissue lysate can now be used as a PCR template.

2.3 Purification

The initial DNA samples revealed high levels of protein and carbohydrate contamination under a NanoDrop spectrophotometer. 50µL of DNA was removed from the original digest and added to 350µl of a Tris EDTA-SDS solution in 1.5mL tubes (34mL H₂O, 5mL 10% SDS, 5mL 0.5M EDTA, 5mL Tris pH8, 0.1mL 5M NaCl). These were placed in a thermomixer at 60°C for 10 minutes at 15rcf. 350µL of 5M LiCl and 80µL of 10% CTAB solution was then added to the samples which were placed back on the thermomixer for a further 10 minutes at 60°C. The contents of each tube were mixed to complete emulsion with 1mL of chloroform, followed by

centrifugation at 3500rcf for 12 minutes. The upper aqueous phase was recovered into separate tubes and an equal volume of isopropanol was added. The resulting mixture was then placed in a -20°C freezer for 30 minutes to precipitate the DNA, and thereafter spun for a further 12 minutes at 3500rcf. The isopropanol was carefully removed, and 1mL of ethanol was added to each sample and re-spun for a further 12 minutes. After a DNA pellet was visualised the ethanol was removed and 20µL of TE buffer (10 mM Tris, 1 mM EDTA, pH8.0) was added to re-suspend the cleaned DNA. The resulting concentration of the clean DNA was confirmed using the NanoDrop spectrophotometer. Ideal DNA concentrations were over 20ng/µL, but often reached well over 100ng/µL, with a 260/280 reading between 1.8-2.0.

2.4 PCR

Following DNA extraction and purification, a 947 base pair (bp) section of the mitochondrial control region was amplified using 0.1µM (10pmol/µl) of the primers MouseCRF (TCTTCTCAAGACATCAAGAAG) (MacKay et al. 2013) and H0072 (TATAAGGCCAGGACCAAACCT) (MacKay et al. 2013) with the Mouse Direct PCR Kit. PCR amplifications were initially performed in 50µL reactions as per the manufacturer's protocol. A modified thermocycler profile was also trialled based on the procedure detailed by MacKay et al. (2013), who employed the same primers in their protocol. However, the M-PCR OPTI Mix did not yield the desired DNA product. After replacing primer and water working stocks, it was clear the M-PCR OPTI Mix had become contaminated.

A HOT FIREPol Blend MasterMix Ready to Load sample from DNature was trialled successfully following the previous setback. PCR amplification was performed following the manufacturer's protocol at 20 μ L reaction volumes. Thermal cycling conditions included initial denaturation at 95°C for 15 min; 30 cycles of 20 s at 95°C, 45 s at 58°C, 1 min at 72°C; and a final extension of 10 min at 72°C. The PCR products were then run on 0.8% agarose gels at 200V for 8 minutes to visualise correct DNA amplification.

2.5 Restriction digest

As per the manufacturer's protocol, 10 μ L of PCR reaction mixture at 0.1-0.5 μ g of DNA was added to 18 μ L of ddH₂O, 2 μ L of 10X Buffer Tango, and 1 μ L of BSU15I (10U/ μ L). This mixture was mixed gently and spun down for 2 minutes, followed by incubation at 37°C in the thermomixer for 1 hour at 2rcf. To inactivate the enzyme, the mixtures were incubated at 65°C for 20 minutes. Each mixture was then run on a 2% agarose gel at 95V for 30 minutes to visualise band separation (cut site would produce a DNA fragment of approximately 100bp from the 947bp section).

2.6 Mandible cleaning

Mouse heads were removed and placed in heat-safe plastic containers with 15g of sodium perborate and 150mL of water (McDonald and Vaughan 1999). The containers were then placed in an oven overnight at 60°C with a loosely fitted lid. Following incubation, the contents of each container were poured into a metal sieve

and washed with water. Any remaining flesh and cartilage was removed with forceps. The mandibles were left out to dry and subsequently stored in labelled vials.

2.7 Photography and landmark placement

Photographs of each mouse mandible were taken using a Leica MZ12 stereomicroscope with a Carl Zeiss Axiocam HRc camera. A separate light source with cold light bulbs allowed illumination of the mandible to be adjusted to give desired contrast for landmarking. In order to capture the mandibles at similar orientations, a clay cradle was made that created a stable base on which to place the specimens. A scale ruler was also included in all images.

Sixteen two-dimensional homologous landmarks were digitized on the lateral mandible using software TPSDig.2 ver.2.19. (Rohlf 2015) (Figure II-A).

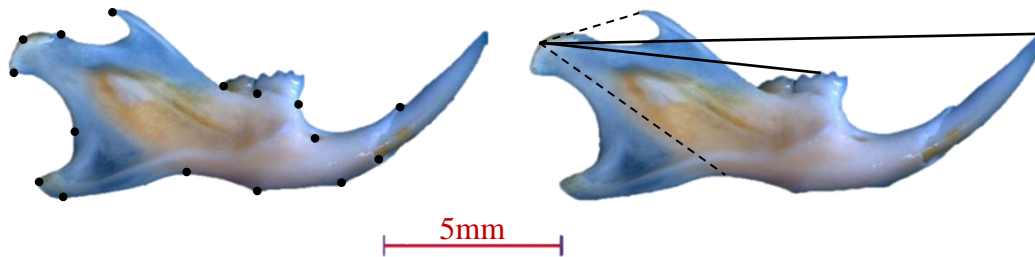


Figure II-A LEFT, placement of 16 landmarks to sample mandible shape. RIGHT, Inlever length (dotted lines) based on muscle attachment zones and Outlever length (solid lines) based on bite zones.

2.8 Biomechanical analysis

Biomechanical advantage is a measure of bite force efficiency by calculating the ratio of inlever to outlever (Figure II-A). These measurements are replicated from Renaud et al. (2015) who conducted a biomechanical analysis on house mouse mandibles

from Guillou Island, sub-Antarctic Kerguelen Archipelago. The inlevers correspond to the distance from the condyle to the attachment zones for the temporalis and masseter muscles. The outlevers are considered to be the distance between the condyle and the tip of the incisor, and the main molar cusp. Four ratios for biomechanical advantage were calculated: masseter/incisor (M/I), masseter/molar (M/M), temporalis/incisor (T/I) and temporalis/molar (T/M). The raw measurements and ratios were compared between mouse populations using Kruskal-Wallis ANOVA in MYSTAT.

2.9 Statistical analysis

A Generalized Procrustes Fit (GPF) was performed on the coordinates obtained from TPSDig.2 in MorphoJ (Klingenberg 2011) to quantify shape differences between individual configurations (Rohlf 1990; Dryden & Mardia 1998; Rohlf 1999). GPF produces a local approximation of the arrangements in Kendall's tangent space in 2-dimensional format for the given data set (Kendall 1984, 1989; Zelditch et al. 2012; Klingenberg 2016). The Procrustes superimposition then removes size (centroid size), position and orientation variables, resulting in Procrustes distances between corresponding landmarks that represents discrepancies between configurations i.e. a measure of shape differences (Dryden & Mardia 1992; Kendall 1989; Zelditch et al. 2012; Klingenberg 2016).

To test for significant allometry in the data set, a multivariate regression of shape (Procrustes coordinates) on log centroid size was performed (Monteiro 1999; Mitteroecker & Gunz 2009; Klingenberg 2016). MANCOVA is included in the

multivariate regression to test the homogeneity of the allometric slopes (Klingenberg 2016). A principal component analysis (PCA) was then conducted on the covariance matrix of the regression residuals to visualise variation between individual mandible shapes (Zelditch et al. 2012). Overall mandible shape change along each principal component axis was visualised using ‘warped outline drawings’ (Slice 2007). A canonical variate analysis (CVA) was used to obtain Procrustes distance and Mahalanobis distance values between samples, and investigate differences between pre-defined groups. Discriminant Function Analysis (DFA) was also used to confirm the distinctness of sample groups by the number of miss-assigned individuals with permutation values (1000 repeats). A partial least squares analysis was conducted to investigate the covariation of mandible shape with abiotic variables between sample locations. These statistical analyses were carried out using MorphoJ ver.1.06d (Klingenberg, 2011). Centroid sizes and Procrustes distances were exported to MYSTAT for Kruskal-Wallis ANOVA comparison.

2.10 Notes

Unfortunately, the restriction digest results are not included in this study because I had difficulty obtaining consistent target PCR products. The samples that were successfully digested with the restriction enzyme also did not run positive for the *M. m. musculus* haplotype. After 4 months of struggling to produce amplified DNA that could be run with the restriction enzyme, I eventually resigned to focus on the rest of my research.

2.11 References

- Bradley E, Trewick SA, Morgan-Richards M 2017. Genetic distinctiveness of the Waikawa Island mouse population indicates low rate of dispersal from mainland New Zealand. *New Zealand Journal of Ecology* 41(2).
- Chubb T 2008. Phylogeography and hybridisation of the New Zealand house mouse. Unpublished Masters thesis, University of Waikato.
- Dryden IL, Mardia KV 1998. *Statistical shape analysis*. Chichester; New York, John Wiley & Sons.
- Dryden IL, Mardia KV 1992. Size and shape analysis of landmark data. *Biometrika* 79(1): 57-68.
- Kendall DG 1984. Shape manifolds, procrustean metrics, and complex projective spaces. *Bulletin of the London Mathematical Society* 16(2): 81-121.
- Kendall DG 1989. A survey of the statistical theory of shape. *Statistical Science* 4(2): 87-99.
- King CM, Innes JG, Flux M, Kimberley MO, Leathwick JR, Williams DS 1996. Distribution and abundance of small mammals in relation to habitat in Pureora Forest park. *New Zealand Journal of Ecology* 20(2): 214-240.
- King CM 1983. The relationships between beech (*Nothofagus* sp.) seedfall and populations of mice (*Mus musculus*), and the demographic and dietary responses of stoats (*Mustela erminea*), in three New Zealand forests. *Journal of Animal Ecology* 52(1): 141-166.
- Klingenberg CP 2011. MorphoJ: an integrated software package for geometric morphometrics. *Molecular Ecology Resources* 11: 353-357.

- Klingenberg CP 2016. Size, shape, and form: concepts of allometry in geometric morphometrics. *Development Genes and Evolution* 226(3): 113-137.
- MacKay JWB, Alexander A, Hauber ME, Murphy EC, Clout MN 2013. Does genetic variation among invasive house mice in New Zealand affect eradication success? *New Zealand Journal of Ecology* 37(1): 18-25.
- McDonald RA and Vaughan N 1999. An efficient way to prepare mammalian skulls and bones. *Mammalian Review* 29: 265-266.
- Mitteroecker P, Gunz P 2009. Advances in geometric morphometrics. *Evolutionary Biology* 36(2): 235-247.
- Monteiro LR 1999. Multivariate regression models and geometric morphometrics: The search for causal factors in the analysis of shape. *Systematic Biology* 48(1): 192-199.
- Renaud S, Gomes Rodrigues H, Ledevin R, Pisanu B, Chapuis J-L, Hardouin EA 2015. Fast evolutionary response of house mice to anthropogenic disturbance on a Sub-Antarctic island. *Biological Journal of the Linnean Society* 114(3): 513-526.
- Rohlf FJ 2015. TPSDig. SUNY Stony Brook Morphometrics.
- Rohlf FJ 1990. Morphometrics. *Annual Review of Ecology and Systematics* 21(1): 299-316.
- Rohlf FJ 1999. Shape statistics: Procrustes superimpositions and tangent spaces. *Journal of Classification* 16(2): 197-223.
- Searle JB, Jamieson PM, Gündüz I, Stevens MI, Jones EP, Gemmill CEC, King CM 2009. The diverse origins of New Zealand house mice. *Proceedings of the Royal Society B: Biological Sciences* 276(1655): 209-217.

Slice DE 2007. Geometric morphometrics. *Annual Review of Anthropology* 36: 261-268.

Zelditch M, Swiderski DL, Sheets HD 2012. *Geometric morphometrics for biologists: a primer*. Elsevier/Academic Press, Amsterdam.

III. Comparing house mouse populations in New Zealand Forests

3.1 Introduction

This chapter compares the size and shape of house mouse mandibles and body measurements from five New Zealand forest habitats (Figure III-A). The variation in plant species between habitat types is likely to influence the major dietary components of house mouse populations. Seed masting, a cycle of periodic heavy seedfall (Norton & Kelly 1988), provides abundant food supplies which facilitate extended winter breeding (King 1983; Murphy 1992; Choquenot & Ruscoe 2000; O'Donnell et al. 2017). House mice populations irrupt in tussock (*Chionochloa*), beech (Nothofagaceae), and hardwood-podocarp forests following seed masting events (King 1983; Murphy 1992; Fitzgerald et al. 1996; Choquenot & Ruscoe 2000; Fitzgerald et al. 2004; Ruscoe et al. 2004; Ruscoe & Murphy 2005; Wilson & Lee 2010; O'Donnell et al. 2017).

A study by Anderson et al. (2014) observed shape changes over 6 months in the alveolar and ramus mandible regions of mice fed either soft or hard food diets. Coronoid and angular processes were extended in hard-food fed individuals, with ventral expansion of alveolar regions. This remodelling related to a higher mechanical advantage, enabling the development of a more efficient bite force compared to mice eating soft food. Conversely, mice fed soft food developed a

slimmer, elongated mandible relative to the hard food mandibles. A slimmer mandible shape reduces the distance of the inlevers, while elongation lengthens the outlevers, reducing the overall mechanical advantage of the jaw. This observation leads to the prediction that biomechanical advantage and mandible shape of mice should vary between populations, presumably with the availability of invertebrates and plant material.

House mice are known to feed on a combination of seeds, invertebrates, and other plant materials (Ruscoe & Murphy 2005; Wilson & Lee 2010; Goldwater et al. 2012; Cuthbert et al. 2013; O'Donnell et al. 2017; Samaniego-Herrera et al. 2017).

However, rats can greatly alter mouse behaviour and restrict their feeding habits through competition and predation (Innes et al. 1995; Caut et al. 2007; Hancock 2008; Ruscoe et al. 2011; Goldwater et al. 2012; Bridgman et al. 2013). In the absence of rats, New Zealand-based studies have shown significant increase in the mean body weight of wild mice (Innes et al. 1995; Goldwater et al. 2012).

The body size of small mammals can also increase with rising latitude, although there are several conflicting studies for Rodentia (Ashton et al. 2000; Meiri & Dayan 2003; Medina et al. 2007; Alhajeri & Stepan 2016). This observation is a general ecogeographic trend first put forward by Bergmann in 1847. Bergmann's proposed mechanism for observing larger animals at greater latitudes was a relationship between heat conservation and environmental temperature. However, several other mechanisms have been debated, including primary productivity, competition and fasting endurance (Burnett 1983; Geist 1987; Ashton et al. 2000; Rodríguez et al. 2006; McNab 2010; Huston & Wolverton 2011; Alhajeri & Stepan 2016). There is much discussion about which climatic variables are most influential to body size at

higher latitudes. Several studies found rainfall, temperature and productivity to be the most significant covariates (Boyce 1978; Burnett 1983; Rodríguez et al. 2006; Alhajeri & Steppan 2016).

In terrestrial ecosystems, primary production is positively correlated with temperature, precipitation, and, of course, sunlight (Huston & Wolverton 2011).

Rodent densities were found to increase with greater plant productivity in the Palearctic (Jędrzejewski & Jędrzejewska 1996). However, house mouse densities tend to be lower in wetter forest habitats compared to drier areas (King 1991). Ruscoe & Murphy (2005) also note that mouse density can fluctuate considerably with seasons and sporadic heavy seed masts that effect food resources. Geographical variation in net primary productivity (NPP) is said to influences the development of body size, especially during growing and reproductive periods (McNab 2010; Huston & Wolverton 2011). Huston & Wolverton (2011) propose that the NPP available during development periods is the most important influence on body size, and name this concept ecologically and evolutionarily relevant NPP (eNPP).

This study investigates the differences in size and shape of house mouse mandibles between forests differing in climate, plant community, and presence or absence of other invasive mammals. The study areas of interest are Eglinton Valley, Hollyford Valley, Craigieburn Forest, Zealandia Wildlife Sanctuary, and Pureora Forest (Figure III-A).

3.2 Material

The five samples available are described in Table III-1, along with any published data (Table III-2). The forests are at least 200km apart (Figure III-A), with the exception of Hollyford and Eglinton Valleys, that are separated by <50km on opposite sides of the South Island Main Divide.

Pureora Forest Park

House mice inhabiting Pureora forest (North Island) are assumed to belong to haplotype *M. m. domesticus* NZ.4, the most prevalent haplotype throughout New Zealand (especially the northern North Island) and Europe (King et al. 2016). Pureora supports a mixture of native podocarp (including: tawa, rimu, matai, miro, totara, kamahi, rata and tree fern) and exotic *Pinus radiata* forest (King et al. 2015). A previous study by King et al. (1996) found mice were most abundant in young plantation areas, where ground cover is most dense.

Zealandia Wildlife Sanctuary

Mice in the Zealandia Wildlife Sanctuary sampled independently by Paul Jamieson and Tanya Chubb were mostly *castaneus*NZ.1 hybrids, with a few *domesticus* and *M. m. musculus* individuals (Searle et al. 2009). As the mice included in this study could not be successfully haplotyped, it is assumed they are mostly *castaneus*NZ.1 hybrids. The Zealandia Wildlife Sanctuary spans a 252 ha section of regenerating broadleaf forest enclosed by a predator-proof fence (Blick et al. 2008). In this region, the vegetation is dominated by coastal broadleaf-conifers such as māhoe, five finger, and pate, interspersed with exotic pine stands (Blick et al. 2008). As the Zealandia forest is in succession, tree ferns, vines and shrubs (hangehange and kawakawa) contribute to a dense understory beneath a closed-canopy, with few emergent trees.

Craigieburn Forest Park

Craigieburn Forest house mice are also likely to belong to *domesticus*NZ.4 because the surrounding sites sampled by King et al (2016) were all of this haplotype.

Craigieburn Forest Park (South Island) is predominantly mountain beech (*Nothofagus solandri*), giving way to alpine grasslands above the treeline (King 1983), which are the only two major seed-bearing plants available over wide areas.

Eglinton and Hollyford Valleys

Mice from the Eglinton and Hollyford Valleys (South Island) are *castaneus*NZ.1 – *domesticus* hybrids (King et al. 2016). Red beech (*Nothofagus fusca*), one of eight food source species, dominates Eglinton Valley Forest (King 1983). By contrast, Hollyford Valley is more diverse, supporting 28 species of food-bearing plants including silver beech (*Nothofagus menziesii*). King (1983) observed significant relationships between beech seedfall and mouse populations in all three South Island sites of this study. This does not necessarily imply that mice were feeding on the beech seeds themselves rather than on other food resources that also responded to beech seeding, simply that there was a correlation between increased seedfall and mouse density.

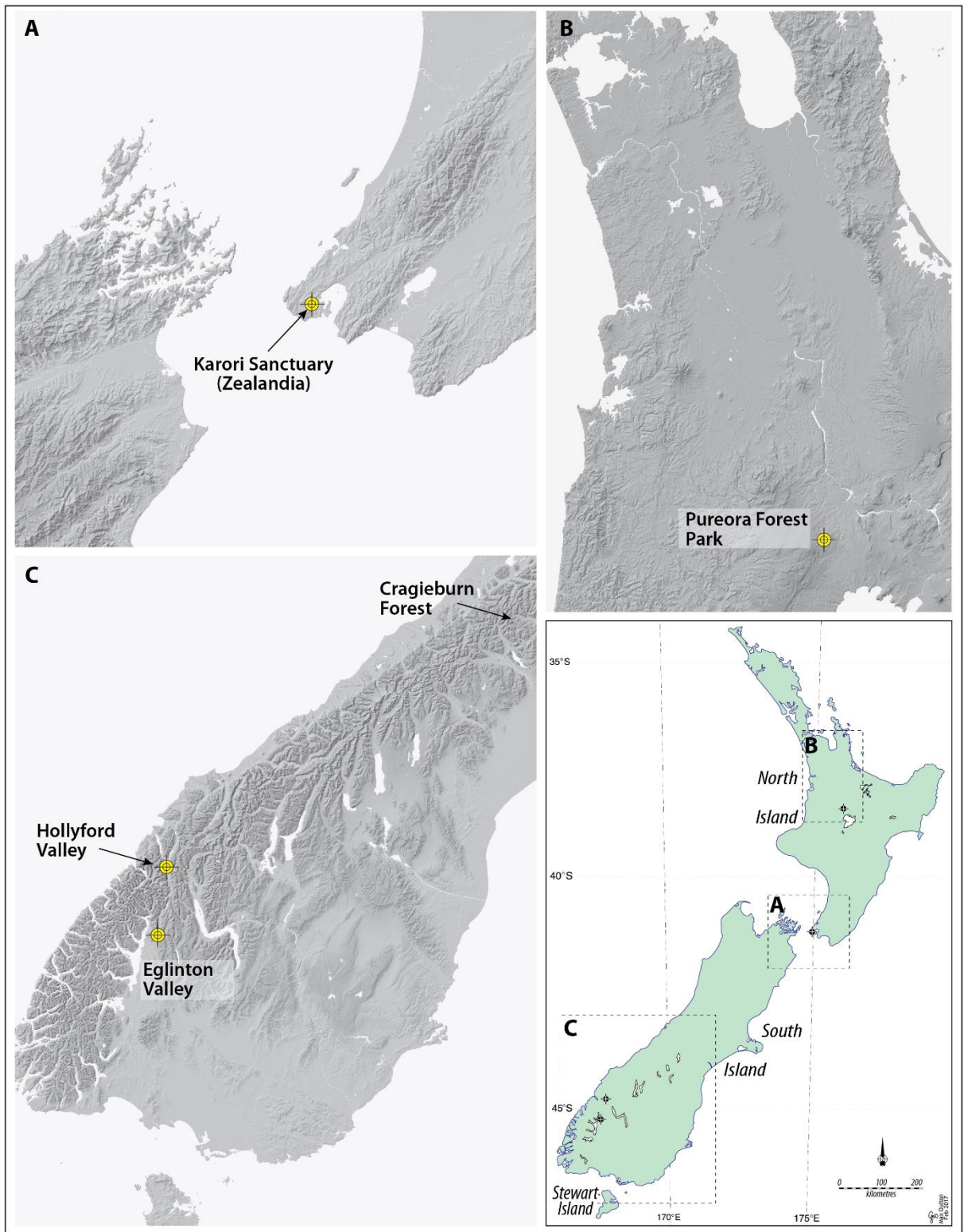


Figure III-A Locations of New Zealand forests included in this study. Drawn up by Max Oulton, University of Waikato.

Table III-1 Published and raw body measurements of adult mice in New Zealand forests (mean \pm SD).

	Weight (g)	n	Total length (mm)	n	Head-body length (mm)	n	Reference
Pureora	17.3 \pm 2.2	14	169.5 \pm 9.3	13	86.1 \pm 5.9	15	King et al. (1996)
Craigieburn	20.0 \pm 2.2	14	179.2 \pm 3.9	14	94.6 \pm 3.5	14	King (1983)
Hollyford	19.1 \pm 2.5	66	175.5 \pm 9.5	68	90.1 \pm 6.3	68	King (1983)
Eglinton	21.1 \pm 2.7	77	178.8 \pm 10.8	77	93.0 \pm 6.3	76	King (1983) and Murphy (unpub.)
Zealandia							Blick et al. (2007)
Raw data	Weight (g)	n	Tail length (mm)	n	Head-body length (mm)	n	
Pureora	16.9 \pm 2.1	37	81.0 \pm 5.0	36	82.2 \pm 4.5	38	
Craigieburn	19.4 \pm 2.8	27	92.5 \pm 5.4	27	81.3 \pm 4.7	27	
Hollyford	18.2 \pm 1.8	15	86.8 \pm 4.9	15	81.9 \pm 7.2	15	
Eglinton	23.5 \pm 2.8	16	88.7 \pm 5.7	17	83.4 \pm 5.8	17	
Zealandia	18.7 \pm 3.6	16	76.4 \pm 5.6	16	78.7 \pm 4.2	16	

Table III-2 Environmental variables associated with each forest habitat.

	Altitude (m)	Annual Rainfall (mm)	Latitude	Habitat	Rats	Reference
Pureora	550-700	1759	38.6947° S, 175.5612° E	Pine and podocarp forest	Yes	King et al. (1996)
Craigieburn	790-1340	1450	43.1509° S, 171.7119° E	Mountain beech forest	Yes	King (1983)
Hollyford	90-370	4250	44.45°S, 168.10° E	Mixed and beech forest	Yes	King (1983)
Eglinton	270-550	2300	44.50°S, 168.05°E	Beech forest	Yes	King (1983) and Murphy (unpub.)
Zealandia	160-380	1265	41.2838° S, 174.7409° E	Young podocarp	No	Blick et al. (2007)

3.3 Traditional measurements

3.2.1 Body Weight

Significant variation in body weight between forest habitats was found among all but three of ten pairwise comparisons (Table III-3). Eglinton Valley mice were the heaviest, and Pureora Forest mice were the lightest (Figures III-B and III-C).

Table III-3 P-values from Kruskal-Wallis ANOVA pairwise comparison of forest mouse body weight. Bold, red text indicates significant p-values ≤ 0.05 .

WEIGHT	Hollyford	Craigieburn	Pureora	Eglinton
Craigieburn	0.17			
Pureora	0.0023	≤ 0.0001		
Eglinton	≤ 0.0001	≤ 0.0001	≤ 0.0001	
Zealandia	0.72	0.6	0.024	≤ 0.0001

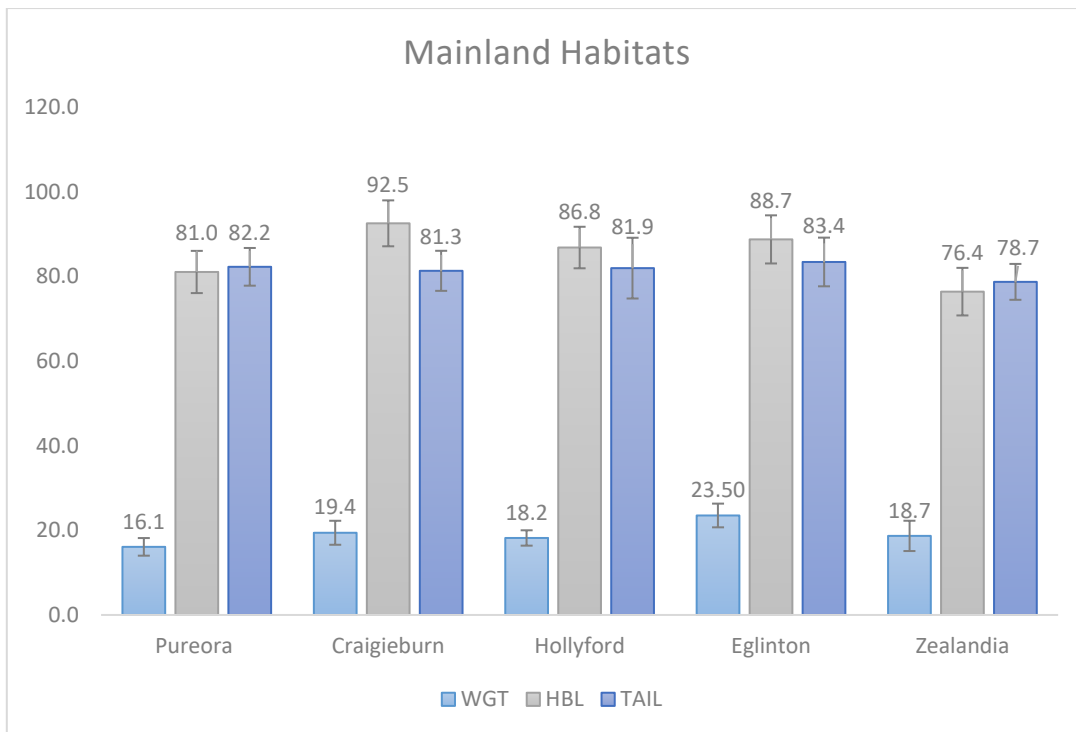


Figure III-B Histogram showing mean body weight, head-body length, and tail length values between forest mouse populations.

3.2.2 Head-Body Length

All but one pairwise comparison produced significant p-values for head-body length (Table III-4). Craigieburn was the longest, and Zealandia was the shortest (Figures III-B and III-C).

Table III-4 P-values from Kruskal-Wallis ANOVA pairwise comparison of forest mouse head-body length. Bold, red text indicates significant p-values ≤ 0.05 .

HBL	Hollyford	Craigieburn	Pureora	Eglinton
Craigieburn	0.0025			
Pureora	0.001	≤ 0.0001		
Eglinton	0.43	0.025	≤ 0.0001	
Zealandia	0.0001	≤ 0.0001	0.0063	≤ 0.0001

3.2.3 Tail Length

Significant variation in tail length was found only between three pairs (Table III-5).

Eglinton mice had the longest tails; Zealandia were the shortest (Figures III-B and III-C).

Table III-5 P-values from Kruskal-Wallis ANOVA pairwise comparison of forest mouse tail lengths. Bold, red text indicates significant p-values ≤ 0.05 .

TAIL	Hollyford	Craigieburn	Pureora	Eglinton
Craigieburn	0.28			
Pureora	0.52	0.46		
Eglinton	0.77	0.22	0.31	
Zealandia	0.016	0.12	0.0043	0.0069

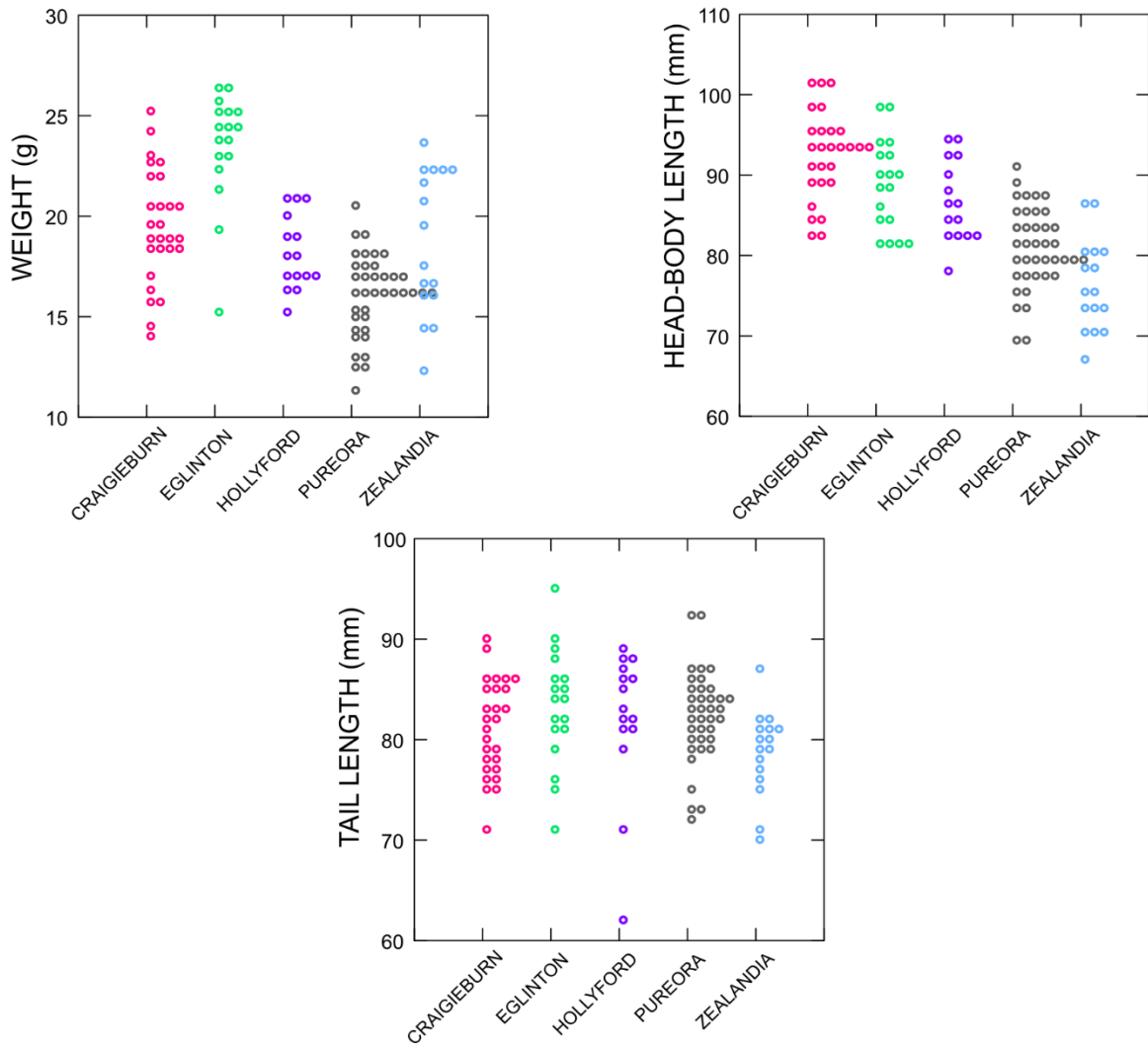


Figure III-C Dot density plots showing the distribution of raw physical measurements within each forest population. Each icon corresponds to an individual mouse.

3.2.4 Regression

Genetic haplotype, ambient temperature, latitude and habitat type varied significantly with mouse body weight, latitude accounting for the most variation (Table III-6). By contrast, only rat presence and high temperature explained significant variation in head-body length.

Table III-6 Regression percentages of total variation in body weight and length explained by each environmental and genetic covariate. Bold, red text indicates significant percentages with p -values ≤ 0.05 .

Regression %	Weight	Head-body length
Rainfall	1.19	0.76
Genetics	7.66	0.10
Presence of rats	0.18	4.91
Temp low	21.0	0.23
Temp high	5.67	5.22
Latitude	22.0	0.13
Habitat	18.2	0.97
Alt low	0.64	0.04
Alt high	0.35	0.13

3.3 Biomechanical analysis

Biomechanical advantage is a measure of the efficacy of the mandible to exert bite force and occlude the incisor teeth.

Significant variation in the masseter/incisor (M/I) ratio were found between Eglinton and Zealandia mandibles with all other populations, except each other (Table III-7).

Zealandia held the highest M/I advantage (0.468), and Craigieburn had the lowest (0.445). The order of mechanical advantage ranged from highest to lowest: Zealandia, Eglinton, Hollyford, Pureora, Craigieburn.

Table III-7 P-values from Kruskal-Wallis ANOVA pairwise comparison of the masseter/incisor biomechanical advantage ratio for forest mandibles. Bold, red text indicates significant p-values ≤ 0.05 .

Masseter/Incisor	Craigieburn	Eglinton	Hollyford	Pureora
Eglinton	0.0007			
Hollyford	0.2	0.0062		
Pureora	0.5	0.0031	0.63	
Zealandia	≤ 0.0001	0.14	0.0007	≤ 0.0001

Significant variation in masseter/molar (M/M) ratio followed that of M/I, with the addition of significant p-values between Pureora with all other populations (Table III-8). Zealandia had the highest M/M advantage (0.865), and Hollyford had the lowest (0.821). In order of mechanical advantage: Zealandia, Eglinton, Pureora, Craigieburn, Hollyford.

Table III-8 P-values from Kruskal-Wallis ANOVA pairwise comparison of the masseter/molar biomechanical advantage ratio for forest mandibles. Bold, red text indicates significant p-values ≤ 0.05 . Bold italicised text indicates p-values close to 0.05.

Masseter/Molar	Craigieburn	Eglinton	Hollyford	Pureora
Eglinton	0.0005			
Hollyford	0.38	0.0005		
Pureora	0.053	0.045	0.015	
Zealandia	<i>≤ 0.0001</i>	0.27	<i>≤ 0.0001</i>	0.0026

Significant variation in the temporalis/incisor (T/I) ratio were found between Pureora and Zealandia mandibles with all other populations, except each other (Table III-9).

Eglinton held the highest T/I advantage (0.222), while Zealandia had the lowest (0.194). In order of mechanical advantage: Eglinton, Hollyford, Craigieburn, Pureora, Zealandia.

Table III-9 P-values from Kruskal-Wallis ANOVA pairwise comparison of the temporalis/incisor biomechanical advantage ratio for forest mandibles. Bold, red text indicates significant p-values ≤ 0.05 .

Temporalis/Incisor	Craigieburn	Eglinton	Hollyford	Pureora
Eglinton	0.18			
Hollyford	0.73	0.45		
Pureora	0.011	0.0007	0.022	
Zealandia	0.0023	0.0005	0.0051	0.14

Significant variation in the temporalis/molar (T/M) ratio followed that of T/I (Table III-10). Eglinton had the highest T/M advantage (0.411), and Zealandia had the lowest (0.358). In order of mechanical advantage: Eglinton, Craigieburn, Hollyford, Pureora, Zealandia.

Table III-10 P-values from Kruskal-Wallis ANOVA pairwise comparison of the temporalis/molar biomechanical advantage ratio for forest mandibles. Bold, red text indicates significant p-values ≤ 0.05 . Bold italicised text indicates p-values close to 0.05.

Temporalis/Molar	Craigieburn	Eglinton	Hollyford	Pureora
Eglinton	0.31			
Hollyford	0.78	0.21		
Pureora	0.012	0.0014	<i>0.09</i>	
Zealandia	0.001	0.0003	0.0077	<i>0.087</i>

Overall, at Zealandia the masseter muscle had the highest mechanical advantage, and the temporalis muscle had the lowest. In Eglinton Valley forest the temporalis had the highest mechanical advantage, while Craigieburn and Hollyford forests had the lowest masseter mechanical advantage.

3.4 Centroid size

Centroid size is used as the standard size variable in geometric morphometric analyses, derived from the square root of the sum of squared distances of all the landmarks.

Kruskal-Wallis ANOVA results found that mice from Craigieburn and Pureora had the smallest average mandible centroid size, significantly different from all other forest populations except each other (Table III-11). Zealandia had the largest mandible centroid size, and did not significantly differ to Eglinton or Hollyford centroid sizes (Figure III-D).

Under regression, centroid size did not vary significantly with weight (1.432%, p-value 0.23) or head-body length (0.58%, p-value 0.45).

Table III-11 P-values from Kruskal-Wallis ANOVA pairwise comparison of forest mandible centroid size. Bold, red text indicates significant p-values ≤ 0.05 .

Centroid Size	Craigieburn	Eglinton	Hollyford	Zealandia
Eglinton	≤ 0.0001			
Hollyford	0.0039	0.52		
Zealandia	0.0005	1	0.46	
Pureora	0.45	0.0068	0.063	0.018

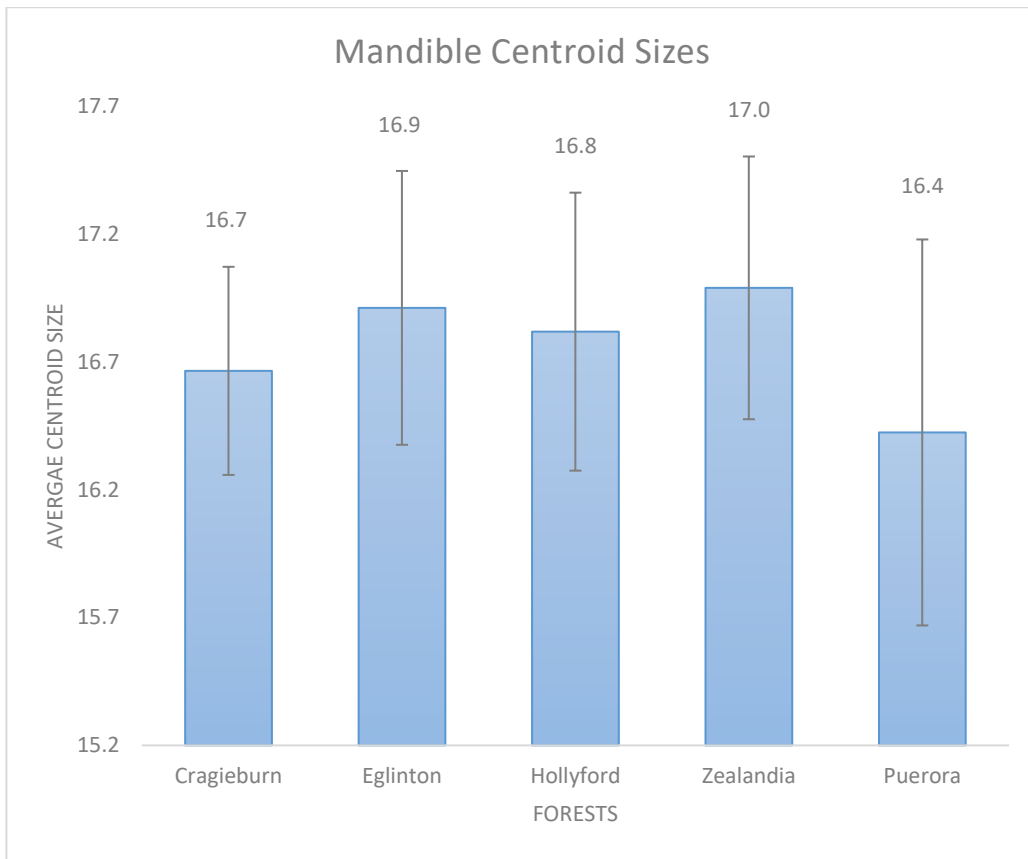


Figure III-D Histogram showing average mandible centroid size values between forest populations.

3.5 Shape analysis

3.5.1 Regression and Principal Component Analysis

The pooled within-group regression was significant for allometry ($p \leq 0.0001$ after 1000 permutations), with size accounting for 4.38% of shape variance (Figure III-E).

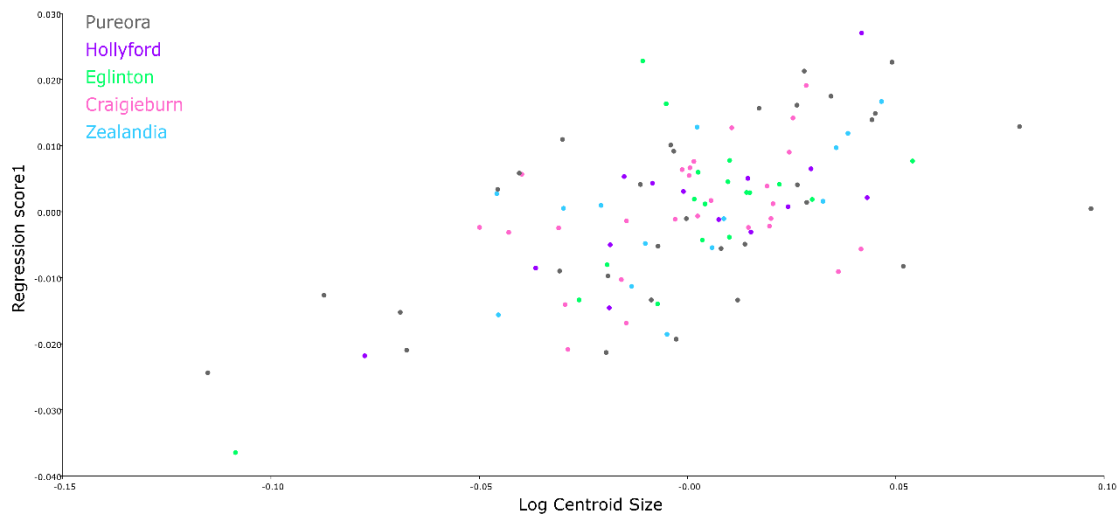


Figure III-E Group-centred regression of forest mandible shape on log centroid size.

All subsequent analyses were performed using the regression residuals in order to visualise variation in shape without allometric influence. Principal components that represent >5% variance are often considered significant. An alternative interpretation of significance is to interpret only those PCs/eigenvalues falling above the inflection point of a scree plot as ‘biologically significant’ to shape variation. In this analysis, the latter method is favoured, however, all PCs >5% are still reported.

The first six principal components accounted for >5% variance, accumulating to 65.7% of total variance (Table III-12).

There is no obvious inflection point on the scree plot (Figure III-F), so a second PCA plot is presented to show differentiation of individuals along the third PC axis.

Table III-12 Eigenvalues for the forest PCA plot that represent more than 5% variance.

	EV1	EV2	EV3	EV4	EV5	EV6
Eigenvalues	0.000228	0.000154	0.000106	0.0000809	0.0000696	0.0000614
Variance (%)	21.35	14.46	9.94	7.62	6.56	5.78
Cumulative (%)	21.35	35.82	45.75	53.37	59.93	65.71

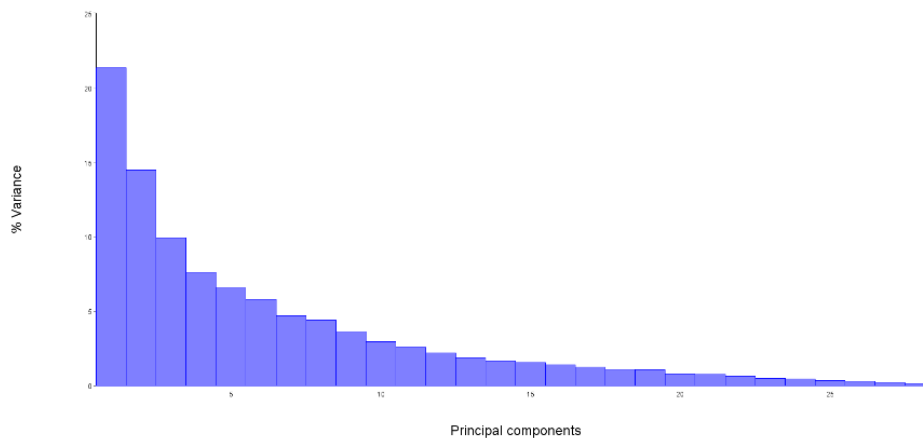


Figure III-F Scree plot of the variance explained by each eigenvalue for forest mandibles.

PC1 accounted for 21.35% of mandible shape variance (Table III-12). The 90% equal frequency ellipses do not help to distinguish the forest populations on the PCA plot (Figure III-G). However, the 90% confidence ellipses of each mean show a clear separation between the North and South Island samples along the first PC axis (Figure III-H). The PC1 warped outline plot depicts a broader alveolar profile, shifted coronoid process, and expanded condyle and angular processes along the PC1 axis

(pink outline). This mandible shape is associated with individuals at the positive PC1 axis end (Hollyford, Eglinton and Craigieburn).

PC2 accounts for 14.46% of mandible shape variation (Table III-12). The second PC axis differentiates Pureora and, to some degree, Craigieburn from the other three samples (Figure III-H). The PC2 warped outline plot displays a shorter, shifted molar region, with a smaller condyle process and longer, slimmer angular process along the second PC axis (pink outline). Individuals at the positive end of the PC2 axis have this mandible shape (Zealandia, Craigieburn, Eglinton and Hollyford).

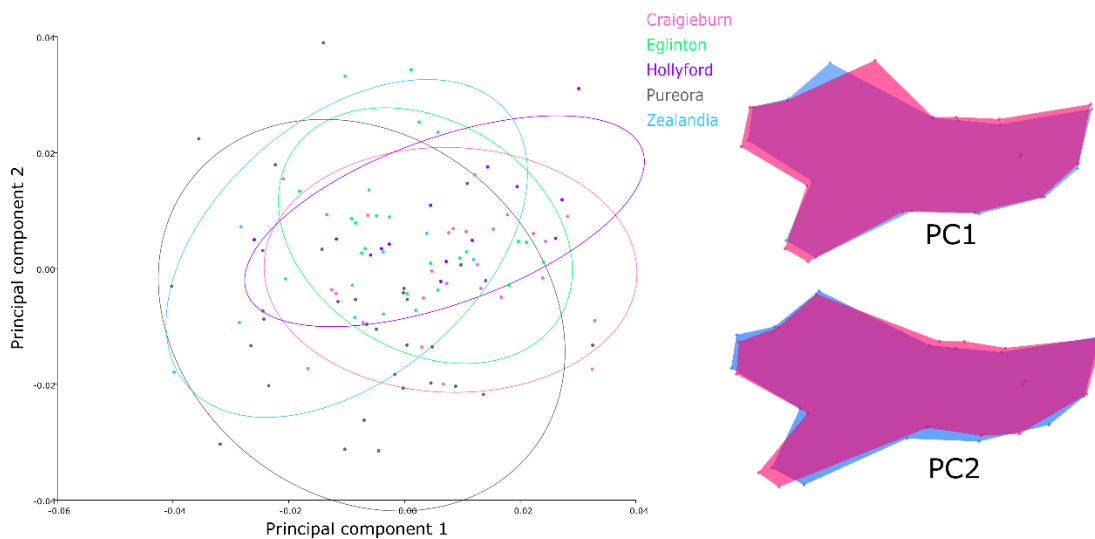


Figure III-G LEFT PCA plot of mandible shape differences between forest populations with PC1 and PC2. Each dot represents a specimen, surrounded by equal frequency ellipses. RIGHT Procrustes deformation warped outlines depicting the change in mandible shape along each axis; blue represents mandible shape at far left of the axis, pink represents the mandible shape at far right of the axis.

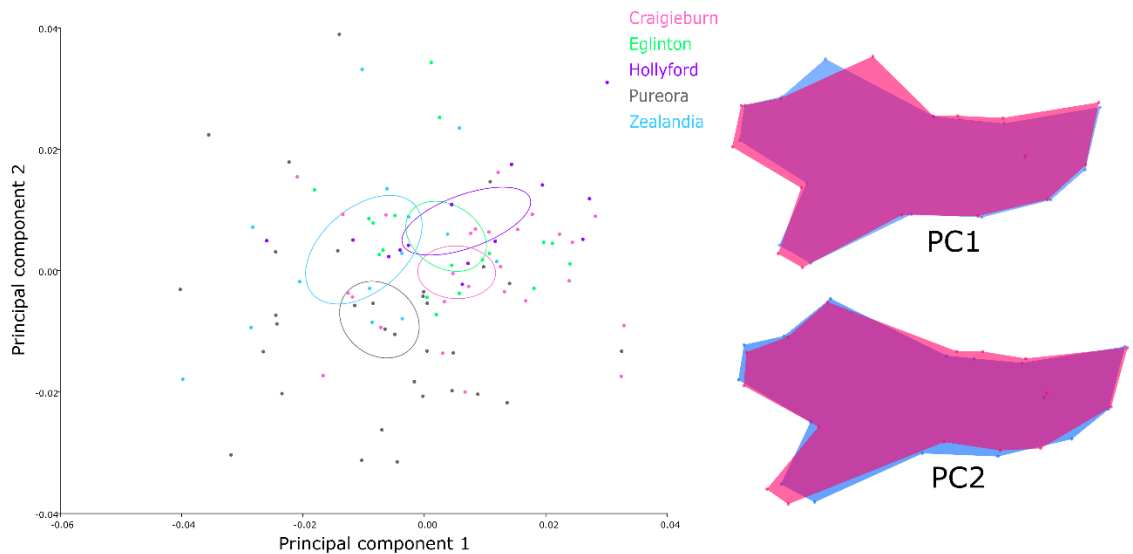


Figure III-H LEFT PCA plot of mandible shape differences between forest populations with PC1 and PC2. Each dot represents a specimen, with 90% confidence ellipses around the mean. RIGHT Procrustes deformation warped outlines depicting the change in mandible shape along each axis; blue represents mandible shape at far left of the axis, pink represents the mandible shape at far right of the axis.

PC3 describes 9.94% of the total variation in mandible shape (Table III-12; Figure III-I). The third PC axis reveals extreme separation of Eglinton and Zealandia mandibles. Craigieburn, Hollyford, and Pureora cluster together at the centre of the axis. The warped outline plot depicts a much slimmer mandible profile with a longer condyle process along the third PC axis (pink outline). This mandible shape is associated with Eglinton individuals at the positive end of the axis, and is much less mechanically efficient than the broader profile of the Zealandia individuals.

The fourth and fifth PCA plots show separation of Zealandia individuals, with substantial overlap of the other mean ellipses. There was little differentiation on the sixth PCA plot.

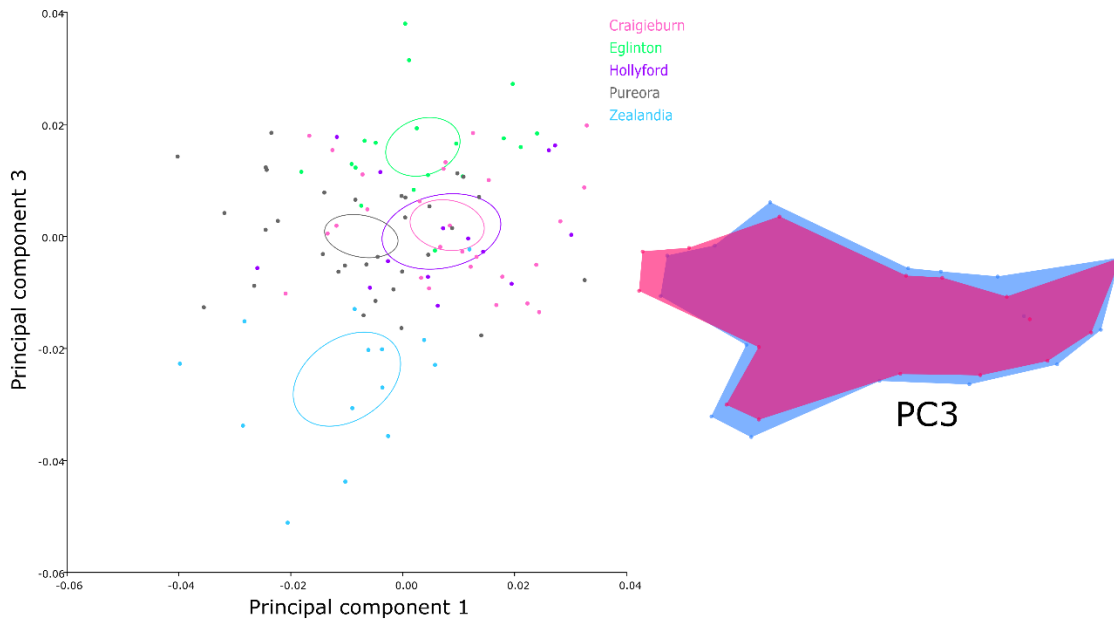


Figure III-1 LEFT PCA plot of mandible shape differences between forest populations with PC1 and PC3. Each dot represents a specimen, with 90% confidence ellipses around the mean. RIGHT Procrustes deformation warped outlines depicting the change in mandible shape along each axis; blue represents mandible shape at far left of the axis, pink represents the mandible shape at far right of the axis.

Kruskal-Wallis pairwise comparison revealed all of the significant variation in PC1 is associated with Zealandia mandible shape (Table III-13).

Table III-13 P-values from Kruskal-Wallis ANOVA pairwise comparison of PC1 between forest populations. Bold, red text indicates significant p-values ≤ 0.05 .

PC1	Craigieburn	Eglinton	Hollyford	Zealandia
Eglinton	0.59			
Hollyford	0.099	0.29		
Zealandia	0.0003	0.0011	0.012	
Pureora	0.12	0.59	0.72	0.0033

Hollyford is solely responsible for significant variation in PC2 (Table III-14), while Zealandia, Pureora, and Hollyford represent the majority of significant variation in PC3 (Table III-15).

Table III-14 P-values from Kruskal-Wallis ANOVA pairwise comparison of PC2 between forest populations. Bold, red text indicates significant p-values ≤ 0.05 . Bold, italicised text indicates p-values close to 0.05.

PC2	Craigieburn	Eglinton	Hollyford	Zealandia
Eglinton	0.71			
Hollyford	0.045	0.03		
Zealandia	0.26	0.6	0.0077	
Pureora	0.055	0.19	0.0008	0.6

Table III-15 P-values from Kruskal-Wallis ANOVA pairwise comparison of PC3 between forest populations. Bold, red text indicates significant p-values ≤ 0.05 .

PC3	Craigieburn	Eglinton	Hollyford	Zealandia
Eglinton	0.13			
Hollyford	0.021	0.18		
Zealandia	0.0001	0.0001	≤ 0.0001	
Pureora	≤ 0.0001	≤ 0.0001	≤ 0.0001	0.83

Significant variation in PC4 is driven by Hollyford and Zealandia mandibles (Table III-16), while Hollyford, Zealandia, and Pureora are responsible for significant variation in PC5 (Table III-17).

Table III-16 P-values from Kruskal-Wallis ANOVA pairwise comparison of PC4 between forest populations. Bold, red text indicates significant p-values ≤ 0.05 . Bold, italicised text indicates p-values close to 0.05.

PC4	Craigieburn	Eglinton	Hollyford	Zealandia
Eglinton	0.89			
Hollyford	0.04	<i>0.074</i>		
Zealandia	0.0006	0.0044	<i>0.066</i>	
Pureora	0.64	0.72	<i>0.07</i>	0.0016

Table III-17 P-values from Kruskal-Wallis ANOVA pairwise comparison of PC5 between forest populations. Bold, red text indicates significant p-values ≤ 0.05 . Bold, italicised text indicates p-values close to 0.05.

PC5	Craigieburn	Eglinton	Hollyford	Zealandia
Eglinton	0.96			
Hollyford	0.019	<i>0.07</i>		
Zealandia	0.0003	0.017	0.0001	
Pureora	0.012	0.045	0.0003	0.14

Overall, Zealandia, Hollyford and Pureora mandibles are mostly responsible for significant variation in mandible shape across the PCA plot.

By genetic haplotype

The position of individual points on these PCA plots and the warped outline changes are the same as the previous plot; only the colour coding differs. Genetic haplotype assignment shows there is significant overlap of *domesticus* and *domesticus* – *castaneus*NZ.1 hybrid individuals on both axes (Figure III-J). However, there is clear separation of haplotype mean ellipses along the first principal axis (Figure III-K).

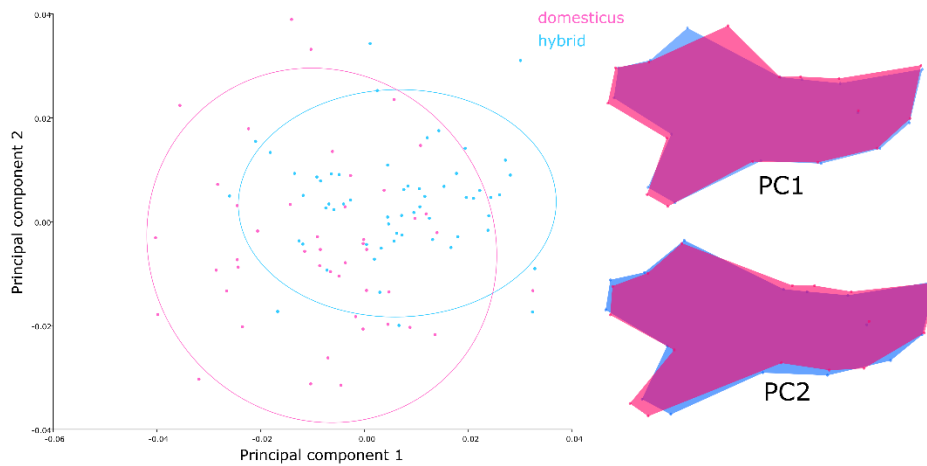


Figure III-J PCA plot of mandible shape differences between forest genetic haplotypes. Each dot represents a specimen, surrounded by equal frequency ellipses.

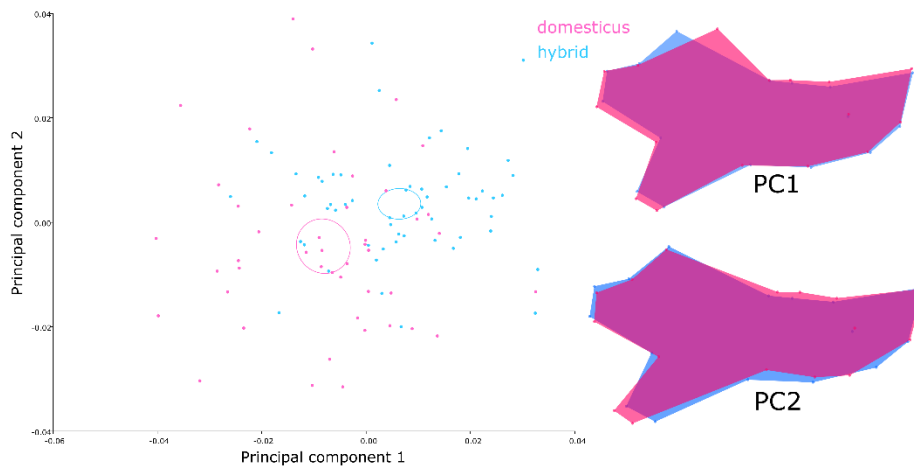


Figure III-K PCA plot of mandible shape differences between forest genetic haplotypes. Each dot represents a specimen, with 90% confidence ellipses around the mean.

3.5.2 Discriminant Function Analysis

The cross-validated DFA separated three groups with >95% accuracy (Table III-18). Figure X shows the Procrustes-based superimposition of mean mandible shape for the four locations with over 89% accuracy. The superimposition of Eglinton and Craigieburn reveals the two mean shapes are very similar (Figure III-L: A), so must significantly differ at their extreme mandible shapes. The same can be said for the superimpositions of Craigieburn – Pureora (Figure III-L: B), and Eglinton – Pureora (Figure III-L: C). The superimposition of Zealandia and Pureora, however, shows that Zealandia mean mandible shape has a broader alveolar profile, with slightly expanded coronoid and angular processes (Figure III-L: D).

Table III-18 Misclassification percentages of cross-validation discriminant function analysis for forest mandibles. Bold, red text indicates misclassification levels of $\leq 5\%$. Bold italicised text indicates $\leq 11\%$.

	Craigieburn	Eglinton	Hollyford	Zealandia
Eglinton	4.4			
Hollyford	22	34.4		
Zealandia	14.6	18.8	35.7	
Pureora	3.4	2	15.2	<i>10.9</i>

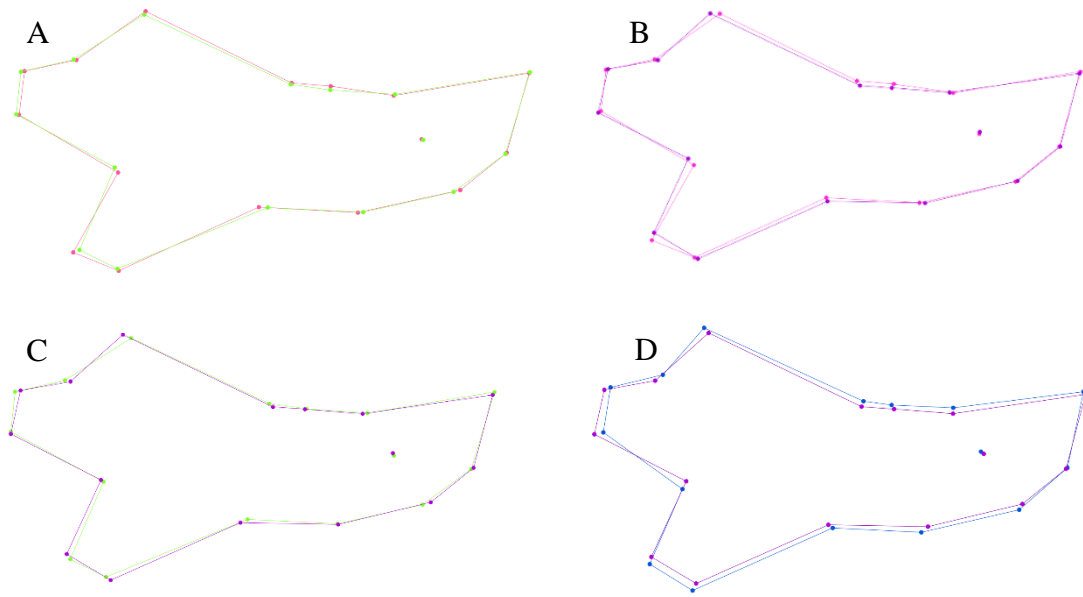


Figure III-L Procrustes-based superimposition of forest mean mandible shapes obtained from discriminant function analysis. A: Craigieburn (pink) and Eglinton (green), B: Craigieburn (pink) and Pureora (purple), C: Eglinton (green) and Pureora (purple), D: Pureora (purple) and Zealandia (blue).

By genetic haplotype

DFA separated *domesticus* and *domesticus* – *castaneus*NZ.1 hybrid groups with 98.1% accuracy and found significant variation between group means with both Procrustes and Mahalanobis distances (p-value ≤ 0.001 after 1000 permutations).

When overlaid with hybrid mean mandible shape, *domesticus* shows decreased distance between the condyle and coronoid processes, with a slightly broader angular process (Figure III-M).

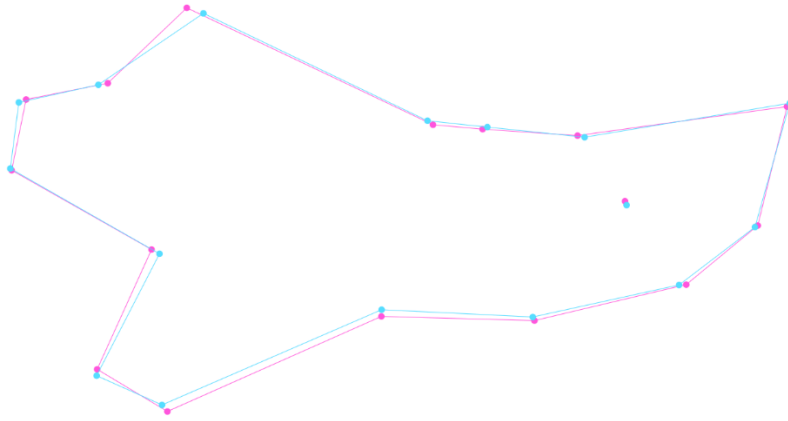


Figure III-M Procrustes-based superimposition of forest haplotype mean mandible shapes obtained from discriminant function analysis. *Domesticus* (pink) and hybrid (blue).

3.5.3 Canonical Variate Analysis

CVA effectively separates Zealandia and Pureora (North Island) from the other three populations (all South Island), overlapping together at the far right of the first canonical axis, and with no overlap on the second CV axis (Figure III-N). The other three populations cluster together on the left of the first canonical axis, and midway between Zealandia and Pureora on the second axis. The first CV represents 47.2% of the total variation, while CV2 accounts for 28.4% (Table III-19: A). Together, the first two CVs represent over 75% of the total variation between groups.

The CV1 warped outline plot depicts a broader mandible profile (pink outline), with an extended coronoid process and wider angular process associated with Zealandia and Pureora groups at the positive end of the first axis (Figure III-N). The slimmer mandible shapes (blue outline) are associated with the South Island groups (Craigieburn, Hollyford, and Eglinton).

The CV2 warped outline plot displays a change from Zealandia mandible shape (blue outline) to Pureora mandible shape (pink outline; Figure III-N). Zealandia mandibles have a broader alveolar and ramus profile, with a slightly shortened condyle process. Pureora mandibles have a slimmer alveolar profile, with smaller coronoid and angular processes, and an extended condyle process. The other three groups cluster between these two mandible shape extremes.

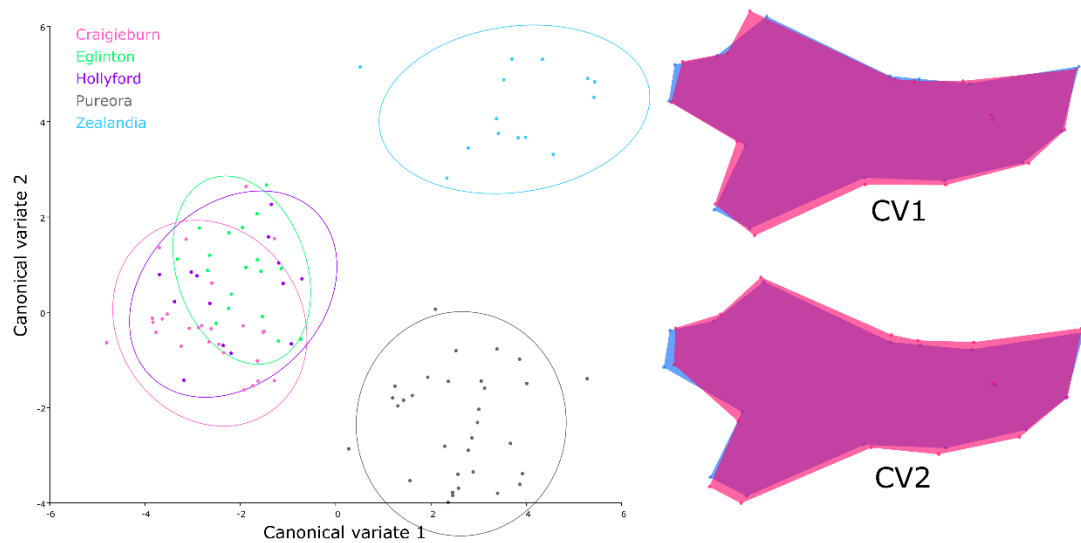


Figure III-N LEFT CVA plot displaying maximum differentiation of pre-defined forest groups with CV1 and CV2. RIGHT Procrustes deformation warped outlines depicting the change in mandible shape along each axis; blue represents mandible shape at far left of the axis, pink represents the mandible shape at far right of the axis.

The third canonical axis represents a differentiation of Eglinton to all other groups (Figure III-O). The CV3 warped outline plot shows reduced coronoid and angular processes with and extended condyle process associated with Eglinton mandibles (pink outline).

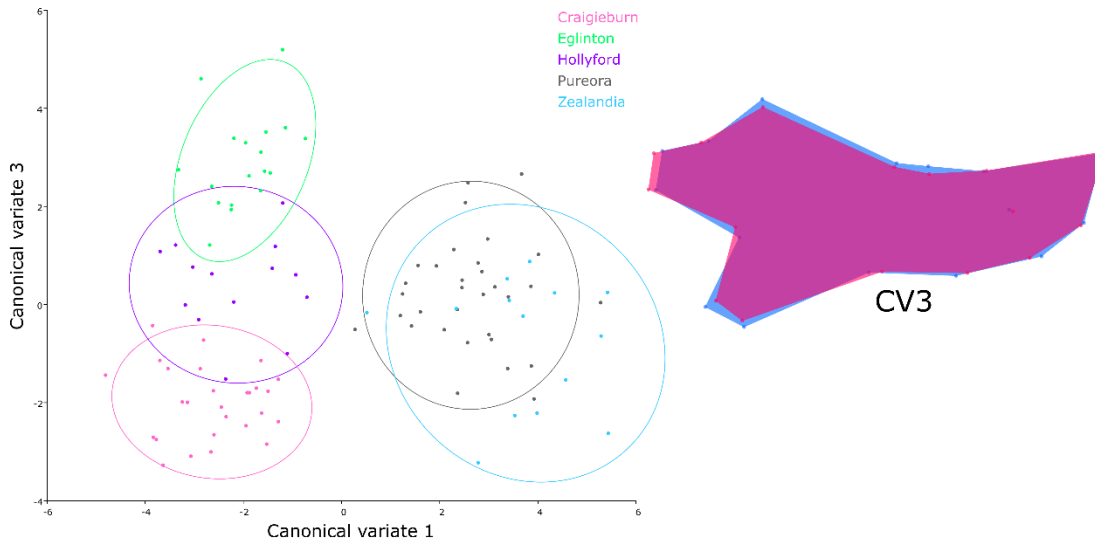


Figure III-O LEFT CVA plot displaying maximum differentiation of pre-defined forest groups with CV1 and CV3. RIGHT Procrustes deformation warped outlines depicting the change in mandible shape along each axis; blue represents mandible shape at far left of the axis, pink represents the mandible shape at far right of the axis.

The Mahalanobis distances and Procrustes distances of the first canonical axis were significantly different between all pairwise locations (Table III-19: B and C). The largest and smallest distances between groups mirror the separation of groups on the CVA and PCA plots. The largest Mahalanobis distance is between Zealandia and Craigieburn means. However, the largest Procrustes distance is between Zealandia and Eglinton means. The smallest Mahalanobis distance and Procrustes distance are observed between Hollyford and Craigieburn, which overlap significantly on the CV1 axis along with Eglinton.

Table III-19 Canonical Variate Analysis results for forest mandibles. A) Canonical variates and their associated variance percentages. B) Mahalanobis distances between groups along the first CV axis and their associated p-values. C) Procrustes distances between groups along the first CV axis and their associated p-values. Bold, red text indicates significant p-values ≤ 0.05 . Bold text indicates highest and lowest distance values between pairs.

A					
	CV1	CV2	CV3	CV4	
Eigenvalues	7.41934397	4.46420979	2.73746145	1.10594887	
Variance (%)	47.2	28.4	17.4	7.0	
Cumulative (%)	47.2	75.6	93.0	100	
B					
	Craigieburn	Eglinton	Hollyford	Zealandia	Pureora
Craigieburn		≤ 0.0001	≤ 0.0001	≤ 0.0001	≤ 0.0001
Eglinton	5.0983		≤ 0.0001	≤ 0.0001	≤ 0.0001
Hollyford	3.9854	4.2526		≤ 0.0001	≤ 0.0001
Zealandia	7.9227	7.6634	7.588		≤ 0.0001
Pureora	6.1155	6.3206	6.0354	6.7621	
C					
	Craigieburn	Eglinton	Hollyford	Zealandia	Pureora
Craigieburn		≤ 0.0001	0.0021	≤ 0.0001	≤ 0.0001
Eglinton	0.0237		≤ 0.0001	≤ 0.0001	≤ 0.0001
Hollyford	0.0181	0.0218		≤ 0.0001	≤ 0.0001
Zealandia	0.043	0.0494	0.0411		≤ 0.0001
Pureora	0.0283	0.03	0.0283	0.0378	

3.5.4 *Partial Least Squares Analysis*

The two block PLS analysis found a fairly weak but statistically significant correlation between the environmental and genetic covariates (block 1) and mandible shape (block 2) (RV coefficient 0.153, p-value < 0.0001 after 1000 permutations; Table III-20).

Only the first two PLS axes represented more than 5% covariation between the blocks. Rainfall (PLS1) had the greatest covariation with mandible shape, followed by highest altitude (PLS2). Along PLS1, lower rainfall coincided with a broader mandible shape (Zealandia, Pureora, Craigieburn; Figure III-P). Highest rainfall was associated with a depressed coronoid process and slimmer angular process (pink outline; Hollyford). Along PLS2, the highest altitude coincided with a slimmer angular process and alveolar region (pink outline; Craigieburn) in comparison to lower altitude locations (Figure III-Q). Singular and correlation values were significant for both PLS1 and PLS2.

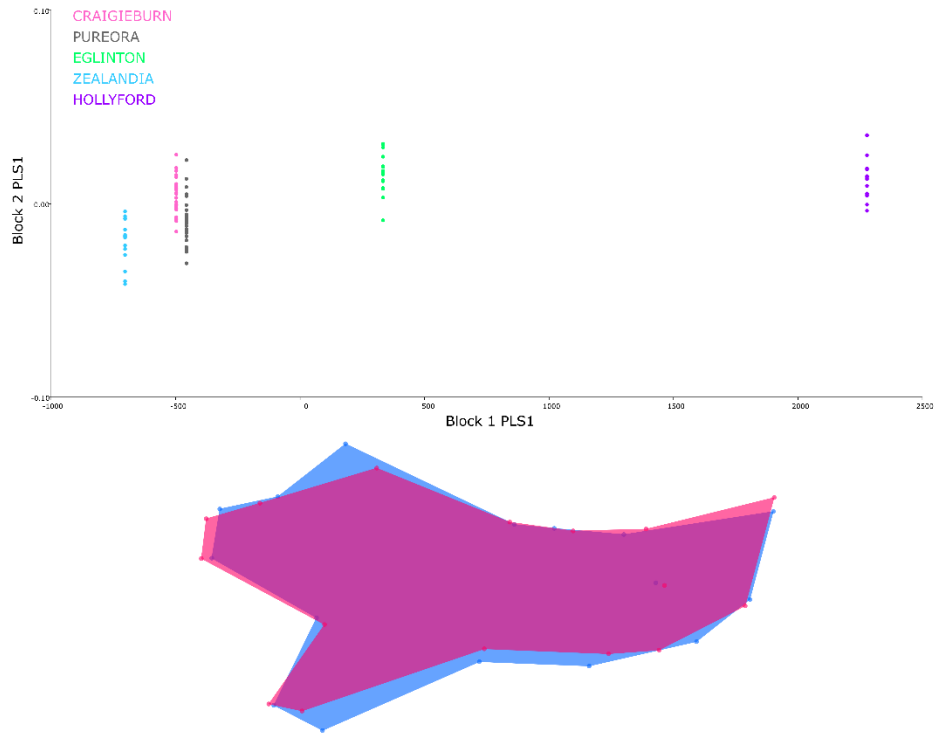


Figure III-P TOP PLS covariation of forest mouse mandible shape with rainfall. Each dot represents an individual specimen. BELOW Warped outline shape change with increasing rainfall.

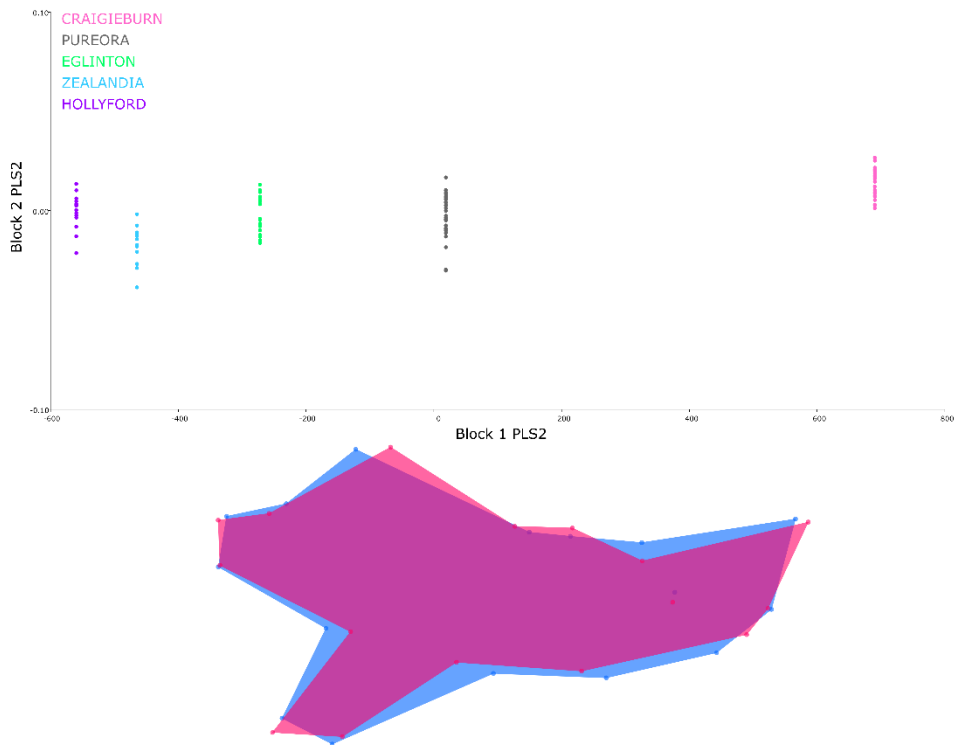


Figure III-Q TOP PLS covariation of forest mouse mandible shape with highest altitude. Each dot represents an individual specimen. BELOW Warped outline shape change with increasing altitude.

Table III-20 PLS forest loading scores for each covariate, correlation percentage of each PLS, and significance test results after 1000 permutations. Bold, red text indicates significant loading scores, covariation percentages, and p-values ≤ 0.05 .

	PLS1	PLS2	PLS3	PLS4	
RAIN	0.99774862	-0.02041439	0.0629174	-0.01091773	
GENETICS	-0.00024602	0.00075845	0.0035335	-0.02454434	
RATS	0.00034012	0.00064234	0.00347953	0.03670839	
HABITAT	0.000696	0.00085422	-0.00278669	0.04859566	
ALT HIGH	0.05055434	0.84970281	-0.52417989	0.00652337	
ALT LOW	-0.04305769	0.52676666	0.84732787	-0.0302503	
TEMP LOW	-0.00196007	-0.00063606	0.03264808	-0.13213894	
TEMP HIGH	-0.00858422	-0.00995521	-0.04055205	-0.96586339	
LATITUDE	0.00312925	0.00201138	-0.02386643	0.21037804	
	Singular value	P-value (perm.)	% total covar.	Correlation	P-value (perm.)
PLS1	7.8553729	<.0001	80.682	0.50445	<.0001
PLS2	3.7922158	<.0001	18.803	0.61089	<.0001
PLS3	0.62719825	<.0001	0.514	0.69855	<.0001
PLS4	0.02931746	<.0001	0.001	0.4765	0.0002

3.6 Discussion

This study found significant variation in body size and mandible shape between five samples of wild house mice living in different forest types of New Zealand.

Zealandia sanctuary mice had the most distinct mandible shape compared with all other populations.

Zealandia mandibles had the highest masseter mechanical advantage, and the lowest temporalis advantage. The masseter muscle is strongly correlated with molar mastication activity, and the processing of resistant, vegetative food (Satoh 1997; Michaux et al. 2007; Baverstock et al. 2013; Renaud et al. 2015). The shape variation associated with Zealandia mandibles repeatedly showed a broad mandible profile with a large angular process that is most efficient for processing tough plant material (Michaux et al. 2007; Anderson et al. 2014; Renaud et al. 2015). These characteristics suggest a diet higher in more resistant food compared with the Pureora and South Island populations. Zealandia mice were also the shortest in both head-body and tail length, but had the largest mandible centroid size. A larger mandible centroid size implies the Zealandia mice experience high mechanical loading on the jaw that may be associated with a resistant food diet (Anderson et al. 2014; Renaud et al. 2015).

Previous studies found house mice to prefer invertebrate prey (Copson 1986; McIntosh 2001; Le Roux et al. 2002; Angel et al. 2009; Renaud et al. 2015) and display increased body size in the absence of rats (Innes et al. 1995; Goldwater et al. 2012). My results do not support the consequent prediction that the mandibles of mice free of competition would be more typical of those feeding on softer foods, or that body size increases in the absence of rats. However, they do support recent findings by Samaniego-Herrera et al. (2017) that house mice on Pa'jaros Island

(Mexico) were smaller and consumed more seeds than house mice inhabiting Muertos Island (Mexico). Pa'jaros was covered in dense native grasses which provided burrowing habitat and abundant seeds. Comparatively, Muertos supported large seabird and purple crab (*Gecarcinus lateralis*) colonies that competed for burrowing habitat in the sparse shrub and herb cover, as well as providing nutritious food resources. The dense understory of the successional Zealandia forest likely provides burrowing and food resources similar to those observed on Pa'jaros Island, lending Zealandia mice to smaller body size with mandibles best adapted to processing plant material. Perhaps in a fenced wildlife sanctuary there is also more competition with birds for invertebrates, and in the absence of large mammalian herbivores (e.g. goats, pigs, deer etc.) there is more plant food available for mice to forage. This is, of course, entirely based on speculation, but presents an interesting topic for further investigation.

Pureora mandible shape appears to represent an intermediate dietary niche, but with a higher consumption of harder than softer foods due to their low temporalis advantage score. Pureora mandibles held significantly greater masseter/molar advantage than Craigieburn and Hollyford samples, but significantly lower advantage than Zealandia and Eglinton. Pureora mice were the lightest in body weight, and held the smallest mean mandible centroid size. They also had a smaller average head-body and tail length than most other locations. King et al. (1996) collected most mice from an area in Pureora Forest with dense ground cover, least frequented by rats. Competition and predation from rats could be confining Pureora mice to a smaller realised niche (Bridgman et al. 2013), constricting body size. Smaller body size may enable mice to

better hide and escape from rats in the dense ground cover, where edible vegetation and invertebrates are abundant (Yom-Tov et al. 1999; Goldwater et al. 2012).

Zealandia and Pureora clustered together along PC1, differentiated from the South Island populations. This separation of North and South Island individuals could reflect higher proportions of hard versus soft food in the diet of North and South Island mice respectively.

All three South Island populations clustered heavily on the PCA and CVA plots, often displaying longer or shifted condyle and coronoid processes, extending the distance of the temporalis inlever. The temporalis muscle acts to move the incisors into occlusion (Sato 1997; Michaux et al. 2007; Baverstock et al. 2013; Anderson et al. 2014; Renaud et al. 2015). The higher mechanical advantage of the temporalis muscle enables more efficient occlusion, thus creating more effective prey catchers. Interestingly, Eglinton mandibles also held the second highest masseter advantage score, suggesting these mice possess a mandible adept for processing both soft and hard food types. This implies Eglinton mice consume resistant food more regularly than Hollyford or Craigieburn mice. Most of Eglinton Valley is covered by beech forest, in comparison to Hollyford Valley where the beech forest cover is interspersed with exotic species. Craigieburn Forest is dominated by mountain beech.

A diet study conducted by Wilson & Lee (2010) on house mice inhabiting Fiordland *Chionochloa* alpine grassland found mice prey heavily on invertebrates such as weta and spiders during non-tussock-mast seed years. During the tussock mast, mice predominantly consumed seeds and caterpillars. Fitzgerald et al (1996) also observed a relationship between mice, Lepidoptera larvae and beech seedfall in Orongorongo

Valley. The increased number of beech flowers on the forest floor preceding a seed mast enabled greater recruitment of larvae that consume the nutritional flowers. Stomach analysis revealed Lepidoptera larvae were the most important component of the house mouse diet, suggesting mouse irruption is closely correlated to caterpillar density. The mice samples from Eglinton and Hollyford Valleys were collected shortly after a heavy seed mast, and Craigieburn mice were collected during a moderate seed masting year.

South Island house mice inhabiting beech forest presented mandible shapes most associated with soft food types, such as invertebrate prey (Renaud et al. 2015). Softer foods require less mechanical force to process, resulting in slimmer mandible profiles (Anderson et al. 2014; Renaud et al. 2015). Eglinton mice had the highest temporalis mechanical advantage, while Craigieburn and Hollyford had the lowest masseter advantages.

Craigieburn, Eglinton and Hollyford did not significantly differ in temporalis advantage, suggesting similarities in their consumption of soft food. With the lowest masseter/molar ratio score, Hollyford mice are certainly not as efficient at processing resistant foods as Eglinton mice. Craigieburn mice appear to have an intermediate phenotype, but possess a mandible shape more suited to catching prey than processing vegetation. Overall, South Island mice possess mandible shapes consistent with a diet based on softer food compared with North Island populations.

PLS analysis showed a significantly greater correlation between mandible shape and rainfall than with any other covariate, including haplotype and presence of rats.

Higher rainfall locations were associated with ‘soft food’ mandibles (Hollyford and

Eglinton). By contrast, lower rainfall areas coincided with mandibles more adept at processing resistant material (Zealandia). Pureora and Craigieburn clustered together on the PLS plot. Both locations represented intermediate mandible phenotypes.

However, covariation of mandible shape and rainfall is only consistent with patterns observed in the biomechanical analysis, and does not follow a latitudinal trend.

The observed trend between shape and rainfall could be tied to net primary productivity (McNab 2010; Huston & Wolverton 2011; Alhajeri & Stepan 2016). Higher annual rainfall is likely to result in elevated plant productivity that supports increased invertebrate density. Greater food availability in Eglinton and Hollyford habitats is consistent with the observed body size and mandible shape, and supports the ‘resource rule’ proposed by McNab (2010), further discussed as eNPP by Huston & Wolverton (2011).

Moreover, the separation pattern across PC2 makes little sense except in light of genetic haplotypes. Pureora and Craigieburn are both likely to be *domesticus* mice, while Hollyford, Eglinton and Zealandia are all assumed to be *domesticus* – *castaneus*NZ.1 hybrids. Renaud et al. (2012) observed laboratory-bred hybrid mouse mandibles to differ in both shape and size from parental groups, suggesting genetic background has a significant influence on mandible shape in the absence of environmental stimuli. Genetic haplotype discriminates between individuals accounting for 14.46% of shape variation with PCA. However, genetic background is not reflected in CVA, where the *groups* are plotted in the direction of most effective discrimination, but not necessarily in the direction of greatest difference. PCA with haplotype assignment showed a clear separation of *domesticus* and hybrid means, while DFA found both group means to differ significantly. It is unclear whether this

significance is actually related to genetic haplotype, but poses interesting questions for further research.

PC3 exaggerates the shape variation between the respective ‘hard food’ and ‘soft food’ mandibles of Zealandia and Eglinton mice. This separation of extreme mandible shapes on the PCA plot was reinforced by CVA where the greatest Mahalanobis distance was found between Eglinton and Zealandia populations. The greatest Procrustes distance, however, was found between Craigieburn and Zealandia, which is more representative of the two populations’ separation along the first PC axis. The smallest Mahalanobis and Procrustes distances were both observed between Craigieburn and Hollyford, suggesting these two populations have the most similar mandible shapes, despite their separation with rainfall on the PLS plot.

Differentiation along the second CV axis may be related to the absence of rats in Zealandia. If so, rats may be an effective tool for discriminating between predefined groups, but that was not apparent when comparing individuals using both PCA and PLS.

The groups with the most accurate cross-validated DFA were Craigieburn – Eglinton, Craigieburn – Pureora, and Eglinton – Pureora, suggesting these samples had the least within-group variation in mandible shape.

Eglinton house mice were the heaviest and had the longest tails, while Craigieburn held the longest head-body length. The larger bodies of South Island mice could be linked to a diet of invertebrates, or to increasing latitude i.e. Bergmann’s rule.

Many studies concur that latitude is a proxy for other environmental trends such as precipitation and temperature, and overall primary productivity (Yom-Tov and

Geffen 2006; Meiri et al. 2007; McNab 2010; Huston & Wolverton 2011; Alhajeri & Steppan 2016). Alhajeri & Steppan (2016) observed a weak correlation between body size with precipitation and temperature in a large scale rodent study between taxonomic orders. McNab (2010) and Huston & Wolverton (2011) argue that primary productivity is a greater influence on body size.

Regression analysis found body weight and length did not significantly vary with the same environmental variables. Latitude, lowest ambient temperature, and habitat explained the most variation in forest mouse body weight, while rat presence and highest ambient temperature represented that greatest variation in head-body length. Body weight exhibited a positive relationship with latitude, while body length increased with the inverse of highest temperature. Both observations support Bergmann's rule that body size increases with cooler climates. Body weight also varied significantly between podocarp and beech forests, the latter supporting heavier mice. It is unclear whether increasing body size is a result of cooler climate, or variation in diet that arises from different forest habitats. More than likely, both environmental variables and major dietary components co-vary with one another, affecting house mouse body size and mandible shape.

3.7 References

- Alhajeri BH, Steppan SJ 2016. Association between climate and body size in rodents: A phylogenetic test of Bergmann's rule. *Mammalian Biology - Zeitschrift für Säugetierkunde* 81(2): 219-225.
- Anderson P, Renaud S, Rayfield E 2014. Adaptive plasticity in the mouse mandible. *BioMed Central Evolutionary Biology* 14(85).
- Angel A, Wanless R, Cooper J 2009. Review of impacts of the introduced house mouse on islands in the Southern Ocean: are mice equivalent to rats? *Biological Invasions* 11(7): 1743-1754.
- Ashton KG, Tracy MC, de Queiroz A 2000. Is Bergmann's rule valid for mammals? *The American Naturalist* 156(4): 390-415.
- Baverstock H, Jeffery NS, Cobb SN 2013. The morphology of the mouse masticatory musculature. *Journal of Anatomy* 223(1): 46-60.
- Blick R, Bartholomew R, Burrell T, Burns KC 2008. Successional dynamics after pest eradication in the Karori Wildlife Sanctuary. *New Zealand Natural Sciences* 33: 3-14.
- Boyce MS 1978. Climatic variability and body size variation in the muskrats (*Ondatra zibethicus*) of North America. *Oecologia* 36(1): 1-19.
- Bridgman LJ, Innes J, Gillies C, Fitzgerald NB, Miller S, King CM 2013. Do ship rats display predatory behaviour towards house mice? *Animal Behaviour* 86(2): 257-268.
- Burnett CD 1983. Geographic and climatic correlates of morphological variation in *Eptesicus fuscus*. *Journal of Mammalogy* 64(3): 437-444.

- Caut S, Casanovas JG, Virgos E, Lozano J, Witmer GW, Courchamp F 2007. Rats dying for mice: Modelling the competitor release effect. *Austral Ecology* 32(8): 858-868.
- Choquenot D, Ruscoe WA 2000. Mouse population eruptions in New Zealand forests: the role of population density and seedfall. *Journal of Animal Ecology* 69(6): 1058-1070.
- Copson GR 1986. The diet of the introduced rodents *Mus musculus* and *Rattus rattus* on sub-Antarctic Macquarie Island. *Wildlife Research* 13(3): 441-445.
- Cuthbert RJ, Louw H, Lurling J, Parker G, Rexer-Huber K, Sommer E, Visser P, Ryan PG 2013. Low burrow occupancy and breeding success of burrowing petrels at Gough Island: a consequence of mouse predation. *Bird Conservation International* 23(2): 113-124.
- Fitzgerald BM, Efford MG, Karl BJ 2004. Breeding of house mice and the mast seeding of southern beeches in the Orongorongo Valley, New Zealand. *New Zealand Journal of Zoology* 31(2): 167-184.
- Fitzgerald BM, Daniel MJ, Fitzgerald AE, Karl BJ, Meads MJ, Notman PR 1996. Factors affecting the numbers of house mice (*Mus musculus*) in hard beech (*Nothofagus truncata*) forest. *Journal of the Royal Society of New Zealand* 26(2): 237-249.
- Geist V 1987. Bergmann's rule is invalid. *Canadian Journal of Zoology* 65(4): 1035-1038.
- Goldwater N, Perry GLW, Clout MN 2012. Responses of house mice to the removal of mammalian predators and competitors. *Austral Ecology* 37(8): 971-979.

- Hancock B 2008. The influence of ship rats (*Rattus rattus*) on the habitat preferences of the house mouse (*Mus musculus*). Unpublished Masters thesis, Victoria University of Wellington.
- Huston MA, Wolverton S 2011. Regulation of animal size by eNPP, Bergmann's rule, and related phenomena. *Ecological Monographs* 81(3): 349-405.
- Innes J, Warburton B, Williams D, Speed H, Bradfield P 1995. Large-scale poisoning of ship rats (*Rattus-rattus*) in indigenous forests of the North-Island, New-Zealand. *New Zealand Journal of Ecology* 19(1): 5-17.
- Jędrzejewski W, Jędrzejewska B 1996. Rodent cycles in relation to biomass and productivity of ground vegetation and predation in the Palearctic. *Acta Theriologica* 41(1): 1-34.
- King CM 1983. The relationships between beech (*Nothofagus* sp.) seedfall and populations of mice (*Mus musculus*), and the demographic and dietary responses of stoats (*Mustela erminea*), in three New Zealand forests. *Journal of Animal Ecology* 52(1): 141-166.
- King CM 1991. Age-specific prevalence and a possible transmission route for *Skrjabingylosis* in New Zealand stoats, *Mustela erminea*. *New Zealand Journal of Ecology* 15(1): 23-30.
- King CM, Gaukrodger DJ, Ritchie NA 2015. The drama of conservation : the history of Pureora Forest, New Zealand, Wellington : Department of Conservaton : Springer.
- King CM, Innes JG, Flux M, Kimberley MO, Leathwick JR, Williams DS 1996. Distribution and abundance of small mammals in relation to habitat in Pureora Forest park. *New Zealand Journal of Ecology* 20(2): 214-240.

- King CM, Alexander A, Chubb T, Cursons R, MacKay J, McCormick H, Murphy E, Veale A, Zhang H 2016. What can the geographic distribution of mtDNA haplotypes tell us about the invasion of New Zealand by house mice *Mus musculus*? *Biological Invasions* 18(6): 1551-1565.
- Le Roux V, Chapuis JL, Frenot Y, Vernon P 2002. Diet of the house mouse (*Mus musculus*) on Guillou Island, Kerguelen archipelago, Subantarctic. *Polar Biology* 25: 49-57.
- McIntosh AR 2001. The impact of mice on the Antipodes Islands. Antipodes Island Expedition; October - November 1995 Southland Conservancy. Wellington, New Zealand, Department of Conservation. Pp. 52-57.
- McNab BK 2010. Geographic and temporal correlations of mammalian size reconsidered: a resource rule. *Oecologia* 164: 13-23.
- Medina AI, Martı DA, Bidau CJ 2007. Subterranean rodents of the genus *Ctenomys* (Caviomorpha, Ctenomyidae) follow the converse to Bergmann's rule *Journal of Biogeography* 34: 1439-1454.
- Meiri S, Dayan T 2003. On the validity of Bergmann's rule. *Journal of Biogeography* 30(3): 331-351.
- Meiri S, Yom-Tov Y, Geffen E 2007. What determines conformity to Bergmann's rule? *Global Ecology & Biogeography* 16: 788-794.
- Michaux J, Chevret P, Renaud S 2007. Morphological diversity of Old World rats and mice (Rodentia, Muridae) mandible in relation with phylogeny and adaptation. *Journal of Zoological Systematics and Evolutionary Research* 45(3): 263-279.

- Murphy EC 1992. The effects of a natural increase in food-supply on a wild population of house mice. *New Zealand Journal of Ecology* 16(1): 33-40.
- Norton D, Kelly D 1988. Mast seeding over 33 years by *Dacrydium cupressinum* Lamb.(rimu)(Podocarpaceae) in New Zealand: the importance of economies of scale. *Functional ecology*: 399-408.
- O'Donnell CF, Weston KA, Monks JM 2017. Impacts of introduced mammalian predators on New Zealand's alpine fauna. *New Zealand Journal of Ecology* 41(1): 01-22.
- Renaud S, Alibert P, Auffray JC 2012. Modularity as a source of new morphological variation in the mandible of hybrid mice. *BioMed Central Evolutionary Biology* 12: 16.
- Renaud S, Gomes Rodrigues H, Ledevin R, Pisanu B, Chapuis J-L, Hardouin EA 2015. Fast evolutionary response of house mice to anthropogenic disturbance on a Sub-Antarctic island. *Biological Journal of the Linnean Society* 114(3): 513-526.
- Rodríguez MÁ, López-Sañudo IL, Hawkins BA 2006. The geographic distribution of mammal body size in Europe. *Global Ecology & Biogeography* 15: 173-181.
- Ruscoe WA, Murphy EC 2005. House Mouse. In: King CM ed. *The Handbook of New Zealand Mammals*. 2nd ed. Melbourne, AUS, Oxford University Press.
- Ruscoe WA, Wilson D, McElrea L, McElrea G, Richardson SJ 2004. A house mouse (*Mus musculus*) population eruption in response to rimu (*Dacrydium cupressinum*) seedfall in southern New Zealand. *New Zealand Journal of Ecology* 28(2): 259-265.

- Ruscoe WA, Ramsey DSL, Pech RP, Sweetapple PJ, Yockney I, Barron MC, Perry M, Nugent G, Carran R, Warne R and others 2011. Unexpected consequences of control: competitive vs. predator release in a four-species assemblage of invasive mammals. *Ecology Letters* 14(10): 1035-1042.
- Samaniego-Herrera A, Clout MN, Aguirre-Muñoz A, Russell JC 2017. Rodent eradications as ecosystem experiments: a case study from the Mexican tropics. *Biological Invasions*: 1-19.
- Satoh K 1997. Comparative functional morphology of mandibular forward movement during mastication of two murid rodents, *Apodemus speciosus* (Murinae) and *Clethrionomys rufocanus* (Arvicolinae). *Journal of Morphology* 231: 131-142.
- Searle JB, Jamieson PM, Gündüz I, Stevens MI, Jones EP, Gemmill CEC, King CM 2009. The diverse origins of New Zealand house mice. *Proceedings of the Royal Society B: Biological Sciences* 276(1655): 209-217.
- Wilson DJ, Lee WG 2010. Primary and secondary resource pulses in an alpine ecosystem: snow tussock grass (*Chionochloa* spp.) flowering and house mouse (*Mus musculus*) populations in New Zealand. *Wildlife Research* 37(2): 89-103.
- Yom-Tov Y, Geffen E 2006. Geographic variation in body size: the effects of ambient temperature and precipitation. *Oecologia* 148: 213-218.
- Yom-Tov Y, Yom-Tov S, Moller H 1999. Competition, coexistence, and adaptation amongst rodent invaders to Pacific and New Zealand Islands. *Journal of Biogeography* 26(5): 947-958.

IV. Comparison of house mice inhabiting New Zealand offshore islands

4.1 Introduction

This chapter compares the mandibles and body measurements of house mice collected from six offshore New Zealand islands (Figure IV-A). Island environments provide opportunities along lines of selection not previously experienced by mainland populations, e.g., differences in available resources and distribution of competitors and predators, that can lead to rapid, if not substantial, evolutionary change shortly after colonisation (Renaud & Auffray 2010; Millien 2006, 2011; Martínková et al. 2013; Cucchi et al. 2014; Gray et al. 2015). Genetic drift and founder effects can also have a major influence on allelic frequency, especially on isolated islands where gene-flow is not present, creating low genetic variation (Pergams & Ashley 2001; Martínková et al. 2013). The remoteness of many New Zealand offshore islands ensures isolation of distinct populations, creating a unique opportunity to investigate the adaptive response of house mice in separate insular settings.

Anderson et al. (2014) showed that captive mice fed on a hard/resistant food resource developed mandible characteristics different from those of mice fed on a diet of softer foods. Again, this observation leads to the prediction that biomechanical advantage and mandible shape of mice should vary between island mouse populations, presumably with the availability of invertebrates and plant material (see CH III).

Over time, the individuals with the most efficient jaw shape suited to a specific island environment are likely to have greater fitness and increase the frequency of this phenotype in subsequent generations. Renaud et al. (2015) investigated mandible changes in house mice that colonised sub-Antarctic Guillo Island two centuries ago. They observed functional changes in the mandible as the colonising population adapted to local food sources, incorporating a greater portion of invertebrates into the diet compared with two Western-Europe populations, supporting previous studies on the diets of insular mice (Copson 1986; Le Roux et al. 2002; Smith et al. 2002; Renaud et al. 2013). As expected, the softer invertebrate-based diet resulted in a mandible shape characterized by smaller muscle attachment processes (Renaud & Auffray 2010; Anderson et al. 2014). Guillo I. mice had significantly shorter body length and smaller mandibles than their continental counterparts, but did not differ in body weight.

The invasion of islands by small continental mammals is often followed by an increase in body size, commonly referred to as the island rule or syndrome (Foster 1964; Adler & Levins 1994; Pergams & Ashley 2001; Millien & Damuth 2004; Lomolino 2005; McNab 2010; Lomolino et al. 2012; Martínková et al. 2013). This change in body mass is typically attributed to resource abundance, which can be influenced by a number of environmental factors including climate and island size (Yom-Tov & Geffen 2006; Medina et al. 2007; Millien 2011; Lomolino et al. 2012; Cucchi et al. 2014). For this reason, the island rule is often studied in conjunction with Bergmann's rule, using latitude as a proxy for climatic variables (see CH III) (Lomolino et al. 2012; Cucchi et al. 2014). Mouse body size is also known to vary with competition and predation, particularly by rats, as they compete for resources

and are restricted to particular activity periods (Innes et al. 1995; Lomolino 2005; Caut et al. 2007; Hancock 2008; McNab 2010; Ruscoe et al. 2011; Goldwater et al. 2012; Bridgman et al. 2013). Lomolino et al. (2012) found a combination of small island size, remoteness, and lack of other mammalian competitors or predators resulted in the largest body size attainable by small mammals on islands (see also Millen 2011).

The house mouse arrived on all the islands presented in this study at least 100 years ago. Past studies on insular rodent populations show that 100 years is enough time for phenotypic changes to develop, especially in the face of substantial habitat differences and genetic drift (Millien 2006; Renaud & Auffray 2010; Millen 2001; Renaud et al. 2013; Cucchi et al. 2014; Renaud et al. 2015). The present study investigates the body size and mandible shape of house mice facing different environmental conditions on the following offshore islands: Antipodes I., Auckland I., Enderby I., Ruapuke I., Waikawa I., and Chatham I.

4.2 Material

The six samples available are described in Table IV-1, with any published data available for them (Table IV-2). The islands are all situated at least 500km apart, with the exception of Auckland I. and Enderby I. that are separated by less than one kilometre (Figure IV-A).

Ruapuke Island

House mice reached Ruapuke I. when the *Elizabeth Henrietta* stranded on the Foveaux Strait island in 1824 (Miskelly 2013; King 2016). The mice that colonised Ruapuke I. are haplotype *domesticus*NZ.19 of Clade C, affiliated with Spain (Searle et al. 2009). The only other incursion of Clade C in the New Zealand archipelago is a *domesticus* population on Antipodes I. more than 800km away, suggesting the Ruapuke I. population has lived in isolation for nearly 200 years. Ruapuke I. was mostly cleared of its native forest for farmland, and is privately owned by descendants of the Kai Tahu chief Tuhawaiki (Miskelly 2013).

Antipodes Island

The Antipodes Islands, 800km south of the New Zealand coast, were discovered in 1800 by Captain Waterhouse of the H.M.S Reliance (Warham & Johns 1975). They make up one of several volcanic, offshore archipelagos that are collectively named the sub-Antarctic Islands (Warham & Johns 1975; Taylor 2006; Russell 2012; Phillips 2013), which include the Auckland, Bounty, Campbell, and Snares Island groups. The high level of biodiversity and endemism on these islands have led to their World Heritage status.

Antipodes I. is the largest island, mostly covered in low vegetation consisting of *Poa litorosa* tussock, *Carex* sedges, ferns and megaherbs (Godley 1989; Taylor 2006; Russell 2012; Rance 2015). The flora is most dense at low-lying coastal regions, dominated by tall *Poa litorosa* and ferns. The resident house mice were the only invasive mammal species on the island up until late 2016, when the population was eradicated. The Antipodes I. mice are haplotype *domesticus*NZ.8, Clade C, and are found nowhere else in the New Zealand archipelago (Searle et al. 2009).

There is much speculation about the first introduction of the house mouse on Antipodes I. It is possible the mice arrived with the first sealers from Sydney in the early 1800s (Taylor 2006; Russell 2012; King 2016). However, Ruapuke I. is the only other Clade C incursion; the other sub-Antarctic island groups are all dominated by Clade E mice. The lack of Clade C mice on any other island suggests they did not coincide with Clade E mice on any of the usual sealing ships. Russell (2012) speculates the invaders on Antipodes I. may have originated from a shipwreck around the turn of the 20th century. Mice were not recorded on the island until 1907 (McIntosh 2001; Russell 2012), however it could be they were simply not observed by earlier visitors.

Antipodes I. was the only site where two separate locations on the island were sampled: Anchorage Bay and North Plains. These two populations differed significantly only in the biomechanical advantage analysis. The two sample sites are combined for all other analyses.

Auckland and Enderby Islands

The Auckland Islands, including Auckland I. and Enderby I., were discovered in 1806 by the whaling brig *Ocean* (Taylor, 1971). During attempts to farm the islands, various mammalian pests were introduced to the Auckland group, including sheep, cattle, goats, pigs, cats, dogs, rabbits, rats, and house mice (Falla 1965; Taylor 1971; Higham & New Zealand. Dept. of Conservation 1999). The sub-Antarctic islands were also popular sealing sites during the early 19th century, providing ample opportunity for house mouse invasions (Higham & New Zealand. Dept. of Conservation 1999; Harper 2010; King 2016). Farming was abandoned in the early 20th century, but had already caused severe modification to original native flora (Torr 2002). In 1934 the islands were made reserves, and are now virtually pest free (Taylor 1971; Russell & Broome 2016). The mouse population inhabiting Auckland I. belongs to *domesticus*NZ.5, Clade E, haplotypes. The Enderby I. population was not haplotyped before their eradication in 1993. However, the proximity of the Enderby I. population to Auckland I. (less than one kilometre) suggests they are likely to be of the same genetic origin.

The vegetation on Enderby I. is characterised by highland rata forest, *Cassinia* scrub, *Bulbinella* and remnant *Poa litorosa* tussock, and large areas of “short lawn-like vegetation” probably induced by grazing mammals (Taylor 1971; Torr 2002). On Auckland I., rata forest frames the coastline, giving way to lowlands and highlands dominated by scrubland and *Chionochloa* tussock grassland (Godley 1965). The climate is bleak, dominated by strong winds, rain, and frequent cloud cover (Taylor 1971; Higham & New Zealand. Dept. of Conservation 1999).

Chatham Island

House mice inhabiting Chatham I. are the only representatives of the *castaneus*NZ.2 haplotype so far known in the New Zealand archipelago (Searle et al. 2009; King et al. 2016). The colonists must have reached Chatham I. via a Pacific Asian trading route, but the date of invasion is not known (King 2016). The first recorded sighting of the Chatham Islands was by Lieutenant William R. Broughton in 1791, followed by sealers from Sydney in the early 1800s (King 2008). Before human colonisation, most of the island was covered by endemic flora such as swamp grass, ferns, rushes, and sedges (Dugdale & Emberson 2008). The remnant forests are dominated by kopi, matipo, akeake and karamu species, with local communities of nikau, Chatham ribbonwood and kowhai (Dugdale & Emberson 2008). The southern region of the island is characterised by peat soil, supporting ferns, rushes, with small tarahinau and pouteretere forest patches. Sheep farming was introduced in 1842, and the native flora has since been confined to fragmented conservation areas. The climate is cool temperate, with frequent gale force winds.

Waikawa Island

Waikawa I., one kilometre off the east coast of the North Island, was discovered by Maori around 600 years ago (Bradley et al. 2017). The name refers to the salty nature of the island's water springs. The island was a centre of learning for the Maori. In 1791, Waikawa I. was sighted by Captain Cook during his navigation of the East Coast, and subsequently named Portland Island. A whaling station was erected during the 1840s, followed by a lighthouse in 1878 to safeguard shipping routes around the point. The transport of supplies required for these commissioned buildings provided ample opportunity for house mouse invasion onto Waikawa I. The lighthouse keepers

were self-sufficient on the island, and kept a few sheep and dairy cows on their allotted 17 acres. The remaining 300 acres were leased as farmland, and have remained privately owned over the last century. The mice inhabiting Waikawa I. did not coexist with rats until recent incursions were discovered by DOC (Bradley et al. 2017). Bradley et al. (2017) observed Waikawa mice to be heavier on average than mice from the mainland areas surrounding the island. The Waikawa I. mouse population is made up of four different *domesticus* haplotypes: domNZ.12, domNZ.14, domNZ.23, and domNZ.24 (Bradley et al. 2017). DomNZ.23 and 24 were not observed in the mainland samples collected by Bradley et al (2017), and may represent strains unique to the island. Waikawa I. samples had the lowest nucleotide diversity, and were significantly differentiated from all other locations, suggesting a lack of gene flow between the island and mainland mice.



Figure IV-A Map of the New Zealand offshore islands included in this study. Drawn up by Max Oulton, University of Waikato.

Table IV-1 Published and raw body measurements of adult mice on New Zealand offshore islands (mean \pm SD).

	Weight (g)	n	Total length (mm)	n	Head-body length (mm)	n	Reference
Antipodes I.	22.1 \pm 3.5	59	172.9 \pm 9.7	36	84.8 \pm 5.0	47	Ruscoe & Murphy (2005), Russell (2012)
Enderby I.	24.9 \pm 1.7	16	180.7 \pm 6.9	16	93.8 \pm 3.0	16	Ruscoe & Murphy (2005), Torr (2002)
Auckland I.	M: 23.1 \pm 2.8 F: 22.5 \pm 1.5	18, 10			M: 92.9 \pm 8.5 F: 90.3 \pm 2.6	18, 10	Harper (2010)
Ruapuke I.							
Chatham I.			136.4 \pm 14.9	7	70.6 \pm 7.9	7	Tanya Chubb (unpublished)
Waikawa I.	20.3 \pm 7.5	10	Tail: 81.7 \pm 7.7	10	81.5 \pm 10.2	10	Bradley et al (2017)
	Weight (g)	n	Tail length (mm)	n	Head-body length (mm)	n	
Antipodes I.	20.95 \pm 3.5	80	82.7 \pm 5.8	43	86.3 \pm 5.2	43	
Enderby I.	22.4 \pm 3.5	45	87.5 \pm 11.3	45	82.6 \pm 12.8	44	
Auckland I.							
Ruapuke I.	19.3 \pm 2.4	6	78.7 \pm 8.3	6	75.8 \pm 4.0	6	
Chatham I.	14.6 \pm 3.8	8	72.3 \pm 8.6	8	76.8 \pm 6.5	8	
Waikawa I.	21.5 \pm 6.7	9	83.3 \pm 9.0	9	83.3 \pm 6.0	9	

Table IV-2 Environmental variables associated with each island habitat.

	Latitude - Longitude	Area (ha)	Rats	Habitat	Annual Rainfall (mm)	Reference
Antipodes I.	49.6643° S, 178.7756° E	2097	No	Tussock and small shrub	650	Ruscoe & Murphy (2005), Russell (2012)
Enderby I.	50.4978° S, 166.2956° E	710	No	Tussock and rātā	1500	Ruscoe & Murphy (2005), Torr (2002)
Auckland I.	50.6218° S, 166.1196° E	45 975	No	Tussock, shrubland, rata	1500	Harper (2010)
Ruapuke I.	46.7673° S, 168.5173° E	1525	Yes	Farmland	1194	
Chatham I.	44.0237° S, 175.9305° W	90 650	Yes	Native forest and farmland	1080	Tanya Chubb (unpublished)
Waikawa I.	39.2934° S, 177.8673° E	120	No	Farmland	1130	Bradley et al (2017)

4.3 Traditional measurements

4.3.1 Body Weight

Significant inter-island variation in body weights were found only in the Enderby I. and Chatham I. populations (Table IV-3; Figures IV-B and IV-C). The Auckland I. population is not included in these Kruskal-Wallis ANOVA analyses as raw data was not available; however, mean values for weight and head-body length published by Harper (2010) show that male Auckland I. mice were the largest. Enderby I. mice tended to be somewhat lighter than the male Auckland I. mice, but similar to Auckland I. female body weight, only 1 km away (Figure IV-B). Enderby I. mice were significantly heavier than Chatham I., Ruapuke I. and Antipodes I. mice, while Chatham I. mice were the lightest (Figure IV-C).

Table IV-3 P-values from Kruskal-Wallis ANOVA pairwise comparison of offshore island mouse body weight. Bold, red text indicates significant p-values ≤ 0.05 . Bold italicised text indicates p-values close to 0.05.

WEIGHT	Antipodes	Chatham	Waikawa	Enderby
Chatham	≤ 0.0001			
Waikawa	0.32	<i>0.067</i>		
Enderby	0.02	≤ 0.0001	0.75	
Ruapuke	0.19	0.033	0.29	0.03

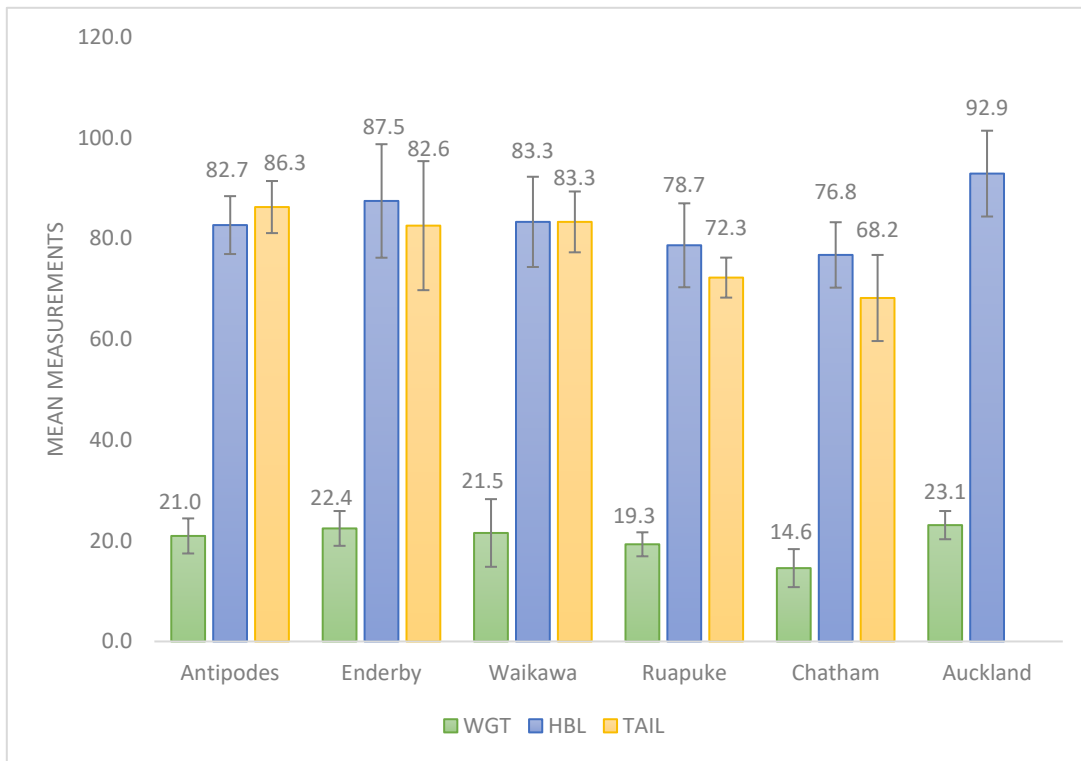


Figure IV-B Histogram showing mean body weight, tail length, and head-body length values between offshore island mouse populations.

4.3.2 Head-Body Length

Significant variation in head-body lengths did not match exactly the variation in body weight (Table IV-4). Enderby I. and Auckland I. mice (both male and female) were the longest (Figures IV-B and IV-C), while Chatham I. mice were the shortest.

Table IV-4 P-values from ANOVA pairwise comparison of offshore island mouse head-body length. Bold, red text indicates significant p-values ≤ 0.05 . Bold italicised text indicates p-values close to 0.05.

HBL	Antipodes	Chatham	Waikawa	Enderby
Chatham	0.0019			
Waikawa	0.85	0.083		
Enderby	≤ 0.0001	0.0002	0.09	
Ruapuke	0.07	0.605	0.35	0.014

4.3.3 Tail Length

All but three pairwise comparisons produced significant p-values for tail length (Table IV-5). Antipodes I. mice had the longest average tail length. Chatham I. tails were the shortest, but did not significantly differ to Ruapuke I. tails (Figures IV-B and IV-C).

Table IV-5 P-values from ANOVA pairwise comparison of offshore island mouse tail length. Bold, red text indicates significant p-values ≤ 0.05 .

TAIL	Antipodes	Chatham	Waikawa	Enderby
Chatham	≤ 0.0001			
Waikawa	0.15	0.016		
Enderby	0.05	0.0001	0.77	
Ruapuke	0.0005	0.245	0.018	0.0036

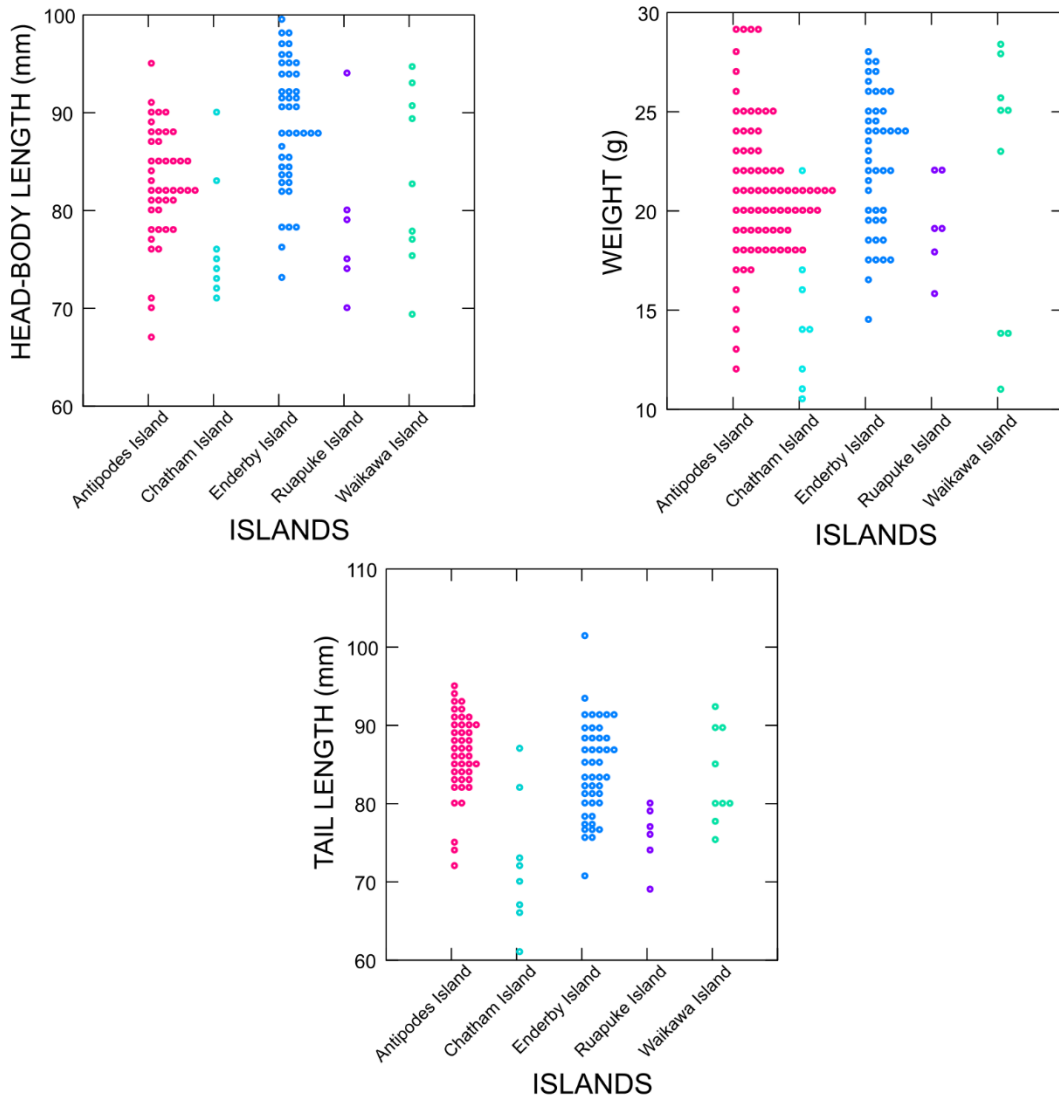


Figure IV-C Dot density plots representing the distribution of body weight, tail length, and head-body length values within offshore populations. Each icon corresponds to an individual mouse.

4.3.4 Regression

Body weight varied significantly with all covariates except lowest temperature (Table IV-6). By contrast, only island size, rainfall, and highest temperature varied significantly with head-body length. Island size explained the most variation in both body weight and head-body length between islands.

Table IV-6 Predicted percentage scores for each island variable. Bold, red text indicates significant regression p -values ≤ 0.05 .

Regression %	Weight	Head-body length
Rainfall	12.6	11.3
Genetics	3.62	0.13
Presence of rats	11.6	0.17
Temp low	2.6	2.29
Temp high	19.5	8.6
Latitude	3.9	1.52
Island size	40.1	20.85

4.5 Biomechanical analysis

Significant inter-island variation in the masseter/incisor (M/I) ratio were found between Chatham I. and Enderby I. mandibles compared with all other populations (Table IV-7). Enderby I. held the highest M/I advantage (0.482), and Chatham I. had the lowest (0.437). The order of mechanical advantage from highest to lowest: Enderby, Anchorage Bay, Auckland, Ruapuke, North Plains, Waikawa, and Chatham.

Table IV-7 P-values from Kruskal-Wallis ANOVA pairwise comparison of the masseter/incisor biomechanical advantage ratio for offshore island mandibles. Bold, red text indicates significant p-values ≤ 0.05 . Bold italicised text indicates p-values close to 0.05.

Masseter/Incisor	North Plain	Anchorage Bay	Chatham	Enderby	Waikawa	Auckland
Anchorage Bay	0.026					
Chatham	0.04	0.003				
Enderby	≤ 0.0001	0.02	0.0001			
Waikawa	0.73	0.014	0.051	≤ 0.0001		
Auckland	0.006	0.95	0.0008	0.0005	0.0012	
Ruapuke	0.41	0.33	0.05	0.0044	0.12	0.11

Significant variation in masseter/molar (M/M) ratio (Table IV-8) did not exactly match the variation in M/I. Enderby I. still held the higher biomechanical advantage for the M/M ratio (0.872), while Chatham I. scored the lowest (0.813). Enderby I. mandibles did not differ significantly to Anchorage bay and Ruapuke I. All pairwise comparisons for Chatham I. mandibles produced significant p-values except for Waikawa I. In order of mechanical advantage: Enderby, Ruapuke, Anchorage Bay, North Plains, Auckland, Waikawa, and Chatham.

Table IV-8 P-values from Kruskal-Wallis ANOVA pairwise comparison of the masseter/molar biomechanical advantage ratio for offshore island mandibles. Bold, red text indicates significant p-values ≤ 0.05 .

Masseter/Molar	North Plain	Anchorage Bay	Chatham	Enderby	Waikawa	Auckland
Anchorage Bay	0.39					
Chatham	0.0075	0.011				
Enderby	0.0082	0.23	0.0007			
Waikawa	0.019	0.017	0.28	0.0001		
Auckland	0.78	0.48	0.012	0.017	0.014	
Ruapuke	0.19	0.65	0.011	0.67	0.0079	0.25

Significant p-values in the temporalis/incisor ratio (T/I) arose from variation in the Enderby I., Chatham I., Auckland I. and Ruapuke I. mandibles (Table IV-9).

Chatham I. held the highest advantage (0.223). while Enderby I. had the lowest (0.186). In order of mechanical advantage: Chatham, Anchorage Bay, North Plains, Waikawa, Auckland, Ruapuke, and Enderby.

Table IV-9 P-values from Kruskal-Wallis ANOVA pairwise comparison of the temporalis/incisor biomechanical advantage ratio for offshore island mandibles. Bold, red text indicates significant p-values ≤ 0.05 .

Temporalis/Incisor	North Plain	Anchorage Bay	Chatham	Enderby	Waikawa	Auckland
Anchorage Bay	0.53					
Chatham	0.19	0.17				
Enderby	≤ 0.0001	≤ 0.0001	0.0003			
Waikawa	0.14	0.36	0.021	0.024		
Auckland	0.0033	0.0003	0.0006	0.029	0.57	
Ruapuke	0.011	0.0037	0.0038	0.73	0.19	0.34

The same pattern was observed between the temporalis/molar (T/M) ratio (Table IV-10) and T/I ratio (Table IV-9). Once more, Chatham I. held the highest mechanical advantage ratio (0.414), and Enderby I. the lowest (0.335). In order of mechanical advantage: Chatham, North Plains, Anchorage Bay, Waikawa, Auckland, Ruapuke, Enderby.

Table IV-10 P-values from Kruskal-Wallis ANOVA pairwise comparison of the temporalis/molar biomechanical advantage ratio for offshore island mandibles. Bold, red text indicates significant p-values ≤ 0.05 . Bold italicised text indicates p-values close to 0.05.

Temporalis/Molar	North Plain	Anchorage Bay	Chatham	Enderby	Waikawa	Auckland
Anchorage Bay	0.83					
Chatham	0.3	0.08				
Enderby	≤ 0.0001	≤ 0.0001	0.0001			
Waikawa	<i>0.052</i>	0.076	0.014	0.0071		
Auckland	0.0003	0.0003	0.0005	0.018	0.48	
Ruapuke	0.011	0.017	0.0055	0.19	0.41	0.92

Overall, on Enderby I. the masseter muscle had the highest mechanical advantage, and the temporalis muscle the lowest. Conversely, on Chatham I. the masseter muscle had the lowest mechanical advantage, and the temporalis muscle the highest.

4.6 Centroid size

Kruskal-Wallis ANOVA results found that Antipodes I. and Chatham I. had the smallest average mandible centroid size, significantly different from all other offshore islands (IV-11; Figure IV-D). Enderby I. had the largest mandible centroid size.

Under regression, centroid size did not vary significantly with weight (0.002%, p-value 0.96) or head-body length (2.12%, p-value 0.13).

Table IV-11P-values from Kruskal-Wallis ANOVA pairwise comparison of offshore island mandible centroid size. Bold, red text indicates significant p-values ≤ 0.05 .

Centroid size	Auckland	Chatham	Enderby	Ruapuke	Waikawa
Chatham	0.0002				
Enderby	0.67	≤ 0.0001			
Ruapuke	0.97	0.0009	0.4		
Waikawa	0.8	0.0024	0.3	0.97	
Antipodes	≤ 0.0001	0.023	≤ 0.0001	0.0001	0.0005

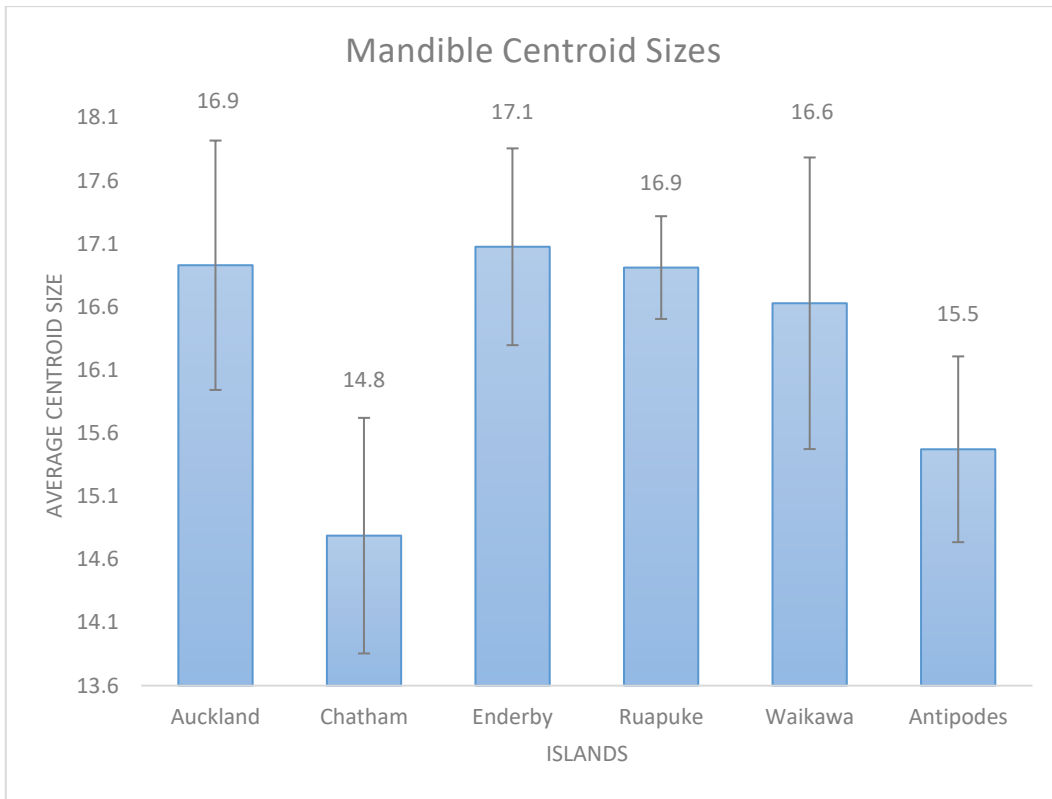


Figure IV-D Histogram showing average centroid size values between offshore island populations.

4.7 Shape analysis

4.7.1 Regression and Principal Component Analysis (PCA)

By location

The pooled within-group regression was significant for allometry ($p \leq 0.0001$ after 1000 permutations), with size accounting for 11.13% of shape variance (Figure IV-E).

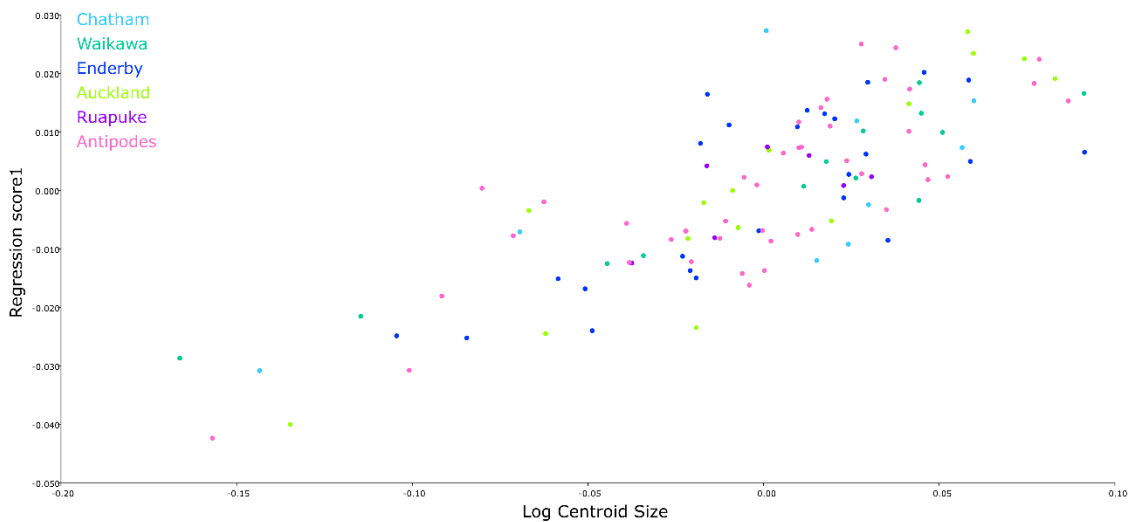


Figure IV-E Group-centred regression of offshore island mandible shape on log centroid size.

The first seven principal components (PCs) of the PCA represent >5% variance, accumulating to a total of 66.91% (Table IV-12). Only the first two eigenvalues were above the inflection point of the scree plot (Figure IV-F). It is unlikely that the other five have any biological significance so are not discussed.

Table IV-12 Eigenvalues for the offshore island PCA plot that represent more than 5% variance. Eigenvalues above the 'lee' point on the scree plot are italicised.

	EV1	EV2	EV3	EV4	EV5	EV6	EV7
Eigenvalues	<i>0.000178</i>	<i>0.000169</i>	0.000103	0.0000993	0.0000871	0.00007233	0.00006683
Variance (%)	<i>15.35</i>	<i>14.60</i>	8.85	8.57	7.52	6.24	5.77
Cumulative (%)	<i>15.35</i>	<i>29.95</i>	38.81	47.38	54.90	61.14	66.91

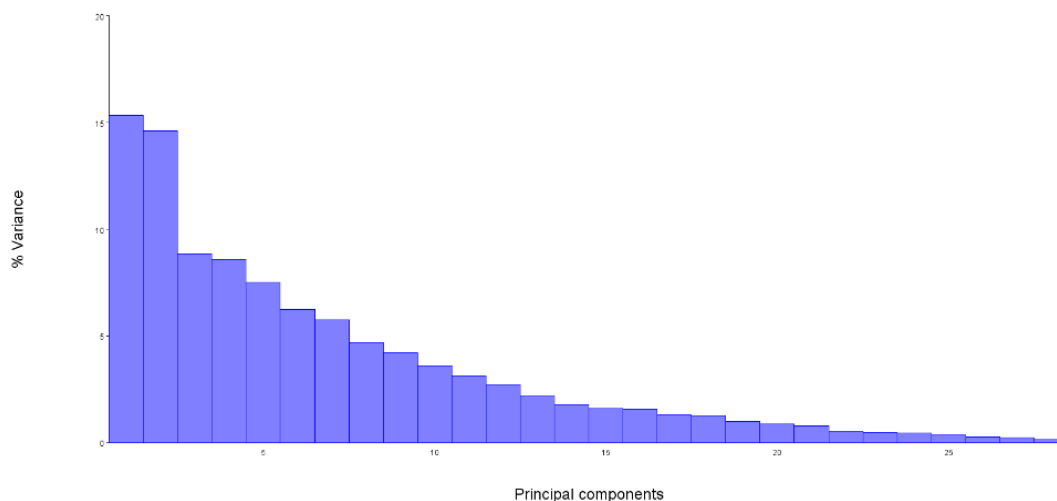


Figure IV-F Scree plot of the variance explained by each eigenvalue for offshore island mandibles.

PC1 accounted for 15.35% of mandible shape variance (Table IV-12; Figure IV-G), driven mostly by the separation Chatham Island mandibles. The PC1 warped outline plot depicts an expansion of the condyle process and a rostral shift of the coronoid process along the first PC axis (pink outline; Figure IV-G). Individuals on the far right of the first PC axis have this mandible shape.

PC2 accounted for 14.6% of shape variance. Waikawa I. mandibles are differentiated from Antipodes I., Auckland I., and Enderby I. (more clearly demonstrated by the mean confidence ellipses; Figure IV-H). Ruapuke I. and Chatham I. mandibles

overlap substantially with all other locations, suggesting high variation between individuals from these populations on this axis.

The PC2 warped outline plot displays a slightly slimmer mandible shape, an inward shift of the coronoid and condyle processes, and a longer angular process along the second PC axis (pink outline). Individuals at the positive end of the PC2 axis have this mandible shape.

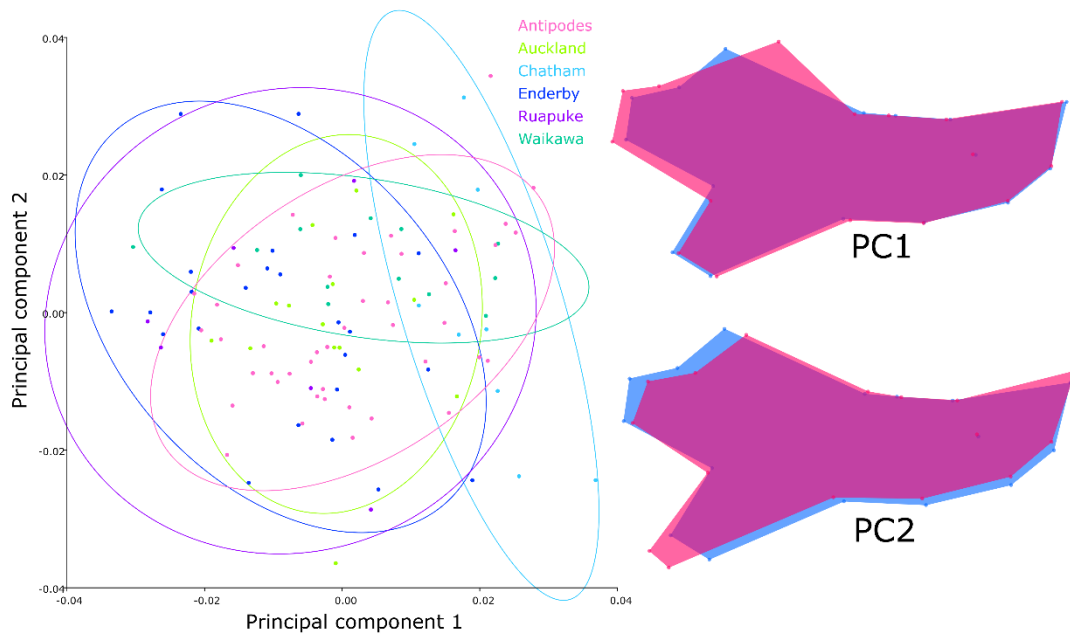


Figure IV-G LEFT PCA plot of mandible shape differences between offshore island populations. Each dot represents a specimen, surrounded by equal frequency ellipses. RIGHT Procrustes deformation warped outlines depicting the change in mandible shape along each axis; blue represents mandible shape at far left of the axis, pink represents the mandible shape at far right of the axis.

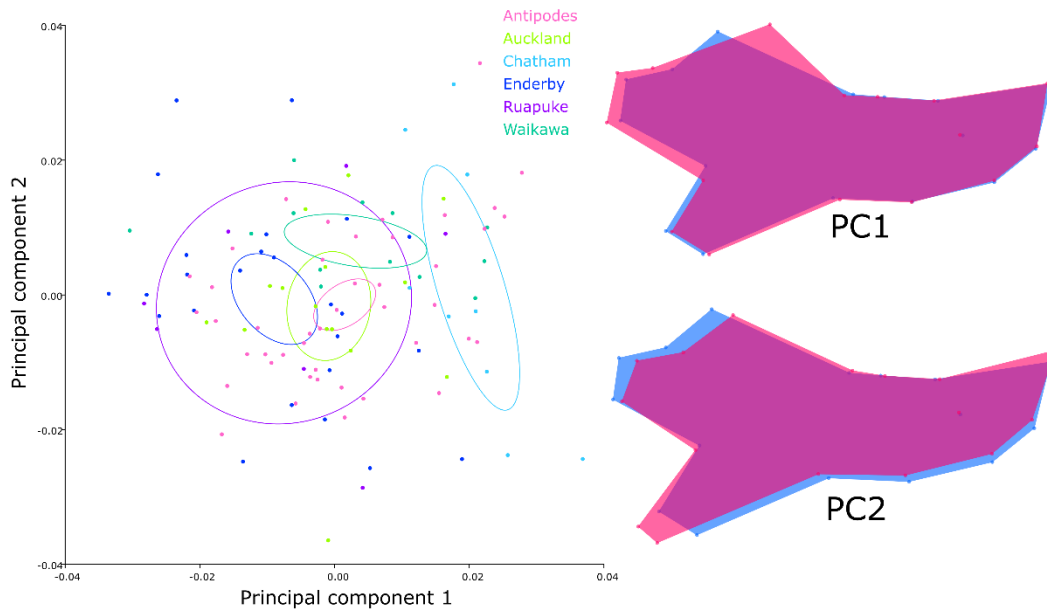


Figure IV-H LEFT PCA plot of mandible shape differences between offshore island populations. Each dot represents a specimen, with 90% confidence ellipses around the mean. RIGHT Procrustes deformation warped outlines depicting the change in mandible shape along each axis; blue represents mandible shape at far left of the axis, pink represents the mandible shape at far right of the axis.

Kruskal-Wallis pairwise comparison revealed much of the significant variation in PC1 is driven by Auckland I., Chatham I., and Enderby I. mandible shapes (Table IV-13).

Table IV-13 P-values from Kruskal-Wallis ANOVA pairwise comparison of PC1 between offshore islands. Bold, red text indicates significant p-values ≤ 0.05 .

PC1	Auckland	Chatham	Enderby	Ruapuke	Waikawa
Chatham	0.0008				
Enderby	0.0022	≤ 0.0001			
Ruapuke	0.045	0.0009	0.8		
Waikawa	0.37	0.0002	0.019	0.14	
Antipodes	0.032	≤ 0.0001	0.046	0.41	0.29

Auckland I., Chatham I., and Waikawa I. are responsible for most of the significant variation across PC2 (Table IV-14).

Table IV-14 P-values from Kruskal-Wallis ANOVA pairwise comparison of PC2 between offshore islands. Bold, red text indicates significant p-values ≤ 0.05 .

PC2	Auckland	Chatham	Enderby	Ruapuke	Waikawa
Chatham	0.0056				
Enderby	0.018	0.0001			
Ruapuke	0.0082	0.0009	0.37		
Waikawa	0.8	0.018	0.0054	0.001	
Antipodes	0.0002	≤ 0.0001	0.26	0.83	≤ 0.0001

Antipodes I. is almost solely responsible for significant variation in PC3 (Table IV-15), while Auckland I., Enderby I., and Waikawa I. represent the majority of significant variation in PC4 (Table IV-16).

Table IV-15 P-values from Kruskal-Wallis ANOVA pairwise comparison of PC3 between offshore islands. Bold, red text indicates significant p-values ≤ 0.05 .

PC3	Auckland	Chatham	Enderby	Ruapuke	Waikawa
Chatham	0.11				
Enderby	0.29	0.033			
Ruapuke	0.15	0.064	0.57		
Waikawa	0.35	0.71	0.088	0.17	
Antipodes	0.0004	0.0003	0.0007	0.08	≤ 0.0001

Table IV-16 P-values from Kruskal-Wallis ANOVA pairwise comparison of PC4 between offshore islands. Bold, red text indicates significant p-values ≤ 0.05 .

PC4	Auckland	Chatham	Enderby	Ruapuke	Waikawa
Chatham	0.0095				
Enderby	0.049	0.064			
Ruapuke	0.0043	0.63	0.021		
Waikawa	≤ 0.0001	0.0083	≤ 0.0001	0.0063	
Antipodes	0.0021	0.69	0.085	0.38	≤ 0.0001

Similarly, significant variation in PC5 is dominated by Auckland I., Enderby I., Waikawa I. and Antipodes I. (Table IV-17), whereas Enderby I. is solely responsible for significant variation in PC6 (Table IV-18).

Table IV-17 P-values from Kruskal-Wallis ANOVA pairwise comparison of PC5 between offshore islands. Bold, red text indicates significant p-values ≤ 0.05 .

PC5	Auckland	Chatham	Enderby	Ruapuke	Waikawa
Chatham	0.0021				
Enderby	0.67	≤ 0.0001			
Ruapuke	0.0082	0.96	0.001		
Waikawa	0.045	0.066	0.017	0.14	
Antipodes	0.0002	0.57	≤ 0.0001	0.93	0.038

Table IV-18 P-values from Kruskal-Wallis ANOVA pairwise comparison of PC6 between offshore islands. Bold, red text indicates significant p-values ≤ 0.05 .

PC6	Auckland	Chatham	Enderby	Ruapuke	Waikawa
Chatham	0.881				
Enderby	0.081	0.38			
Ruapuke	0.113	0.081	0.011		
Waikawa	0.084	0.133	0.003	0.606	
Antipodes	0.741	0.554	0.008	0.08	0.068

Significant variation in PC7 is driven only by Chatham I. and Antipodes I. (Table IV-19).

Table IV-19 P-values from Kruskal-Wallis ANOVA pairwise comparison of PC7 between offshore islands. Bold, red text indicates significant p-values ≤ 0.05 .

PC7	Auckland	Chatham	Enderby	Ruapuke	Waikawa
Chatham	0.005				
Enderby	0.511	≤ 0.0001			
Ruapuke	0.275	0.001	0.399		
Waikawa	0.8	0.001	0.348	0.143	
Antipodes	0.026	≤ 0.0001	0.003	0.262	0.007

By genetic haplotype

The position of individual points on this PCA plot and the warped outline changes (Figure IV-I) are the same as the previous plot (Figure IV-H); only the colour coding differs.

Genetic haplotype assignment shows little separation between the three Clades of *domesticus* across both PC1 and PC2 axes. Employing 90% confidence ellipses around each population's mean elucidates a more distinct separation of Clade B individuals to Clades C and E along the second PC axis (Figure IV-I).

Chatham I. *castaneus*NZ.2 individuals cluster at the positive PC1 axis end, characterised by an expanded condyle process and shifted coronoid process.

Domesticus Clade B Waikawa I. individuals show little scatter across the PC2 axis compared to *domesticus* Clade C, *domesticus* Clade E, and *castaneus*NZ.2 individuals.

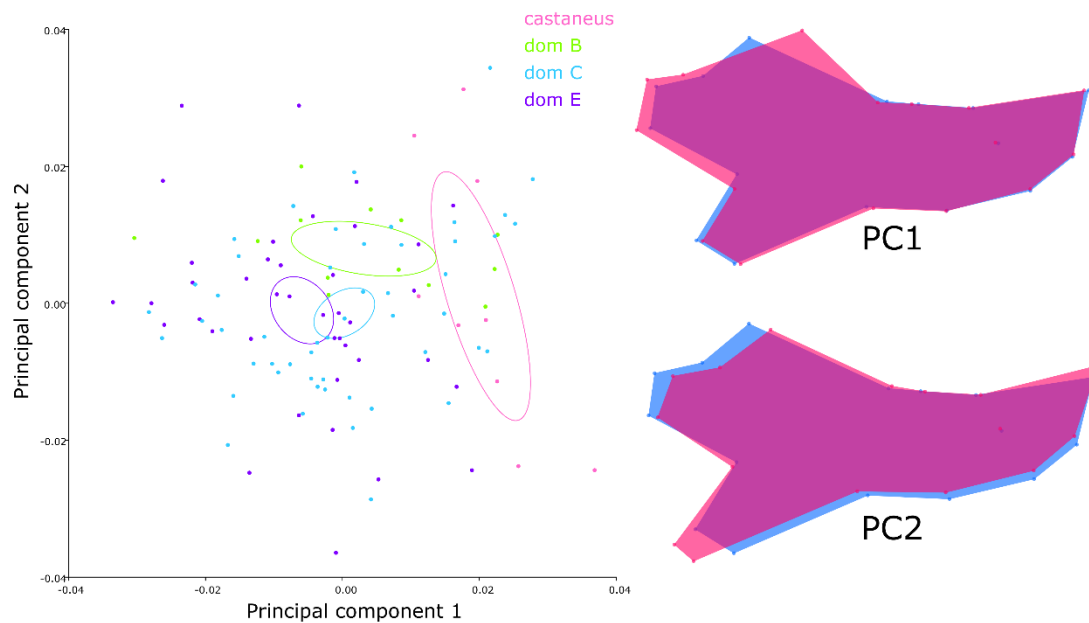


Figure IV-I PCA plot of mandible shape differences between offshore island genetic haplotypes. Each dot represents a specimen, with 90% confidence ellipses around the mean.

4.7.2 Discriminant Function Analysis

By location

The cross-validated DFA separated three groups with 100% accuracy (Table IV-20). Auckland– Enderby Island were separated with a 95% accuracy. Three other pairs were separated with up to 92.8% accuracy. Figure IV-J shows the Procrustes-based superimposition of mean mandible shape for the four locations with 95%+ separation accuracy. The superimposition of Antipodes I. and Chatham I. shows Antipodes I. mandibles have expanded coronoid and angular processes, with a shortened incisor region (Figure IV-J: A). The overlay of Antipodes I. and Waikawa I. displays similar changes, with slight expansion of the coronoid and condylar processes, and a shortened incisor region of the Antipodes I. mean mandible shape (Figure IV-J: B). Enderby I. mandibles have an inward shift of the curve stretching between the condyle and angular processes, with slight expansion of both these processes when overlaid with Auckland I. (Figure IV-J: C). When overlaid with Waikawa I., Enderby I. mandibles have a slimmer alveolar region, with expansion of the coronoid and condyle processes and an inward shift of the condyle-angular curve (Figure IV-J: D).

Table IV-20 Misclassification percentages of cross-validation discriminant function analysis for offshore island mandibles. Bold, red text indicates misclassification levels of $\leq 5\%$. Bold italicised text indicates $\leq 10\%$.

	Antipodes	Auckland	Chatham	Enderby	Ruapuke
Auckland	6.8				
Chatham	0	20.8			
Enderby	7.2	5	23.5		
Ruapuke	5.9	18.2	12.5	28.1	
Waikawa	0	25	13.6	0	15

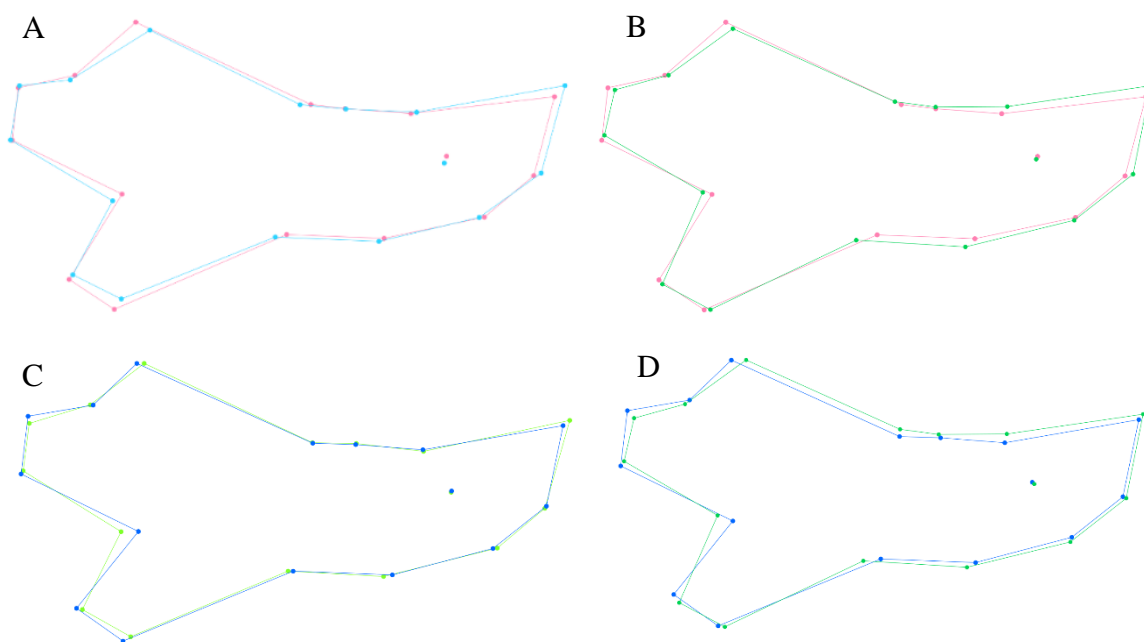


Figure IV-J Procrustes-based superimposition of offshore island mean mandible shapes obtained from discriminant function analysis. A: Antipodes Island (pink) and Chatham Island (light blue), B: Antipodes Island (pink) and Waikawa Island (green), C: Auckland Island (light green) and Enderby Island (blue), D: Enderby Island (blue) and Waikawa Island (green).

By genetic haplotype

The cross-validated DFA separated three groups with >95% accuracy (*castaneus*NZ.2 – *domesticus* Clade C, *domesticus* Clade B – *domesticus* Clade C, and *domesticus* Clade B – *domesticus* Clade E; Table IV-21). Figure IV-K shows the Procrustes-based superimposition of mean mandible shape for the three haplotypes with 95%+ accuracy. *Domesticus* Clade C mandibles show expanded coronoid and angular processes and a slightly shorter incisor region when overlaid with *castaneus* (Figure IV-K: A). Superimposition of *domesticus* Clades C and B reveal clade C mandibles have a slimmer alveolar profile with slightly expanded coronoid and condyle processes (Figure IV-K: B). When overlaid with *domesticus* Clade B, *domesticus* Clade E mean mandible shape displays a slimmer alveolar profile, with a shifted coronoid process and slightly expanded condyle process (Figure IV-K: C).

Table IV-21 Misclassification percentages of cross-validation discriminant function analysis for offshore island haplotypes. Bold, red text indicates misclassification levels of $\leq 5\%$. Bold italicised text indicates $\leq 10\%$.

	<i>Castaneus</i> NZ.2	<i>dom</i> Clade B	<i>dom</i> Clade C
<i>dom</i> Clade B	13.6		
<i>dom</i> Clade C	1.7	3.1	
<i>dom</i> Clade E	14.3	1.9	12.1

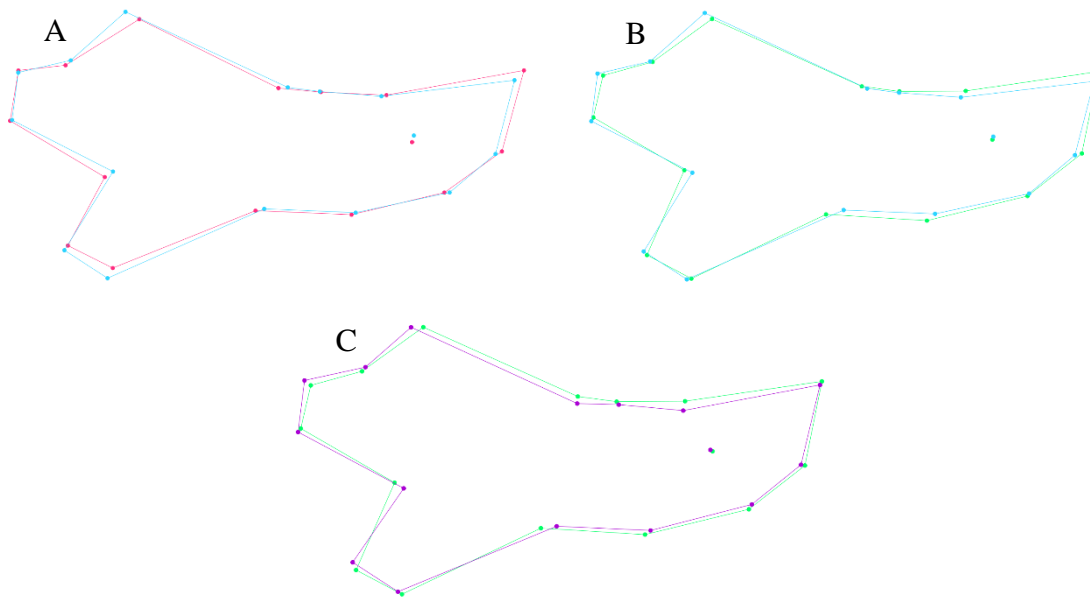


Figure IV-K Procrustes-based superimposition of mean mandible shapes for offshore island haplotypes obtained from discriminant function analysis. A: *Castaneus* (pink) and *domesticus* Clade C (light blue), B: *domesticus* Clade C (light blue) and *domesticus* Clade B (green), C: *domesticus* Clade B (green) and *domesticus* Clade E (purple).

4.7.3 Canonical Variate Analysis

By location

CVA effectively separates Antipodes I. and Enderby I. from all other locations, overlapping together at the far left of the first canonical variate axis (Figure IV-L), with no overlap on the second CV axis. The other four locations cluster together between these two extremes. The first CV accounts for 55.1% of total variation, while CV2 accounts for 20.6% totally more than 75% of shape variation (Table 22; A).

The CV1 warped outline plot (Figure IV-L) depicts a slightly broader alveolar region with a larger angular process (pink outline), associated with groups at the positive (right) end of the first CV axis. Ruapuke I. and Auckland I. are differentiated from Waikawa I., but overlap one another at the positive end of the first CV axis. Chatham I. overlaps Ruapuke I., Auckland I., and Waikawa I. along the first CV axis.

Differentiation among Ruapuke I., Auckland I., Waikawa I. and Chatham I. is driven

only by the first axis. The slimmer mandibles (blue outline) with slightly expanded processes are associated with Antipodes I. and Enderby I. groups.

The CV2 warped outline plot essentially depicts a change from Antipodes I. mandible shape (blue outline) to Enderby I. mandible shape (pink outline; Figure IV-L).

Antipodes I. mandibles have a large upward shift of the coronoid process, with a shorter incisor region. Enderby I. mandibles have an expansion of the condyle process, depressed coronoid process, and a slightly longer alveolar region.

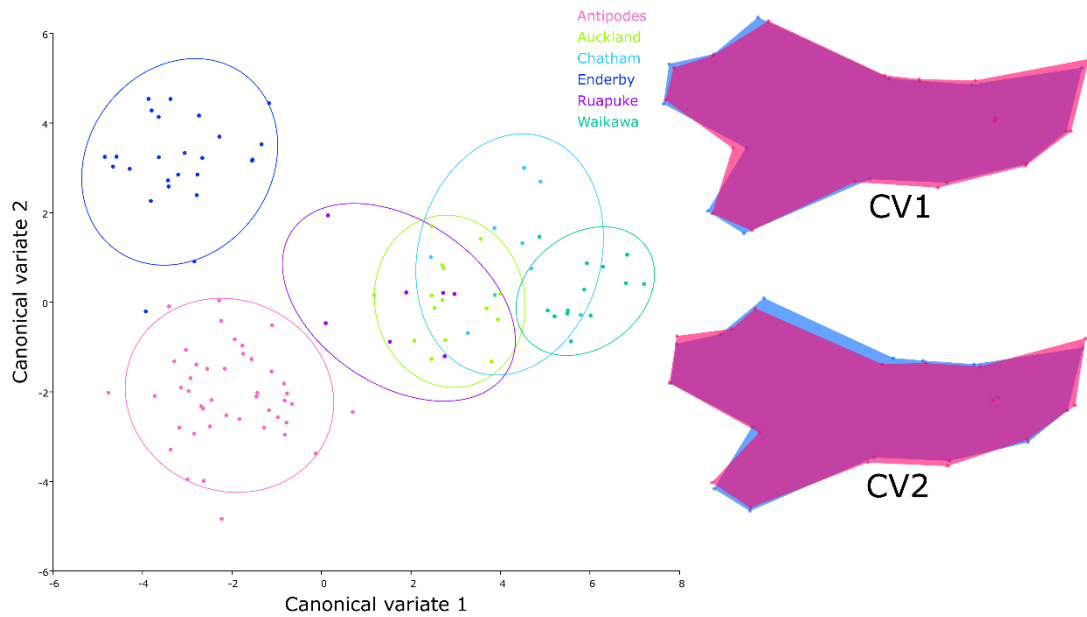


Figure IV-L LEFT CVA plot displaying maximum differentiation of pre-defined offshore island groups. RIGHT Procrustes deformation warped outlines depicting the change in mandible shape along each axis; blue represents mandible shape at far left of the axis, pink represents the mandible shape at far right of the axis.

The Mahalanobis distances and Procrustes distances were significantly different between all pairwise locations (Table IV-22: B and C). The largest and smallest distances between groups mirror the separation of groups on the CVA plot (Figure IV-L). The largest Mahalanobis distance is between Waikawa I. and Enderby I. means. The largest Procrustes distance is between Enderby I. and Chatham I. means. The smallest Mahalanobis distance and Procrustes distance are observed between Antipodes I. and Enderby I., which overlap significantly on the CV1 axis.

Table IV-22 Canonical Variate Analysis results for offshore island mandibles. A) Canonical variates and their associated variance percentages. B) Mahalanobis distances between groups along the first CV axis and their associated p-values. C) Procrustes distances between groups along the first CV axis and their associated p-values. Bold, red text indicates significant p-values ≤ 0.05 . Bold text indicates highest and lowest distances between pairs.

A						
	CV1	CV2	CV3	CV4	CV5	
Eigenvalues	11.14732	4.17263	2.554783	1.772019	0.582338	
Variance (%)	55.105	20.627	12.629	8.76	2.879	
Cumulative (%)	55.105	75.732	88.362	97.121	100	
B						
	Antipodes	Auckland	Chatham	Enderby	Ruapuke	Waikawa
Antipodes		≤ 0.0001	≤ 0.0001	≤ 0.0001	≤ 0.0001	≤ 0.0001
Auckland	6.6815		≤ 0.0001	≤ 0.0001	≤ 0.0001	≤ 0.0001
Chatham	7.7979	6.4381		≤ 0.0001	≤ 0.0001	≤ 0.0001
Enderby	5.3427	7.7854	8.5504		≤ 0.0001	≤ 0.0001
Ruapuke	6.1839	5.9539	7.4549	7.1841		≤ 0.0001
Waikawa	8.5451	6.3725	5.0048	9.73	6.1619	
C						
	Antipodes	Auckland	Chatham	Enderby	Ruapuke	Waikawa
Antipodes		≤ 0.0001	≤ 0.0001	≤ 0.0001	≤ 0.0001	≤ 0.0001
Auckland	0.0364		≤ 0.0001	≤ 0.0001	≤ 0.0001	≤ 0.0001
Chatham	0.0458	0.0343		≤ 0.0001	≤ 0.0001	≤ 0.0001
Enderby	0.0288	0.0345	0.0503		≤ 0.0001	≤ 0.0001
Ruapuke	0.0355	0.0322	0.0494	0.0371		0.0004
Waikawa	0.0458	0.0337	0.035	0.05	0.0317	

By genetic haplotype

Domesticus Clades C and E overlap substantially at the left of the first CV axis, but are effectively separated along the second CV axis (Figure IV-M). *Castaneus*NZ.2 and *domesticus* Clade B groups overlap at the positive end of the first CV axis, and to a lesser extent on the second CV axis, positioned midway between *domesticus* Clades C and E. The first CV axis accounts for 55.4% of total variation, and CV2 accounts for 34.8% totalling more than 90% of shape variation (Table IV-23: A).

The CV1 warped outline plot shows groups at the far right of the CV1 axis possess a broader alveolar region with slightly smaller processes (pink outline; Figure IV-M). Groups at the far left have a slimmer alveolar profile and slightly larger muscle attachment zones (blue outline). The CV2 warped outline plot depicts a slimmer, elongated mandible profile associated with Clade C mandibles at the positive end of the axis (pink outline; Figure IV-M). Groups at the negative end of the axis show enlarged coronoid and angular processes.

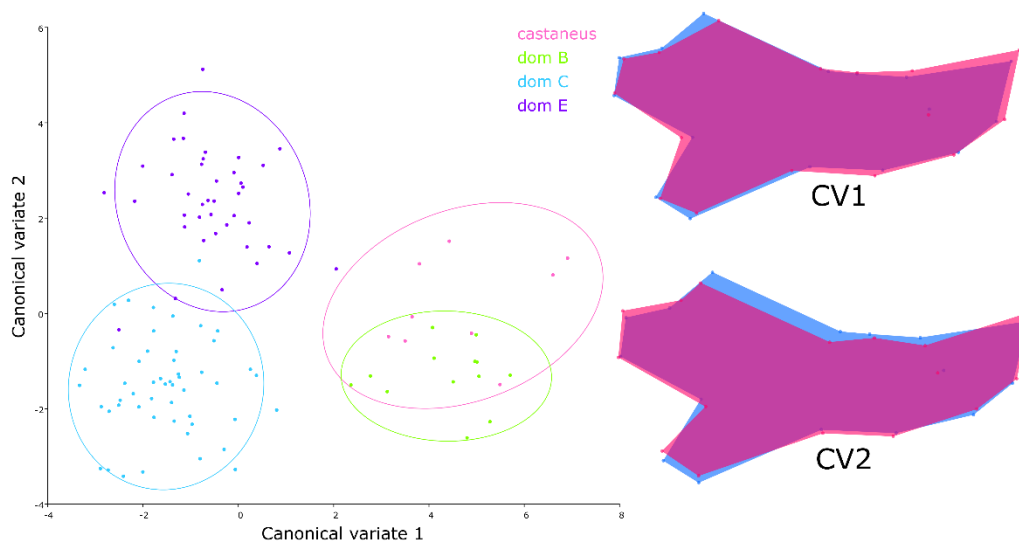


Figure IV-M LEFT CVA plot displaying maximum differentiation of pre-defined offshore island haplotype groups. RIGHT Procrustes deformation warped outlines depicting the change in mandible shape along each axis; blue represents mandible shape at far left of the axis, pink represents the mandible shape at far right of the axis.

The Mahalanobis distances and Procrustes distances were significantly different between all pairwise locations (Table IV-23: B and C), largest between *castaneus* and *domesticus* Clade C and smallest between *domesticus* Clades C and E.

Table IV-23 Canonical Variate results for offshore island mandibles. A) Canonical variates and their associated variance percentages. B) Mahalanobis distances between groups along the first CV axis and their associated p-values. C) Procrustes distances between groups along the first CV axis and their associated p-values. Bold, red text indicates significant p-values ≤ 0.05 . Bold text indicates highest and lowest distance values between pairs.

A				
	CV1	CV2	CV3	
Eigenvalues	5.29259071	3.32546527	0.93058176	
Variance (%)	55.428	34.827	9.746	
Cumulative (%)	55.428	90.254	100	
B				
	<i>Castaneus</i> NZ.2	<i>dom</i> Clade B	<i>dom</i> Clade C	<i>dom</i> Clade E
<i>Castaneus</i> NZ.2		≤ 0.0001	≤ 0.0001	≤ 0.0001
<i>dom</i> Clade B	4.5551		≤ 0.0001	≤ 0.0001
<i>dom</i> Clade C	6.8793	6.1926		≤ 0.0001
<i>dom</i> Clade E	6.3247	6.3124	4.0168	
C				
	<i>Castaneus</i> NZ.2	<i>dom</i> Clade B	<i>dom</i> Clade C	<i>dom</i> Clade E
<i>Castaneus</i> NZ.2		≤ 0.0001	≤ 0.0001	≤ 0.0001
<i>dom</i> Clade B	0.035		≤ 0.0001	≤ 0.0001
<i>dom</i> Clade C	0.0447	0.0424		≤ 0.0001
<i>dom</i> Clade E	0.0418	0.0414	0.0248	

4.7.4 Partial Least Squares Analysis

The two block PLS analysis found a fairly weak but statistically significant correlation between the environmental and genetic covariates (block 1) and mandible shape (block 2) (RV coefficient 0.184; p-value < 0.0001). The first PLS axis, mean annual rainfall, represented 99.9% of covariation with mandible shape (Figure IV-N)

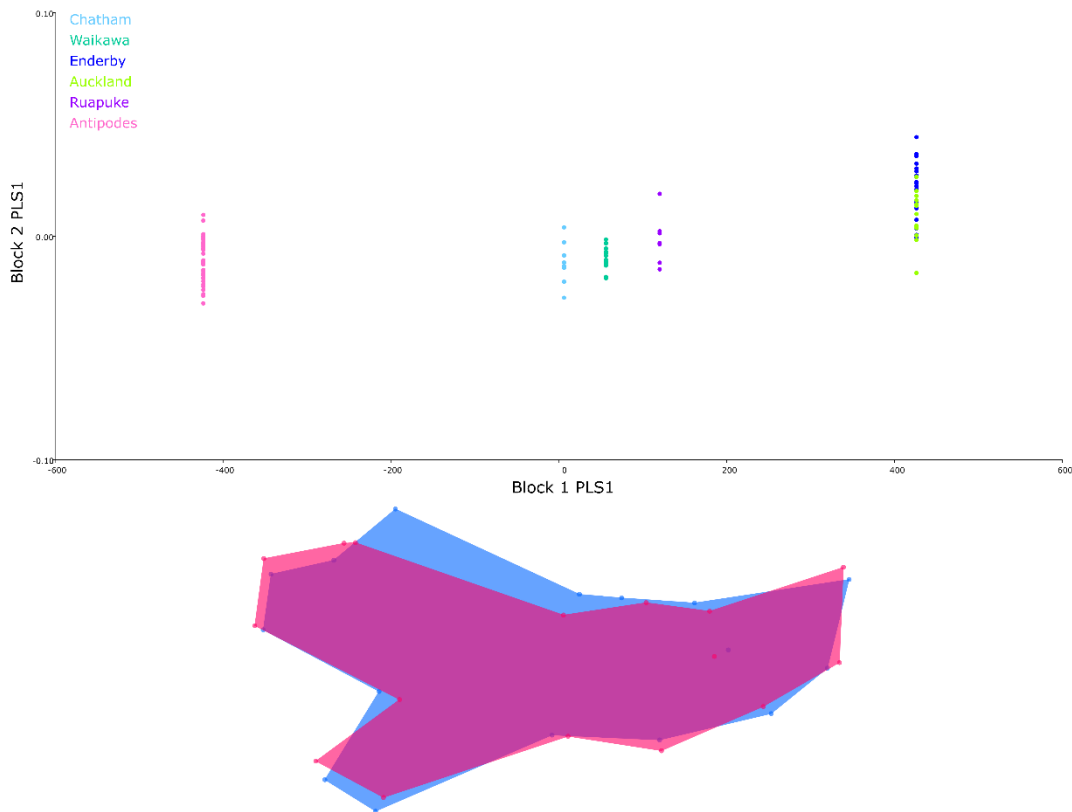


Figure IV-N TOP PLS covariation of offshore island mandible shape with rainfall. Each dot represents an individual specimen. BELOW Warped outline shape change with increasing rainfall.

4.8 Discussion

Significant variation in body size and mandible shape were found between six samples of wild house mice living on offshore islands of New Zealand. Enderby I. and Chatham I. were the most distinct samples of all six locations. Unfortunately, the Ruapuke I. sample size ($n = 6$) was not big enough to accurately describe mandible shape, resulting in a wide spread of Ruapuke I. individuals across the ordination plot.

Enderby I. mice followed Auckland I. with the second largest overall body size. However, the mean physical measurements for Enderby I. mice presented in this study were smaller than previously published values which exceed the Auckland I. sizes quoted here (Ruscoe & Murphy 2005). Enderby I. had the greatest masseter mechanical advantage and the lowest temporalis advantage. The Enderby I. mice were differentiated from Auckland, Antipodes, and Waikawa I. samples at the left of PC1 on the mean ellipse PCA plot. Shape variation associated with Enderby I. mandibles along PC1 showed a smaller condyle process with reduced distance between the coronoid and condyle processes. These characteristics suggest a diet more dominated by resistant food types compared with the other five populations. Enderby I. mandibles also had the largest mean centroid size, but did not significantly differ from Auckland I., Ruapuke I., or Waikawa I. centroid sizes.

Interestingly, Auckland I. and Enderby I. mandibles were significantly distinct from one another in several analyses. This may suggest the two populations do not mix often, despite the small channel distance between the two islands.

By contrast, Chatham I. mice had the smallest overall body size, with the highest temporalis mechanical advantage and the lowest masseter advantage. Both Chatham

I. and Antipodes I. mandibles were significantly smaller in mean centroid size than the other three locations (which did not significantly differ amongst themselves). Chatham I. individuals were also distinctly separated from the other five locations at the far right of the first PC axis. The shape variation associated with Chatham I. mandibles showed an expanded condyle process with increased distance between the condyle and coronoid processes. These observations are consistent with efficient incisor occlusion, suggesting a diet related to catching prey such as invertebrates. On the other hand, the divergence of Chatham I. mandibles may be a reflection of genetic background as the only *castaneus*NZ.2 population.

Waikawa I., Antipodes I., and Auckland I. cluster together in the middle of the PCA plot, and were found to have intermediate biomechanical advantages. This implies the mice inhabiting these islands have broad dietary niches not dominated by any one food type. Antipodes I. mice were observed to feed on both *Carex* seeds and endemic invertebrates in tussock grass habitat where the population was most dense (Berry & Peters 1975; Marris 2000; Russell 2012).

DFA found Antipodes I. and Enderby I. samples to have the least within-group variation in mandible shape.

The factors responsible for between-group variation in the CVA plot with location assignment could not be identified, and certainly do not reflect variation patterns observed with PCA. This observation implies that the factors most useful for group separation with CVA are not the same as those responsible for the greatest variation among individual mouse mandibles with PCA. CVA found the largest Mahalanobis distance between Waikawa I. and Enderby I. Nonetheless, the greatest Procrustes

distance was still observed between Enderby I. and Chatham I. The most similar groups were Antipodes I. and Enderby I.

As previously noted in Chapter III, Samaniego-Herrera et al. (2017) found differences in diet between mouse populations inhabiting Pa'jaros I. and Muertos I. coincided with habitat variation between the two islands. Pa'jaros was covered in dense native grasses which provided burrowing habitat and abundant seeds. Comparatively, Muertos supported large seabird and purple crab (*Gecarcinus lateralis*) colonies that competed for burrowing habitat in the sparse shrub and herb cover, as well as providing nutritious food resources. Mandible shape variation across the six islands presented in this study may also reflect differences in habitat type. Though entirely speculation, the 'soft food' mandibles of Chatham I. mice may reflect a shortage of dense grass cover that is abundant on the sub-Antarctic islands where mouse mandibles have greater masseter advantage and may be consuming greater quantities of seeds.

CVA with haplotype grouping found *domesticus* Clades C and E, and *castaneus*NZ.2 and *domesticus* Clade B mandible shapes to be most similar to one another along CV1. *Castaneus*NZ.2 and *domesticus* Clade B mice represent Chatham and Waikawa I. respectively, while *domesticus* Clades C and E represent Ruapuke I. and Antipodes I., and Auckland I. and Enderby I. The separation along CV1 is consistent with latitude, suggesting environmental factors are more influential than haplotype for maximum separation of predefined groups during CVA. Shape variation along CV1 showed elongation of the mandible profile, with reduced coronoid and angular processes, corresponding to *castaneus*NZ.2 and *domesticus* Clade B groups. These shape changes are usually associated with soft food diets as mechanical stress on the

mandible decreases. *Domesticus* Clade C and *castaneus* were found to be the most dissimilar groups, with the largest Procrustes and Mahalanobis distances between them, while *domesticus* Clades C and E were most similar.

Additionally, annual rainfall was the most significant covariate with mandible shape in the PLS analysis. Antipodes I. experiences the least annual precipitation, while Auckland I. and Enderby I. receive the most. Populations experiencing the least annual rainfall had mandible shapes consistent with softer food diets, whereas high rainfall areas coincide somewhat with 'hard food' mandible shapes. The warped outline shape change associated with PLS, however, is somewhat quizzical, and may not represent any biological significance.

The general pattern in body size follows Bergmann's rule and is consistent with a study by Lomolino et al. (2012), peaking at 50° latitude with cold climates. Increased body size of insular populations has been attributed to ecological release from predation and competition, niche expansion, climate, and resource availability (Lomolino 1985, 2005; White & Searle 2007; Lomolino et al. 2012). Yet Antipodes I., Waikawa I., and Ruapuke I. did not significantly differ in most physical measurements. Regression analysis revealed island size explained the most variation in body weight, body size increasing with the inverse of island size. Lomolino et al. (2012) also found a significant relationship between gigantism in small mammals with small, isolated islands lacking other mammalian competitors.

The small size of Chatham I. and Ruapuke I. mice could be associated with competition and predation from rats. Chatham and Ruapuke are the only two islands in this study where mice co-exist with rats. Body weight varied significantly with rat

presence under regression, but head-body length did not. The small body and centroid size of Chatham I. mice may also pertain to their unique *castaneus*NZ.2 haplotype. Further studies are required to confirm if any of these factors has a significant influence over body size in this context.

The absence of rats on Antipodes I., Auckland I., Enderby I., and Waikawa I. may have enabled access to previously unavailable resources, as well as reducing competition and predation activity that usually alter mouse activity (Lomolino 1985; White & Searle 2007; Lomolino et al. 2012). Furthermore, house mice free from rat predation on islands do not have body size restrictions associated with escape into small burrows (White & Searle 2007). These lifted restrictions may have permitted Auckland I. and Enderby I. mice in particular to attain significantly larger body sizes than other island populations.

Highest ambient temperature, rainfall and genetics were also significant predictors for body size variation between islands, indicating body size is controlled by a combination of factors. In summary, Lomolino et al. (2012) note that “body size evolution is influenced by a combination of forces whose relative importance is contextual, varying in a predictable manner with the body size of the focal ancestral species ... [and] is also strongly influenced by characteristics of the focal islands, including the nature of their ecological communities, their geographic isolation, and climate”, an observation that very likely applies to variation in mandible shape as well.

4.9 References

- Adler GH, Levins R 1994. The island syndrome in rodent populations. *The Quarterly Review of Biology* 69(4): 473-90.
- Anderson P, Renaud S, Rayfield E 2014. Adaptive plasticity in the mouse mandible. *BioMed Central Evolutionary Biology* 14(85).
- Berry RJ, Peters J 1975. Macquarie Island house mice. *Journal of Zoology* 176(3): 375-389.
- Bradley E, Trewick SA, Morgan-Richards M 2017. Genetic distinctiveness of the Waikawa Island mouse population indicates low rate of dispersal from mainland New Zealand. *New Zealand Journal of Ecology* 41(2).
- Bridgman LJ, Innes J, Gillies C, Fitzgerald NB, Miller S, King CM 2013. Do ship rats display predatory behaviour towards house mice? *Animal Behaviour* 86(2): 257-268.
- Caut S, Casanovas JG, Virgos E, Lozano J, Witmer GW, Courchamp F 2007. Rats dying for mice: Modelling the competitor release effect. *Austral Ecology* 32(8): 858-868.
- Copson GR 1986. The diet of the introduced rodents *Mus musculus* and *Rattus rattus* on sub-Antarctic Macquarie Island. *Wildlife Research* 13(3): 441-445.
- Cucchi T, Barnett R, Martínková N, Renaud S, Renvoisé E, Evin A, Sheridan A, Mainland I, Wickham-Jones C, Tougaard C 2014. The changing pace of insular life: 5000 years of microevolution in the Orkney vole (*Microtus arvalis orcadensis*). *Evolution* 68(10): 2804-2820.

- Dugdale J, Emberson RM 2008. Flora. In: Miskelly C, New Zealand. Department of Conservation ed. Chatham Islands: heritage and conservation. Rev. and Enl. ed. Christchurch, N.Z., Canterbury University Press in Association with the Dept. of Conservation.
- Falla RA 1965. Birds and mammals of the Subantarctic Islands. Proceedings of the New Zealand Ecological Society 12: 63-68.
- Foster JB 1964. Evolution of mammals on islands. Nature 202(4929): 234-235.
- Godley EJ 1965. The ecology of the Subantarctic islands of New Zealand: Notes on the vegetation of the Auckland Islands. Proceedings of the New Zealand Ecological Society 12: 57-63.
- Godley EJ 1989. The flora of Antipodes Island. New Zealand Journal of Botany 27(4): 531-564.
- Goldwater N, Perry GLW, Clout MN 2012. Responses of house mice to the removal of mammalian predators and competitors. Austral Ecology 37(8): 971-979.
- Gray MM, Parmenter MD, Hogan CA, Ford I, Cuthbert RJ, Ryan PG, Broman KW, Payseur BA 2015. Genetics of rapid and extreme size evolution in island mice. Genetics 201(1): 213-228.
- Hancock B 2008. The influence of ship rats (*Rattus rattus*) on the habitat preferences of the house mouse (*Mus musculus*). Unpublished Masters thesis, Victoria University of Wellington.
- Harper GA 2010. Habitat use by mice during winter on subantarctic Auckland Island. New Zealand Journal of Ecology 34(2): 262-264.
- Higham T, New Zealand. Dept. of Conservation 1999. New Zealand's Subantarctic Islands. Auckland, N.Z., Reed.

- Innes J, Warburton B, Williams D, Speed H, Bradfield P 1995. Large-scale poisoning of ship rats (*Rattus-rattus*) in indigenous forests of the North-Island, New Zealand. *New Zealand Journal of Ecology* 19(1): 5-17.
- King CM 2016. How genetics, history and geography limit potential explanations of invasions by house mice *Mus musculus* in New Zealand. *Biological Invasions* 18(6): 1533-1550.
- King CM, Alexander A, Chubb T, Cursons R, MacKay J, McCormick H, Murphy E, Veale A, Zhang H 2016. What can the geographic distribution of mtDNA haplotypes tell us about the invasion of New Zealand by house mice *Mus musculus*? *Biological Invasions* 18(6): 1551-1565.
- King M 2008. Human settlement and historic sites. In: Miskelly C, New Zealand. Department of Conservation ed. Chatham Islands: heritage and conservation. Rev. and Enl. ed. Christchurch, N.Z., Canterbury University Press in Association with the Dept. of Conservation.
- Le Roux V, Chapuis JL, Frenot Y, Vernon P 2002. Diet of the house mouse (*Mus musculus*) on Guillou Island, Kerguelen archipelago, Subantarctic. *Polar Biology* 25: 49-57.
- Lomolino MV 1985. Body size of mammals on islands: The island rule reexamined. *The American Naturalist* 125: 310-316.
- Lomolino MV 2005. Body size evolution in insular vertebrates: generality of the island rule. *Journal of Biogeography* 32: 1683-1699.
- Lomolino MV, Sax DF, Palombo MR, van der Geer AA 2012. Of mice and mammoths: evaluations of causal explanations for body size evolution in insular mammals. *Journal of Biogeography* 39(5): 842-854.

- Martínková N, Barnett R, Cucchi T, Struchen R, Pascal M, Pascal M, Fischer MC, Higham T, Brace S, Ho SY 2013. Divergent evolutionary processes associated with colonization of offshore islands. *Molecular ecology* 22(20): 5205-5220.
- McIntosh AR 2001. The impact of mice on the Antipodes Islands. Antipodes Island Expedition; October - November 1995 Southland Conservancy. Wellington, New Zealand, Department of Conservation. Pp. 52-57.
- McNab BK 2010. Geographic and temporal correlations of mammalian size reconsidered: a resource rule. *Oecologia* 164: 13-23.
- Medina AI, Martí DA, Bidau CJ 2007. Subterranean rodents of the genus *Ctenomys* (Caviomorpha, Ctenomyidae) follow the converse to Bergmann's rule *Journal of Biogeography* 34: 1439-1454.
- Millien V 2006. Morphological evolution is accelerated among island mammals. *Public Library of Science (PLOS) Biology* 4(11): 2165-2165.
- Millien V 2011. Mammals evolve faster on smaller islands. *Evolution* 65(7): 1935-1944.
- Millien V, Damuth J 2004. Climate change and size evolution in an island rodent species: New perspectives on the island rule. *Evolution* 58(6): 1353-1360.
- Miskelly C 2013. Blog: Hunting henriettas on Ruapuke Island – on the tail of New Zealand's first mice. Biodiversity, Field trips, History, Mammals. www.Tepapa.govt.nz, Te Papa Museum of New Zealand.
- Pergams ORW, Ashley MV 2001. Microevolution in island rodents. *Genetica* 112(1): 245-256.

- Phillips J 2013. Subantarctic islands-Snares, Antipodes, and Bounty islands.
Retrieved 23-09-2014 2014, from Te Ara – The Encyclopedia of New Zealand. www.teara.govt.nz.
- Rance B 2015 Antipodes Island flora and vegetation. *Trilepidia: Newsletter of the New Zealand plant conservation network*: 2-5.
- Renaud S, Auffray JC 2010. Adaptation and plasticity in insular evolution of the house mouse mandible. *Journal of Zoological Systematics and Evolutionary Research* 48(2): 138-150.
- Renaud S, Hardouin EA, Pisanu B, Chapuis JL 2013. Invasive house mice facing a changing environment on the Sub-Antarctic Guillou Island (Kerguelen Archipelago). *Journal of Evolutionary Biology* 26(3): 612-624.
- Renaud S, Gomes Rodrigues H, Ledevin R, Pisanu B, Chapuis J-L, Hardouin EA 2015. Fast evolutionary response of house mice to anthropogenic disturbance on a Sub-Antarctic island. *Biological Journal of the Linnean Society* 114(3): 513-526.
- Ruscoe WA, Murphy EC 2005. House Mouse. In: King CM ed. *The Handbook of New Zealand Mammals*. 2nd ed. Melbourne, AUS, Oxford University Press.
- Ruscoe WA, Ramsey DSL, Pech RP, Sweetapple PJ, Yockney I, Barron MC, Perry M, Nugent G, Carran R, Warne R and others 2011. Unexpected consequences of control: competitive vs. predator release in a four-species assemblage of invasive mammals. *Ecology Letters* 14(10): 1035-1042.
- Russell JC 2012. Spatio-temporal patterns of introduced mice and invertebrates on Antipodes Island. *Polar Biology* 35(8): 1187-1195.

- Russell JC, Broome KG 2016. Fifty years of rodent eradications in New Zealand: another decade of advances. *New Zealand Journal of Ecology* 40(2): 197-204.
- Samaniego-Herrera A, Clout MN, Aguirre-Muñoz A, Russell JC 2017. Rodent eradications as ecosystem experiments: a case study from the Mexican tropics. *Biological Invasions*: 1-19.
- Searle JB, Jamieson PM, Gündüz I, Stevens MI, Jones EP, Gemmill CEC, King CM 2009. The diverse origins of New Zealand house mice. *Proceedings of the Royal Society B: Biological Sciences* 276(1655): 209-217.
- Smith VV, Avenant NN, Chown SS 2002. The diet and impact of house mice on a sub-Antarctic island. *Polar Biology* 25(9): 703-715.
- Taylor RH 2006. *Straight through from London: the Antipodes and Bounty Islands, New Zealand*. Christchurch, N.Z, Heritage Expeditions New Zealand.
- Taylor RH 1971. Influence of man on vegetation and wildlife of Enderby and Rose Islands, Auckland Islands. *New Zealand Journal of Botany* 9(2): 225-268.
- Torr N 2002. Eradication of rabbits and mice from subantarctic Enderby and Rose Islands. *Turning the tide: the eradication of invasive species*.
- Warham J, Johns PM 1975. The University of Canterbury Antipodes Island expedition 1969. *Journal of the Royal Society of New Zealand* 5(2): 103-131.
- White TA, Searle JB 2007. Factors explaining increased body size in common shrews (*Sorex araneus*) on Scottish Islands. *Journal of Biogeography* 34: 356-363.
- Yom-Tov Y, Geffen E 2006. Geographic variation in body size: the effects of ambient temperature and precipitation. *Oecologia* 148: 213-218.

V. Variation across the Tasman

5.1 Introduction

This chapter compares body size and mandible shape of the forest and offshore island house mouse populations discussed in Chapters III and IV, as well as comparing house mice from Sydney, Australia, to both forest and island populations.

New Zealand is an archipelago of large and small islands, the North and South Islands being considerably larger landmasses than their numerous smaller counterparts. Previous studies suggest small mammals experience more rapid and substantial change on smaller, more remote islands (Lomolino 2005; Millien 2006; Renaud & Auffray 2010; Millien 2011; Lomolino et al. 2012; Martínková et al. 2013). Increasing island size is often associated with more complex ecology, such as increased competition, predation, and habitat diversity (Simberloff et al. 2000; Grant & Grant 2006; Lomolino et al. 2012). Smaller islands with lower diversity would result in the ecological release of small mammalian invaders. This investigation presents an opportunity to compare the mandible shape and body size of house mouse colonies on small and large islands.

Founded in 1788, Sydney is believed to have been an important port for traders and sealers operating in New Zealand during the late 18th and early 19th centuries (King 2016). British cargo ships sailed frequently to Australia, carrying essential supplies for the expanding Sydney settlement. These ships provided ample opportunity for the transport and subsequent invasion of *M. m. domesticus* in Sydney, particularly clades E and F (King 2016). From Sydney, sealing gangs sailed out to the Foveaux Strait and Subantarctic Islands, carrying provisions for the men to set up camps for

extended periods until the ships returned for both the men and seal skins (Taylor 2006; King 2016). Whaling stations, settlements and trading from both Sydney and Europe further enabled clade E house mice to colonise and dominate most of northern New Zealand. It is likely that modern Sydney house mice are descendants of the original population from which New Zealand *domesticus* mice are derived, and thus present an interesting comparison prospect.

5.2 Material

Sydney

Sydney, Eastern Australia, was established as “a port of call for trading and ship maintenance after 1788” (King 2016). A previous study by Gabriel et al. (2011) on house mice across Australia found only *domesticus* DNA elements. AUSTRALIA0.1 is the most common type of *domesticus* Clade E haplotype currently known in Australia (Gabriel et al. 2011). The 12 Sydney samples used in this study include one *domesticus* Clade A individual, and 11 *domesticus* Clade E individuals that are probably representatives of the AUSTRALIA0.1 haplotype. The samples were collected from several different poultry farms in North and West Sydney regions.

The reported Sydney mice do not have any associated body measurements as the heads were removed before physical measurements were taken, so only mandible shape is compared.

5.3 Comparison of offshore island and forest mice within the New Zealand archipelago

5.3.1 Physical measurements and centroid size

Average body weight and tail length differed significantly between island and forest mice, but head-body length did not (Table V-1). Average centroid size also differed significantly between island and forest groups.

Table V-1 P-values from Kruskal-Wallis ANOVA pairwise comparison between offshore island and forest body measurements and mandible centroid size. Bold, red text indicates significant p-values ≤ 0.05 .

Island vs. Mainland	Weight	Head-body length	Tail	Centroid size
P-value	≤ 0.0001	0.702	0.006	≤ 0.0001

5.3.2 Shape analysis

5.3.2.1 Regression and Principal Component Analysis (PCA)

The pooled within-group regression was significant for allometry ($p \leq 0.0001$ after 1000 permutations), with size accounting for 8.47% of shape variance (Figure V-A).

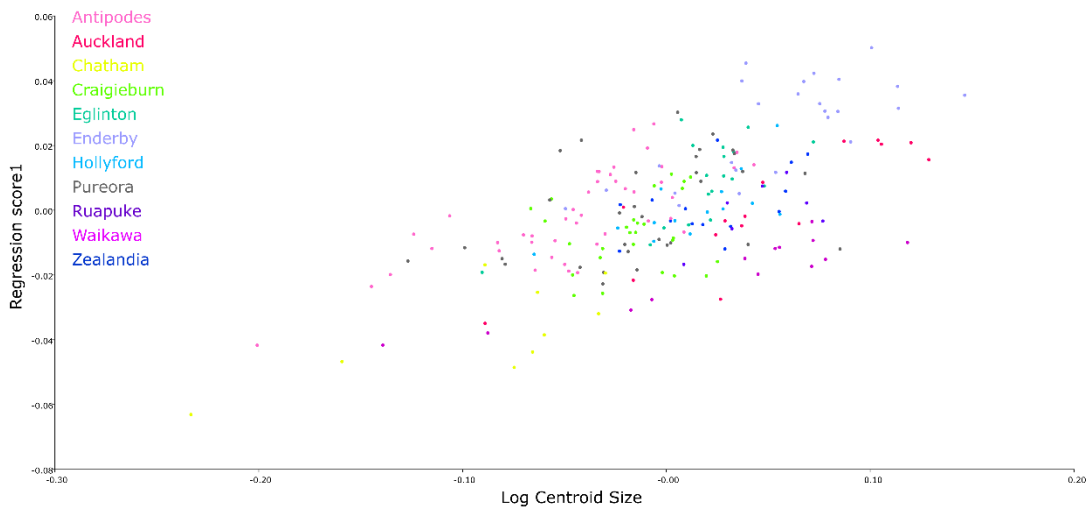


Figure V-A Group-centred regression of mandible shape on log centroid size for forest and offshore island mandibles.

The first seven principal components of the PCA represent >5% variance, accumulating to a total of 67.04% (Table V-2). However, only the first eigenvalue falls above the inflection point of the scree plot (Figure V-B). It is unlikely that the other five have any biological significance so are not discussed.

Table V-2 Eigenvalues for the offshore island and forest PCA plot that represent more than 5% variance. Eigenvalues above the 'lee' point on the scree plot are italicised.

	EV1	EV2	EV3	EV4	EV5	EV6
Eigenvalues	<i>0.000386</i>	0.000231	0.000178	0.000127	9.7E-05	9.07E-05
Variance (%)	<i>23.331</i>	13.959	10.743	7.675	5.855	5.477
Cumulative (%)	<i>23.331</i>	37.291	48.034	55.708	61.563	67.04

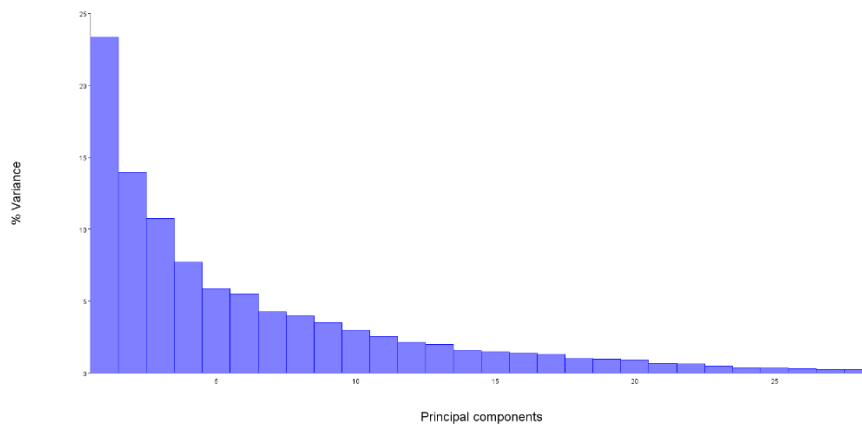


Figure V-B Scree plot of the variance explained by each eigenvalue for forest and offshore island mandibles.

PC1 accounted for 23.33% of mandible shape variance (Table V-2). The 90% confidence ellipses of each mean show a clear separation of populations along the first PC axis that follows previously observed patterns in diet variation (Figure V-C). Eglinton, Craigieburn, Hollyford, Chatham I. and Waikawa I. cluster together at the far left of PC1. Zealandia, Pureora, Ruapuke I. and Auckland I. cluster midway along

PC1, while Antipodes I. and Enderby I. cluster to the far right. The warped outline plot (Figure V-C) depicts a shift from a broader mandible shape with increased distance between the condyle and coronoid processes and a smaller angular process (blue outline), to a shorter mandible with extended condyle and angular processes and a posterior shifted coronoid process from left to right along the first PC axis (pink outline).

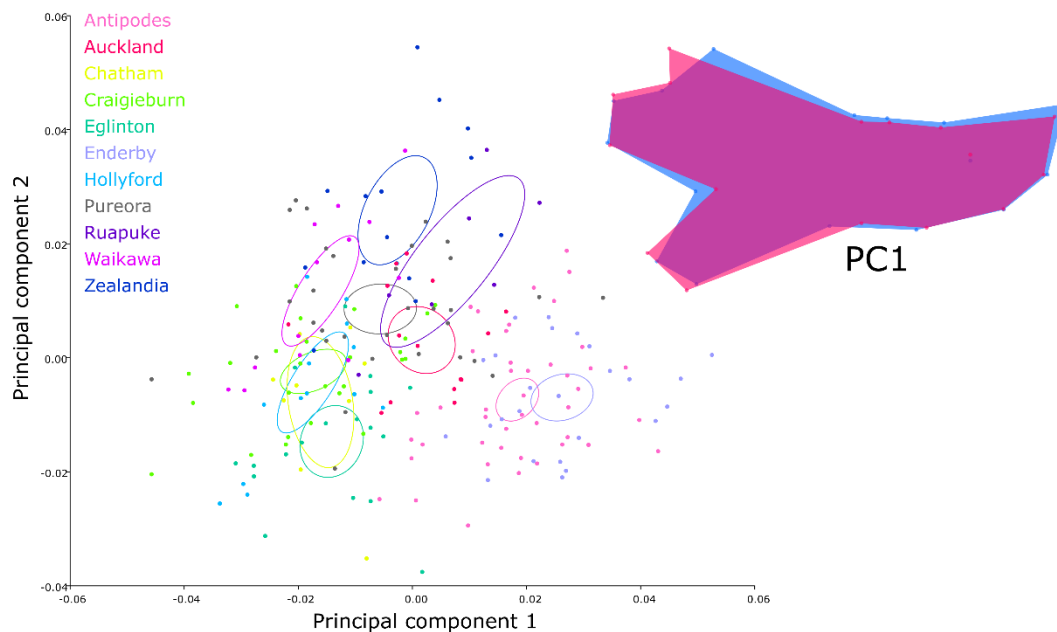


Figure V-C LEFT PCA plot of mandible shape differences between offshore island and forest populations. Each dot represents a specimen, with 90% confidence ellipses around the mean. RIGHT Procrustes deformation warped outlines depicting the change in mandible shape along each axis; blue represents mandible shape at far left of the axis, pink represents the mandible shape at far right of the axis.

5.3.2.2 Discriminant Function Analysis

DFA separated island and forest groups with 84.4% accuracy and found significant variation between group means with both Procrustes and Mahalanobis distances (p-

value ≤ 0.001 after 1000 permutations). The superimposition of island versus forest reveal the two mean shapes are very similar (Figure V-D).

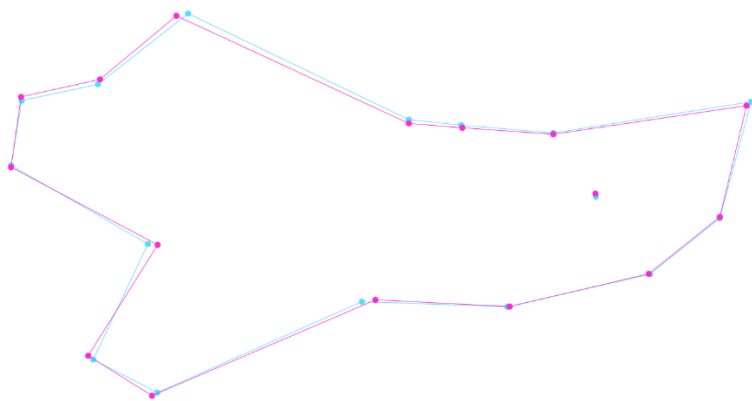


Figure V-D Procrustes-based superimposition of mean mandible shapes for forest and offshore island mandibles obtained from discriminant function analysis. Forest: pink, offshore islands: blue.

5.3.3 Discussion

The North and South Islands of New Zealand cannot be classified as ‘mainland’ areas, despite being significantly larger landmasses than any of their offshore islands, and therefore impose ecological pressures unique to island environments. House mouse body weight and tail length were significantly larger on offshore islands compared with North and South Island forest samples, supporting previous observations that the body size of small mammals increases on smaller, more isolated islands (Lomolino 1985, 2005; Lomolino et al. 2012). Head-body length did not significantly differ between populations in this study, but is much more difficult to measure accurately on a soft body than weight and tail length, so should be interpreted with care.

The increased body size of small mammal colonies on smaller remote islands has been attributed to ecological release from predation and competition, niche expansion, climate, and resource availability (Lomolino 1985, 2005; White & Searle 2007; Millien 2011; Lomolino et al. 2012; Martínková et al. 2013). The absence of rats on several offshore islands may have enabled access to previously unavailable resources, as well as reducing competition and predation activity that usually alter mouse activity (Lomolino 1985; White & Searle 2007; Lomolino et al. 2012).

Furthermore, house mice free from rat predation on islands do not have body size restrictions associated with escape into small burrows (White & Searle 2007). Habitat variation between forest and offshore island environments may have also enabled niche expansion, leading to the larger body size of offshore insular mice. Without further data, it is impossible to conclude precisely which variables are responsible for the increased body size of offshore island populations. However, it is likely to be

selected for by a number of factors that cannot be easily differentiated and “whose relative importance is contextual” (Lomolino et al. 2012).

The differentiation of mouse populations on the ordination plot followed previously observed patterns in diet variation. Eglinton, Craigieburn, Hollyford, Chatham I. and Waikawa I. cluster together to the left of PC1, showing mandible shape variation consistent with a diet of softer foods. At the other extreme, Antipodes I. and Enderby I. display mandible shapes associated with processing resistant plant material (Satoh 1997; Baverstock et al. 2013; Renaud et al. 2015). Intermediate phenotypes between these two extreme mandible shapes are represented by Zealandia, Pureora, Ruapuke I. and Auckland I. mice.

When pooled together, DFA found significant variation in mean mandible shape between island and forest groupings, further confirming that evolutionary processes differ between islands of varying size.

In conclusion, the evolution of house mice in the New Zealand archipelago is certainly contextual, and varies with each island’s unique environment. The factors underlying the direction of change within each population cannot be easily identified or separated, but could be linked to variation in habitat, climate, competition, and diet.

5.4 Trans-Tasman forest and Sydney comparison

5.4.1 Centroid size

Kruskal-Wallis ANOVA results revealed mice from Sydney had the smallest average centroid size compared with all forest populations (Table V-3; Figure V-E).

Table V-3 P-values from Kruskal-Wallis ANOVA pairwise comparison of mandible centroid size between forest and Sydney mice. Bold, red text indicates significant p-values ≤ 0.05 .

Centroid Size	Craigieburn	Eglinton	Hollyford	Pureora	Zealandia
Sydney	0.041	≤ 0.0001	0.001	0.023	≤ 0.0001

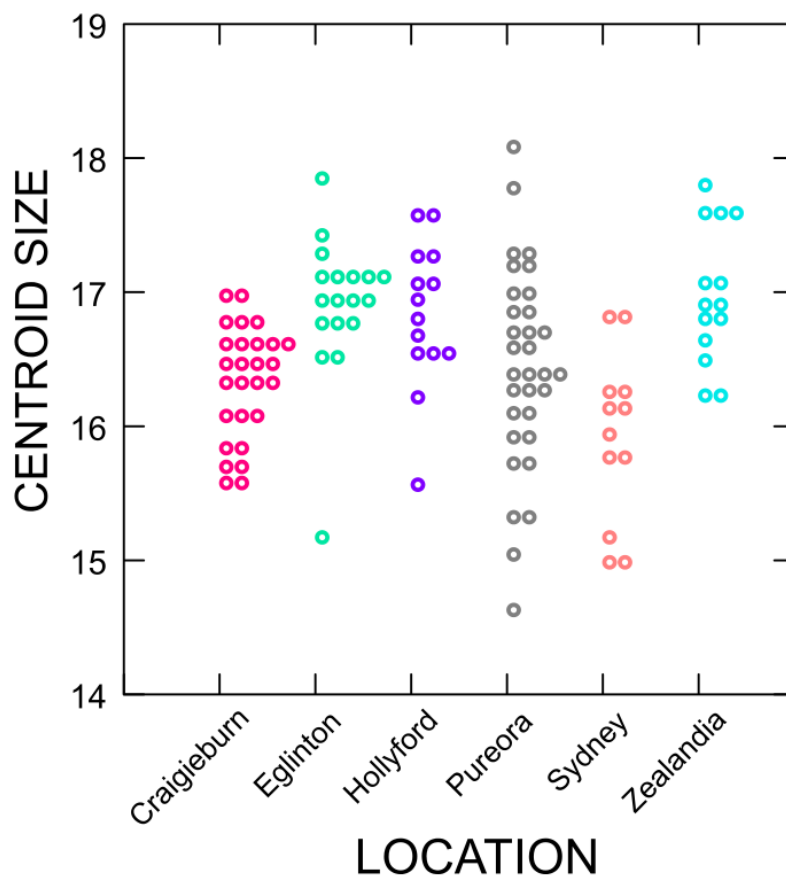


Figure V-E Dot density plot showing the distribution of centroid size within forest and Sydney populations. Each icon represents an individual mouse.

5.4.2 Biomechanical analysis

Sydney mandibles had significantly greater temporalis mechanical advantage compared with Zealandia and Pureora mandibles, and did not differ significantly to South Island mandibles (Table V-4). Only Zealandia mandibles had significantly greater masseter advantage than Sydney.

Table V-4 P-values from Kruskal-Wallis ANOVA pairwise comparison of the biomechanical advantage ratios between forest and Sydney mandibles. Bold, red text indicates significant p-values ≤ 0.05 . Bold italicised text indicates p-values close to 0.05.

	Craigieburn	Eglinton	Hollyford	Pureora	Zealandia
Masseter/Incisor					
Sydney	0.54	<i>0.059</i>	0.41	0.89	0.007
Masseter/Molar					
Sydney	0.14	0.13	0.07	0.87	0.018
Temporalis/Incisor					
Sydney	0.16	0.87	0.5	0.009	0.008
Temporalis/Molar					
Sydney	<i>0.088</i>	0.5	<i>0.08</i>	0.006	0.002

5.4.3 Shape analysis

5.4.3.1 Regression and Principal Component Analysis

The pooled within-group regression was significant for allometry ($p \leq 0.0001$ after 1000 permutations), with size accounting for 4.89% of shape variance (Figure V-F).

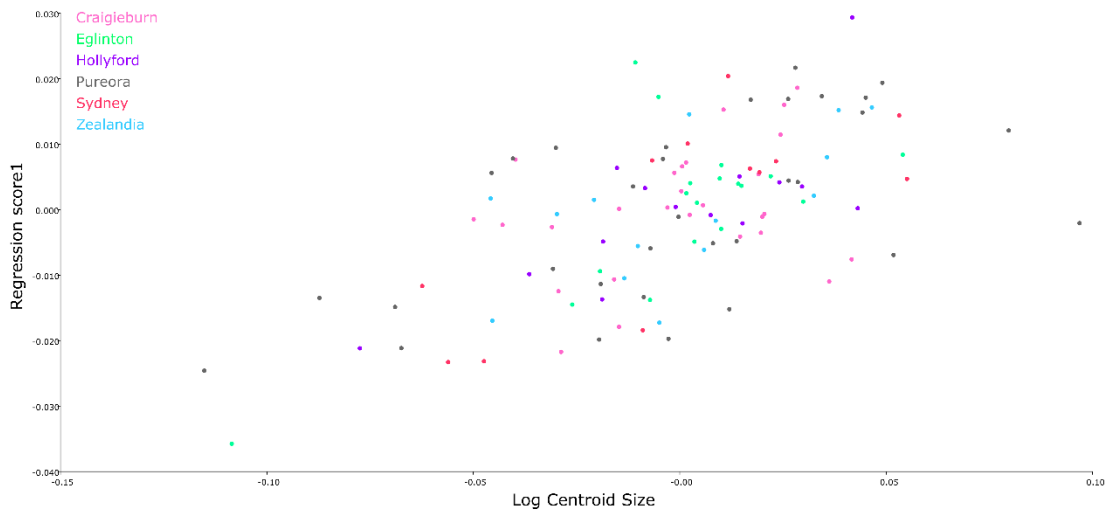


Figure V-F Group-centred regression of mandible shape on log centroid size for forest and Sydney mandibles.

The first six principal components accounted for >5% variance, accumulating to 65.2% of total variance (Table V-5). Only the first eigenvalue falls above the inflection point on the scree plot (Figure V-G). However, PCA produces conflicting results with CVA and DFA, so a second PCA plot is presented to show differentiation of individuals along the third PC axis.

Table V-5 Eigenvalues for the forest and Sydney PCA plot that represent more than 5% variance. Eigenvalues above the 'lee' point on the scree plot are italicised.

	EV1	EV2	EV3	EV4	EV5	EV6
Eigenvalues	<i>0.000229</i>	0.000148	0.000103	8.07E-05	7.46E-05	5.86E-05
Variance (%)	<i>21.549</i>	13.908	9.641	7.574	7.003	5.505
Cumulative (%)	<i>21.549</i>	35.457	45.098	52.671	59.674	65.178

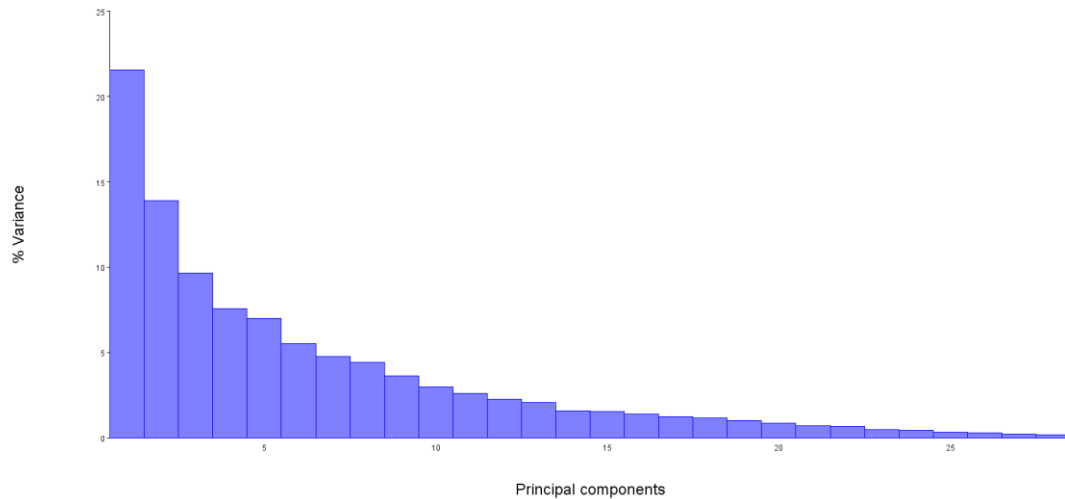


Figure V-G Scree plot of the variance explained by each eigenvalue for forest and Sydney mandibles.

PC1 accounted for 21.6% of total shape variation (Table V-5; Figure V-H). The 90% confidence ellipses surrounding the mean of each location indicate Sydney mandibles cluster to the far right of the first PC axis, most similar to South Island samples (Figure V-H). The PC1 warped outline plot depicts a forward shift of the coronoid process, a slightly longer angular process, with expansion of condylar process and alveolar region associated with Sydney mandibles at the positive end of PC1 (pink outline).

PC2 accounts for 13.9% of mandible shape variation. Sydney mandibles mostly cluster with Pureora mandibles along PC2 (Figure V-H). The PC2 warped outline plot shows broader and shorter angular process, expanded condyle process, and broader alveolar profile associated with Sydney and Pureora mandibles (pink outline).

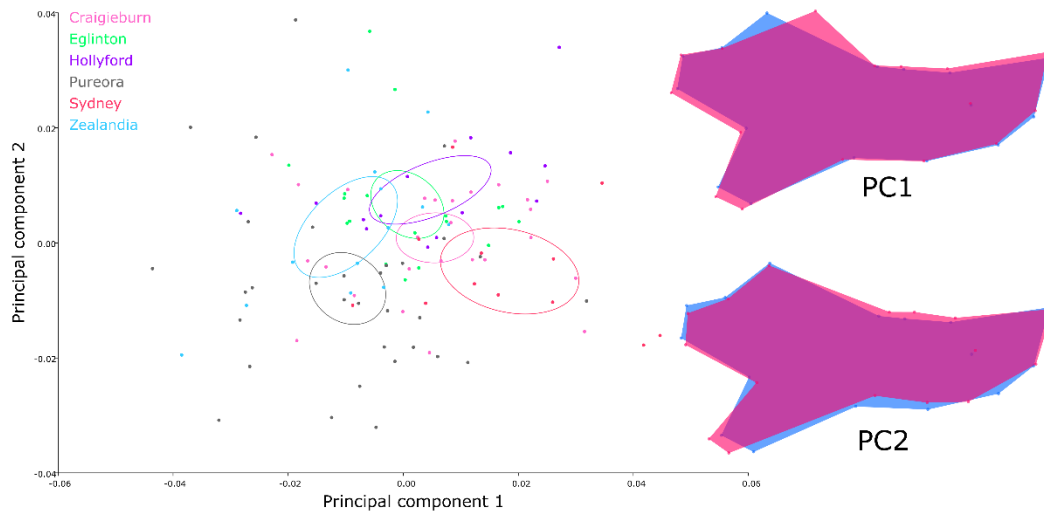


Figure V-H LEFT PCA plot of mandible shape differences between forest and Sydney populations. Each dot represents a specimen, surrounded by equal frequency ellipses. RIGHT Procrustes deformation warped outlines depicting the change in mandible shape along each axis; blue represents mandible shape at far left of the axis, pink represents the mandible shape at far right of the axis.

PC3 describes 9.6% of the total variation in mandible shape (Figure V-I). Sydney mandibles cluster with Zealandia mandibles in extreme separation to the other 4 populations. The warped outline plot depicts a much broader mandible profile with a larger angular and coronoid processes along the third PC axis associated with Sydney and Zealandia mandibles (blue outline).

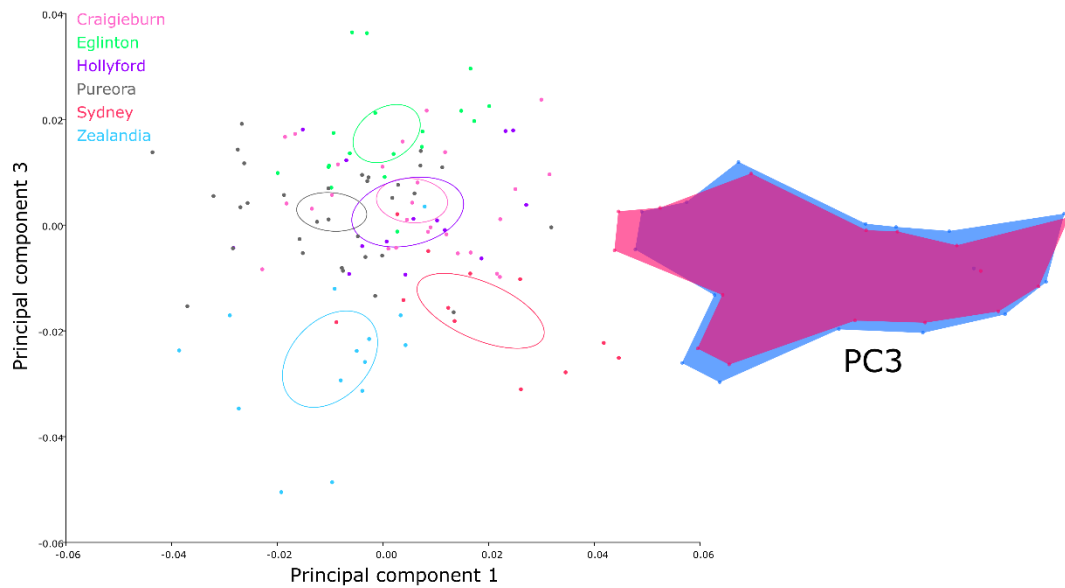


Figure V-1 LEFT PCA plot of mandible shape differences between forest and Sydney populations with PC1 and PC3. Each dot represents a specimen, with 90% confidence ellipses around the mean. RIGHT Procrustes deformation warped outlines depicting the change in mandible shape along each axis; blue represents mandible shape at far left of the axis, pink represents the mandible shape at far right of the axis.

Kruskal-Wallis analysis revealed significant variation in PC1 is associated with Sydney, Hollyford, Zealandia and Pureora mandibles (Table V-6). Although Sydney mandibles did not cluster closely to Hollyford mandibles along PC2, their PC2 coordinates did not significantly differ with Kruskal-Wallis ANOVA. Sydney mandibles differed significantly with Craigieburn and Eglinton mandibles across all PCs except PC1. Pureora mandibles varied significantly to Sydney mandibles with all PCs except PC3. Zealandia mandibles did not differ significantly to Sydney mandibles with PC3 and PC4.

Table V-6 P-values from Kruskal-Wallis ANOVA pairwise comparison of the first five PCs between forest and Sydney mandible shapes. Bold, red text indicates significant p-values ≤ 0.05 .

	Craigieburn	Eglinton	Hollyford	Zealandia	Pureora
Sydney					
PC1	0.162	0.108	0.027	≤ 0.0001	0.020
PC2	0.036	0.018	0.572	0.007	0.001
PC3	≤ 0.0001	≤ 0.0001	≤ 0.0001	0.165	0.163
PC4	≤ 0.0001	≤ 0.0001	0.001	0.440	≤ 0.0001
PC5	≤ 0.0001	≤ 0.0001	≤ 0.0001	0.024	≤ 0.0001

By genetic haplotype

The position of individual points on this PCA plot and the warped outline changes (Figure V-J) are the same as the previous PC1-PC2 plot (Figure V-H); only the colour coding differs.

Genetic haplotype assignment shows the Sydney *domesticus* haplotype mean ellipse is effectively separated from the mean ellipses of forest haplotypes, which overlap considerably, along CV1. Along CV2, Sydney *domesticus* mandibles cluster closely with *domesticus* Clade E forest mandibles (Pureora and Craigieburn).

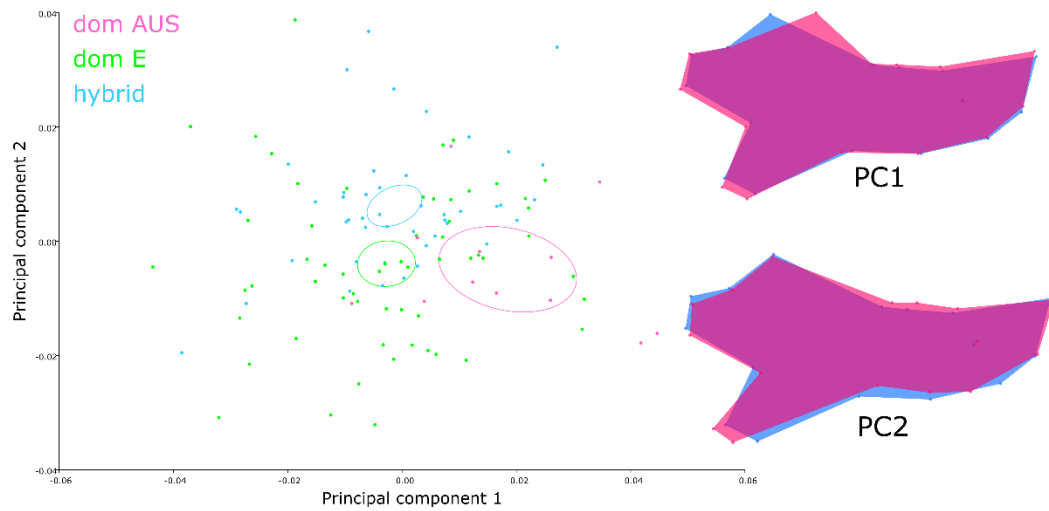


Figure V-J PCA plot of mandible shape differences between forest and Sydney genetic haplotypes. Each dot represents a specimen, with 90% confidence ellipses around the mean.

5.4.3.2 Discriminant Function Analysis

The cross-validated DFA separated three groups with >93% accuracy (Table V-7).

Sydney mandibles were most similar to Zealandia mandibles. Figure V-K shows the Procrustes-based superimposition of mean mandible shape for these three locations.

The superimposition of Eglinton and Sydney mice reveals the mean shape of Sydney mandibles has a broader mandible profile with expanded processes (Figure V-K: A).

The same shape variation is observed with superimposition of Hollyford and Pureora samples with Sydney (Figure V-K: B and C).

Table V-7 Misclassification percentage of cross-validation discriminant function analysis for forest and Sydney mandibles. Bold, red text indicates misclassification levels of $\leq 5\%$. Bold italicised text indicates $\leq 10\%$.

	Craigieburn	Eglinton	Hollyford	Zealandia	Pureora
Sydney	12.8	3.3	3.1	53.8	6.8

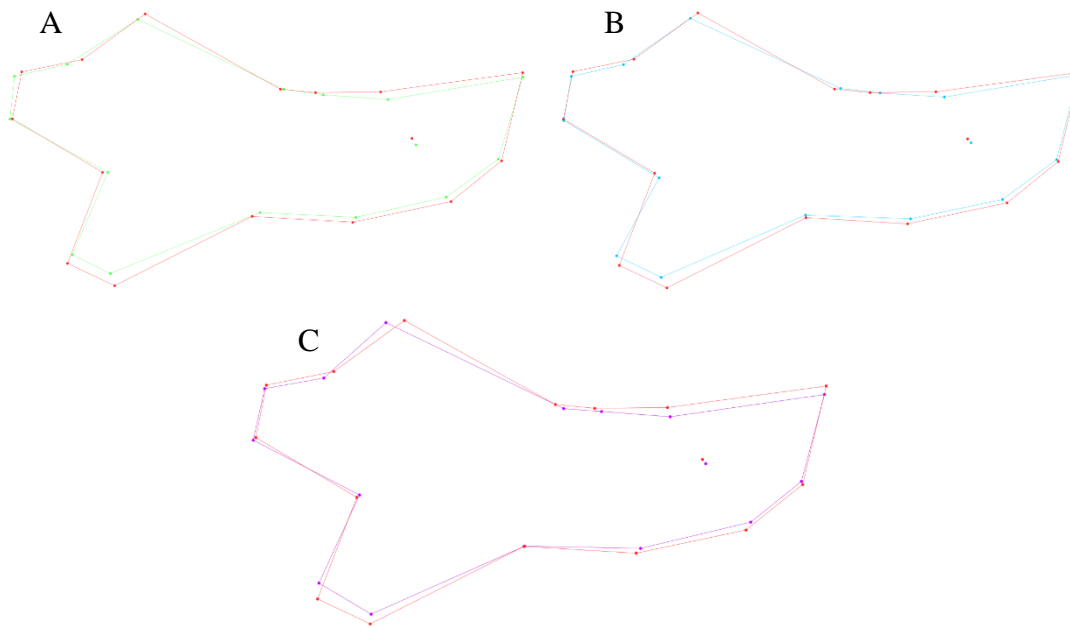


Figure V-K Procrustes-based superimposition of forest and Sydney mean mandible shapes obtained from discriminant function analysis. A: Sydney (orange) and Craigieburn (light green), B: Sydney (orange) and Hollyford (blue), C: Sydney (orange) and Pureora (purple).

By genetic haplotype

The cross-validated DFA separated Sydney *domesticus* mandibles from *domesticus* Clade E and *domesticus* – *castaneus*NZ.1 hybrid groups with >96% accuracy (Table V-8). The superimposition of Sydney *domesticus* with hybrid and Clade E mean mandible shapes show the Sydney *domesticus* haplotype has a slightly broader shape with larger angular processes (Figure V-L).

Table V-8 Misclassification percentage of cross-validation discriminant function analysis for forest and Sydney haplotypes. Bold, red text indicates misclassification levels of $\leq 5\%$.

	<i>Dom-cas</i> NZ.1 hybrid	<i>Domesticus</i> Clade E
<i>Sydney domesticus</i>	3.5	1.4

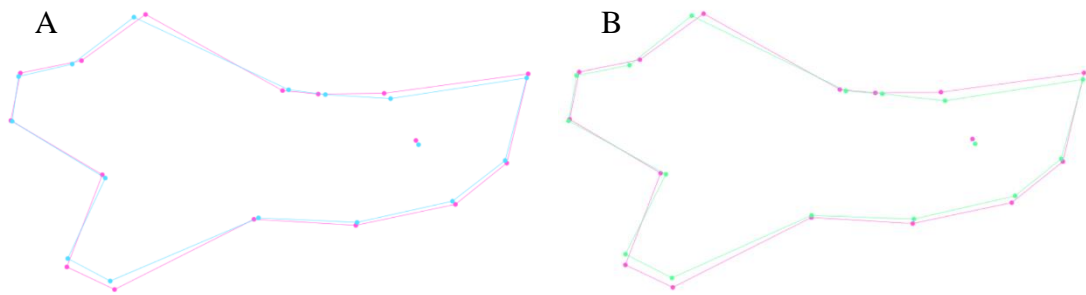


Figure V-L Procrustes-based superimposition of mean mandible shapes from forest and Sydney haplotypes obtained from discriminant function analysis. A: Sydney domesticus (pink) and domesticus-castaneusNZ.1 hybrids (blue), B: Sydney domesticus (pink) and forest domesticus Clade E (green).

5.4.3.3 Canonical Variate Analysis

CVA reveals Sydney mice overlap with Zealandia and Pureora at the far right of the first canonical axis (Figure V-M). Along the second CV axis Sydney and Zealandia overlap again at the positive end of CV2, separated from the other four populations. The first CV represents 39% of the total variation, while CV2 accounts for 28.3% (Table V-9: A). Together, the first two CVs represent over 67% of the total variation between groups.

The CV1 warped outline plot depicts the same shape change observed in Chapter III: a broader mandible profile (pink outline), with an extended coronoid process and wider angular process associated with Sydney, Zealandia and Pureora groups at the positive end of the first axis (Figure V-M).

The CV2 warped outline plot, however, depicts a broader mandible profile associated with Sydney and Zealandia mandibles at the positive end of the second CV axis (pink outline; Figure V-M). This shape change differs from the elongated profile observed in Chapter III.

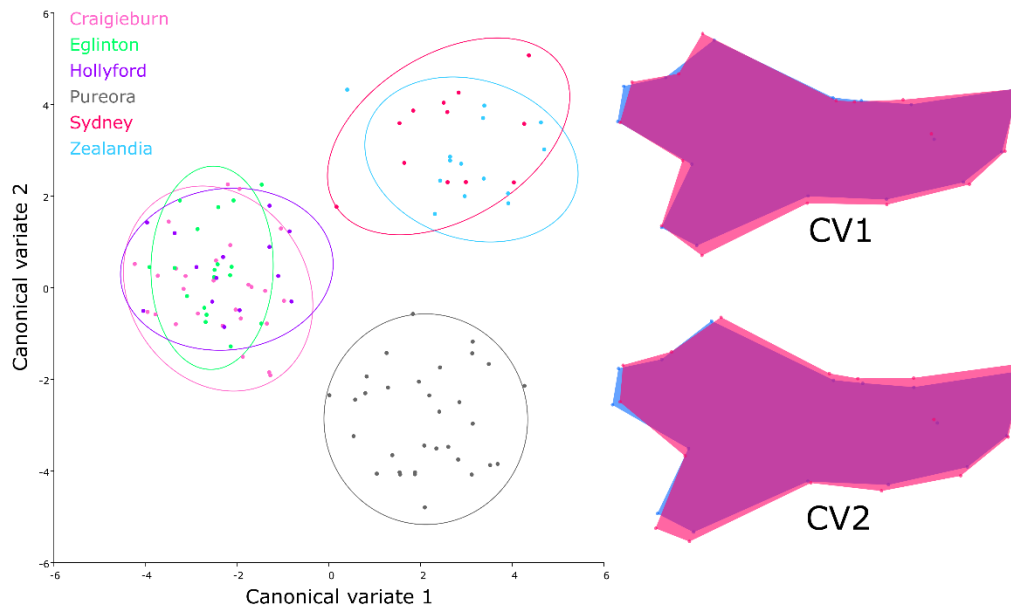


Figure V-M LEFT CVA plot displaying maximum differentiation of pre-defined forest and Sydney groups. RIGHT Procrustes deformation warped outlines depicting the change in mandible shape along each axis; blue represents mandible shape at far left of the axis, pink represents the mandible shape at far right of the axis.

The Mahalanobis distances and Procrustes distances of the first canonical axis were significantly different between all pairwise locations (Table V-9: B and C). The largest Mahalanobis and Procrustes distances are observed between Eglinton and Sydney. The smallest Mahalanobis and Procrustes distances are observed between Sydney and Zealandia, which overlap considerably on the CVA plot and PC3.

Table V-9 Canonical Variate Analysis results for forest and Sydney mandibles. A) Canonical variates and their associated variance percentages. B) Mahalanobis distances between groups along the first CV axis and their associated p-values. C) Procrustes distances between groups along the first CV axis and their associated p-values. Bold, red text indicates significant p-values ≤ 0.05 . Bold text indicates highest and lowest distance values between pairs.

A					
	CV1	CV2	CV3	CV4	CV5
Eigenvalues	6.345801	4.59398	2.335799	2.034797	0.953305
Variance (%)	39.018	28.247	14.362	12.511	5.862
Cumulative (%)	39.018	67.265	81.627	94.138	100
B					
Sydney	Craigieburn	Eglington	Hollyford	Zealandia	Pureora
Mahalanobis distance	7.2217	7.2581	7.0714	6.167	6.9194
P-value	≤ 0.0001	≤ 0.0001	≤ 0.0001	≤ 0.0001	≤ 0.0001
C					
Sydney	Craigieburn	Eglington	Hollyford	Zealandia	Pureora
Procrustes distance	0.0397	0.0454	0.0396	0.039	0.0444
P-value	≤ 0.0001	≤ 0.0001	≤ 0.0001	≤ 0.0001	≤ 0.0001

By genetic haplotype

CVA reveals Sydney *domesticus* mice are well differentiated from forest haplotypes at the far right of the first canonical axis (Figure V-N). Along the second CV axis Sydney overlaps somewhat with *domesticus* Clade E forest mandibles at the negative end of the axis. The first CV represents 61% of the total variation, while CV2 accounts for 39% (Table V-10: A).

The CV1 warped outline plot depicts a broader mandible profile with an extended angular process associated with Sydney *domesticus* mice at the positive end of the first axis (pink outline; Figure V-N). The CV2 outline shows slightly larger coronoid and angular processes associated with Sydney *domesticus* mandibles at the negative end of the second axis (blue outline).

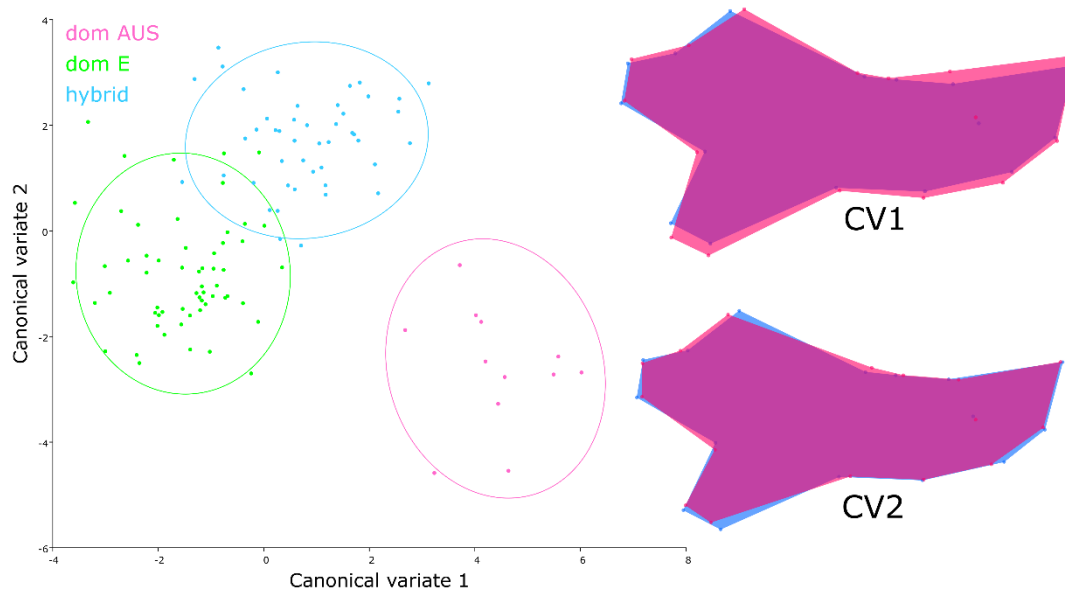


Figure V-N LEFT CVA plot displaying maximum differentiation of pre-defined forest and Sydney haplotype groups. RIGHT Procrustes deformation warped outlines depicting the change in mandible shape along each axis; blue represents mandible shape at far left of the axis, pink represents the mandible shape at far right of the axis.

The Mahalanobis distances and Procrustes distances of the first canonical axis were significantly different between all pairwise locations (Table V-10: B and C). The largest Mahalanobis and Procrustes distances are observed between Sydney *domesticus* and *domesticus* – *castaneus*NZ.1 hybrid groups. The smallest Mahalanobis and Procrustes distances are observed between Sydney *domesticus* and *domesticus* Clade E groups.

Table V-10 Canonical Variate Analysis results for forest and Sydney haplotype groups. A) Canonical variates and their associated variance percentages. B) Mahalanobis distances between groups along the first CV axis and their associated p-values. C) Procrustes distances between groups along the first CV axis and their associated p-values. Bold, red text indicates significant p-values ≤ 0.05 . Bold text indicates highest and lowest distance values between pairs.

A		
	CV1	CV2
Eigenvalues	3.507036	2.242779
Variance (%)	60.994	39.006
Cumulative (%)	60.994	100
B		
<i>Sydney domesticus</i>	<i>Dom-casNZ.1 hybrid</i>	<i>Domesticus Clade E</i>
Mahalanobis distance	6.1866	5.6103
P-value	≤ 0.0001	≤ 0.0001
C		
<i>Sydney domesticus</i>	<i>Dom-casNZ.1 hybrid</i>	<i>Domesticus Clade E</i>
Procrustes distance	0.0399	0.0353
P-value	≤ 0.0001	≤ 0.0001

5.4.4 Discussion

This study found significant variation between Sydney and New Zealand forest mouse mandibles, but produced conflicting results for Sydney mandible shape. PCA found Sydney mandibles to cluster with South Island samples at the far right of PC1, and overlap with *Pureora* mandibles along the second axis.

However, CVA and DFA results suggest Sydney mandibles are most similar to *Zealandia* mandible shape, overlapping considerably on the CVA ordination plot. Sydney mandibles had greater temporalis mechanical advantage than *Pureora* and

Zealandia mandibles, lending Sydney mice an occlusion efficiency similar to South Island mice. In Chapter III, South Island mice were suggested to consume a greater portion of soft foods such as invertebrates compared with North Island mice (Renaud et al. 2015). Furthermore, Sydney mandibles had significantly lower masseter advantage than Zealandia mice, suggesting Zealandia mice may incorporate a greater proportion of resistant plant material into their diet than Sydney mice (Satoh 1997; Baverstock et al. 2013; Renaud et al. 2015).

Yet the smallest Procrustes and Mahalanobis distances were observed between Sydney and Zealandia mandibles. Zealandia and Sydney only clustered together on the PCA plot with PC3, which explained 9.6% of the total variation in mandible shape. Average Sydney centroid size was significantly smaller than all New Zealand forest centroid sizes, implying they had the smallest mandible size.

Haplotype was a very effective discriminating factor for Sydney mandible shape, especially along the first axes of PCA and CVA plots. Sydney *domesticus* mandibles were most similar to New Zealand forest *domesticus* Clade E mandibles along the second axes of both PCA and CVA plots. Sydney *domesticus* shape was very different to *Domesticus – castaneus*NZ.1 hybrid mandible shapes, showing a broader mandible profile with a forward-shifted coronoid process.

These results suggest Sydney mandibles represent an efficient intermediate phenotype that is very different from the observed New Zealand mouse phenotypes. Genetic haplotype may be an important variable contributing to this variation in Sydney mandible shape.

5.5 Offshore island and Sydney comparison

5.5.1 Centroid size

Sydney mandible centroid size differed significantly to all New Zealand offshore island mandibles (Table V-11). Antipodes I. produced a p-value slightly above 0.05, and in this study is considered biologically significant. Average Sydney centroid size was significantly greater than Chatham I. and Antipodes I., but significantly smaller than the other four islands (Figure V-O).

Table V-11 P-values from Kruskal-Wallis ANOVA pairwise comparison of mandible centroid size between offshore island and Sydney mice. Bold, red text indicates significant p-values ≤ 0.05 . Bold, italicised text indicates p-values close to 0.05.

Centroid Size	Auckland	Chatham	Enderby	Ruapuke	Waikawa	Antipodes
Sydney	0.007	0.004	≤ 0.0001	0.002	0.030	<i>0.053</i>

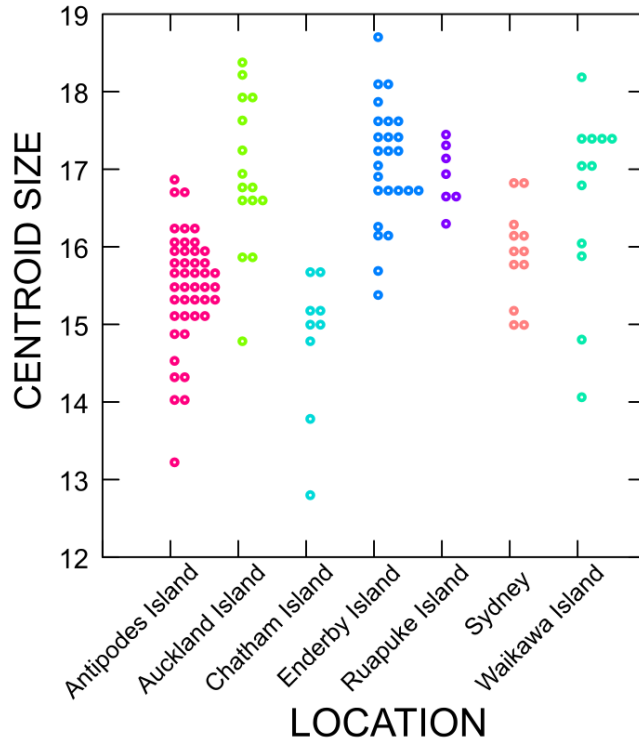


Figure V-O Dot density plot showing the distribution of centroid size within offshore island and Sydney populations. Each icon represents an individual mouse.

5.5.2 Biomechanical analysis

Sydney mandibles had significantly greater temporalis mechanical advantage compared to four of the seven island samples (although Antipodes I. was nearly so; Table V-12). Sydney was most similar to Chatham I. in temporalis advantage. Significantly lower masseter advantage was found between Sydney and Enderby I., and to some extent Anchorage Bay and Auckland I. Overall, Sydney mandibles were most similar in mechanical efficiency to Chatham I. mandibles, and most dissimilar to Enderby I.

Table V-12 P-values from Kruskal-Wallis ANOVA pairwise comparison of the biomechanical advantage ratios between offshore island and Sydney mandibles. Bold, red text indicates significant p-values ≤ 0.05 . Bold italicised text indicates p-values close to 0.05.

	North Plain	Anchorage Bay	Chatham	Enderby	Waikawa	Auckland	Ruapuke
Masseter/Incisor							
Sydney	0.113	0.004	0.19	≤ 0.0001	0.355	0.002	0.128
Masseter/Molar							
Sydney	0.249	0.14	0.054	0.002	0.253	0.262	0.076
Temporalis/Incisor							
Sydney	0.077	0.113	0.877	≤ 0.0001	0.0009	≤ 0.0001	0.002
Temporalis/Molar							
Sydney	0.072	0.016	0.817	≤ 0.0001	0.004	≤ 0.0001	0.003

5.5.3 Shape analysis

5.5.3.1 Regression and Principal Component Analysis

The pooled within-group regression was significant for allometry ($p \leq 0.0001$ after 1000 permutations), with size accounting for 10.94% of shape variance (Figure V-P).

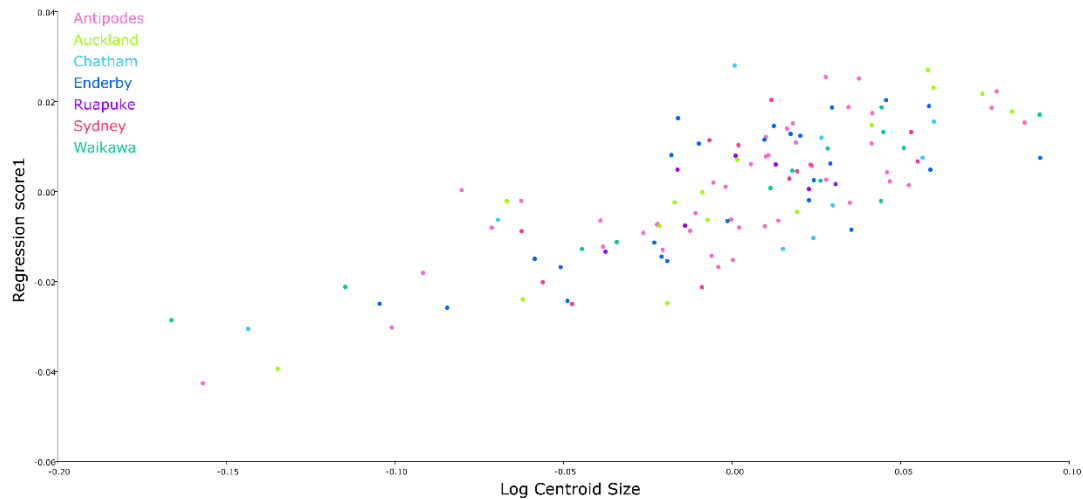


Figure V-P Group-centred regression of mandible shape on log centroid size for offshore island and Sydney mandibles.

The first seven principal components accounted for >5% variance, accumulating to 66.5% of total variance (Table V-13). Only the first two eigenvalues fall above the inflection point of the scree plot (Figure V-Q). It is unlikely that the other five have any biological significance so are not discussed.

Table V-13 Eigenvalues for the offshore island and Sydney PCA plot that represent more than 5% variance. Eigenvalues above the 'lee' point on the scree plot are italicised.

	EV1	EV2	EV3	EV4	EV5	EV6	EV7
Eigenvalues	<i>0.000183</i>	<i>0.000162</i>	0.000104	9.54E-05	8.68E-05	7.07E-05	6.46E-05
Variance (%)	<i>15.868</i>	<i>14.096</i>	9.001	8.276	7.529	6.131	5.604
Cumulative (%)	<i>15.868</i>	<i>29.964</i>	38.965	47.241	54.771	60.901	66.505

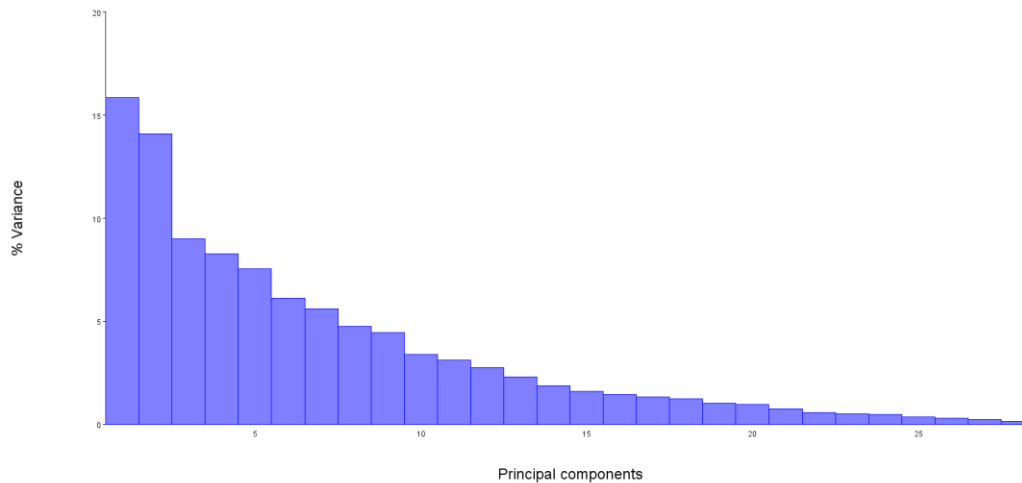


Figure V-Q Scree plot of the variance explained by each eigenvalue for offshore island and Sydney mandibles.

PC1 accounted for 15.9% of total shape variation (Table V-13; Figure V-R). The 90% confidence ellipses surrounding the mean of each location indicate Sydney mandibles cluster to the far right of the first PC axis, most similar to Chatham I. samples. The PC1 warped outline plot depicts a forward shift of the coronoid process, a longer angular process, with expansion of condylar process and shifted alveolar region associated with Sydney mandibles at the positive end of PC1 (pink outline; Figure V-R).

PC2 accounts for 14.1% of mandible shape variation (Table V-13; Figure V-R). Sydney mandibles mostly cluster with Auckland I., Antipodes I., and Waikawa I. mandibles along PC2. The PC2 warped outline plot shows reduced coronoid and condyle processes, longer angular process and upwards shift of the incisor region with positive change along the axis (pink outline; Figure V-R). Sydney mandibles fall between the two extremes depicted by the PC2 warped outlines.

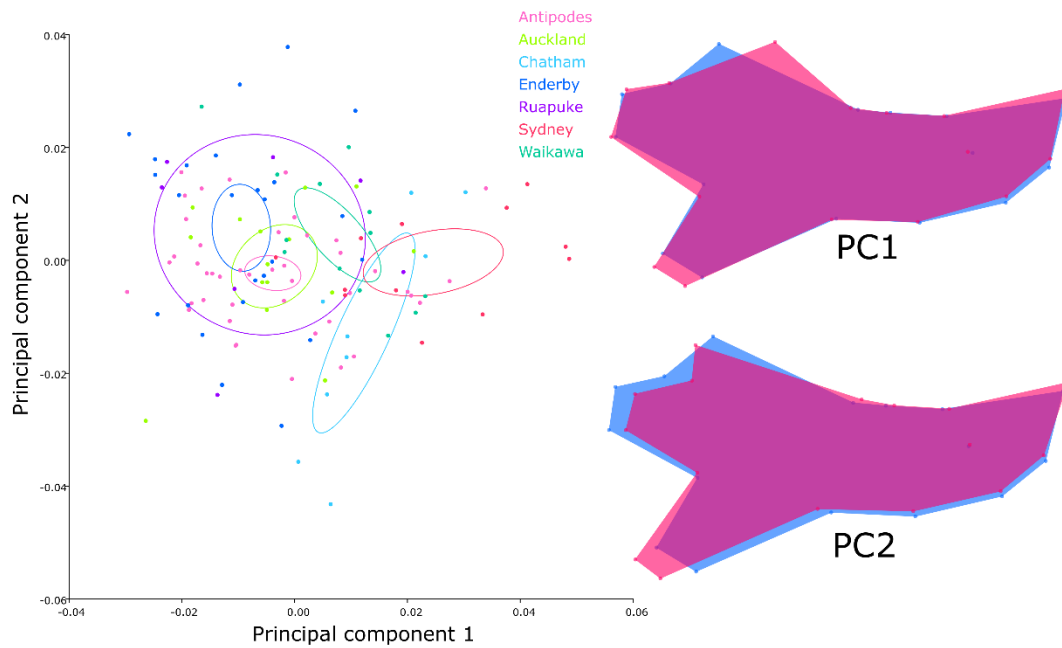


Figure V-R LEFT PCA plot of mandible shape differences between offshore island and Sydney populations. Each dot represents a specimen, surrounded by equal frequency ellipses. RIGHT Procrustes deformation warped outlines depicting the change in mandible shape along each axis; blue represents mandible shape at far left of the axis, pink represents the mandible shape at far right of the axis.

Kruskal-Wallis analysis revealed Sydney mandible shape varied significantly to all island mandible shapes within PC1 (Table V-14), consistent with the separation of Sydney mice on the ordination plot. Although Antipodes I. mandibles clustered within the mean ellipse of Auckland I., Antipodes I. significantly differed to Sydney mandibles along PC2 while Auckland I. and Waikawa I. did not. Sydney mandibles differed significantly with Enderby I. and Ruapuke I. mandibles across all PCs. Of the 30 pairwise comparisons, only five were not significant.

Table V-14 P-values from Kruskal-Wallis ANOVA pairwise comparison of the first five PCs between offshore island and Sydney mandible shapes. Bold, red text indicates significant p-values ≤ 0.05 . Bold, italicised text indicates p-values close to 0.05.

	Auckland	Chatham	Enderby	Ruapuke	Waikawa	Antipodes
Sydney						
PC1	0.025	0.004	≤ 0.0001	0.002	0.007	≤ 0.0001
PC2	0.77	0.016	0.006	0.004	0.957	≤ 0.0001
PC3	0.002	0.001	0.001	0.043	≤ 0.0001	0.119
PC4	≤ 0.0001	0.004	≤ 0.0001	0.002	0.55	≤ 0.0001
PC5	≤ 0.0001	<i>0.055</i>	≤ 0.0001	0.011	≤ 0.0001	0.001

By genetic haplotype

The position of individual points on this PCA plot and the warped outline changes (Figure V-S) are the same as the previous plot (Figure V-R); only the colour coding differs.

Genetic haplotype assignment shows the Sydney *domesticus* haplotype mean ellipse is effectively separated from the mean ellipses of offshore island *domesticus* Clades C, B and E haplotypes along CV1. (Figure V-S). New Zealand *Domesticus* Clades C and E mandibles are widespread throughout the ordination plot, whereas *domesticus* Clade B and Sydney *domesticus* mandible shapes are more localised. *Castaneus*NZ.2 mandible shapes are localised along PC1, but spread out along PC2. Sydney *domesticus* mandibles cluster somewhat closely with *castaneus*NZ.2 mandibles along PC1, and overlap with all New Zealand *domesticus* Clades along PC2.

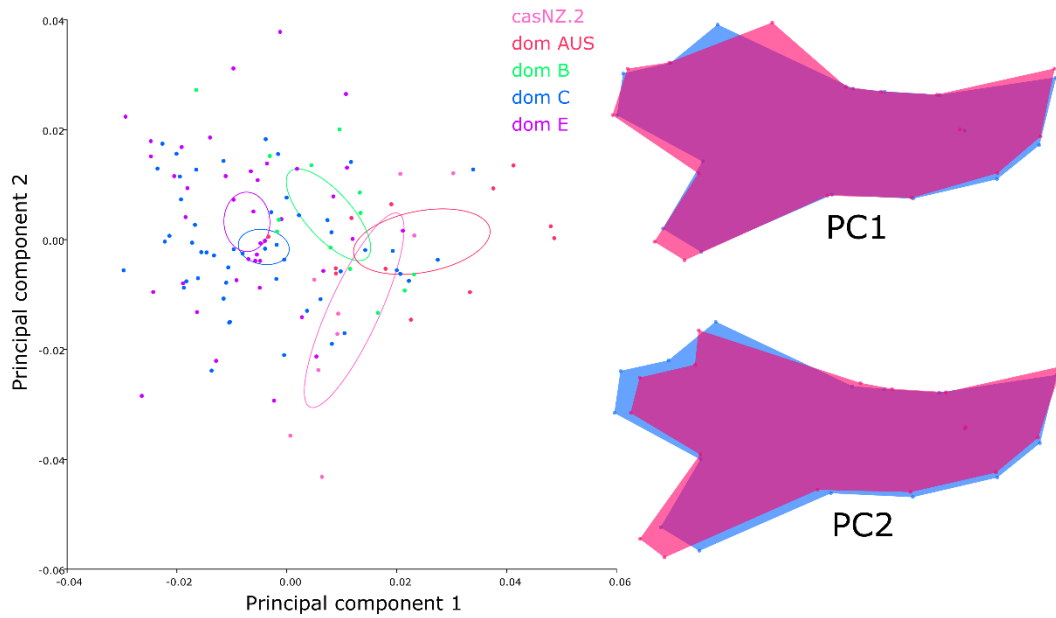


Figure V-S PCA plot of mandible shape differences between offshore island and Sydney genetic haplotypes. Each dot represents a specimen, with 90% confidence ellipses around the mean.

5.5.3.2 Discriminant Function Analysis

The cross-validated DFA separated three groups with >90% accuracy (Table V-15). Sydney mandibles were most similar to Waikawa mandibles. Figure V-T shows the Procrustes-based superimposition of mean mandible shape for these three locations.

Table V-15 Misclassification percentages of cross-validation discriminant function analysis for offshore island and Sydney mandibles. Bold, red text indicates misclassification levels of $\leq 5\%$.

	Antipodes	Auckland	Chatham	Enderby	Ruapuke	Waikawa
Sydney	0	25.9	9.5	10.8	5.3	40

When overlaid with Antipodes I., Sydney mean mandible shape depicts a broader mandible profile, with slightly shifted coronoid and angular processes (Figure V-T: A). The superimposition of Chatham I. and Sydney is similar to that of Antipodes I. and Sydney, but with the addition of an extended angular process in Sydney mean

mandible shape (Figure V-T: B). The mean shape of Ruapuke I. mandibles displays an almost identical superimposition to Antipodes I., with the exception of Sydney not exhibiting such a broad alveolar change (Figure V-T: C).

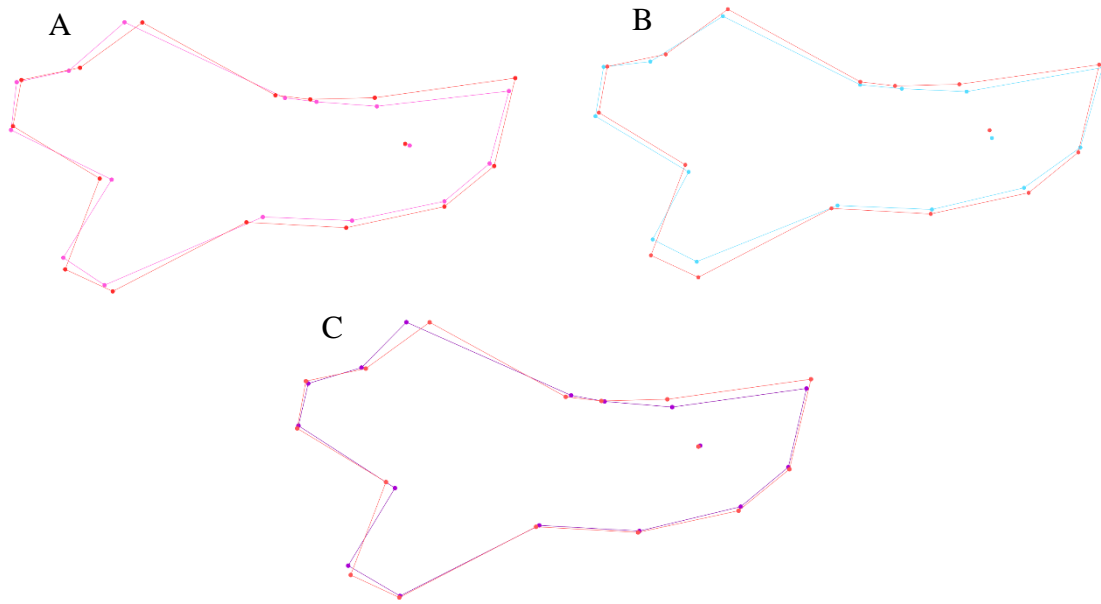


Figure V-T Procrustes-based superimposition of offshore island and Sydney mean mandible shapes obtained from discriminant function analysis. A: Sydney (orange) and Antipodes I. (pink), B: Sydney (orange) and Chatham I. (blue), C: Sydney (orange) and Ruapuke I. (purple).

By genetic haplotype

Cross-validated DFA separated Sydney *domesticus* mandibles from three of four haplotype groups with >95% accuracy (Table V-16). Figure V-U shows the Procrustes-based superimposition of mean mandible shape for these three pairwise comparisons.

Table V-16 Misclassification percentages of cross-validation discriminant function analysis for offshore island and Sydney haplotypes. Bold, red text indicates misclassification levels of $\leq 5\%$.

	<i>castaneus</i> NZ.2	<i>dom</i> Clade B	<i>dom</i> Clade C	<i>dom</i> Clade E
Sydney <i>domesticus</i>	4.8	28	0	3.9

In all three superimpositions, the Sydney *domesticus* haplotype has a much broader mean mandible shape with larger angular processes (Figure V-U: A, B and C).

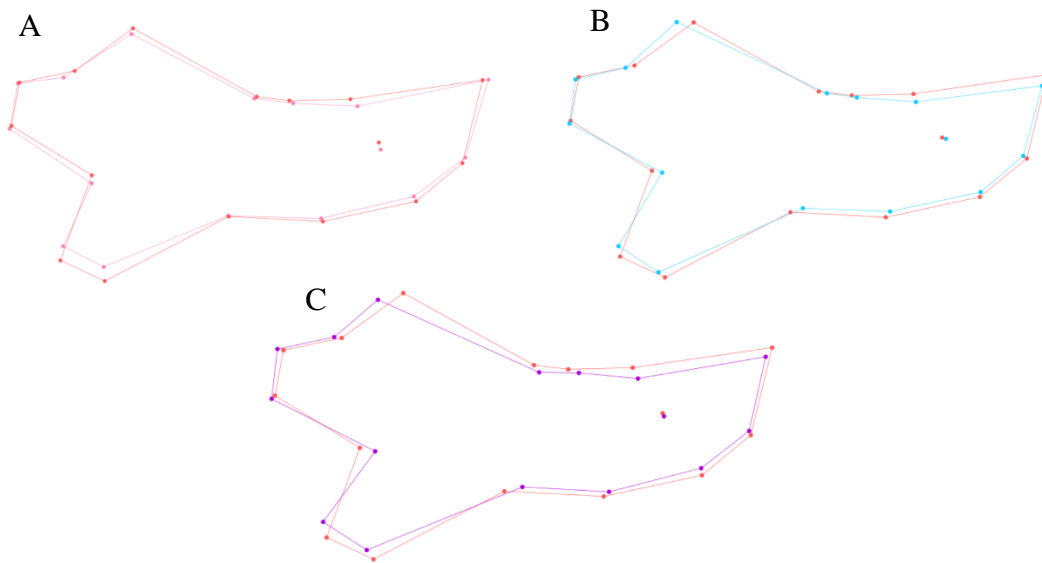


Figure V-U Procrustes-based superimposition of mean mandible shapes for offshore island and Sydney haplotypes obtained from discriminant function analysis. A: Sydney *domesticus* (orange) and *castaneus* (pink), B: Sydney *domesticus* (orange) and dom Clade C (blue), C: Sydney *domesticus* (orange) and dom Clade E (purple).

5.5.3.3 Canonical Variate Analysis

CVA reveals Sydney mice overlap with Chatham I. and Waikawa I. at the far right of the first canonical axis (Figure V-V). Along the second CV axis Sydney, Chatham I. and Waikawa I. overlap again with Ruapuke I. and Auckland I. at the positive end of CV2, midway between Antipodes I. and Enderby I. The first CV represents 56.4% of the total variation, while CV2 accounts for 15.8% (Table V-17: A). Together, the first two CVs represent over 72% of the total variation between groups.

The CV1 warped outline plot depicts the same shape change observed in Chapter IV: a broader alveolar profile with a shorter angular process (pink outline), associated with Sydney, Chatham I. and Waikawa I. groups at the positive end of the first axis (Figure V-V).

The CV2 warped outline plot is also similar to that of CH IV, depicting an expanded condyle process, depressed coronoid process, and a slightly longer alveolar region associated with Enderby I. mandibles at the positive end of the second CV axis (pink outline; Figure V-V). Sydney mandibles fall between the two wifeframe shapes that represent Enderby I. and Antipodes I. mandibles at opposing ends of the second axis.

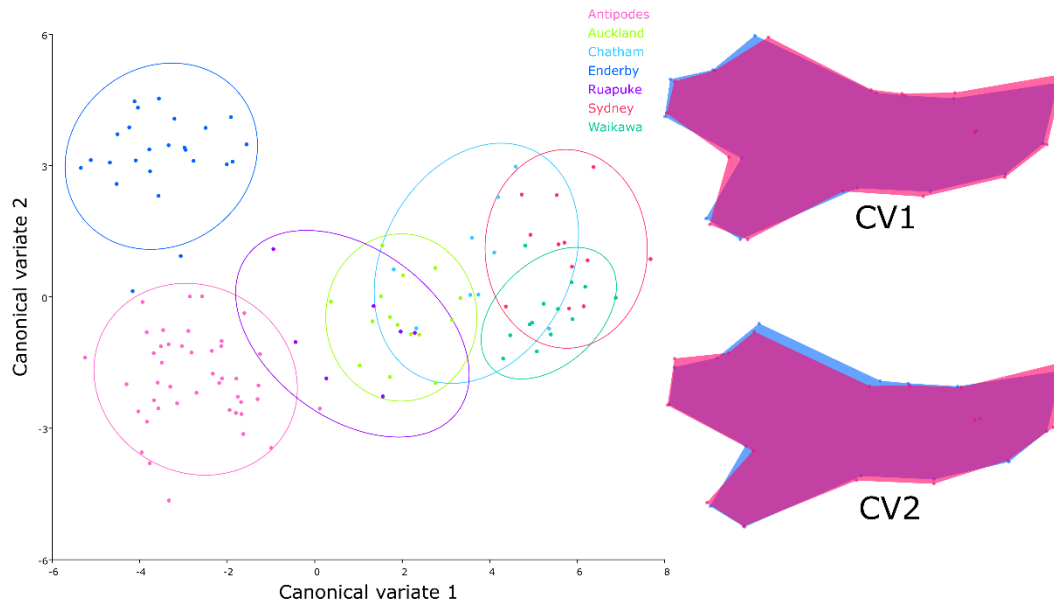


Figure V-V LEFT CVA plot displaying maximum differentiation of pre-defined offshore island and Sydney groups. RIGHT Procrustes deformation warped outlines depicting the change in mandible shape along each axis; blue represents mandible shape at far left of the axis, pink represents the mandible shape at far right of the axis.

The Mahalanobis distances and Procrustes distances of the first canonical axis were significantly different between all pairwise locations (Table V-17: B and C). The largest Mahalanobis and Procrustes distances are observed between Enderby I. and Sydney. The smallest Mahalanobis and Procrustes distances are observed between Sydney and Waikawa I., which overlap considerably on the CVA plot.

Table V-17 Canonical Variate Analysis results for offshore island and Sydney mandibles. A) Canonical variates and their associated variance percentages. B) Mahalanobis distances between groups along the first CV axis and their associated p-values. C) Procrustes distances between groups along the first CV axis and their associated p-values. Bold, red text indicates significant p-values ≤ 0.05 . Bold text indicates highest and lowest distance values between pairs.

A						
	CV1	CV2	CV3	CV4	CV5	CV6
Eigenvalues	13.47343	3.761371	2.949575	1.744383	1.456683	0.489427
Variance (%)	56.434	15.755	12.354	7.306	6.101	2.05
Cumulative (%)	56.434	72.188	84.542	91.849	97.95	100
B						
Sydney	Antipodes	Auckland	Chatham	Enderby	Ruapuke	Waikawa
Mahalanobis distance	9.5099	7.8725	6.7319	10.2561	8.2268	5.4465
P-value	≤ 0.0001	≤ 0.0001	≤ 0.0001	≤ 0.0001	≤ 0.0001	≤ 0.0001
C						
Sydney	Antipodes	Auckland	Chatham	Enderby	Ruapuke	Waikawa
Procrustes distance	0.0576	0.0498	0.0505	0.0641	0.0437	0.0325
P-value	≤ 0.0001	≤ 0.0001	≤ 0.0001	≤ 0.0001	≤ 0.0001	≤ 0.0001

By genetic haplotype

CVA grouping by genetic haplotype show *Sydney domesticus* overlaps with *castaneus*NZ.2 and *domesticus* Clade B groups at the negative end of the first axis, and midway along the second axis (Figure V-W). *Sydney domesticus* mandibles are effectively separated from *domesticus* Clades C and E along CV1, and fall midway between the two groups on CV2. The first CV axis accounts for 55.1% of total

variation, and CV2 accounts for 23.8% totalling more than 78% of shape variation (Table V-18). The CV1 warped outline plot shows Sydney *domesticus* mandibles at the far left of the CV1 axis possess slightly broader alveolar regions with a smaller condyle processes (blue outline; Figure V-W). *Domesticus* Clades C and E mandibles at the far right have a slimmer alveolar profile and slightly larger coronoid and condyle zones.

The CV2 warped outline plot indicates a shift from broader, shorter mandibles to slimmer, elongated mandibles with positive change along the second axis (Figure V-W). Sydney *domesticus* mandible shape falls between these two extremes of CV2.

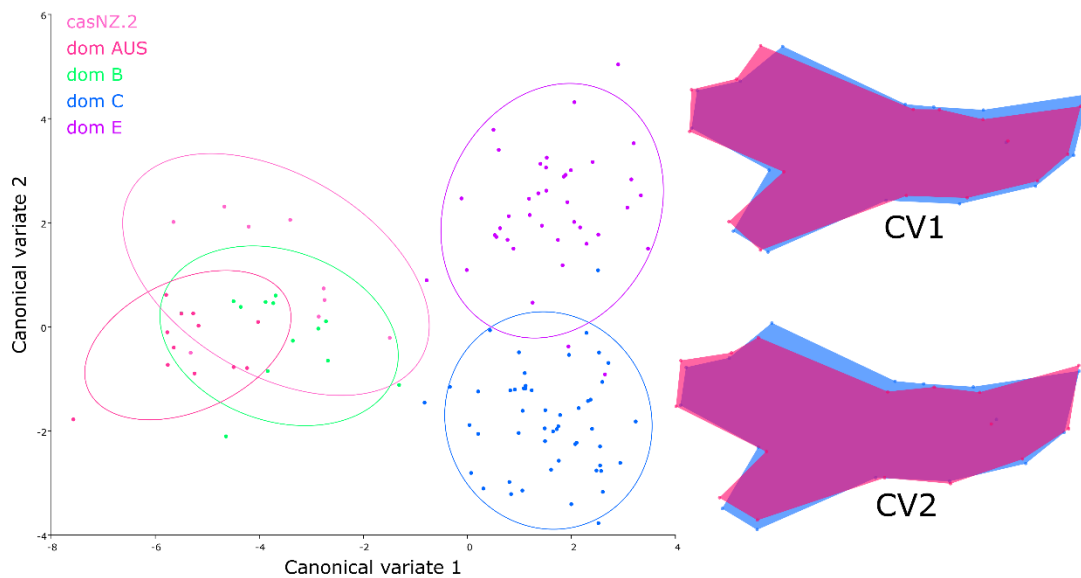


Figure V-W LEFT CVA plot displaying maximum differentiation of pre-defined offshore island and Sydney haplotype groups. RIGHT Procrustes deformation warped outlines depicting the change in mandible shape along each axis; blue represents mandible shape at far left of the axis, pink represents the mandible shape at far right of the axis.

The Mahalanobis distances and Procrustes distances were significantly different between all pairwise locations, largest between Sydney *domesticus* and *domesticus* Clade E and smallest between Sydney *domesticus* Clades B (Table V-18: B and C).

Table V-18 Canonical Variate Analysis results for offshore island and Sydney haplotypes. A) Eigenvalues and their associated variance percentages. B) Mahalanobis distances between groups along the first CV axis and their associated p-values. C) Procrustes distances between groups along the first CV axis and their associated p-values. Bold, red text indicates significant p-values ≤ 0.05 . Bold text indicates highest and lowest distance values between pairs.

A				
	CV1	CV2	CV3	CV4
Eigenvalues	7.238493	3.127148	1.823341	0.952551
Variance (%)	55.081	23.796	13.875	7.248
Cumulative (%)	55.081	78.877	92.752	100
B				
<i>Sydney domesticus</i>	<i>castaneusNZ.2</i>	<i>dom Clade B</i>	<i>dom Clade C</i>	<i>dom Clade E</i>
Mahalanobis distance	6.6445	5.3416	7.6784	7.9056
P-value	≤ 0.0001	≤ 0.0001	≤ 0.0001	≤ 0.0001
C				
<i>Sydney domesticus</i>	<i>castaneusNZ.2</i>	<i>dom Clade B</i>	<i>dom Clade C</i>	<i>dom Clade E</i>
Procrustes distance	0.0459	0.0367	0.0516	0.0674
P-value	≤ 0.0001	≤ 0.0001	≤ 0.0001	0.0003

5.5.4 Discussion

This study found significant variation between Sydney mandibles and mouse mandibles from New Zealand offshore islands. Mandibles of Sydney mice repeatedly showed shape variation consistent with efficient jaw occlusion associated with catching prey (Renaud et al. 2015). Average Sydney centroid size was significantly larger than Chatham I. and Antipodes I., but smaller than Auckland I., Enderby I., Ruapuke I., and Waikawa I. centroid sizes, suggestive of an intermediate mandible size.

Biomechanical analysis revealed Sydney mandibles had significantly greater temporalis advantage than (essentially) all island populations except Chatham I. mandibles. In Chapter IV, Chatham I. mice had the greatest temporalis advantage of all island populations, implying they were most adept at catching prey. Sydney mandibles had significantly less masseter advantage than Enderby I. mandibles, but similar advantage to all other locations, suggesting they are also fairly adept at processing resistant plant material (Sato 1997; Baverstock et al. 2013; Renaud et al. 2015).

Sydney mandibles clustered closely with Chatham I. and Waikawa I. mandibles at the far right of PC1, associated with an extended angular process, slightly larger condyle process, and increased distance between the coronoid and condyle processes. This shape variation is further indication that catching invertebrate prey forms an important portion of mouse diet in these locations. Variation in diet between locations may be a product of habitat type, with dense grass cover supporting increased plant consumption on the more southern islands compared with Sydney, Chatham I. and Waikawa I. populations (Samaniego-Herrera et al. 2017).

With PC2, Sydney mandibles cluster beside Auckland I., Antipodes I., and Waikawa I. midway along the axis. Further studies are required to confirm the variables that explain variation in mandible shape beyond PC1. Kruskal-Wallis ANOVA revealed Sydney mandible shape differed significantly to New Zealand island mandibles across the first five PCs.

CVA found Sydney mandibles were differentiated to the far right of the first canonical axis alongside Chatham I. and Waikawa I. groups. Shape change along the first axis showed a slightly broader mandible profile and shortened angular process associated with Sydney mandibles at the positive end of CV1. Sydney mandibles were most dissimilar to Enderby I. mandible shape, previously noted to be most efficient at processing plant material in Chapter IV. DFA results also found a broader mandible profile was consistently portrayed by mean Sydney mandible shape.

Haplotype analyses found that *domesticus* Sydney mandibles were consistently associated with broader mandible shapes. DFA found *domesticus* Clade B (Waikawa I.) to be the most similar New Zealand mean mandible shape to *domesticus* Sydney mice. *Domesticus* Clade B and Sydney *domesticus* mandibles clustered closely on the CVA plot, but were slightly more differentiated with PCA. Interestingly, *domesticus* Clade E represented the most dissimilar mandible shape to Sydney *domesticus* mice. These results suggest factors other than genetics are important influencers of mandible shape on the small, remote Auckland Islands where these *domesticus* Clade E mice are found.

Overall, Sydney mice possess mandible shapes most similar to Chatham I. and Waikawa I. mice, and most dissimilar to Enderby I. mice. This study found Sydney

mouse mandible shape and function is more consistent with efficient incisor occlusion, suggesting a diet higher in softer rather than hard foods. However, my results do not support previous studies that suggest a diet of softer foods results in a slimmer mandible profile, not broader, as the mechanical force required to breakdown soft foods is considerably less compared with more resistant food (Anderson et al. 2014; Renaud et al. 2015). Sydney mandibles are biomechanically efficient in both temporalis and masseter zones, suggesting considerable variation in the Sydney house mouse diet compared with New Zealand offshore island populations, which may explain the unexpected broader profile.

5.6 New Zealand mice compared to Sydney mice

5.6.1 Shape analysis

5.6.1.1 Regression and Principal Component Analysis

The pooled within-group regression was significant for allometry ($p \leq 0.0001$ after 1000 permutations), with size accounting for 7.69% of shape variance (Figure V-X).

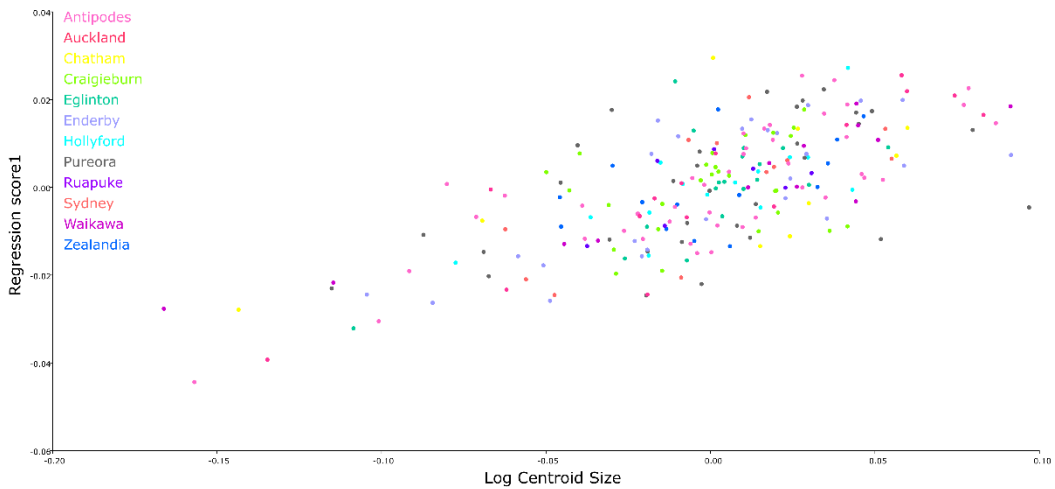


Figure V-X Group-centred regression of mandible shape on log centroid size for New Zealand and Sydney mandibles.

The first six principal components accounted for >5% variance, accumulating to 67.8% of total variance (Table V-19). Only the first eigenvalue falls above the inflection point of the scree plot (Figure V-Y). It is unlikely that the other five have any biological significance so are not discussed.

Table V-19 Eigenvalues for the New Zealand - Sydney PCA plot that represent more than 5% variance. Eigenvalues above the 'lee' point on the scree plot are italicised.

	EV1	EV2	EV3	EV4	EV5	EV6
Eigenvalues	<i>0.00041</i>	0.000246	0.000188	0.000132	0.000102	9.32E-05
Variance (%)	<i>23.736</i>	14.238	10.896	7.636	5.9	5.391
Cumulative (%)	<i>23.736</i>	37.975	48.871	56.507	62.407	67.798

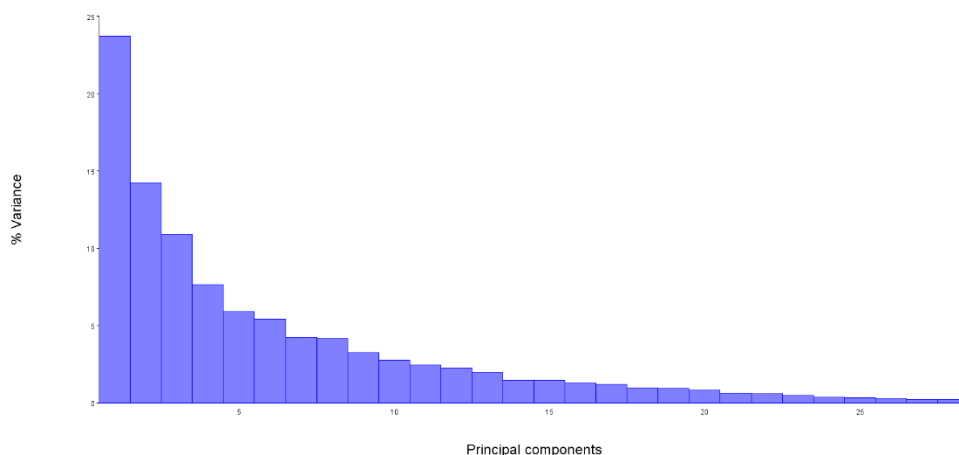


Figure V-Y Scree plot of the variance explained by each eigenvalue for New Zealand and Sydney.

PC1 accounted for 23.7% of total shape variation (Table V-19; Figure V-Z). The 90% confidence ellipses surrounding the mean of each location indicate Sydney mandibles cluster to the far left of the first PC axis, most similar to South Island, Chatham I. and Waikawa I. samples. Antipodes I. and Enderby I. are most differentiated from Sydney mandibles at the far right of the first axis. The PC1 warped outline plot depicts a forward shift of the coronoid process, smaller condyle and angular processes, and a broader alveolar region associated with Sydney mandibles at the negative end of PC1 (blue outline; Figure V-Z). At the far right, Enderby I. and Antipodes I. display a

slimmer, shorter mandible profile, with a longer angular process and greatly reduced distance between the coronoid and condyle processes (pink outline).

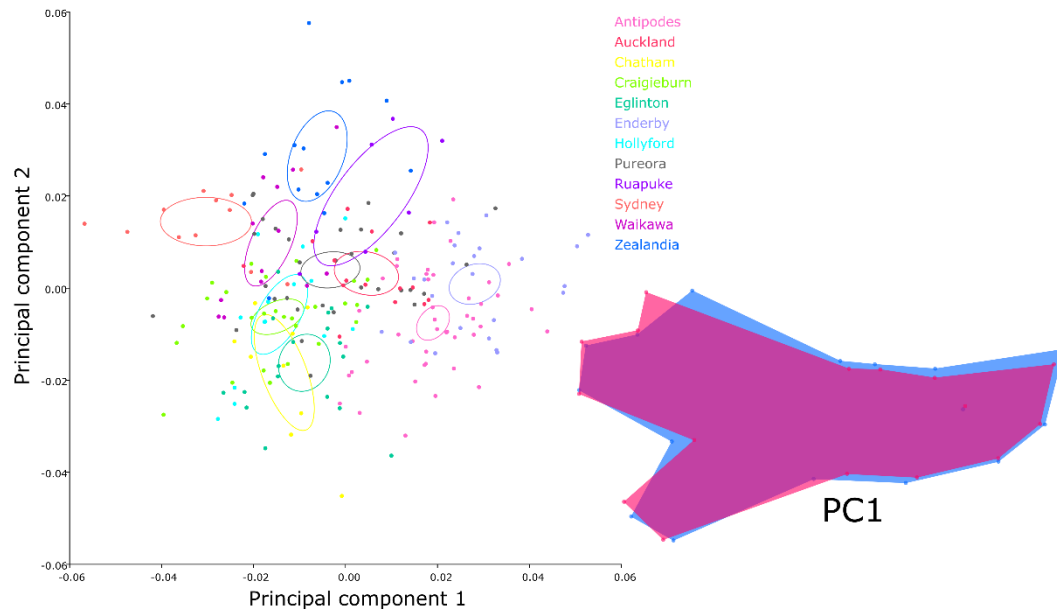


Figure V-Z LEFT PCA plot of mandible shape differences between New Zealand and Sydney populations. Each dot represents a specimen, surrounded by equal frequency ellipses. RIGHT Procrustes deformation warped outlines depicting the change in mandible shape along each axis; blue represents mandible shape at far left of the axis, pink represents the mandible shape at far right of the axis.

5.6.1.2 Canonical Variate Analysis

The first CV represents 45.8% of the total variation, while CV2 and CV3 account for 14.0% and 11.5% respectively (Table V-20). Together, the first three CVs represent over 71% of the total variation between groups.

The CV1 warped outline plot depicts a shift from broader mandible shape with reduced processes to a slimmer mandible profile with enlarged processes and a shifted coronoid process along the first axis from left to right (Figure V-AA). Sydney mandibles fall between these two extreme shapes, overlapping considerably with

Auckland I., Waikawa I., Chatham I., Zealandia, and the South Island mandibles in the negative axis region.

The CV2 warped outline plot depicts a mandible shape with an enlarged coronoid process, smaller condyle process, and slimmer alveolar profile associated with Antipodes I and Pureora mandibles at the positive end of the second canonical axis (pink outline; Figure V-AA). Sydney mandibles overlap with Enderby I., Ruapuke I., Auckland I., Waikawa I., Chatham I., and to some extent Zealandia and Hollyford mandibles towards the negative region of the axis. These mandibles show reduced coronoid processes, a larger condyle process, and a broader alveolar profile (blue outline).

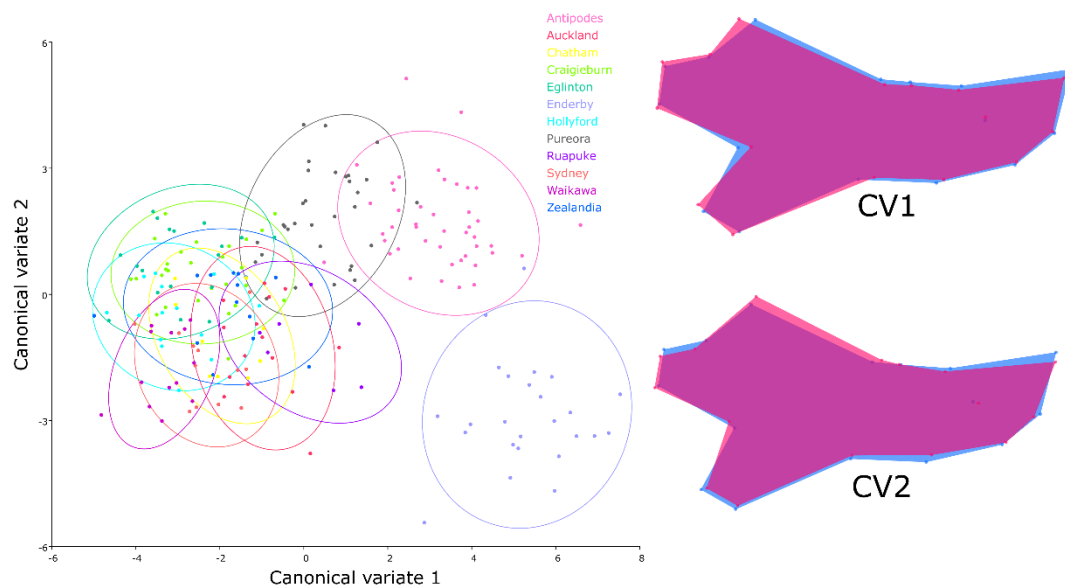


Figure V-AA LEFT CVA plot displaying maximum differentiation of pre-defined New Zealand and Sydney groups. RIGHT Procrustes deformation warped outlines depicting the change in mandible shape along each axis; blue represents mandible shape at far left of the axis, pink represents the mandible shape at far right of the axis.

Sydney mandibles cluster with Zealandia mandible shape along CV3, differentiated from all other populations (Figure V-BB). The CV3 warped outline plot suggests Zealandia and Sydney mandibles possess much broader mandible profiles than the other New Zealand mice, with enlarged coronoid and angular processes, but a reduced condyle process (pink outline).

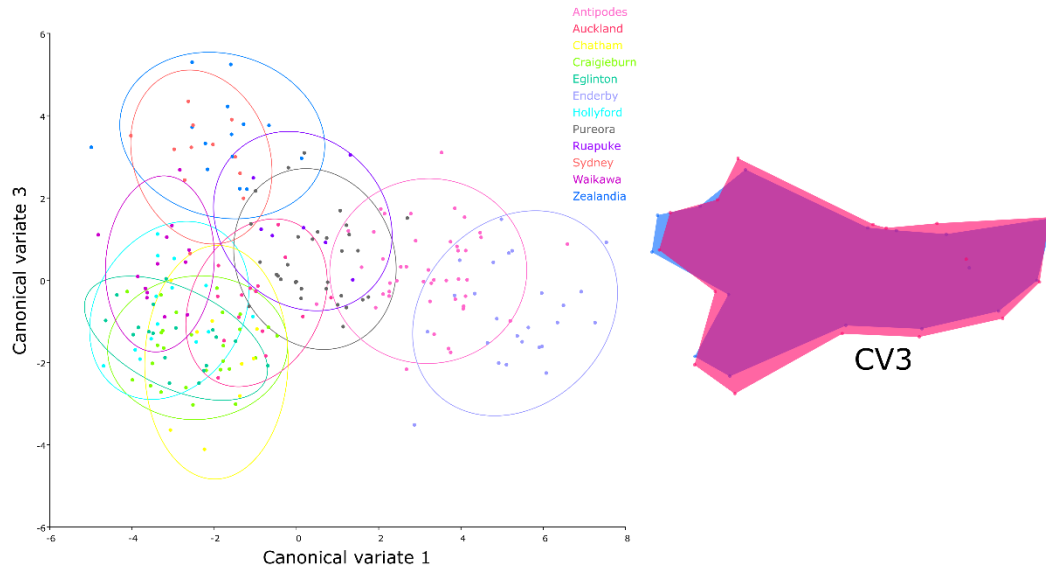


Figure V-BB LEFT CVA plot displaying maximum differentiation of pre-defined New Zealand and Sydney groups with CV1 and CV3. RIGHT Procrustes deformation warped outlines depicting the change in mandible shape along each axis; blue represents mandible shape at far left of the axis, pink represents the mandible shape at far right of the axis.

The Mahalanobis distances and Procrustes distances of the first canonical axis were significantly different between all pairwise locations (Tables V-22 and V-23). The largest Mahalanobis distance is observed between Eglinton and Enderby I, whereas the largest Procrustes distance is found between Enderby I. and Sydney. The smallest Mahalanobis and Procrustes distances are observed between Craigieburn and Hollyford.

Table V-20 Canonical variates and their associated variance percentages for New Zealand and Sydney mandibles.

	CV1	CV2	CV3	CV4	CV5	CV6	CV7	CV8	CV9	CV10	CV11
Eigenvalues	8.77699	2.67849	2.203643	1.309552	1.146722	0.947297	0.877288	0.622547	0.253564	0.208108	0.150465
Variance (%)	45.774	13.969	11.492	6.83	5.98	4.94	4.575	3.247	1.322	1.085	0.785
Cumulative (%)	45.774	59.743	71.235	78.065	84.045	88.986	93.561	96.808	98.13	99.215	100

Table V-21 Mahalanobis distances between groups along the first CV axis and their associated p-values for New Zealand and Sydney mandibles. Bold, red text indicates significant p-values ≤ 0.05 . Bold text indicates highest and lowest distance values between pairs.

Mahalanobis	Antipodes	Auckland	Chatham	Craigieburn	Eglinton	Enderby	Hollyford	Zealandia	Pureora	Ruapuke	Sydney	Waikawa
Antipodes		<.0001	<.0001	<.0001	<.0001	<.0001	<.0001	<.0001	<.0001	<.0001	<.0001	<.0001
Auckland	6.3849		<.0001	<.0001	<.0001	<.0001	<.0001	<.0001	<.0001	<.0001	<.0001	<.0001
Chatham	7.3006	5.7859		<.0001	<.0001	<.0001	<.0001	<.0001	<.0001	<.0001	<.0001	<.0001
Craigieburn	6.5322	4.9194	5.0047		<.0001	<.0001	<.0001	<.0001	<.0001	<.0001	<.0001	<.0001
Eglinton	6.7355	5.0313	4.4321	4.0919		<.0001	<.0001	<.0001	<.0001	<.0001	<.0001	<.0001
Enderby	5.4355	7.5343	8.228	8.7705	9.3806		<.0001	<.0001	<.0001	<.0001	<.0001	<.0001
Hollyford	7.1182	5.1598	4.0377	3.5566	3.5972	8.9651		<.0001	<.0001	<.0001	<.0001	<.0001
Zealandia	7.0241	5.9726	6.732	6.1342	6.2858	9.0954	5.5397		<.0001	<.0001	<.0001	<.0001
Pureora	4.431	5.4366	5.6164	5.2022	5.5404	7.186	5.4283	5.7987		<.0001	<.0001	<.0001
Ruapuke	5.6284	5.4216	7.0234	5.494	6.573	7.0504	5.709	5.2517	5.6599		<.0001	<.0001
Sydney	7.721	6.3735	6.911	6.3988	6.2941	9.2572	5.6094	5.7592	6.5922	6.3778		<.0001
Waikawa	7.8701	5.5179	5.2563	5.059	4.4704	9.2023	3.6328	5.7365	6.1711	5.4926	5.24	

Table V-22 Procrustes distances between groups along the first CV axis and their associated p-values for New Zealand and Sydney mandibles. Bold, red text indicates significant p-values ≤ 0.05 . Bold text indicates highest and lowest distance values between pairs.

Procrustes	Antipodes	Auckland	Chatham	Craigieburn	Eglinton	Enderby	Hollyford	Zealandia	Pureora	Ruapuke	Sydney	Waikawa
Antipodes		<.0001	<.0001	<.0001	<.0001	<.0001	<.0001	<.0001	<.0001	<.0001	<.0001	<.0001
Auckland	0.0351		<.0001	<.0001	<.0001	<.0001	<.0001	<.0001	<.0001	<.0001	<.0001	<.0001
Chatham	0.0464	0.0346		<.0001	0.0016	<.0001	0.0015	<.0001	<.0001	<.0001	<.0001	<.0001
Craigieburn	0.0392	0.0321	0.0293		<.0001	<.0001	0.0027	<.0001	<.0001	<.0001	<.0001	<.0001
Eglinton	0.0362	0.0317	0.0229	0.0236		<.0001	0.0002	<.0001	<.0001	<.0001	<.0001	<.0001
Enderby	0.0285	0.0346	0.0517	0.0488	0.0481		<.0001	<.0001	<.0001	<.0001	<.0001	<.0001
Hollyford	0.04	0.0321	0.0258	0.0177	0.0218	0.0479		<.0001	<.0001	<.0001	<.0001	0.0014
Zealandia	0.0471	0.0376	0.0534	0.0423	0.0493	0.051	0.0409		<.0001	0.0031	<.0001	<.0001
Pureora	0.0345	0.0258	0.0351	0.0283	0.03	0.0429	0.0281	0.0372		<.0001	<.0001	<.0001
Ruapuke	0.0353	0.0322	0.0508	0.0365	0.0444	0.0371	0.0378	0.0259	0.0313		<.0001	0.0002
Sydney	0.0573	0.05	0.0508	0.0396	0.0454	0.0646	0.039	0.0379	0.0445	0.0444		<.0001
Waikawa	0.0456	0.0335	0.0364	0.0253	0.032	0.05	0.0217	0.0322	0.0284	0.0317	0.0328	

5.6.2 Discussion

Sydney mandibles varied consistently with different New Zealand populations occupying opposite ends of the shape spectrum. PCA and CVA results suggest Sydney mandible shape adheres to both soft and hard dietary patterns discussed throughout this thesis. Variation across PC1 and CV1 imply Sydney mandibles are most similar to forest and island mice, which are thought to consume a greater portion of soft foods that may be associated with soft-bodied invertebrates, such as caterpillars, compared to other New Zealand populations (Fitzgerald et al. 1996; Ruscoe & Murphy 2005; Wilson & Lee 2010; Russell 2012; Anderson et al. 2014; Renaud et al. 2015).

On the other hand, Sydney mandibles consistently group with Zealandia mandibles along the second canonical and principal axes, as well as the third canonical axis. CV3 exaggerates the broader mandible profile previously observed with Sydney and Zealandia mice, suggesting Sydney mice are also similar to mice sampled from Zealandia Sanctuary (which may represent mixed haplotypes), but to a lesser extent. Zealandia mice were previously suggested to possess a very efficient mandible shape for processing hard, resistant foods that may be related to a greater consumption of tough plant material (Sato 1997; Baverstock et al. 2013; Anderson et al. 2014; Renaud et al. 2015).

Sydney mandibles are most dissimilar to Enderby I. with Procrustes distance, yet with Mahalanobis distance Enderby I. differs most with Eglinton mandibles.

Sydney mice are clearly very efficient at processing both hard and soft food types, suggesting perhaps several New Zealand house mouse populations have experienced

a directional selection towards either a harder or softer based diet. Of course, without dietary data this is purely hypothetical, but lays the foundation for further study on house mice across the Tasman.

5.7 References

- Anderson P, Renaud S, Rayfield E 2014. Adaptive plasticity in the mouse mandible. *BioMed Central Evolutionary Biology* 14(85).
- Baverstock H, Jeffery NS, Cobb SN 2013. The morphology of the mouse masticatory musculature. *Journal of Anatomy* 223(1): 46-60.
- Fitzgerald BM, Daniel MJ, Fitzgerald AE, Karl BJ, Meads MJ, Notman PR 1996. Factors affecting the numbers of house mice (*Mus musculus*) in hard beech (*Nothofagus truncata*) forest. *Journal of the Royal Society of New Zealand* 26(2): 237-249.
- Gabriel SI, Stevens MI, Mathias MdL, Searle JB 2011. Of Mice and ‘Convicts’: Origin of the Australian House Mouse, *Mus musculus*. *PLOS ONE* 6(12): e28622.
- Grant PR, Grant BR 2006. Evolution of character displacement in Darwin's finches. *Science* 313(5784): 224-226.
- King CM 2016. How genetics, history and geography limit potential explanations of invasions by house mice *Mus musculus* in New Zealand. *Biological Invasions* 18(6): 1533-1550.
- Lomolino MV 1985. Body size of mammals on islands: The island rule reexamined. *The American Naturalist* 125: 310-316.
- Lomolino MV 2005. Body size evolution in insular vertebrates: generality of the island rule. *Journal of Biogeography* 32: 1683-1699.

- Lomolino MV, Sax DF, Palombo MR, van der Geer AA 2012. Of mice and mammoths: evaluations of causal explanations for body size evolution in insular mammals. *Journal of Biogeography* 39(5): 842-854.
- Martínková N, Barnett R, Cucchi T, Struchen R, Pascal M, Fischer MC, Higham T, Brace S, Ho SY 2013. Divergent evolutionary processes associated with colonization of offshore islands. *Molecular ecology* 22(20): 5205-5220.
- Millien V 2006. Morphological evolution is accelerated among island mammals. *Public Library of Science (PLOS) Biology* 4(11): 2165-2165.
- Millien V 2011. Mammals evolve faster on smaller islands. *Evolution* 65(7): 1935-1944.
- Renaud S, Auffray JC 2010. Adaptation and plasticity in insular evolution of the house mouse mandible. *Journal of Zoological Systematics and Evolutionary Research* 48(2): 138-150.
- Renaud S, Gomes Rodrigues H, Ledevin R, Pisanu B, Chapuis J-L, Hardouin EA 2015. Fast evolutionary response of house mice to anthropogenic disturbance on a Sub-Antarctic island. *Biological Journal of the Linnean Society* 114(3): 513-526.
- Ruscoe WA, Murphy EC 2005. House Mouse. In: King CM ed. *The Handbook of New Zealand Mammals*. 2nd ed. Melbourne, AUS, Oxford University Press.
- Russell JC 2012. Spatio-temporal patterns of introduced mice and invertebrates on Antipodes Island. *Polar Biology* 35(8): 1187-1195.

- Samaniego-Herrera A, Clout MN, Aguirre-Muñoz A, Russell JC 2017. Rodent eradications as ecosystem experiments: a case study from the Mexican tropics. *Biological Invasions*: 1-19.
- Satoh K 1997. Comparative functional morphology of mandibular forward movement during mastication of two murid rodents, *Apodemus speciosus* (Murinae) and *Clethrionomys rufocanus* (Arvicolinae). *Journal of Morphology* 231: 131-142.
- Simberloff D, Dayan T, Jones C, Ogura G 2000. Character displacement and release in the small Indian mongoose, *Herpestes javanicus*. *Ecology* 81(8): 2086-2099.
- Taylor R 2006. Straight through from London: the Antipodes and Bounty Islands, New Zealand. Christchurch, N.Z, Heritage Expeditions New Zealand.
- White TA, Searle JB 2007. Factors explaining increased body size in common shrews (*Sorex araneus*) on Scottish Islands. *Journal of Biogeography* 34: 356-363.
- Wilson DJ, Lee WG 2010. Primary and secondary resource pulses in an alpine ecosystem: snow tussock grass (*Chionochloa* spp.) flowering and house mouse (*Mus musculus*) populations in New Zealand. *Wildlife Research* 37(2): 89-103.

VI. General discussion and conclusions

This thesis project began with the aim of qualifying specific biotic and abiotic variables that might influence the mandible shape and body size of house mice inhabiting the New Zealand archipelago. The initial questions I developed searched for find changes in mandible shape and body size that could be precisely pinpointed to genetic origins or island ecological processes.

Shortly after the project began, it became apparent that a substantial proportion of the house mouse samples collected by previous researchers intended to be included in this study were not available. Undeterred, I arranged to collect samples from Zealandia (Karori Wildlife Sanctuary) to pursue my first chapter question: Did mandible shape and body size differ significantly between hybrid and ‘purebred’ populations? In order to answer this query, the Zealandia mice needed to be haplotyped to identify *musculus-domesticus* hybrid individuals. Unfortunately, despite months of endeavour, I could not yield any successful or positive results. At this stage, I concluded that the same question could still be asked of the known pure *castaneus*NZ.2 and hybrid *castaneus*NZ.1 - *domesticus* samples, excluding the *musculus* Zealandia population.

As it happens, a comparison between ‘pure’ and hybrid mouse strains could not be investigated as there were too many other variables that could not be controlled for. First and foremost, the pure and hybrid strains did not co-exist in the same habitat, and so mandible changes related to habitat type could not be controlled. Furthermore,

I could not control for island size when selecting the pure *castaneus* individuals, which were only found on Chatham I. Chatham I. mice also represent a slightly different *castaneus*NZ.2 haplotype compared to the *castaneus*NZ.1 strain found in the hybrid mice. In summary, a hybrid analysis would not have been an appropriate nor accurate reflection of the material.

My second chapter question asked which abiotic and/or biotic factors were the greatest influence on mandible shape and body size between offshore islands? I did indeed find significant variation between island mouse populations, but pinpointing the exact variables responsible for these changes proved to be a fruitless exercise.

The more I began to understand the output of the statistical methods underpinning this investigation, the more I realised the original questions asked of the material at hand were inappropriate, and littered with assumptions. Physiological traits cannot be defined by any one variable, biotic or abiotic. The observable phenotype is the result of a complex relationship with its genetic blueprint, and the ever-changing surrounding environment. My original questions evolved over the course of the investigation, finally forming the crucial queries introduced at the beginning of this thesis:

1. Does mandible shape and body size vary significantly between house mouse populations inhabiting different forest habitats of the New Zealand North and South Islands? If so, what are the covariates available that explain a significant proportion of this observed variation?
2. Does mandible shape and body size of house mice vary significantly between smaller, offshore New Zealand islands that differ significantly in ecology and

habitat to the North and South Islands? If so, what are the covariates available that explain a significant proportion of this observed variation?

3. Does mouse mandible shape and body size vary significantly between the larger and smaller islands of New Zealand i.e. comparing forest and offshore island populations?

In Chapter V I extended the study to include 12 house mice from Sydney, Australia. Regrettably, amidst all the excitement I processed the Sydney mouse mandibles (removed the head) before taking any physical weight or length measurements. This meant that the only question I could ask of the Sydney material was whether mandible shape varied significantly to New Zealand house mouse mandibles. As Sydney *domesticus* house mice likely represent an ancestral population from which northern New Zealand *domesticus* mice are descended, this opportunity enabled a brief glimpse into the intraspecific variation between island and continental populations.

The preceding chapters all found significant variation in house mouse body size, mandible shape and biomechanical advantage between forest, offshore island, and Sydney populations. Geometric morphometric analyses revealed significant patterns of discrimination across PCA and CVA ordination plots. The variation in mandible shape associated with significant PC and CV axes followed biomechanical advantage patterns that suggested hard versus soft food diets were the greatest influence on mandible shape and function from previously published data. South Island, Waikawa I., and Chatham I. mandible shapes were consistent with soft food diets, while North Island, Antipodes I., and Enderby I. mandibles were much more indicative of a diet

high in resistant food types. Other population mandibles shapes fell between these two extremes, suggesting intermediate phenotypes and diets.

To my surprise, the comparison between Sydney and New Zealand mandibles yielded some of the most interesting results of this project. Sydney clustered closely with soft food mandible shapes, but also with mandible shapes related to hard food diets too. Sydney mandibles were most similar to Chatham I. mandibles across most analyses, with high temporalis mechanical advantage and an extended coronoid process. However, Sydney mice were consistently associated with a generally broader mandible profile that strongly related to Zealandia mandible shape. This final results chapter introduced a continental mandible shape that displayed affinities to both hard and soft food-related variation within New Zealand mandibles.

Rainfall was a significant abiotic factor that co-varied with both island and forest mandible shapes, and tended to increase with latitude within each chapter. Greater annual rainfall is likely to be associated with increased primary productivity, which may represent an important factor determining the proportion of soft-bodied invertebrates included in the house mouse diet. When reviewing rainfall data from both chapters, Hollyford and Eglinton Valleys experience the most annual precipitation of all locations, yet cluster closely with Chatham and Waikawa Islands along the first principal component axis in Chapter V. Both Waikawa I. and Chatham I. experience almost half the annual precipitation of Hollyford and Eglinton Valleys, suggesting rainfall is not the only factor influencing the consumption of invertebrates in these mouse populations. Of these four populations, only Waikawa I. mice are free from the competition and predation restrictions imposed by rats, suggesting rat presence is not a significant influence on invertebrate consumption.

Furthermore, Antipodes I. and Enderby I. often grouped together on ordination plots, yet Enderby I.'s annual rainfall is almost three times greater than Antipodes I. Mice on Antipodes I. are known to consume a mix of *Carex* seeds and invertebrates, and displayed intermediate mandible shape and mechanical advantage. Enderby I. mandibles had the greatest masseter advantage, suggesting hard seeds probably make up a majority of their feeding habits, yet they experience more annual rainfall than Chatham I. Unfortunately, the potential link between rainfall, primary productivity, and dietary habits could not be explored further in this thesis without supporting dietary data.

Genetic haplotype was a less significant but recurring explanation for variation in mandible shape in New Zealand results chapters, but very relevant for the Trans-Tasman Sydney comparison. Sydney mandible shape was very clearly separated from those representing New Zealand forest haplotypes. However, Sydney *domesticus* mandibles clustered closely with *castaneus*NZ.2 (Chatham I.) and *domesticus* Clade B (Waikata I.) in the offshore island comparison. Genetics may impose constraints on the direction that shape can adapt along, thus leading to subtle differences between different haplotypes and subspecies. It is also possible that the similarities in mandible shape observed between Sydney *domesticus*, *castaneus*NZ.2 and *domesticus* Clade B are a response to environmental variables rather than genetic constraints. Without more data, it is unwise to draw any further conclusions.

Body size varied significantly between islands, with largest body size observed on smaller and more remote areas. Chapters III and IV also found body size to generally increase with rising latitude, larger mice observed in wetter, cooler climates. The greatest instance of gigantism was observed on the Auckland Islands, found at 50°

latitudes, otherwise known as the Furious Fifties. These findings support previous research by Lomolino et al. (2012) that suggest small mammals attain greatest possible body size on small, moderately remote islands, especially at 50° latitudes, that are free from other mammalian competitors. Mouse body size also varied significantly with temperature, habitat type, presence of rats, and genetic haplotype. Evidently, the growth and eventual body size of a house mouse is influenced by many environmental and physiological variables that interrelate, and is thus very difficult to isolate any one factor.

All in all, this Master's thesis provides an observation of significant patterns of variation within New Zealand house mice that lays the foundation for future investigation. It is my recommendation that further environmental, dietary, and genetic data be collected in order to clarify the shape variation found between mouse mandibles that could not be obtained for this study.

VII. Appendices

APPENDIX 1

Raw physical body measurements for forest and offshore island mice.

LOCATION	WEIGHT (g)	TAIL (mm)	HBL (mm)
Antipodes	22	90	82
Antipodes	29	95	82
Antipodes	25	88	78
Antipodes	29	91	85
Antipodes	25	86	82
Antipodes	27	85	78
Antipodes	23	93	84
Antipodes	29	91	85
Antipodes	29	91	81
Antipodes	21	85	85
Antipodes	14	74	85
Antipodes	12	72	78
Antipodes	13	75	77
Antipodes	20	87	81
Antipodes	21	87	81
Antipodes	22	88	76
Antipodes	19	84	82
Antipodes	25	90	76
Antipodes	28	91	82
Antipodes	24	92	81
Antipodes	18	82	82
Antipodes	25	91	87
Antipodes	21	84	95
Antipodes	17	86	88
Antipodes	22	82	91
Antipodes	19	90	87
Antipodes	23	90	88
Antipodes	24	85	85
Antipodes	17	94	90
Antipodes	25	88	89
Antipodes	24	85	82
Antipodes	19	86	70
Antipodes	23	88	67

Antipodes	22	83	71
Antipodes	15	83	83
Antipodes	17	87	80
Antipodes	21	89	85
Antipodes	21	83	80
Antipodes	16	83	90
Antipodes	20	80	90
Antipodes	18	80	88
Antipodes	21	82	78
Antipodes	21	93	88
Antipodes	20		
Antipodes	21		
Antipodes	20		
Antipodes	19		
Antipodes	18		
Antipodes	18		
Antipodes	22		
Antipodes	19		
Antipodes	20		
Antipodes	20		
Antipodes	19		
Antipodes	18		
Antipodes	21		
Antipodes	25		
Antipodes	20		
Antipodes	18		
Antipodes	19		
Antipodes	24		
Antipodes	26		
Antipodes	19		
Antipodes	18		
Antipodes	20		
Antipodes	20		
Antipodes	23		
Antipodes	18		
Antipodes	18		
Antipodes	21		
Antipodes	22		
Antipodes	20		
Antipodes	21		
Antipodes	22		

Antipodes	20		
Antipodes	21		
Antipodes	20		
Antipodes	18		
Antipodes	21		
Antipodes	21		
Chatham	12	67	73
Chatham	14	70	74
Chatham	22	87	90
Chatham	16	72	76
Chatham	14	73	75
Chatham	11	66	71
Chatham	10.5	61	72
Chatham	17	82	83
Waikawa	13.8	77.7	77
Waikawa	25.04	89.3	90.7
Waikawa	25.21	90	94.7
Waikawa	10.98	75.3	69.3
Waikawa	25.67	79.7	82.7
Waikawa	28.37	92.3	93
Waikawa	22.97	85	89.3
Waikawa	13.95	80.3	75.3
Waikawa	27.89	80.2	77.8
Enderby	17.5	76.3	78.3
Enderby	18.5	81.2	78
Enderby	17.5	77.2	84.7
Enderby	14.5	70.7	73.1
Enderby	26	89.3	92.2
Enderby	26.5	86.5	94.8
Enderby	24.5	87.4	92.4
Enderby	24	91.2	88.3
Enderby	17.5	77.3	78.4
Enderby	25	88.7	94.1
Enderby	22	91.9	83
Enderby	27.5	85.8	95.9
Enderby	19.5	79.7	85.4
Enderby	27	88.5	90.3
Enderby	26	93.4	96.1
Enderby	22.5	83.7	87.9
Enderby	28	91	91.2
Enderby	22	85.8	88.2

Enderby	21	82.7	81.9
Enderby	24.5	87.4	90.8
Enderby	20	81.9	87.7
Enderby	20	83.6	87.9
Enderby	16.5	75.3	76.2
Enderby	22	83.3	84.4
Enderby	24	81.6	93.9
Enderby	25	89.3	97
Enderby	24	101.4	95.5
Enderby	26	84.9	97
Enderby	17.5	76.3	82.8
Enderby	23	81.6	91
Enderby	24	88	87.6
Enderby	25	91.2	98.3
Enderby	24	88	90.6
Enderby	20	80.9	86.5
Enderby	21.5	83	83.1
Enderby	27	86.9	98.1
Enderby	26	91	99.5
Enderby	27.5	78.3	91.8
Enderby	24	89.8	92.1
Enderby	18.5	80.2	84.7
Enderby	19.5	76	85.5
Enderby	18.5	80.6	83.6
Enderby	22	86.6	94.9
Enderby	23.5	77.7	94
Enderby	19.5	77.6	
Ruapuke	19.2	77	75
Ruapuke	21.9	80	94
Ruapuke	17.9	76	79
Ruapuke	15.8	69	70
Ruapuke	18.96	74	74
Ruapuke	22	79	80

LOCATION	WEIGHT (g)	TAIL (mm)	HBL (mm)
Hollyford	20.7	88	93
Hollyford	21	88	90
Hollyford	16.3	62	84
Hollyford	20.8	81	94
Hollyford	20	81	94
Hollyford	16.5	79	85
Hollyford	18.2	89	83
Hollyford	19.1	87	92
Hollyford	18	86	83
Hollyford	17.1	82	83
Hollyford	17	85	86
Hollyford	15.2	86	82
Hollyford	17	81	78
Hollyford	18.8	71	88
Hollyford	17.1	83	87
Craigieburn	15.7	79	84
Craigieburn	15.8	78	86
Craigieburn	21.8	83	89
Craigieburn	23	77	95
Craigieburn	22.7	86	102
Craigieburn	19	85	94
Craigieburn	19.6	75	94
Craigieburn	18.7	85	93
Craigieburn	19.4	76	101
Craigieburn	22.5	79	101
Craigieburn	24.2	89	94
Craigieburn	18.6	78	91
Craigieburn	25.2	82	94
Craigieburn	18.5	71	82
Craigieburn	20.3	86	93
Craigieburn	20.6	80	99
Craigieburn	22.2	86	98
Craigieburn	17	83	91
Craigieburn	18.2	90	89
Craigieburn	18.8	83	94
Craigieburn	16.3	81	89
Craigieburn	14	76	83
Craigieburn	18.7	86	91
Craigieburn	20.3	78	96
Craigieburn	14.5	75	85
Craigieburn	20.4	83	95
Craigieburn	18.2	85	95
Pureora	18.1	80	88

Pureora	14.8	84	85
Pureora	14.1	83	82
Pureora	16	84	78
Pureora	16.8	85	85
Pureora	16.3	85	78
Pureora	18.9	85	84
Pureora	18.3	87	89
Pureora	15.2	84	85
Pureora	19.2	85	79
Pureora	18.2	82	77
Pureora	17.5	83	82
Pureora	12.6	80	76
Pureora	12.3	73	69
Pureora	16.4	79	82
Pureora	13.8	81	75
Pureora	18.2	92	87
Pureora	12.8	83	91
Pureora	16.4	84	70
Pureora	17.2	80	77
Pureora	16.8	72	83
Pureora	15.3	80	80
Pureora	13.2	75	80
Pureora	16.2	84	78
Pureora	14.3	82	80
Pureora	14.8	82	80
Pureora	16.3	87	74
Pureora	16.2	78	81
Pureora	16.1	86	84
Pureora	16.9	82	73
Pureora	13.8	83	79
Pureora	17	73	83
Pureora	11.3	82	86
Pureora	17.7	80	80
Pureora	17.2	92	87
Pureora	20.5	87	82
Pureora	18.3	79	87
Pureora	16.3		84
Pureora			80
Eglinton	15.2	85	94
Eglinton	19.3	85	93
Eglinton	24	81	89
Eglinton	22.8	82	86
Eglinton	25.4	90	99
Eglinton	25.7	76	88

Eglinton	24.5	86	98
Eglinton	23	88	85
Eglinton	24.4	75	90
Eglinton	22.3	82	81
Eglinton	25	86	92
Eglinton	23.6	79	82
Eglinton	25.2	71	81
Eglinton	24.4	85	81
Eglinton	21.3	82	90
Eglinton	26.6	95	90
Eglinton	26.2	84	84
Eglinton		89	94
Zealandia	16.1	81	80
Zealandia	22.3	80	79
Zealandia	14.4	82	80
Zealandia	16.63	81	78
Zealandia	17.51	75	76
Zealandia	16.03	78	75
Zealandia	19.51	77	71
Zealandia	12.28	81	74
Zealandia	20.72	76	81
Zealandia	22.28	79	70
Zealandia	21.64	82	86
Zealandia	14.53	71	74
Zealandia	16.63	87	87
Zealandia	22.39	70	67
Zealandia	23.63	80	73
Zealandia	22.28	79	71

APPENDIX 2

Environmental and genetic variables used for PLS in Chapters III and IV.

LOCATION	RAIN (mm)	RATS	GENETICS	HABITAT	ALT-LOW (m)	ALT-HIGH (m)	TEMP LOW	TEMP HIGH	LAT
ZEALANDIA	1265	0	0	0	160	380	0.5	28.6	41.2
PUREORA	1759	1	1	0	550	700	6	15.3	38.3
CRAIGIEBURN	1450	1	1	1	790	1340	1	13	43.1
HOLLYFORD	4520	1	0	1	90	370	1	10	44.45
EGLINTON	2300	1	0	1	270	550	0	8	44.5

LOCATION	RAIN (mm)	RATS	GENETICS	LOG ISLAND SIZE (ha)	TEMP LOW	TEMP HIGH	LAT
CHATHAM I.	1080	1	0	4.957368	-0.8	29.6	43.8
WAIKAWA I.	1130	0	1	2.079181	2.9	30.9	39.3
RUAPUKE I.	1194	1	1	3.18327	-3	21	46.8
ANTIPODES I.	650	0	1	3.321598	-3	13	49.7
ENDERBY I.	1500	0	1	2.851258	-3	20	50.5
AUCKLAND I.	1500	0	1	4.662522	-3	20	50.6

ERRATUMS

Several of the PCA plots featured in this thesis were created using a pooled within-group variance-covariance matrix instead of the standard variance-covariance matrix (Figures III-G to K, IV-G to I, V-C, V-H to J, and V-R to S). The pooled within-group option is used when wanting to investigate group variation, similar to a CVA plot. The intention of using a PCA plot in this study was to emphasise the variation between individuals, not the pooled within-group variation. The correct PCA plots are shown and discussed in this section.

New Zealand Forest Comparison

The corrected forest PCA plot reveals a much greater separation of Zealandia mandibles from the other four forest populations than previously observed (Figure VII-A). Craigieburn, Eglinton, and Hollyford mandibles still cluster together along PC1, while Pureora mandibles fall between the two extremes. The PC1 warped outline plot depicts a broader mandible profile with a shifted coronoid process and smaller condyle process associated with Zealandia individuals at the positive end of the axis (pink outline). South Island mandibles show a much reduced angular process and slightly longer mandible profile (blue outline). Differentiation across PC2 is quite different to the original plot, with Pureora and Eglinton mandibles clustered at the negative end, and Zealandia mandibles clustered at the positive. The PC2 warped outline plot shows a much broader and shorted mandible shape associated with Zealandia individuals at the positive end of PC2 (pink outline). In this instance, only the first eigenvalue falls above the inflection point on the scree plot. The overall conclusions drawn from these PCA results still match those drawn from the original plot.

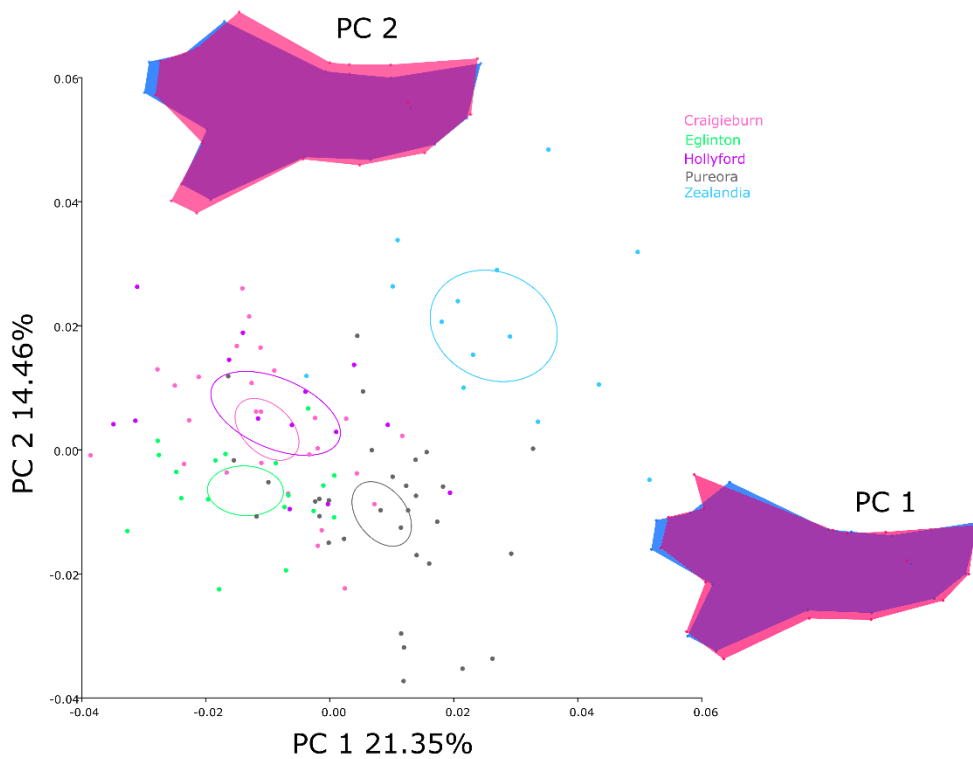


Figure VII-A Corrected PCA plot of mandible shape variation between forest populations with PC1 and PC2. Warped outline plots depict shape change along each axis; blue represents mandible shape at far left of the axis, pink represents mandible shape at far right of the axis.

When grouped by genetic haplotype, the forest PCA plot shows similar overlap of *domesticus* and *domesticus* – *castaneus*NZ.1 hybrid individuals, but with closer clustering of *domesticus* individuals (Figure VII-B). As before, the position of individual points on this PCA plot and the warped outline changes are the same as the forest plot above.

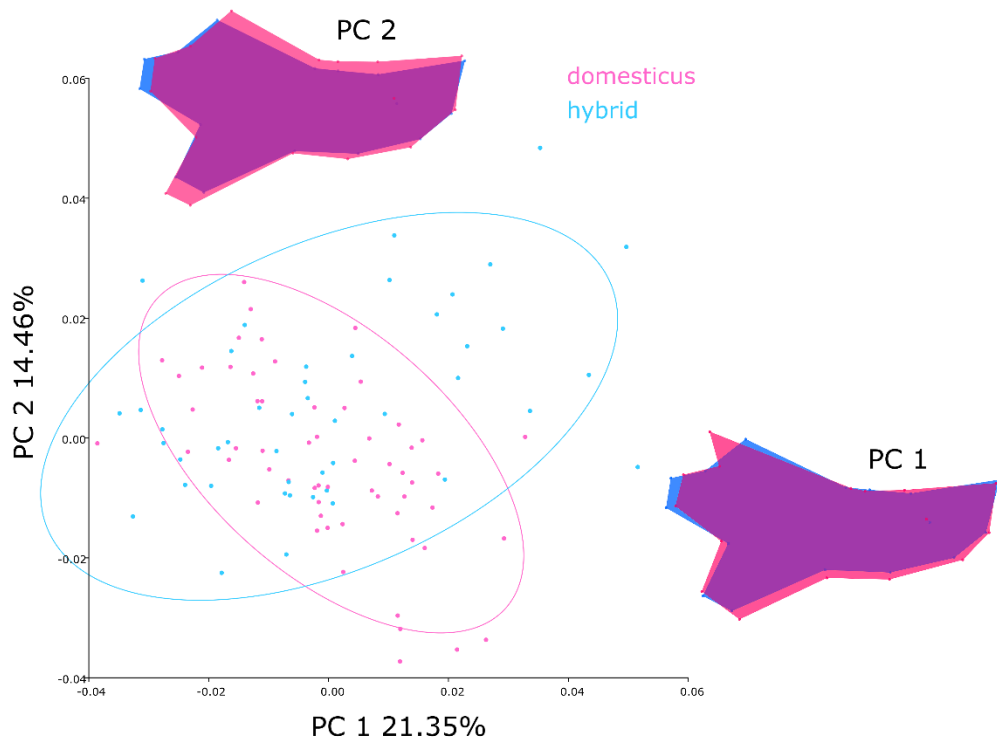


Figure VII-B Corrected PCA plot of mandible shape variation between forest genetic haplotypes with PC1 and PC2. Warped outline plots depict shape change along each axis; blue represents mandible shape at far left of the axis, pink represents mandible shape at far right of the axis.

Offshore Island Comparison

The corrected offshore island PCA plot (Figure VII-C) differs considerably from the original plot. First and foremost, the Ruapuke I. individuals cluster more closely than previously observed. There is also definite separation of island populations along the first axis. Chatham I. and Waikawa I. group together at the negative PC1 axis end, opposing Enderby I. and Antipodes I. at the positive axis end. Ruapuke I. and Auckland I. group together between these two extremes in the middle of the PC1 axis. The PC1 warped outline plot depicts a slimmer mandible profile and extended attachment processes with positive shape change along the first axis (pink outline).

By contrast, Chatham I. and Antipodes I. cluster together at the negative end of the second PC axis, separated from the other four populations. The PC2 warped outline plot shows an enlargement of coronoid and condyle processes associated with Chatham I. and Antipodes I. mandibles (blue outline). However, only the first eigenvalue falls above the inflection point of the scree plot.

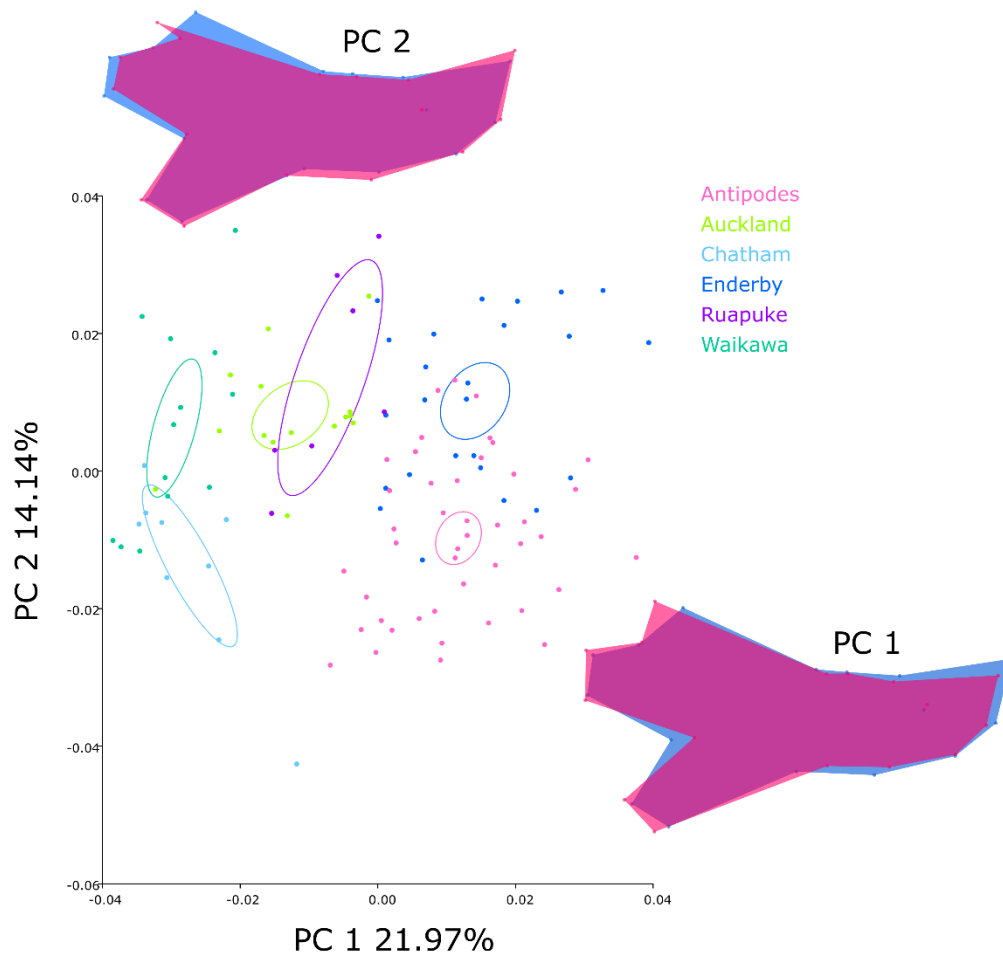


Figure VII-C Corrected PCA plot of mandible shape variation between offshore island populations with PC1 and PC2. Warped outline plots depict shape change along each axis; blue represents mandible shape at far left of the axis, pink represents mandible shape at far right of the axis.

When grouped by genetic haplotype there is clear separation of *castaneus*NZ.2 and *domesticus* Clade B with *domesticus* Clades C and E along the first PC axis (Figure

VII-D). This observation differs considerably to the original island haplotype PCA plot, where only *castaneus*NZ.2 individuals showed clear separation along PC1. As before, the position of individual points on this PCA plot and the warped outline changes are the same as the forest plot above.

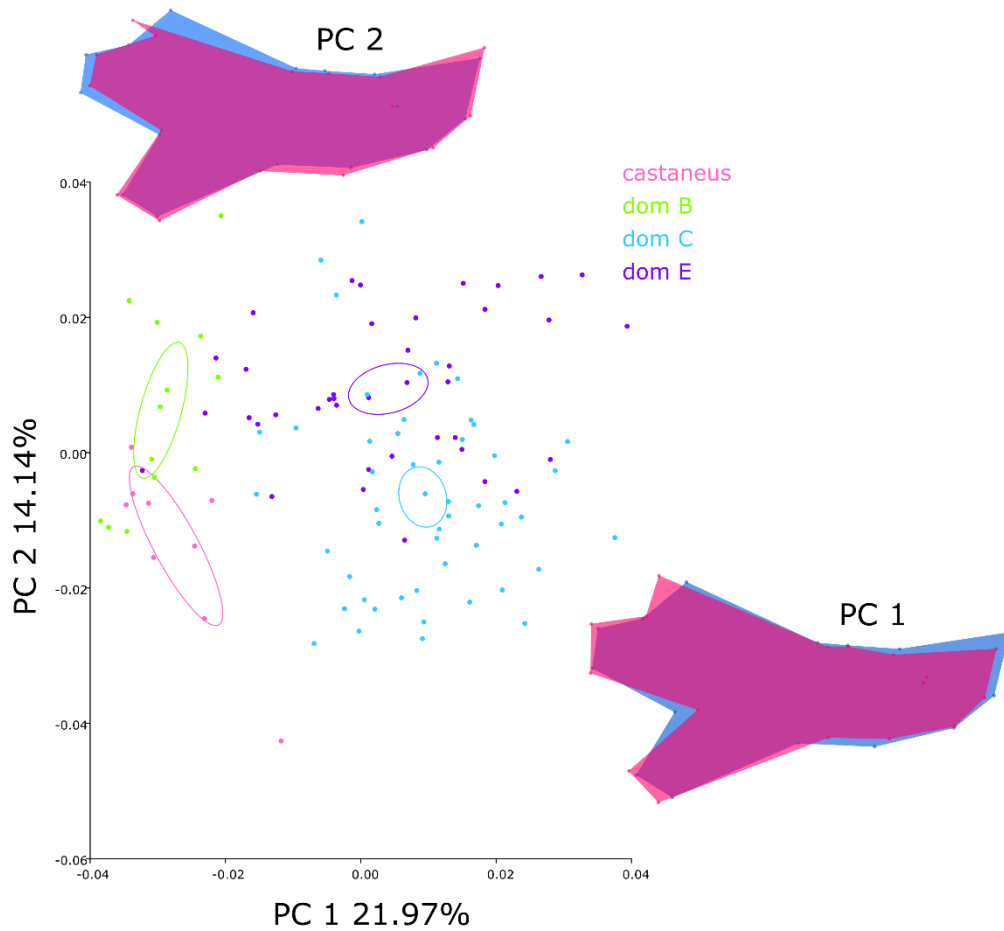


Figure VII-D Corrected PCA plot of mandible shape variation between offshore island genetic haplotypes with PC1 and PC2. Warped outline plots depict shape change along each axis; blue represents mandible shape at far left of the axis, pink represents mandible shape at far right of the axis.

New Zealand Forest and Offshore Island Combined Comparison

The combined forest and offshore island corrected PCA plot is very similar to the original plot, including the warped outline shape change plot (Figure VII-E). The

only obvious difference is a greater separation between the confidence ellipses of Enderby I. and Antipodes I. along PC1.

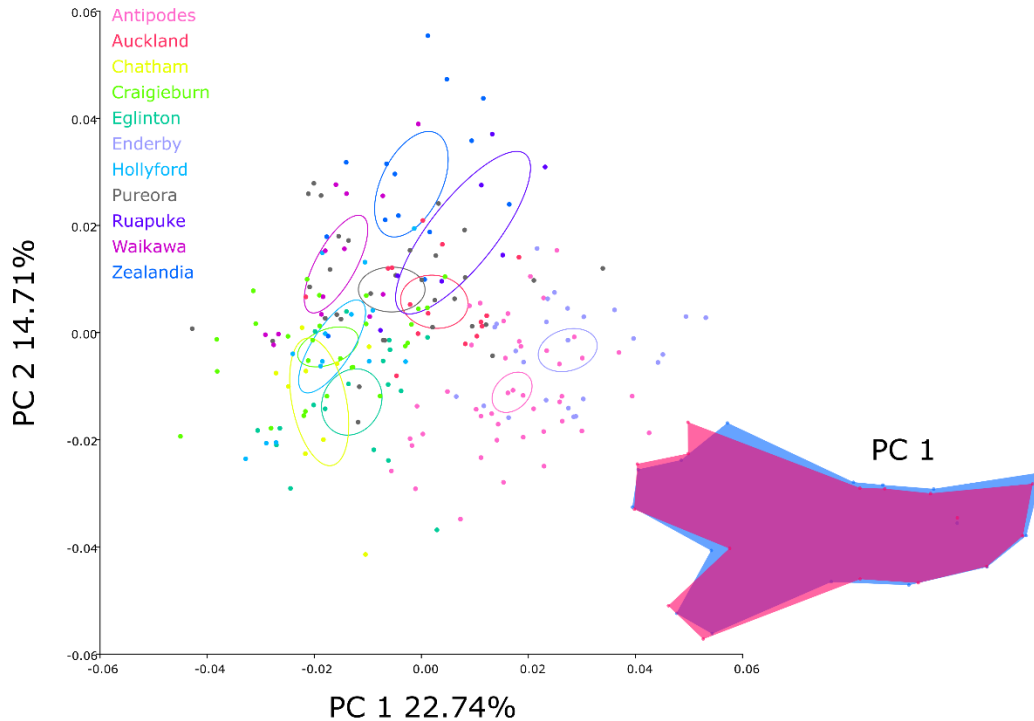


Figure VII-E Corrected PCA plot of mandible shape variation between offshore island and forest populations with PC1 and PC2. Warped outline plots depict shape change along each axis; blue represents mandible shape at far left of the axis, pink represents mandible shape at far right of the axis.

New Zealand Forest and Sydney Comparison

The differentiation of individuals across PC1 of the corrected New Zealand forest and Sydney PCA plot is very similar to the original plot (Figure VII-F). The second PC axis, however, accounts for 7% more mandible shape variation than the original plot, revealing a substantial separation of Zealandia and Sydney mandibles to the other New Zealand forest populations. Zealandia and Sydney mandibles show much broader mandible profiles with extended coronoid and angular processes (blue

outline) compared with South Island and Pureora forest mandible shapes.

Unsurprisingly, both eigenvalues fall above the inflection point on the scree plot. This change in PC2 likely accounts for the conflicting results initially observed in Chapter V.

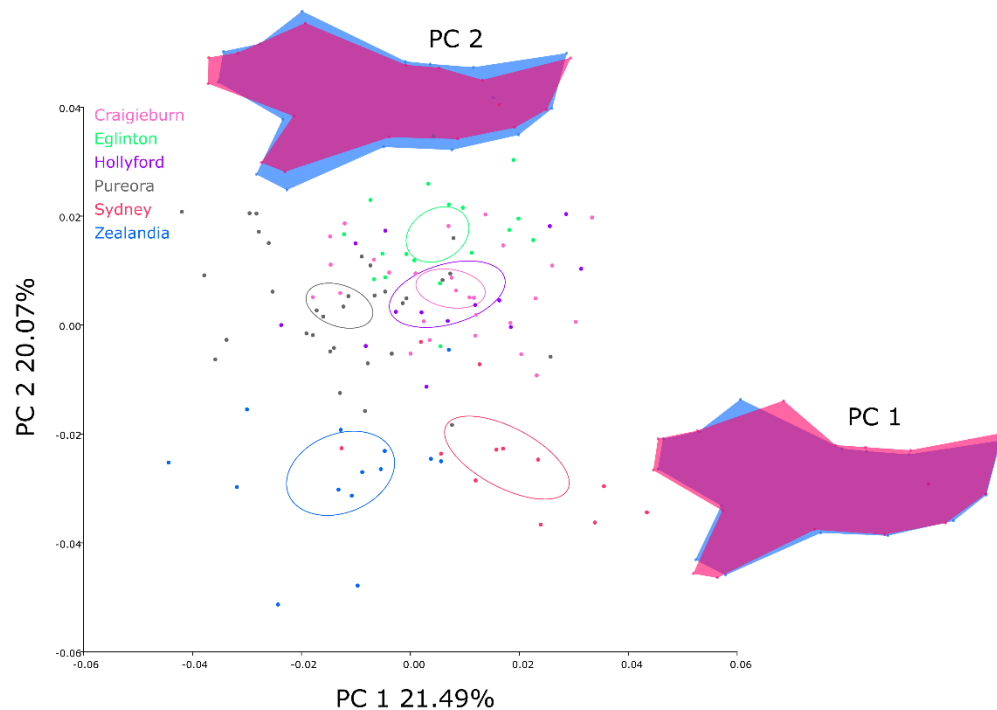


Figure VII-F Corrected PCA plot of mandible shape variation between New Zealand forest and Sydney populations with PC1 and PC2. Warped outline plots depict shape change along each axis; blue represents mandible shape at far left of the axis, pink represents mandible shape at far right of the axis.

When grouped by genetic haplotype, Sydney mandibles are clearly separated from *domesticus* Clade E mandibles, but overlap slightly with *domesticus* – *castaneus*NZ.1 hybrid mandibles on both axes (Figure VII-G). As before, the position of individual points on this PCA plot and the warped outline changes are the same as the forest plot above. Despite these visual changes, the overall conclusions drawn remain similar, if not reinforced by these observations.

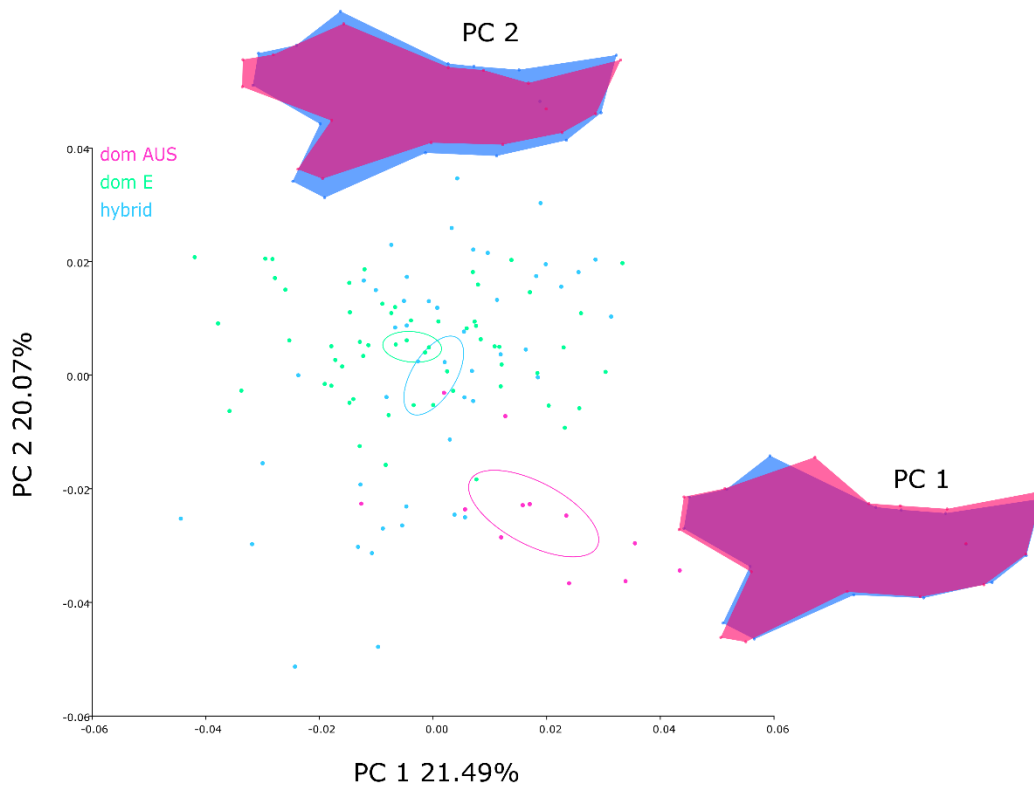


Figure VII-G Corrected PCA plot of mandible shape variation between New Zealand forest and Sydney genetic haplotypes with PC1 and PC2. Warped outline plots depict shape change along each axis; blue represents mandible shape at far left of the axis, pink represents mandible shape at far right of the axis.

Offshore Island and Sydney Comparison

The corrected PCA plot of New Zealand offshore island and Sydney mandibles is similar to the corrected offshore island PCA, and once again considerably different to the original plot in Chapter V (Figure VII-H). Sydney mandibles cluster left of the offshore island mandibles, near Waikawa I. and Chatham I, along PC1. Sydney mandibles show a broader mandible profile, with a larger angular process and shifted coronoid process in the PC1 warped outline plot (blue outline) compared with offshore islands clustering at the positive end of the axis (namely Antipodes I. and Enderby I.). Along PC2, Sydney mandibles cluster at an intermediary position, similar to that of the original plot. Only the first eigenvalue falls above the inflection

point of the scree plot. Despite visual changes across PC1, the overall conclusions drawn remain relatively similar.

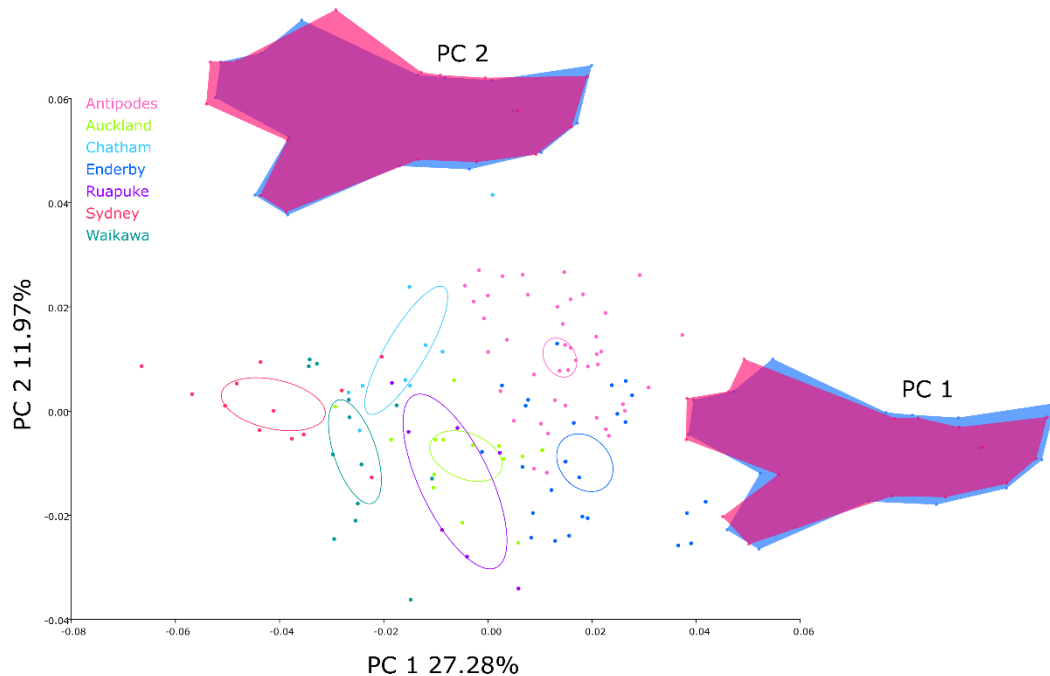


Figure VII-H Corrected PCA plot of mandible shape variation between New Zealand offshore island and Sydney populations with PC1 and PC2. Warped outline plots depict shape change along each axis; blue represents mandible shape at far left of the axis, pink represents mandible shape at far right of the axis.

When grouped by genetic haplotype, the new PCA plot of New Zealand offshore island and Sydney mandibles is almost a mirror of the original plot (Figure VII-I).

Once again, Sydney mandibles are found close to *domesticus* Clade B and *castaneus*NZ.2 mandible shapes, and extremely differentiated from *domesticus* Clades C and E. The warped outline plot shape changes are also similar to the original outline plots.

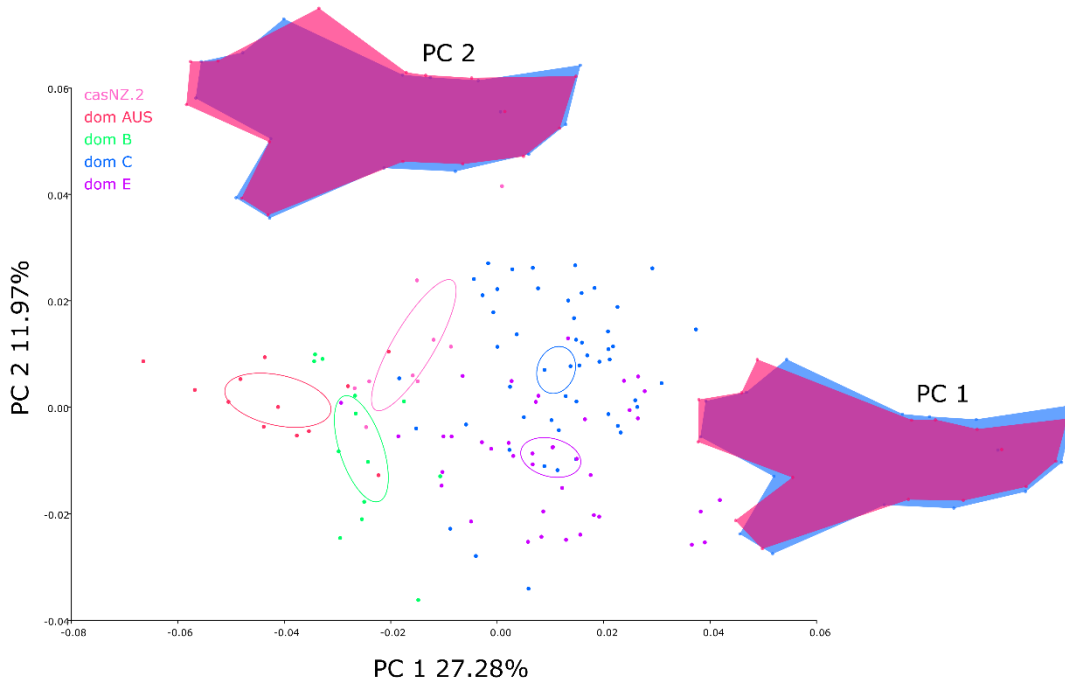


Figure VII-I Corrected PCA plot of mandible shape variation between New Zealand offshore island and Sydney genetic haplotypes with PC1 and PC2. Warped outline plots depict shape change along each axis; blue represents mandible shape at far left of the axis, pink represents mandible shape at far right of the axis.

Overall, the greatest changes are observed in the corrected offshore island PCA plots, while the forest and Sydney plots remain similar to their respective originals.